

The cell walls and arabinogalactan-proteins of streptophyte algae, bryophytes and ferns in the context of evolution

Dissertation

zur Erlangung des Doktorgrades

(*Doctor rerum naturalium*)

der Mathematisch-Naturwissenschaftlichen Fakultät

der Christian-Albrechts-Universität zu Kiel

vorgelegt von

Kim-Kristine Müller

Kiel, 2024

Erste Gutachterin: Prof. Dr. Birgit Classen
Pharmazeutisches Institut
Abteilung Pharmazeutische Biologie
Gutenbergstraße 76
24118 Kiel

Zweiter Gutachter: Prof. Dr. Christian Peifer
Pharmazeutisches Institut
Abteilung Pharmazeutische Chemie
Gutenbergstraße 76
24118 Kiel

Tag der mündlichen Prüfung: 22.02.2024

Für meine Familie,

für meine Freundinnen!

Abstract

More than 500 million years ago, plant terrestrialization was the most significant event for life on land, as we know it today. The common ancestor of all land plants colonised the land from the freshwater habitat and had to cope with a variety of abiotic and biotic stressors to ensure survival. This required various adaptations, including changes of the cell wall.

While much is known about the cell walls of seed plants, there is a significant gap in the knowledge on the cell walls of streptophyte algae and spore-producing land plants. To expand this knowledge, the cell walls of several streptophyte algae (*Chara* spp.), bryophytes (*Anthoceros agrestis* and *Physcomitrium patens*) and ferns (*Psilotum nudum*, *Salvinia* spp. and *Ceratopteris richardii*) were isolated and characterized in this work by using gas chromatography, mass spectrometry, photometry and immunocytochemistry. Analytical investigations revealed that the main polysaccharide classes of the cell walls of seed plants were also present in the cell walls of the species investigated, although there were differences in quantity and structure within the subclasses. Epitopes of the pectic polysaccharides homogalacturonan and rhamnogalacturonan-I and of the hemicelluloses xylans and xyloglucans were also detected by antibodies directed against glycan epitopes via indirect enzyme-linked immunosorbent assays.

In addition to polysaccharides, cell wall glycoproteins, especially arabinogalactan-proteins (AGPs), are also part of the cell wall. In this work, these glycoproteins, if present, were also isolated and characterized in the different species. The search for these AGPs in the cell walls of the *Charales* members demonstrated that only the galactan core structure of pyranosidic 1,3-, 1,6- and 1,3,6-galactose (Galp) known from seed plant AGPs was found, but not the connection of the carbohydrate and the protein part *via* hydroxyproline. Furthermore, the branched galactans were characterized by a unique feature: high amounts of the unusual monosaccharide 3-*O*-methyl Gal.

In all investigated land plant species, AGPs were present. In contrast to seed plant AGPs, the galactan core structure of the AGPs of bryophytes and ferns contained lower amounts of 1,6-linked Galp, indicating highly branched, shorter side chains. Within the bryophytes, a hornwort AGP was isolated for the first time and revealed an unusual 1,3,4-Galp branching point. Furthermore, differences were determined with regard to the terminal residues. Angiosperm AGPs contain mainly 1,5-linked and terminal furanosidic arabinose (Araf) residues, which was comparable in the moss AGP of *Physcomitrium*. In *Anthoceros* AGP, t-Araf residues dominated and were accompanied by low amounts of pyranosidic t-Ara and 1,3-Araf. The AGP of the eusporangiate fern *Psilotum* exhibited mainly 1,3-linked Araf and both t-Ara residues, but these in an equal ratio and thus resembled the AGP isolated from a lycophyte. In contrast, all leptosporangiate ferns were characterized by 1,2-linked Araf and t-Araf. All AGPs of the analysed species had in common that they contained end groups with rhamnose (Rha) and/or the unusual 3-*O*-methylated Rha, which is not part of angiosperm cell walls. A principal component analysis of AGP linkage structures over the streptophyte lineage revealed that angiosperm AGPs are highly conserved, whereas AGPs of bryophytes and ferns show much more varieties.

Zusammenfassung

Vor mehr als 500 Millionen Jahren war der Landgang der Pflanzen das bedeutsamste Ereignis für Leben an Land, wie wir es heute kennen. Der gemeinsame Vorfahre aller Landpflanzen siedelte aus dem Süßwasser auf das Land über und musste mit einer Vielzahl von abiotischen und biotischen Stressoren umgehen, um das Überleben zu sichern. Dies erforderte verschiedene Anpassungen, die auch die Veränderung der Zellwand umfasste. Während schon viel über die Zellwände von Samenpflanzen bekannt ist, gibt es jedoch eine erhebliche Wissenslücke über die Zellwände von streptophytischen Algen und sporen-produzierenden Landpflanzen. Um dieses Wissen zu erweitern, wurden in dieser Arbeit die Zellwände von mehreren Algen (*Chara* spp.), Bryophyten (*Anthoceros agrestis* und *Physcomitrium patens*) und Farnen (*Psilotum nudum*, *Salvinia* spp. und *Ceratopteris richardii*) isoliert und mit Hilfe von Gaschromatographie, Massenspektrometrie, Photometrie und über Immunchemie charakterisiert. Analytische Untersuchungen zeigten, dass die wichtigsten Polysaccharidklassen der Zellwände von Samenpflanzen auch in den Zellwänden der untersuchten Arten vorkommen, allerdings Unterschiede in Menge und Aufbau innerhalb der Subklassen aufweisen. Epitope der Pektin-Polysaccharide Homogalacturonan und Rhamnogalacturonan-I sowie die der Hemicellulosen Xylane und Xyloglucane wurden außerdem mit Antikörpern, die gegen Glykanepitope gerichtet sind, über indirekte Enzym-Immunoassays nachgewiesen.

Neben den Polysacchariden sind auch Zellwand-Glykoproteine, insbesondere Arabinogalaktan-Proteine (AGPs), Teil der Zellwand. In dieser Arbeit wurden diese Glykoproteine, sofern vorhanden, aus allen untersuchten Arten isoliert und charakterisiert. Die Suche nach diesen AGPs zeigte in den Zellwänden der *Charales*-Mitglieder, dass nur das aus Samenpflanzen bekannte Galaktan-Rückgrat aus pyranosidischer 1,3-, 1,6- und 1,3,6-Galaktose (Galp) gefunden wurde, nicht aber die Verbindung des Kohlenhydrat- und des Proteinteils über Hydroxyprolin. Außerdem zeichneten sich die verzweigten Galaktane durch ein einzigartiges Merkmal aus: einen hohen Gehalt der ungewöhnlichen 3-*O*-Methylgalaktose.

In allen untersuchten Landpflanzenarten waren AGPs vorhanden. Im Gegensatz zu den AGPs der Samenpflanzen enthielt das Galaktan-Rückgrat der AGPs von Bryophyten und Farnen geringe Mengen an 1,6- verknüpfter Galp, was auf stark verzweigte, kürzere Seitenketten hindeutet.

Innerhalb der Bryophyten wurde zum ersten Mal ein Hornmoos-AGP isoliert, dass eine ungewöhnliche 1,3,4-Galp Verknüpfung aufwies. Außerdem wurden Unterschiede bei den terminalen Resten festgestellt. Angiospermen-AGPs enthalten hauptsächlich furanosidische 1,5-verknüpfte und terminale Arabinose-Reste (Araf), was im Moos-AGP von *Physcomitrium* vergleichbar war. Im AGP von *Anthoceros* dominierte t-Araf, die mit geringen Mengen an pyranosidischer t-Ara und 1,3-Araf einhergingen. Das AGP des eusporangiaten Farns *Psilotum* wies hauptsächlich 1,3-verknüpfte Araf und beide t-Ara-Reste auf, allerdings im gleichen Verhältnis und ähnelte damit dem aus einem Lycophyten isolierten AGP. Alle leptosporangiaten Farne waren dagegen durch 1,2-verknüpfte Araf und t-Araf gekennzeichnet. Allen AGPs der untersuchten Arten war gemeinsam, dass sie Endgruppen mit Rhamnose und/oder der ungewöhnlichen 3-*O*-Methylrhamnose enthielten, das in den Zellwänden von Angiospermen nicht vorkommt. Eine Hauptkomponenten-Analyse der AGP-Verknüpfungsstrukturen über die Streptophyten-Linie ergab, dass die AGPs der Angiospermen hoch konserviert sind, während die AGPs der Bryophyten und Farne eine viel größere Vielfalt aufwiesen.

Table of Contents

Abstract.....	I
Zusammenfassung	III
Introduction	1
The Terrestrialization and the Evolution of Land Plants	1
The Plant Cell Wall.....	2
Arabinogalactan-proteins.....	3
The Investigated Plants	5
1. Streptophyte Algae	5
2. Bryophytes.....	9
3. Ferns	12
Aim of this Work.....	21
Results and Contributions.....	22
1. The cell walls of different <i>Chara</i> species are characterized by branched galactans rich in 3- <i>O</i> -methylgalactose and absence of AGPs	24
ABSTRACT	24
INTRODUCTION	25
RESULTS	27
DISCUSSION.....	36
CONCLUSION	44
EXPERIMENTAL PROCEDURES	45
ACKNOWLEDGEMENTS	49
AUTHORS CONTRIBUTIONS and CONFLICT OF INTEREST	49
DATA AVAILABILITY STATEMENT	49
SUPPORTING INFORMATION	50
2. The cell wall of hornworts and liverworts: Innovations in early land plant evolution?	56
ABSTRACT	56
INTRODUCTION	57
Cellulose	60
Hemicelluloses	62
Pectic polysaccharides.....	68
Callose	70

Hydroxyproline-rich glycoproteins (HRGPs).....	72
Lignin.....	75
CONCLUDING REMARKS.....	79
ACKNOWLEDGEMENTS.....	80
AUTHORS CONTRIBUTIONS and CONFLICT OF INTEREST.....	80
3. The model organisms <i>Anthoceros agrestis</i> and <i>Physcomitrium patens</i> : Insights into their cell walls and arabinogalactan-proteins.....	81
ABSTRACT.....	81
INTRODUCTION.....	82
RESULTS.....	85
DISCUSSION.....	94
CONCLUSION.....	102
EXPERIMENTAL PROCEDURES.....	103
ACKNOWLEDGEMENTS.....	106
AUTHORS CONTRIBUTION and CONFLICT OF INTEREST.....	106
DATA AVAILABILITY STATEMENT.....	106
SUPPORTING INFORMATION.....	106
4. Sequential extraction of fern cell walls and characterization of arabinogalactan-proteins from the “living fossil” <i>Psilotum nudum</i>	109
ABSTRACT.....	109
INTRODUCTION.....	110
RESULTS.....	112
DISCUSSION.....	118
CONCLUSION.....	126
EXPERIMENTAL PROCEDURES.....	126
ACKNOWLEDGEMENTS.....	129
AUTHORS CONTRIBUTION and CONFLICT OF INTEREST.....	129
DATA AVAILABILITY STATEMENT.....	129
SUPPORTING INFORMATION.....	129
5. Fern cell walls and the evolution of arabinogalactan-proteins in streptophytes ..	135
ABSTRACT.....	135
INTRODUCTION.....	136
RESULTS.....	139
DISCUSSION.....	151

CONCLUSION	156
EXPERIMENTAL PROCEDURES	157
ACKNOWLEDGEMENTS	163
AUTHORS CONTRIBUTIONS and CONFLICT OF INTEREST.....	163
DATA AVAILABILITY STATEMENT.....	163
SUPPORTING INFORMATION	164
Discussion, Conclusion and Outlook	173
References	186
Acknowledgements	203
Declaration.....	204

Introduction

The Terrestrialization and the Evolution of Land Plants

The terrestrialization was one of the most significant events in the evolution of plants. More than 500 million years ago (mya), the first plant organisms successfully conquered the land and land plants, the embryophytes, emerged (Füirst-Jansen *et al.*, 2020; Domozych & Bagdan, 2022).

It is assumed that the latest common ancestor of the embryophytes evolved from the streptophyte algae. These belong, together with the embryophytes, to the streptophytes (Delaux *et al.*, 2019). Approximately 1200 – 725 mya, the *green lineage* split into two clades: the chlorophytes and the streptophytes (Fig. 1; Füirst-Jansen *et al.*, 2020). The most streptophyte algae first colonized fresh water until the common ancestor of land plants ventured onto land. These algae are separated into the lower-branching KCM-grade (Klebsormidiophyceae, Chlorokybophyceae and Mesostigmatophyceae) and the higher-branching ZCC-grade (Zygnematophyceae, Coleochaetophyceae and Charophyceae). The latest common ancestor of all embryophytes is phylogenetically most closely related to the Zygnematophyceae (de Vries & Archibald, 2018; Füirst-Jansen *et al.*, 2020).

The embryophytes can be divided into vascular and non-vascular plants (Harris *et al.*, 2022). Around 470 mya, the non-vascular plants, the bryophytes, evolved, which can be further subdivided into hornworts, liverworts and mosses (Wang *et al.*, 2022). The vascular plants, can be separated into spore-bearing or seed-bearing plants. The spore-bearing vascular plants, which include the lycophytes and ferns, emerged around 440 mya and 400 mya (Pires & Dolan, 2012). The first seed plants, which can be further subdivided into gymnosperms and angiosperms, emerged around 310 mya, with the latter evolving around 180 mya and representing the fruit-bearing plants (Dehors *et al.*, 2019). To date, more than 370,000 species of embryophytes have been discovered (Harris *et al.*, 2022).

Before this biodiversity could develop, terrestrialization required enormous adaptations to the environment conditions on land. The greatest challenges included abiotic stressors such as drought, dehydration, unfiltered UV radiation, and fluctuating temperature changes (Popper *et al.*, 2011; de Vries & Archibald, 2018; Becker *et al.*, 2020; Füirst-Jansen *et al.*, 2020; Harris *et al.*, 2022).

These adaptations are particularly evident on a morphological, physiological, and molecular level (Becker *et al.*, 2020) and are thus also reflected in the plant cell wall. This also needed to change to cope successfully with these new environmental conditions (de Vries & Archibald, 2018).

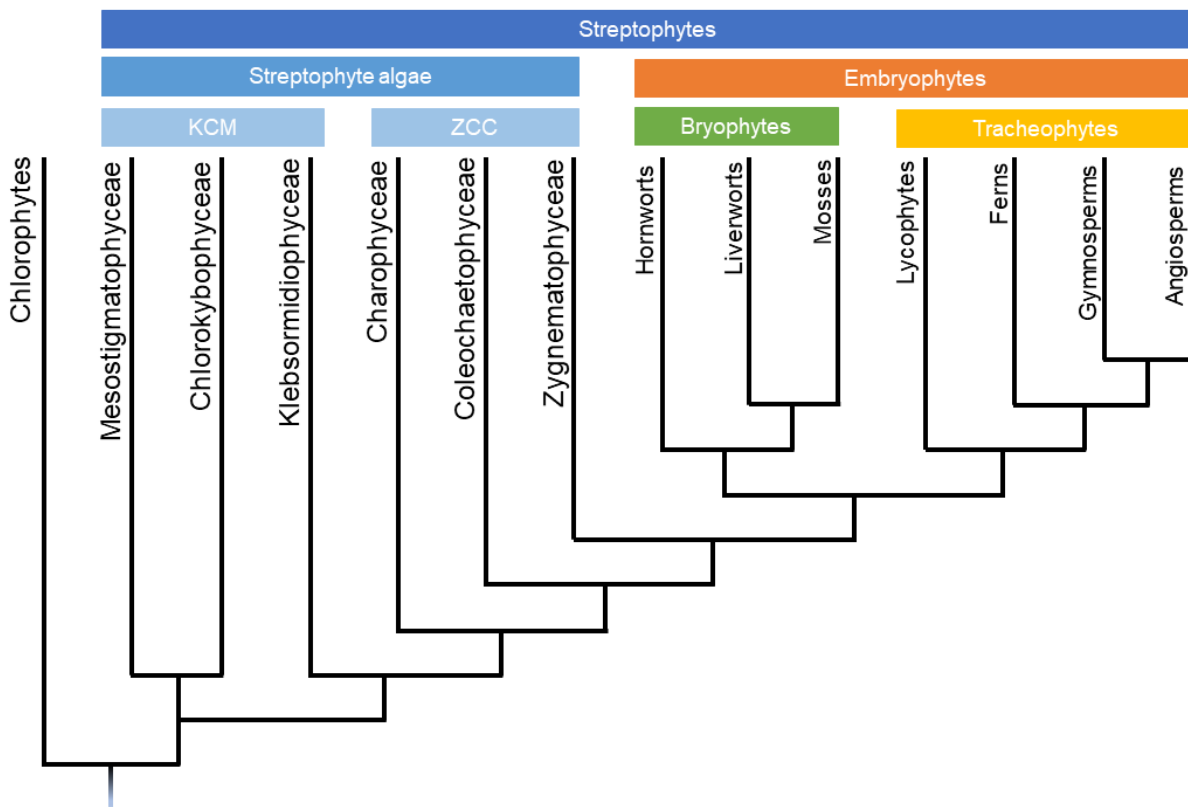


Figure 1. Phylogenetic tree of the *green lineage* (according to Delaux *et al.*, 2019). KCM: Klebsormidiophyceae, Chlorokybophyceae, Mesostigmatophyceae; ZCC: Zygnematophyceae, Coleochaetophyceae and Charophyceae.

The Plant Cell Wall

The plant cell wall is a complex, highly dynamic and polysaccharide-rich construct that surrounds every plant cell (Popper *et al.*, 2011) and is important in all stages of plant morphology, growth, and development (Leroux *et al.*, 2013a).

These cell walls mainly provide the cell with stabilization and protection against external influences, such as pressure differences or infections by pathogens (Sarkar *et al.*, 2009). In addition, cells can communicate with neighboring cells beyond the cell walls, for example to deal more rapidly with changing environmental circumstances. Thus, the cell wall not only defines the cell in its structure, but also plays a crucial role in its survival (Scheller *et al.*, 2007).

The first wall between two cells after mitosis is the middle lamella, a thin pectin-rich layer. Afterwards, the primary wall is built, in some cases supplemented by a secondary cell wall.

The primary cell wall is ubiquitous in every plant cell and is only 0.1 - 10 µm thick and consists mainly of polysaccharides and cell wall proteins (Popper, 2008).

The main polysaccharides are cellulose, hemicelluloses and pectins. The cellulose is preferably present in microfibrils that are cross-linked with hemicelluloses. This cross-linked network is embedded in a matrix of pectin.

Cell wall proteins are also part of this architecture. The hydroxyproline-rich glycoproteins (HRGPs) represent one of the major groups. These proteins can be subdivided in three classes, which are characterized by their glycosylation pattern: arabinogalactan-proteins (AGPs), extensins (EXT) and proline-rich proteins (PRPs). Glycosylation decreases in these groups from 90 % to 50 % to marginally glycosylated (Johnson *et al.*, 2018).

The different components of the cell wall are summarized and described in detail in the result chapter of the review "The cell wall of liverworts and hornworts" (see chapter 2 of the results). It should be taken into account that the composition of the cell walls can vary greatly depending not only on the species, organ or tissue, but also on the cell wall type (Sarkar *et al.*, 2009; Smith *et al.*, 2017).

In addition to the primary wall mentioned above, there is sometimes also a secondary wall, which is a layer on top of the primary wall as soon as it has completed its growth. This type of wall is generally found in wood tissue, increases the stability and strength of the cells during growth and tends to have a hydrophobic character due to lignin incorporation (Popper, 2006; Sørensen *et al.*, 2010).

Arabinogalactan-proteins

AGPs are cell wall glycoproteins that belong to the HRGPs (see above). These glycoproteins consist of a protein and a carbohydrate part and are structurally represented by the most commonly accepted “wattle-blossom” model of Fincher *et al.* (1983), modified by Ellis *et al.* (2010), which is shown in Figure 2A. AGPs can be classified in classical, hybrid and chimeric. The protein of classical AGPs consists of a N-terminus, 100 – 150 amino acids and, in some AGPs, a hydrophobic C-terminal glycosylphosphatidylinositol (GPI) anchor (Youl *et al.*, 1998; Seifert & Roberts, 2007; Ma *et al.*, 2018). Hybrid AGPs show motifs of AGPs and additionally other HRGP-motifs (Classen *et al.*, 2005) and chimeric AGPs show in addition non-HRGP protein domains (Showalter & Basu, 2016). In AGPs, the protein content accounts for 2 – 10 % of the total molecule and is rich in the amino acids proline (P), alanine (A), serine (S) and threonine (T; Showalter *et al.*, 2010). Within the sequence, the occurrence of characteristic dipeptide motifs of AP, PA, SP, TP as well as of valine and glycine followed by proline (VP and GP) is common (Showalter & Basu, 2016). The protein part is mostly covalently linked to the carbohydrate moiety via hydroxyproline (Hyp), which is post-translationally modified from proline by prolyl 4-hydroxylase (P4H; Seifert & Roberts, 2007; Seifert *et al.*, 2021). The polysaccharide part mainly contains the monosaccharides Ara and Gal and is classified as type II arabinogalactan (AG-II) due to the linkage patterns of these monosaccharides (Ellis *et al.*, 2010). These AG-II moieties consist mainly of a pyranosidic 1,3-, 1,6- and 1,3,6-galactose

(Galp) core structure, to which are attached mostly furanosidic arabinose (Araf) residues, which occur terminally, 1,3- or 1,5-linked (Fig. 2B). In addition, some minor pyranosidic monosaccharides like rhamnose (Rhap), fucose (Fucp) or glucuronic acid (GlcAp) are also present as terminal end groups (Showalter & Basu, 2016).

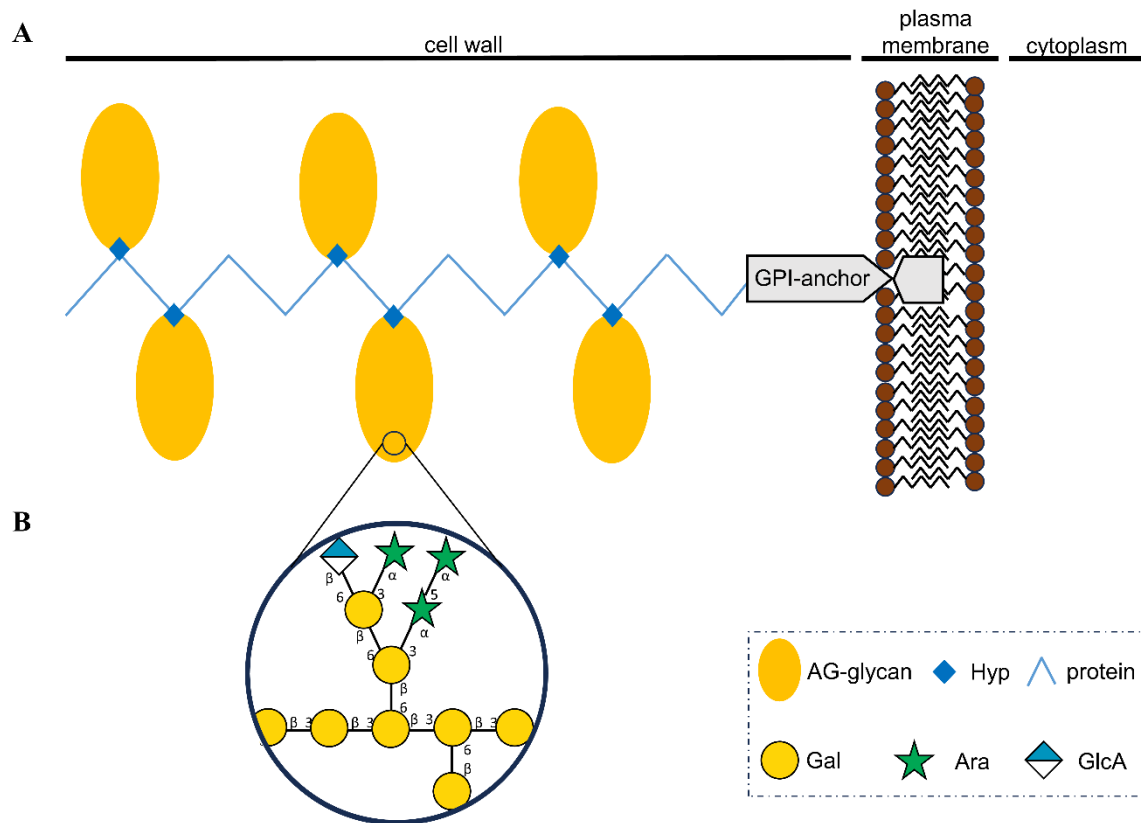


Figure 2. Structural proposal of AGPs. **A:** AGP localization in the cell wall, attached to the plasma membrane via GPI-anchor according to Youl *et al.* (1998) and Ellis *et al.* (2010). **B:** Detailed view of the glycan part of AGPs according to Classen *et al.* (2000) and Ruprecht *et al.* (2017).

The synthesis of AGPs takes place in the endoplasmic reticulum (ER) and the Golgi apparatus, whereby the transport of AGPs to the cell wall and the plasma membrane is transported *via* Golgi vesicles (Youl *et al.*, 1998). In addition to the hydroxylation of Hyp by P4H (mentioned above), glycosylation of the glycan part by glycosyltransferases (GT) also occurs post-translationally (Ma *et al.*, 2018). The GTs belong to different GT families, which are categorized in the carbohydrate active enzymes database (CAZy; www.cazy.org). To date, only a few GTs involved in AGP biosynthesis have been characterized. These include, for example, members of the GT 29 and GT31 family, which are responsible for galactosylation, GT14

members for glucuronosylation and GT77 members for arabinosylation (Showalter & Basu, 2016).

Furthermore, this AG-glycan part is essential for the various functions of AGPs. To name only a few, they are involved in somatic embryogenesis, cell division and growth, pattern formation, xylem differentiation, pollen tube formation, plant microbe interactions and programmed cell death (Seifert & Roberts, 2007; Ma *et al.*, 2018).

The Investigated Plants

More than 1200 – 750 mya, the *green lineage* divided into chlorophytes and streptophytes (Fürst-Jansen *et al.*, 2020). The streptophytes, in turn, can be classified in streptophyte algae and embryophytes, the land plants. Thus, all extant land plants are sister to these algae (de Vries & Archibald, 2018).

To get more information about the latest common ancestor of all land plants, it is necessary to study both the streptophyte algae and the land plants to gain a complete picture of its development and evolution.

Therefore, in this work, both streptophyte algae as well as bryophytes and ferns were investigated in order to obtain a wide spectrum of plants that live both in water and on land.

1. Streptophyte Algae

The streptophyte algae belong to the green algae and grow mainly in freshwater or terrestrial environments (Fürst-Jansen *et al.*, 2020). Phylogenetically, these algae can be classified into six classes, separated into two grades, the lower-branching KCM-grade and the higher branching ZCC-grade, mentioned above (de Vries & Archibald, 2018).

It is generally accepted that the latest common ancestor of all land plants originated from the ZCC-grade, but it has long been discussed to which class of these three the latest common ancestor belongs (Becker & Marin, 2009). Phylogenetic studies have completed this understanding, leading to the conclusion that the common ancestor is most closely related to the Zygnematophyceae.

Previously, it was thought to belong to the Charophyceae, mainly due to their more complex morphological structure and multicellularity (Karol *et al.*, 2001; McCourt *et al.*, 2004).

Cell walls of a member of the Zygnematophyceae have been analysed in the working group and confirmed presence of AGP-like molecules (Pfeifer *et al.*, 2022). To characterize the cell walls of members of the Charophyceae and to search for AGPs in this group, three further species of this class were investigated.

Chara globularis, *Chara subspinos*, *Chara tomentosa*

The genus *Chara* belongs to the streptophyte algae and most species are found in ponds, lakes or streams (Arbeitsgruppe Characeen Deutschlands, 2016). These macrophytic algae have in common a complex structure with an apical growth, which resembles that of horsetails. This thallus consists of nodes, internodes and rhizoids for anchoring in the soil. Additionally, side branches extend from the nodes (Fig. 3A; Arbeitsgruppe Characeen Deutschlands, 2016). Each node bears a whole of branchlets, which has bract cells. The gametangia are located at these bract cells (Fig. 3A; Schneider *et al.*, 2016). In case of a dioecious *Chara* species either the oogonium or the antheridium is situated there (Urbaniak & Gąbka, 2014).

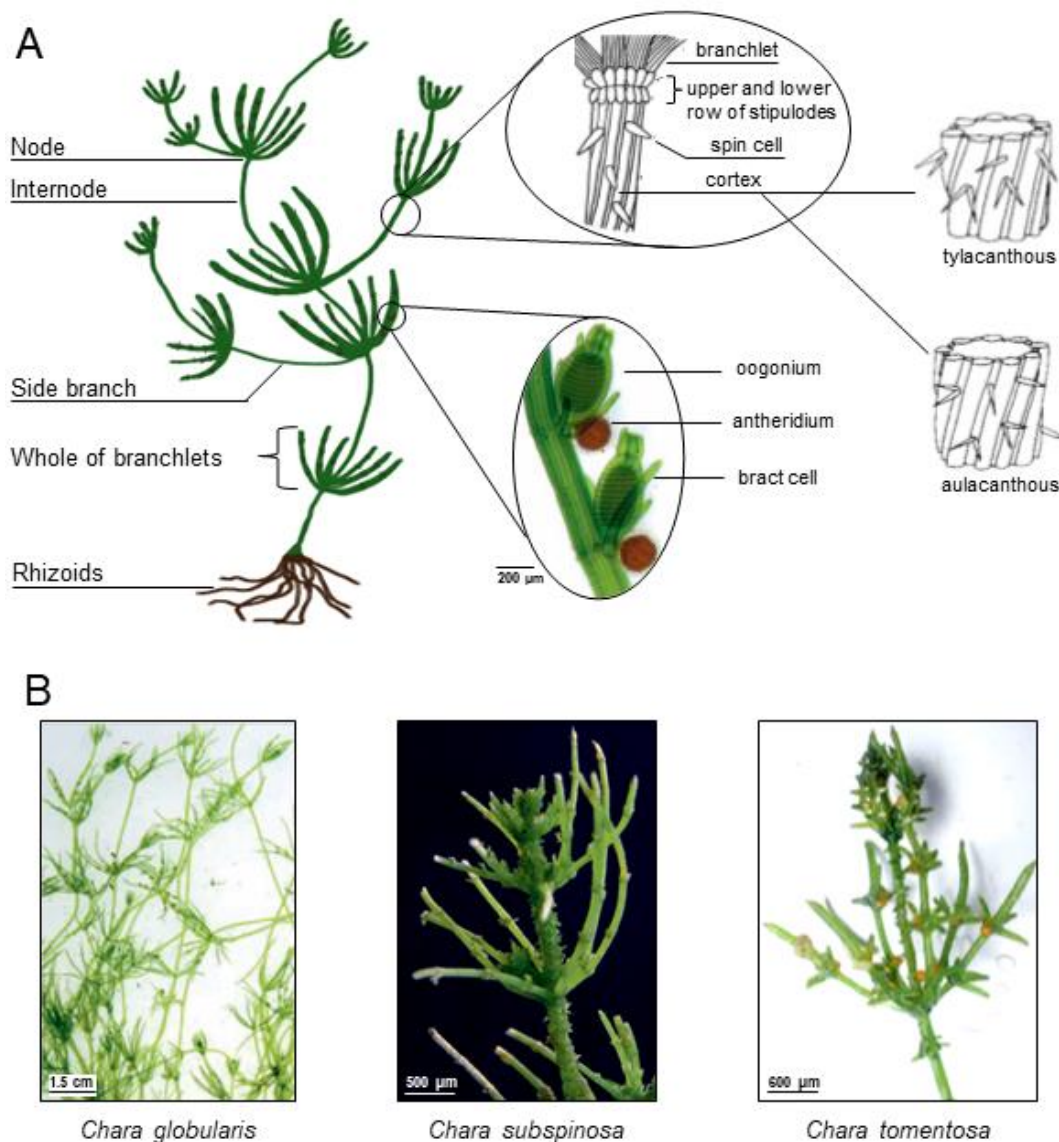


Figure 3. Morphological features of the genus *Chara*. **A:** Schematic illustration of the *Chara* individual with a detailed view of the node, the cortex and the gametangia (according to Schneider *et al.*, 2016; Arbeitsgruppe Characeen Deutschlands, 2016; Urbaniak & Gąbka, 2014). **B:** Illustrations of the individuals (images based on Urbaniak & Gąbka, 2014).

Stipulodes are attached to the internodes below each node. The cortex of the internodes is very characteristic for different *Chara* species, as this can be classified according to the arrangement of cortical cell rows, their ratio to the whole of branchlets, and their spination. If the number of the cortical cell rows is equal to the number of the branchlets, the cortex is haplostichous. If the cortical cell rows are twice or three times as high, it is called di- or triplostichous. The cortical cell rows can also be divided into primary and secondary rows. As soon as both are equally prominent, the cortex is isostichous, otherwise heterostichous. If the primary cortex is more prominent and covered with spin cells, the cortex is called tylacanthous, if the secondary cortex is more dominant, but the spin cells are covered at the primary rows, it is aulacanthous (Arbeitsgruppe Characeen Deutschlands, 2016; Schneider *et al.*, 2016). In addition to the cortex, there are other features to distinguish *Chara* species, like the stipulodes, the spin cells or the branchlet structures.

The streptophyte algae *Chara globularis* THUILL., *Chara subspinoso* RUPR. and *Chara tomentosa* L. belong to this genus *Chara* and are members of the family Characeae (Arbeitsgruppe Characeen Deutschlands, 2016). These individuals are shown in Figure 3B and their features are summarized in Table 1.

Table 1. Characteristic features of the investigated *Chara* spp.*

	<i>Chara globularis</i>	<i>Chara subspinoso</i>	<i>Chara tomentosa</i>
Distribution	cosmopolitan, mainly northern hemisphere; fresh water and brackish water	mainly Central Europe, Scandinavia, Russia	cosmopolitan
Habitus	olive to dark green; up to 120 cm; highly branched	dark green to greyish green; 50–70 cm; branched	green to reddish-brown; 25–200 cm antler-like,
Sex	monoecious	monoecious	dioecious
Cortification	triplostichous; commonly isostichous	diplostichous, strongly heterostichous and aulacanthous	diplostichous, tylacanthous
Shoot diameter	0.3–1.4 mm	1–1.2 mm	2–3 mm
Spin cells	without	mostly in pairs, grow in the opposite direction with different lengths; located in the furrows	solitary or 2–3 in bunches; broad at the base, tapering to a tip
Stipulodes	arranged in two rows, either warty or absent	arranged in two rows, spiky and short	arranged in two rows, uppers mostly more intensive developed
Number of branchlets	6–9	7–10	6–7
Branchlet structure	1–6 corticated cells followed by 2–3 ecorticated cells,	5–6 corticated cells followed by 2–3 ecorticated cells, the last cell is clearly offset	4–5 corticated cells followed by 1–2 ecorticated cells (one is swollen, the terminal cell reduced)
Special features	nodes of the whole branchlets dark colored; long internodes with short branches	distinct manifestation of the heterostichous aulacanthous cortex	inflated bract cells and end cells of the branchlets, the form of the spine cells; individuals growing close to the water surface are reddish, in deeper water greenish

*Arbeitsgruppe Characeen Deutschlands, 2016; Urbaniak & Gąbka, 2014

2. Bryophytes

The common ancestor of all extant bryophytes evolved around 470 mya (Morris *et al.*, 2018). Beside the angiosperms, the bryophytes contain the second greatest diversity of species with around 20,000 species and can be classified into hornworts, liverworts and mosses. The mosses are the most numerous group with 30 orders and approximately 13,000 species, followed by the liverworts with 15 orders and approx. 7,000 species and finally the hornworts with 5 orders and 215 species (Wang *et al.*, 2022).

Phylogenetically, there is increasing support for the monophyly of bryophytes with hornworts sister to the liverworts and the mosses. Liverworts and mosses were classified as setaphytes due to the formation of a seta (Zhang *et al.*, 2020; Wang *et al.*, 2022).

Similar to all embryophytes, the bryophytes reproduce within a life cycle that is divided into two alternating multicellular generations: the haploid gametophyte and the diploid sporophyte (Pires & Dolan, 2012). However, only within the bryophytes, the gametophyte is the dominant generation and determines the phenotype. The diploid sporophyte is partially or completely dependent on the gametophyte (Frangedakis *et al.*, 2021).

Bryophytes represent the only clade of the embryophytes without vascular tissues and nevertheless colonize a wide variety of habitats today. In addition to moist areas and forests, the habitats also include deserts, tropics, and the Antarctic (Hodgetts *et al.*, 2019; Roig-Oliver *et al.*, 2021; Wang *et al.*, 2022). Their enormous adaptability qualifies them as excellent and indispensable candidates for the evolutionary study of cell walls.

Anthoceros agrestis

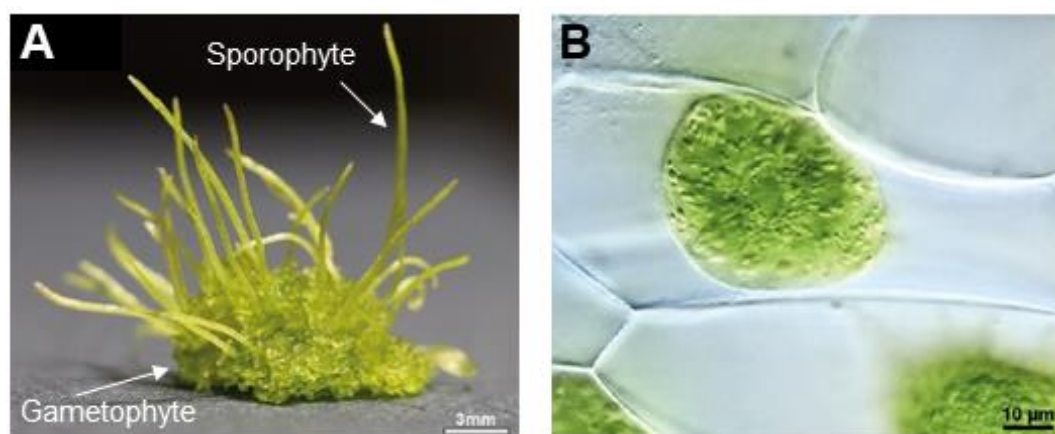


Figure 4. *Anthoceros agrestis*. **A:** Individual illustration (according to Szövényi *et al.*, 2015). **B:** Gametophyte cells with a single chloroplast (Frangedakis *et al.*, 2021).

Anthoceros agrestis PATON is a hornwort of the genus *Anthoceros* of the family Anthocerotaceae (Fig. 4A). The name "*Anthoceros*" is derived from the Greek, where "Anthos" means flower and "Ceras" refers to horn. It is an annual species that is widespread in northern areas (Frangedakis *et al.*, 2021).

The gametophyte is thallose, monoecious with embedded antheridia and archegonia, and forms unicellular rhizoids. These are root-like structures that resemble the root hairs of angiosperms. However, their main function is to anchor in the soil rather than to absorb water and nutrients (Wang *et al.*, 2022).

Anthoceros agrestis can be symbiotic with fungi (the arbuscular mycorrhizal fungi, AMF) as well as with endophytic cyanobacteria, which primarily belong to the genus *Nostoc*. These N₂-fixing bacteria are found in so-called mucilage clefts, which are two-cell epidermal cavities filled with mucilage (Frangedakis *et al.*, 2021). While symbiosis with AMF is widespread among land plants, such *Nostoc* symbiosis is only found in a few representatives, one of the best-known examples being that with *Azolla filiculoides* (Li *et al.*, 2018).

In addition, the cells of the gametophyte have a special feature: they have only one single chloroplast per cell, which is equipped with a pyrenoid. These pyrenoids are compartments that can accommodate a mechanism for concentration carbon (Fig. 4B; Li *et al.*, 2020; Frangedakis *et al.*, 2021).

The gametophyte is attached to the elongated sporophyte *via* a basal meristem. The sporophyte grows upwards as a horn, giving the hornwort its name. The sporangium, in which the spores are formed, is located in the horn. Pseudoelaters are involved in spore dispersal (Renzaglia *et al.*, 2017; Frangedakis *et al.*, 2021). In addition, the sporophytes contain stomata which, however, differ morphologically and physiologically from those of the tracheophytes. For example, the opening and closing of the stomata cannot be controlled by the CO₂-concentration or the availability of water. Their function is not primarily to optimize photosynthetic performance or prevent desiccation, but rather to ensure a certain degree of desiccation of the sporophyte to improve spore dispersal (Frangedakis *et al.*, 2021; Wang *et al.*, 2022).

Anthoceros agrestis is nowadays a model organism as the hornwort is easy to cultivate, has a small size and can be propagated vegetatively (Szövényi *et al.*, 2015; Frangedakis *et al.*, 2021). Therefore, *Anthoceros agrestis* is suitable for studying various biological processes and is also an interesting organism to study cell wall composition in the context of evolution of the cell wall. In addition, the genomes of *Anthoceros agrestis* and those of two relatives (*Anthoceros angustus* and *Anthoceros punctatus*) have been published and offer further insights into the genus *Anthoceros* (Li *et al.*, 2020; Zhang *et al.*, 2020).

Physcomitrium patens

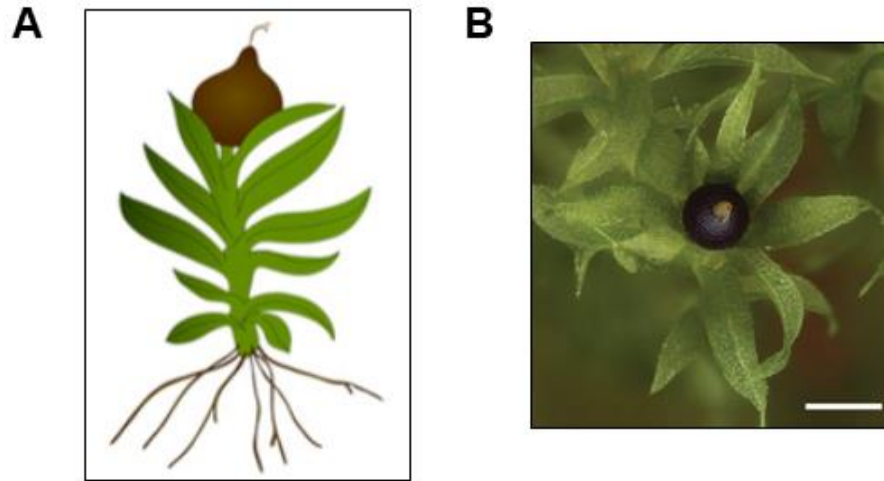


Figure 5. *Physcomitrium patens*. **A:** Individual illustration. **B:** Gametophore with a mature sporophyte. Scales bare \triangleq 1 mm (according to Lang *et al.*, 2018 and Rensing *et al.*, 2020).

Physcomitrium patens (HEDW.) BRUCH & SCHRIMP. is a moss of the genus *Funariales* of the family Funariaceae (Fig. 5A). The moss is native to Europe, North America and East Asia and prefers to grow in moist habitats at low or moderate elevations (Rensing *et al.*, 2020).

A distinctive feature in the development of *Physcomitrium* is the multicellular protonema. This is a tip growing filament that develops from the spore. The protonema generates buds that grow into a leafy gametophore. It consists of a short, mostly unbranched stem and oval leaf like structures, which are also called phyllids, and rhizoids (Rensing *et al.*, 2020; Ye *et al.*, 2022). The moss is monoecious, because of the development of male and female gametangia on the same gametophore (Cove, 2001).

The sporophyte is connected to the gametophore apex by a foot structure and further consists of a seta, which ends in a single globular capsule bearing a thin cap, the calyptra (Fig. 5B). The spores develop inside this capsule. In addition, the sporophyte is equipped with stomata, but these are only controlled by a single guard cell (Ligrone *et al.*, 2012; Rensing *et al.*, 2020).

Physcomitrium is one of the model organisms of the non-vascular plants. It is used for a variety of evolutionary developmental studies (Rensing *et al.*, 2020; Yadav *et al.*, 2023). In addition, *Physcomitrium* was the first seedless plant which genome was sequenced (Rensing *et al.*, 2008).

3. Ferns

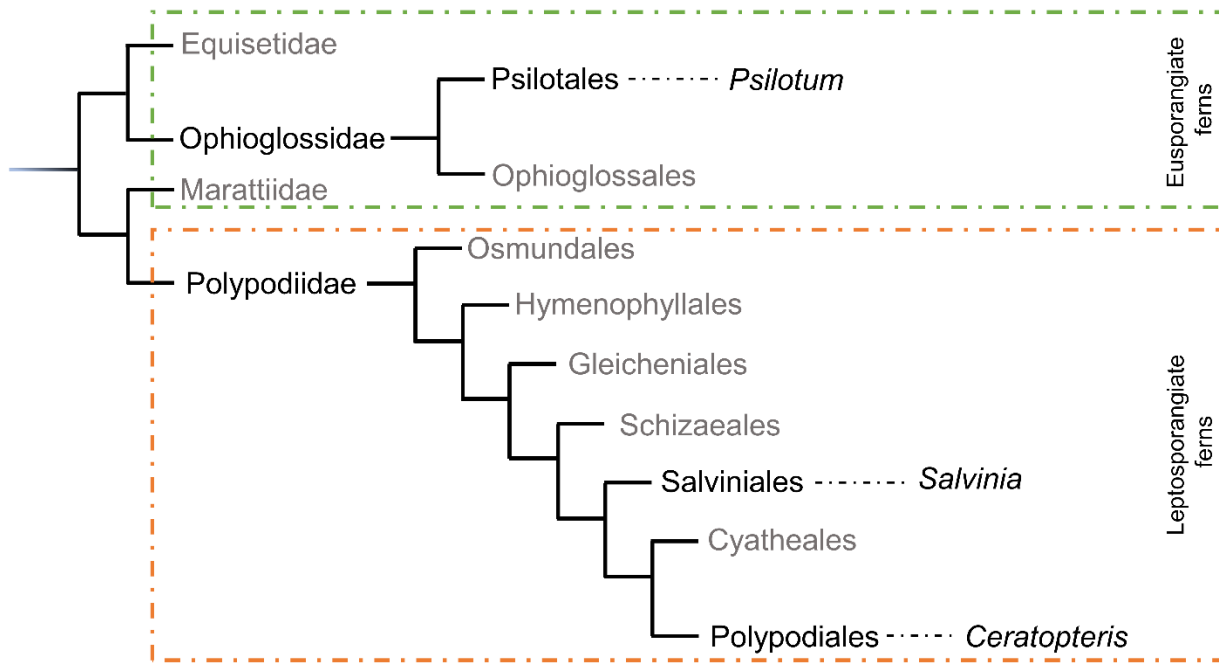


Figure 6. Phylogenetic tree of ferns, including categorisation into eusporangiate and leptosporangiate ferns and classification of the investigated fern genera *Psilotum*, *Salvinia* and *Ceratopteris* (according to Pryer *et al.*, 2004 and Nitta *et al.*, 2022).

Ferns are the second most diverse group of vascular plants and contain around 12,000 species. Ferns colonize a wide variety of habitats and ecosystems (Marchant *et al.*, 2022). The phylogenetic tree of ferns is shown in Figure 6.

Around 400 mya, the common ancestors of ferns evolved and with them, among other developments, the formation of "true" leaves, which can also be found in the extant seed plants (Pryer *et al.*, 2004). These megaphyllous leaves are structurally more complex than the microphylls of the lycophytes (Leroux *et al.*, 2013a). Due to this similarity, ferns and seed plants are classified as "euphyllophytes" (Pryer *et al.*, 2004). Ferns can in turn be subdivided into eusporangiate and leptosporangiate species. The difference depends on the structure of the sporangia walls. The sporangium wall of eusporangiate ferns consists of two or more layers, while that of leptosporangiates has only one layer (Popper, 2006).

The main differences between ferns and seed plants are the spore dispersal and the life cycle of ferns. Whereas in ferns both generations are almost completely independent of each other and autotrophic, the gametophyte of seed plants is completely dependent on the sporophyte, does not form a division-active meristem and is greatly reduced in size. In these plants, the sporophyte is responsible for the growth and development of the individual, in which it mainly forms pluripotent apical meristems (Geng *et al.*, 2022).

Phylogenetically, the ferns are sister to seed plants and are therefore very important in the study of cell wall evolution of land plants (Delaux *et al.*, 2019; Fang *et al.*, 2022).

Psilotum nudum

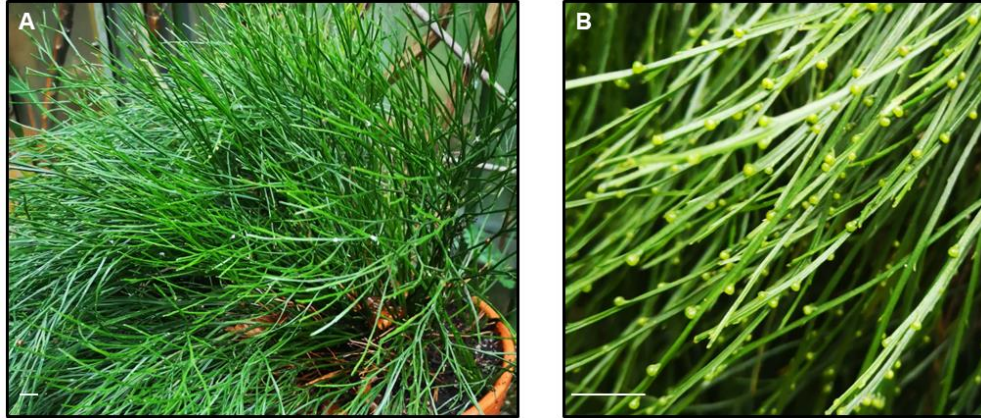


Figure 7. *Psilotum nudum*. **A:** Individual illustration. **B:** Shoot ends with synangia. Images by K. Mueller. Scales bare \triangleq 1.0 cm.

Psilotum nudum (L.) BEAUV. is an eusporangiate fern of the genus *Psilotum* and a member of the family Psilotaceae (Fig. 7A). This family contains only the two genera *Psilotum* and *Tmesipteris* (Šamec *et al.*, 2019). The fern is perennial and native to tropical, subtropical and rocky landscapes or occurs epiphytically (Brownsey & Lovis, 1987; Chernova *et al.*, 2020). In India and Hawaii, for example, parts of this fern are used medicinally to heal wounds or against diarrhea (Valavan *et al.*, 2016). The phenotype of *Psilotum* differs from most other ferns in that *Psilotum* lacks leaves. Instead, this fern morphologically consists of a shoot and an underground rhizome part.

The aerial section resembles a stem and is highly forked, from which the common name whisk fern originates, which is typical for this genus (Valavan *et al.*, 2016; Chernova *et al.*, 2020). The branched shoots contain tiny enations, which are scale-like appendages. Located above these enations are the synangia (Fig. 7B). These arise from the fusion of three neighboring sporangia and contain the spores (Šamec *et al.*, 2019). The rhizome bears rhizoids and can be symbiotic with mycorrhizal fungi (Šamec *et al.*, 2019).

Due to its fern-like and reduced appearance, *Psilotum* is often called “living fossil” (Chernova *et al.*, 2020). Phylogenetically, the extant individuals belong to a clade, which is separated from all other fern species by the first split within the ferns (Nitta *et al.*, 2022). *Psilotum* is therefore also of interest for evolutionary research on the cell wall.

Salvinia x molesta, *Salvinia auriculata*, *Salvinia cucullata*, *Salvinia natans*

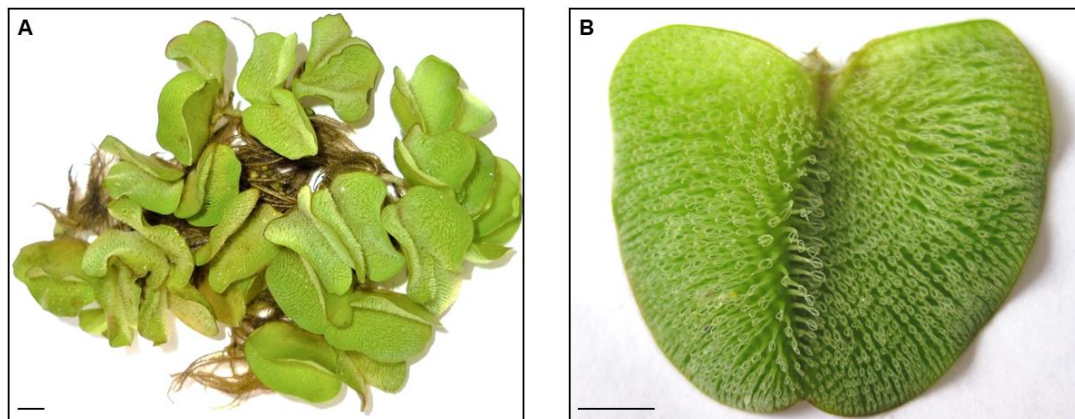


Figure 8. *Salvinia x molesta*. **A:** Individuals (Mueller *et al.*, 2023). **B:** Floating fronds with whisk-like hairs (Image by K. Mueller). Scales bare \triangleq 0.5 cm.

Salvinia x molesta D.S. MITCHELL is a species of the genus *Salvinia* and belongs to the leptosporangiate, free-floating ferns. This fern is a member of the family Salviniaceae (Fig. 8A). It is native to Brazil and has now been introduced to many tropical and subtropical countries around the world. Its habitat is mainly water surfaces of calm and still waters, slow-flowing rivers or canals (Forno & Harley, 1979; Room, 1985; Oliver, 1993; Pryer *et al.*, 2004; Nagalingum *et al.*, 2006; Leterme *et al.*, 2008).

Morphologically, the floating fern consists of a horizontal shoot axis that is attached to each node with three fronds, two floating fronds and one water frond, which is dissected (Miranda & Schwartsburd, 2016). The roots are absent; the function is taken over by the water frond (Room, 1983).

The two floating fronds are oval and have a circumference of 1 – 5 cm. On the adaxial side of the frond, which is directed towards the atmosphere, there are characteristic hairs, which are explained in more detail later in this section. The abaxial, water-facing side of the frond, on the other hand, has simple hairs.

Each frond is divided into two lobes by a lamella and is dissected up to a third. The fronds are arranged in a heart shape at the base (Fig. 8B; Miranda & Schwartsburd, 2019).

The water frond, on the other hand, is submerged. It is brownish, highly branched and covered with simple hairs. It is filamentous and can grow up to 24 cm long (Miranda & Schwartsburd, 2016; 2019).

The sorophores, which are arranged in spikes, are attached to the base of these fronds. The sori are ovoid (Mitchell & Thomas, 1972; Miranda & Schwartsburd, 2019).

The hairs on the upper side of the floating fronds are a very characteristic and striking feature of this fern. They have a special shape that resembles a whisk and consist of a long papilla and four trichomes (Fig. 8B; McFarland, 2004). The four trichomes are located above the papilla

and are stuck together at the tip. This hair tip is hydrophilic, but the inner body shows a hydrophobic character, which encloses air. The fronds gain buoyancy, which protects them from sinking. This is also known as the "*Salvinia* effect" (Barthlott *et al.*, 2009; 2010; Ensikat *et al.*, 2010; Miranda & Schwartzburd, 2019).

This air-enveloping and air-holding effect, even in turbulent flows, could be used in the future for the design of artificial surfaces such as ship coatings, low-friction fluid transport or heat-insulating interfaces (Barthlott *et al.*, 2010).

This whisk-like hair shape was discovered in three other *Salvinia* species: *S. auriculata*, *S. biloba* and *S. herzogii*. Due to this unique characteristic, these four floating ferns form the *Salvinia-auriculata*-complex among the *Salvinia* species (Mitchell & Thomas, 1972).

Salvinia x molesta can go through three stages of development. In the primary stage, short and flat floating fronds (up to 1.5 cm in width) are formed. The internodes are relatively long in relation to the fronds. In the secondary state, these fronds still grow flat on the water surface, up to 2 cm, and form a boat shape. The internodes are still relatively long. In the final stage, the tertiary state, a mat of individuals spread out. The floating fronds have reached a size of up to 6 cm in width, protruding for the most part from the water surface and overlapping each other. The internodes are short (Mitchell & Thomas, 1972; George & Jothi, 2015). The three stages of growth are shown in Figure 9 for illustration.

Salvinia x molesta differs from the other *Salvinia-auriculata*-complex species in the way it reproduces. Reproduction is only vegetative through distribution of the nodes (Mitchell & Thomas, 1972; Room, 1983; Miranda & Schwartzburd, 2019). This fern is not capable of developing mature spores (Loyer & Grewal, 1966; Forno, 1983; Miranda & Schwartzburd, 2016). The sorophores at the base of the frond each have a sorus. These contain the sporangia, which, however, are mostly hollow inside (Mitchell & Thomas, 1972; Forno, 1983; Oliver, 1993). Based on this, it is postulated that *Salvinia x molesta* originated as a hybrid from two other *Salvinia* species, most likely due to the inheritance of the whisk-like hairs from two species of the *Salvinia-auriculata*-complex (Mitchell & Thomas, 1972; Forno, 1983).

Vegetative reproduction has a very high growth rate, which is exponential (Mitchell & Tur, 1975). It has been shown that growth can double in mass in 2.2 to 4 days under optimal conditions (Mitchell & Tur, 1975; Cary & Weerts, 1983). The growth is so massive, mat-like and competitive that it can have a negative impact on the environment and is therefore referred to as a plague in many countries (Mitchell & Tur, 1975). The species has been included in the "100 of the World's Worst Invasive Alien Species" list since 2013 and still is today (Motitsoe, 2020).

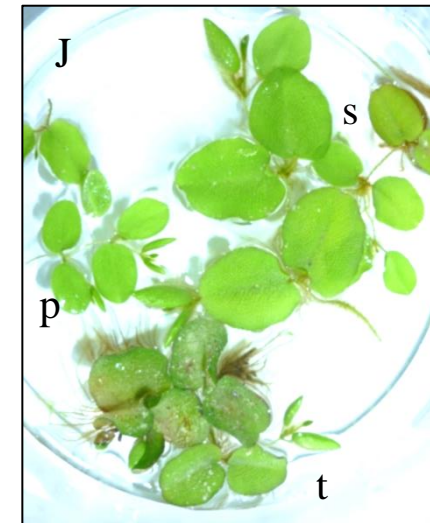
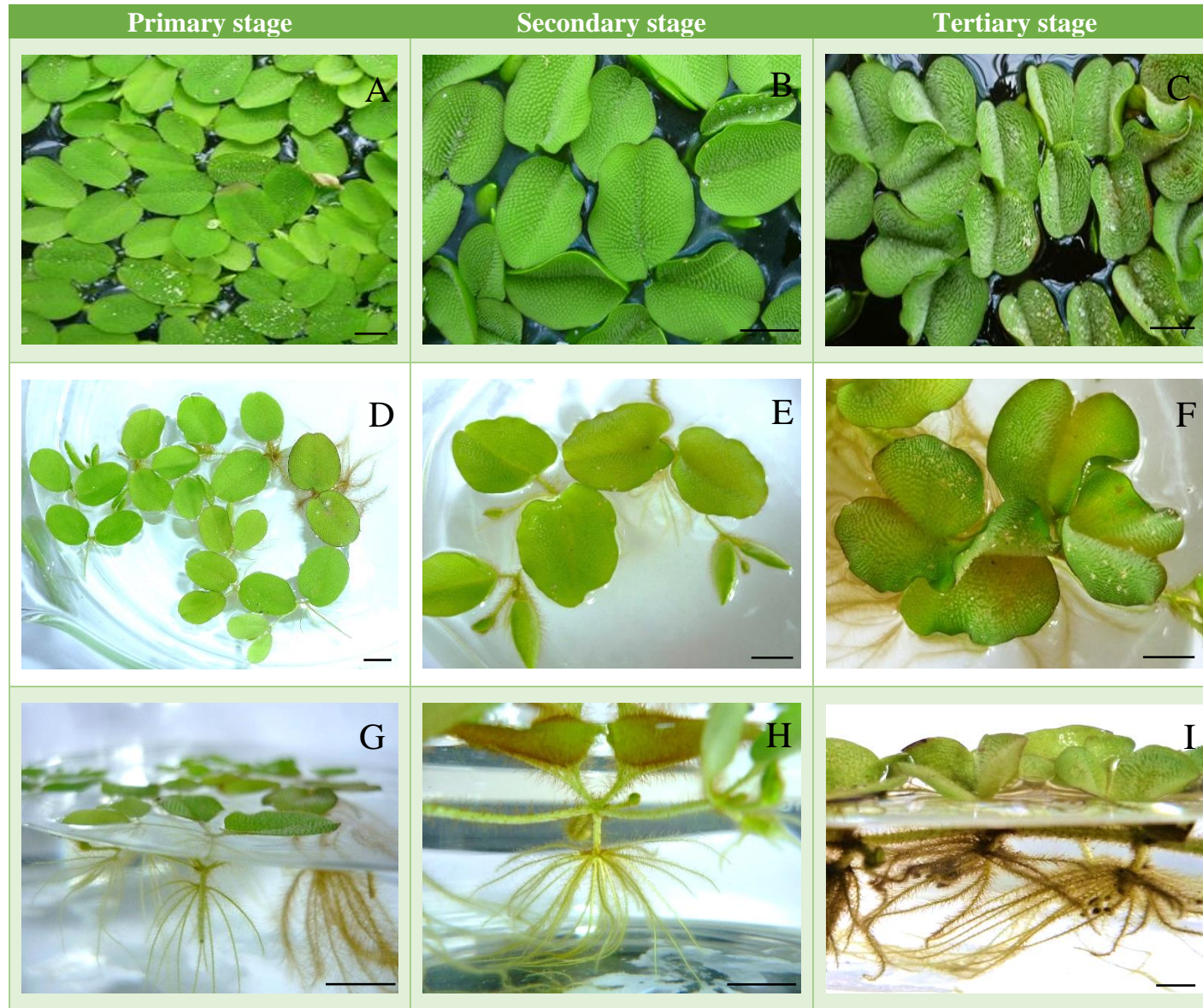


Figure 9.
Developmental stages of *Salvinia x molesta*.
A, D, G: primary stage;
B, E, H: secondary stage;
C, F, I: tertiary stage;
J: primary (p), secondary (s),
tertiary (t) stage.
Images by K. Mueller.

Scales bar \cong 1 cm.

Identification of *Salvinia x molesta*:

Due to the close growing location of *Salvinia x molesta* to another *Salvinia* species, *Salvinia natans*, the close relationship of the *Salvinia* species belonging to the *Salvinia-auriculata*-complex and the morphological special characteristics of these floating ferns, this species was identified (Fig. 10A-J).

The investigated species consists of two floating fronds and one water frond, which arise from the node on the horizontal shoot axis (Fig. 10D,G). The roots are absent.

The sorophores are embedded in the water frond and are arranged in spikes with an egg-shaped sori (Fig. 10F). The sporangia contained therein are hollow (Fig. 10H-J).

The shoot axis, the underside of the floating fronds, the water fronds and the sorophores bear multicellular simple hairs (Fig. 10E).

The floating fronds show whisk-like hairs on the upside. These consist of a protruding papilla bearing four trichomes, which in turn are stuck together at the tip (Fig. 10A-C).

Two identification keys (described in Mitchell & Thomas, 1972; Miranda & Schwartzburd, 2019) were used to determine the three species of the *Salvinia-auriculata*-complex.

The fronds of these *Salvinia* species are very similar and differ only in size in the tertiary stage or in the length of the incision on the middle lamella. However, as this is development-dependent, the structure of the sorophores and the sori were also examined, which can be used to determine major macroscopic distinguishing features.

The sorophores of *Salvinia auriculata* are umbel-shaped and the sori are globose, whereas in *Salvinia biloba*, these are arranged in racemes, but the sori are oval, as in *Salvinia x molesta*. In *Salvinia herzogii*, however, the sorophores are also arranged in spikes, as in *Salvinia x molesta*, and the sori are also oval. However, the spikes of *Salvinia herzogii* are highly constricted.

The morphological differentiation from the species *Salvinia natans*, however, is determined by the characteristic hairs on the floating fronds. These are not whisk-shaped in *Salvinia natans*. There are three to four trichomes on the top of a papilla, but these are not stuck together. This means that the plant species under investigation cannot be assigned to *Salvinia natans* (Barthlott *et al.*, 2009). Based on the morphological identification and the additional exclusion of close relatives and *Salvinia* species close to the location, the species investigated has been identified as *Salvinia x molesta*.

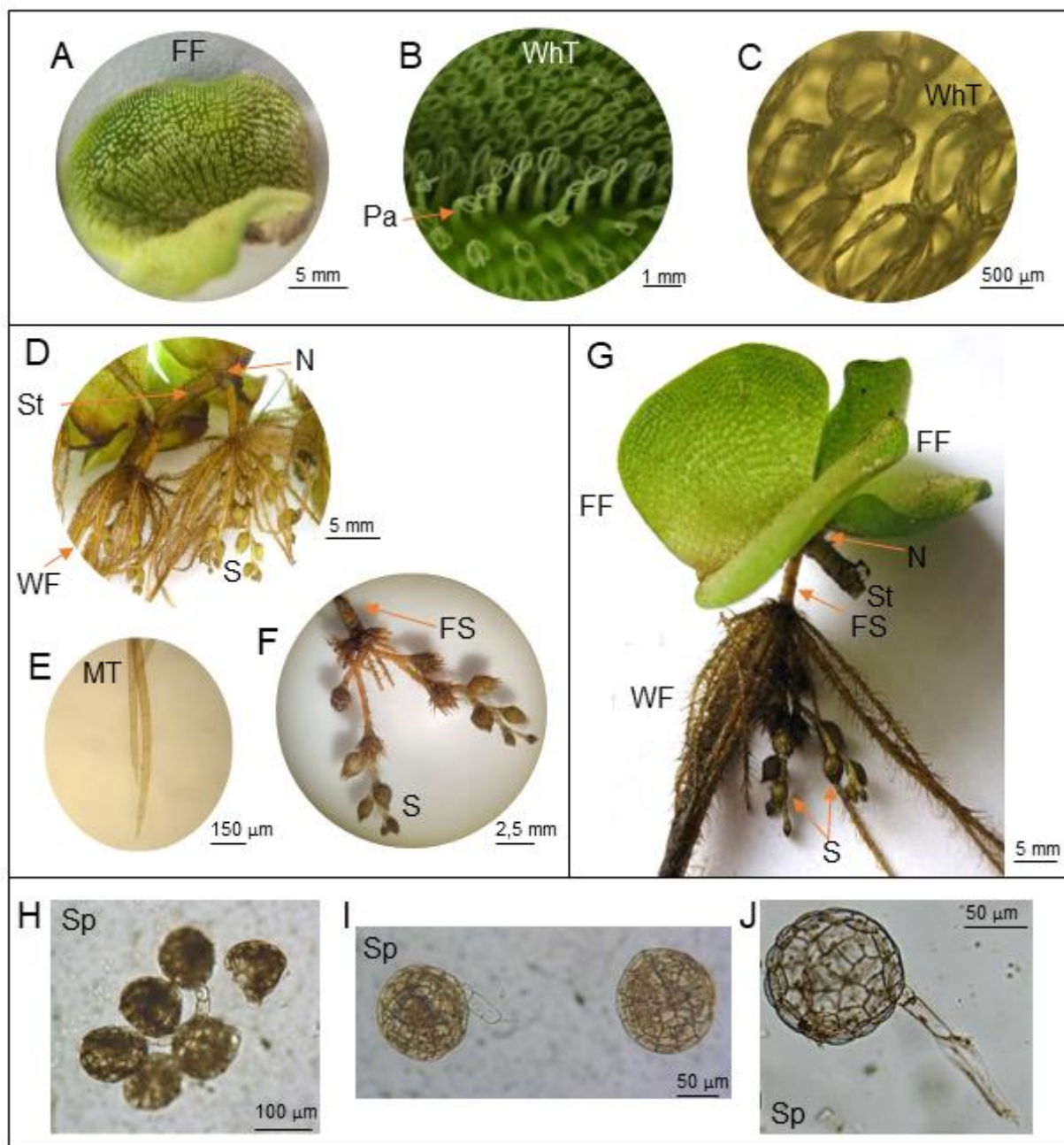


Figure 10. Identification of *Salvinia x molesta*. **A:** floating fronds with whisk-shaped trichomes; **B, C:** whisk-shaped trichomes; **D:** submerged organs; **E:** multicellular trichomes of the water frond; **F:** sorophores; **G:** plant individuum; **H, I, J:** sporangia; N: node; MT: multicellular trichomes; Pa: papilla; S: sorophores; St: Stem; Sp: Sporangium/Sporangia; WhT whisk-shaped trichomes; FF: floating fronds; WF: water frond; FS: frond stalks. Images by K. Mueller.

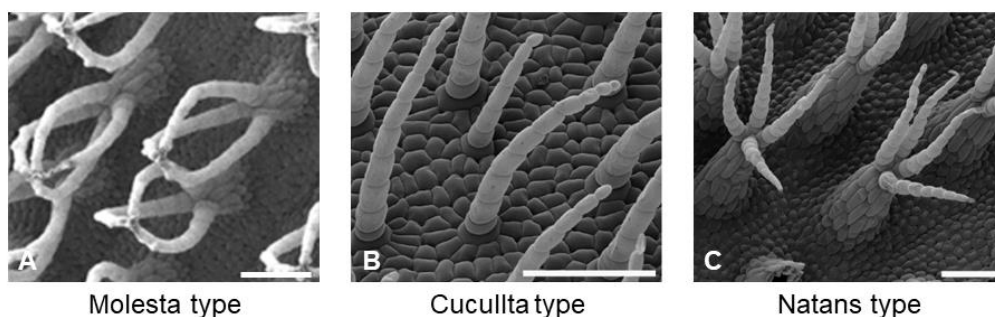


Figure 11. Electron micrographs of three trichome types of *Salvinia*, assigned to the investigated *Salvinia* species (according to Barthlott *et al.*, 2009 and Gomez *et al.*, 2023). **A:** Image of *S. auriculata*. **B:** Image of *S. cucullata*. **C:** Image of *S. minima*. Scales bar \triangleq 200 μ m.

The floating ferns *Salvinia auriculata* AUBL., *Salvinia cucullata* ROXB. and *Salvinia natans* (L.) ALL. also belong to the Salviniaceae.

Salvinia auriculata is originally from Central and South America, especially Brazil. *Salvinia cucullata* is also found in Brazil, as it was imported from its native India and cultivated there. *Salvinia natans*, on the other hand, is widespread in Europe, including Germany, and East Asia (Herzog, 1934; Miranda & Schwartzburd, 2016; 2019).

The basic structure of the three other *Salvinia* species corresponds to that of *Salvinia x molesta*: each fern consists of a horizontal shoot axis, which is linked to two floating fronds and a dissected water frond at each node. Also here, the water frond replaces the role and function of the root, as these are also absent (Miranda & Schwartzburd, 2019).

However, there are differences in macroscopic features. The floating fronds of *Salvinia auriculata* are heart-shaped at the base and slightly emarginated at the tip. These can get up to 3 cm long. There are adaxially fouet-like hairs, which are typical of the *Salvinia-auriculata*-complex (Fig. 11A), and abaxially simple hairs. The sorophores are arranged in umbels and the sori are globose. (Miranda & Schwartzburd, 2016).

In *Salvinia cucullata*, the floating fronds only reach a length of up to 1 cm. These fronds are rounded at the tip and truncate at the base. The hair system on the upper side of the frond consists of only one hair on the papilla (Fig. 11B). The underside is bare. *Salvinia cucullata* lacks sorophores and thus also the sori (Miranda & Schwartzburd, 2019).

The floating fronds of *Salvinia natans*, in contrast, are spread out flat on the water surface, truncate at the tip with a length up to 1.4 cm. On the upper side of the frond, there are hump-shaped papillae, each with three to four hairs, which are free at the tip (Fig. 11C). Abaxially, the fronds are covered with simple hairs. The sorophores each bear 3 - 8 globular sori (Herzog, 1934; Barthlott *et al.*, 2009).

Ceratopteris richardii



Figure 12. *Ceratopteris richardii* individuals. **A:** Fertile stage. **B:** Buds on a withered frond. **C:** Development of a sterile to a fertile stage (Mueller *et al.*, 2023). Images A and B by K. Mueller. Scales bar \triangleq 1.0 cm.

Ceratopteris richardii BRONGN. is a species of the genus *Ceratopteris* and belongs to the family Pteridaceae (Fig. 12A-C). The annual fern is native to the Caribbean and West Africa, in tropical to subtropical areas. It grows in both aquatic and semi-aquatic habitats, such as rivers or rice fields (Hickok *et al.*, 1995; Banks, 1999; Kinosian & Wolf, 2022).

The phenotype of *Ceratopteris richardii* is characterized by roots, a short rhizome, a shoot axis, and fronds (Leroux *et al.*, 2013a). The fronds differ considerably in the sterile and fertile state (Fig. 12A,C). While in the sterile stage the fronds are delta-shaped to ovate-lanceolate and with dissected pinnae, the fertile fronds only have this frond structure in the bottom area. During development, these transform into a linear to lanceolate, unpaired pinnate frond with rolled margins. These enclose the sporangia, which form a false indusium. The sori are absent. The number of spores per sporangium is 16, which is atypical for leptosporangiate ferns with 64 spores (Lloyd, 1974, Hickok *et al.*, 1995, Kinosian & Wolf, 2022).

In addition, *Ceratopteris* can reproduce vegetatively by forming buds in the axils of the pinnae (Figure 12B). These fronds often wither (Hickok *et al.*, 1995).

Besides the use of *Ceratopteris* as an aquarium plant or as food in Southeast Asian countries, *Ceratopteris* gained the greatest popularity as a model organism for studying various biological processes as the so-called "C-Fern" (Hickok *et al.*, 1995; Banks, 1999).

Advantages as a model organism are the short life cycle of about 120 days, the simple cultivation in the laboratory or greenhouse, the abundant spore production and the fact that the sporophyte and the gametophyte are independent of each other and viable and both generations can thus be studied separately (Hickok *et al.*, 1987).

Thus, *Ceratopteris* is ideal for biological studies, such as developmental biology and sex determination, apogamy, hybridization, reproductive barriers and genetic and transgenic studies (Kinosian & Wolf, 2022). These studies will be supported by elucidation of the *Ceratopteris* genome (Marchant *et al.*, 2022).

Aim of this Work

More than 500 mya ago, the common ancestor of all land plants colonised land. During this process, abiotic and biotic stressors affected this ancestor, resulting in essential adaptations to the new habitat. This also involved changes in the cell wall.

While the cell wall structure and its components of seed plants have been extensively studied and characterized, knowledge on the cell wall composition of algae and spore-producing plants is still limited.

In order to fill this gap, this work analyses the cell walls of streptophyte algae, bryophytes and ferns in the evolutionary context. Thereby, the occurrence and evolutionary development of unusual methylated monosaccharides in polysaccharides of cell walls of algae and spore-producing plants is of special interest. In addition to polysaccharides, the cell wall also consists of glycoproteins, like arabinogalactan-proteins (AGPs). The presence of AGPs in algae was previously only demonstrated *via* antibody binding to epitopes of the polysaccharide moiety with the disadvantage of possible cross-reactivities of these antibodies. To date, isolation of an AGP-like molecule was only successful from one streptophyte alga and detected an altered rhamnogalactan-protein (Pfeifer *et al.*, 2022).

In addition, no AGP has ever been isolated from a hornwort, thus this and the comparison with moss and liverwort AGPs provide further insights into the evolution of AGPs.

These investigations have been completed by AGP isolation and characterization from cell walls of different ferns. To elucidate differences in the fine structure, a eusporangiate fern was analysed besides leptosporangiate ferns. Furthermore, aquatic ferns and a semi-aquatic fern were used to compare the isolated AGPs with previously isolated AGPs from terrestrial ferns. For additional information about the cell wall of the latest common ancestor of all land plants, it is essential to study the cell wall of algae as well as those of land plants. Thus, this work contributes to a clearer picture of the cell wall composition before and after colonisation of land, thus supporting the understanding of cell wall evolution.

Furthermore, the decoding of cell wall modifications caused by adaptations of the aquatic habitat to extreme dry environments provides knowledge how plants might adapt to drought that will accompany climate change through targeted genetic cell wall modifications.

Results and Contributions

This chapter summarises the results of the work in form of published research paper (1. & 5.), unpublished research paper in preparation (3. & 4.) and a published review (2.). The published paper of the subchapters 1. and 5. are adapted to the design of this work.

General contributions can be found within the paper subchapter. The focus here is primarily on the personal contribution according to the Doctoral Degree Regulation of the Faculty of Mathematics and Natural Sciences and the Faculty of Engineering (§8 (2), PromO MNF und TF 2018):

1. ¹Pfeifer, L., ¹Mueller, K.-K., Utermöhlen, J., Erdt, F., Zehge, J. B. J., Schubert, H., Classen, B. (2023) The cell walls of different *Chara* species are characterized by branched galactans rich in 3-*O*-methylgalactose and absence of AGPs. *Physiologia Plantarum*, 175:e13989.

doi: 10.1111/ppl.13989

¹shared first authorship

Contribution: BC and LP planned and designed the research with assistance of KM. KM performed extractions, carbohydrate and ELISA experiments; KM and LP instructed and assisted FE in the analytical work as part of her master thesis; KM analysed the data with the help of BC, LP and FE, except of the bioinformatic search (performed and analysed by LP). BC, KM and LP wrote and edited the draft manuscript; KM and LP created all figures and tables.

2. Pfeifer, L., Mueller, K.-K., Classen, B. (2022) The cell wall of hornworts and liverworts: innovations in early land plant evolution? *Journal of Experimental Botany*, **73**, 4454–4472. doi: 10.1093/jxb/erac157

Contribution: BC, KM and LP planned and designed the review. All authors performed literature research and evaluation. The manuscript was drafted and edited by all authors equally. LP created all Figures, KM all Tables.

3. **Mueller, K.-K. & Classen, B.** (2023) The model organisms *Anthoceros agrestis* and *Physcomitrium patens*: Insights into their cell walls and arabinogalactan-proteins.
Paper unpublished, in preparation

Contribution: BC and KM planned and designed the research. KM performed all experiments and created all figures and tables. All authors analysed the data. KM wrote the draft manuscript with the help of BC. BC and KM revised the manuscript and approved the final manuscript.

4. **Mueller, K.-K., Pfeifer, L., Schuldt, L., Classen, B.** (2023) Sequential extraction of fern cell walls and characterization of arabinogalactan-proteins from the “living fossil” *Psilotum nudum*.
Paper unpublished, in preparation

Contribution: BC, KM and LP planned and designed the research. KM, LP and LS cultivated the plant material. KM performed the extractions and the carbohydrate experiments of *Salvinia*, *Ceratopteris*, and *Psilotum* (with the help of LP) as well as the ELISA experiment. KM created all main text figures with the help of LP (Figure 1). All authors analysed the data. KM and BC wrote and edited the draft manuscript.

5. **¹Mueller, K.-K., ¹Pfeifer, L., Schuldt, L., Szövényi, P., de Vries, S., de Vries, J., Johnson, K. L., Classen, B.** (2023) Fern cell walls and the evolution of arabinogalactan proteins in streptophytes. *The Plant Journal*, **114**, 875–894.
doi: 10.1111/tpj.16178
¹shared first authorship

Contribution: BC and LP planned and designed the research with the help of KM. KM, LP, and LS cultivated the plant material and performed the extractions as well as the carbohydrate and the ELISA experiment. KM prepared all main text tables. LP created all main text figures with the help of KM (Figure 1 & 2). All authors analysed the data (KM, LS and LP: carbohydrate analysis). BC wrote the draft manuscript with the help of KM and LP. All authors revised the manuscript.

1. The cell walls of different *Chara* species are characterized by branched galactans rich in 3-*O*-methylgalactose and absence of AGPs

Lukas Pfeifer^{1,†}, Kim-Kristine Mueller^{1,†}, Jon Utermöhlen¹, Felicitas Erdt¹, Jean Bastian Just Zehge¹, Hendrik Schubert² and Birgit Classen¹

¹Pharmaceutical Institute, Department of Pharmaceutical Biology, Christian-Albrechts-University of Kiel, 24118 Kiel, Germany

²Aquatic Ecology, Institute of Biosciences, University of Rostock, 18059 Rostock, Germany

[†]Authors contributed equally to the publication.

ABSTRACT

Streptophyte algae are the closest relatives to land plants; their latest common ancestor performed the most drastic adaptation in plant evolution around 500 million years ago: the conquest of land. Besides other adaptations, this step required changes in cell wall composition. Current knowledge on the cell walls of streptophyte algae and especially on the presence of arabinogalactan-proteins (AGPs), important signaling molecules in all land plants, is limited. To get deeper insights into the cell walls of streptophyte algae, especially in Charophyceae, we performed sequential cell wall extractions of four *Chara* species. The three species *Chara globularis*, *Chara subspinoso* and *Chara tomentosa* revealed comparable cell wall compositions, with pectins, xylans and xyloglucans, whereas *Chara aspera* stood out with higher amounts of uronic acids in the pectic fractions and lack of reactivity with antibodies binding to xylan- and xyloglucan epitopes. Search for AGPs in the four *Chara* species and in *Nitellopsis obtusa* revealed the presence of galactans with pyranosidic galactose in 1,3-, 1,6- and 1,3,6-linkage, which are typical galactan motifs in land plant AGPs. A unique feature of these branched galactans was high portions of 3-*O*-methylgalactose. Only *Nitellopsis* contained substantial amounts of arabinose. A bioinformatic search for prolyl-4-hydroxylases, involved in the biosynthesis of AGPs, revealed one possible functional sequence in the genome of *Chara braunii*, but no hydroxyproline could be detected in the four *Chara* species or in *Nitellopsis obtusa*. We conclude that AGPs that is typical for land plants are absent, at least in these members of the Charophyceae.

INTRODUCTION

More than 500 million years ago (mya), one of the most significant events for life on Earth occurred: plant terrestrialization (Domozych & Bagdan, 2022). Land plants (bryophytes, lycophytes, ferns, gymnosperms, and angiosperms) descended from a common algal ancestor that would be classified (if alive today) as a member of the streptophyte algae (Bowman, 2022). Extant streptophyte algae are divided into two grades: the lower-branching KCM-grade (Klebsormidiophyceae, Chlorokybophyceae and Mesostigmatophyceae) and the higher-branching ZCC-grade (Zygnematophyceae, Coleochaetophyceae and Charophyceae; de Vries & Archibald, 2018). The genus *Chara* is an important part of the natural aquatic ecosystems, commonly beneficial to lakes and ponds by providing food and cover to wildlife (DiTomaso & Kyser *et al.*, 2013). Due to the morphological complexity of the Charophyceae, it was first assumed that these streptophyte algae were the closest relatives of extant land plants (Domozych & Bagdan, 2022). However, recent phylogenomic studies have shown that land plants evolved from algal ancestors most closely related to extant Zygnematophyceae (Domozych & Bagdan, 2022; Leebens-Mack *et al.*, 2019; Wickett *et al.*, 2014). This group of streptophyte algae is further classified in a recently proposed five-order system of Desmidiales, Spirogyrales, Zygnematales, Serritaeniales and Spirogloales (Hess *et al.*, 2022).

To cope with life on land, the terrestrial algal species had to adapt to enormous changes in the environment, such as UV radiation and drought. This also meant that the cell wall needed to adapt by changing its composition (Harholt *et al.*, 2016). The plant cell wall is generally a highly dynamic system consisting mainly of polysaccharides and cell wall proteins. It has many essential functions, such as mechanical stability and protection against abiotic and biotic stressors (Silva *et al.*, 2020). The main polysaccharides of spermatophyte cell walls include cellulose, pectins, hemicelluloses and lignin. Hemicelluloses are cross-linked in a highly branched network of cellulose microfibrils, which are embedded in a matrix of pectins (Sørensen *et al.*, 2011). Important cell wall proteins are hydroxyproline-rich glycoproteins (HRGPs). These comprise arabinogalactan-proteins (AGPs), proline-rich proteins (PRPs) and extensins (EXT; Johnson *et al.*, 2018), differing mainly in their carbohydrate moiety. While the glycan part is about 90% in AGPs, it is about 50% in EXT. In PRPs, the protein part is only marginally glycosylated (Johnson *et al.*, 2018).

The AG moiety of AGPs consists of arabinogalactans type II (AG II) with a (1→3)-β-D-galactan core structure carrying (1→6)-β-D-galactan side chains at position O-6. These side chains are decorated with α-L-Araf and other monosaccharides, like L-Rha, L-Fuc or D-GlcAp (Kitazawa *et al.*, 2013). AGs in AGPs are covalently linked to the protein moiety *via*

hydroxyproline (Hyp). The hydroxylation of Pro to Hyp is post-translationally catalyzed by prolyl-4-hydroxylase (P4H; Seifert *et al.*, 2021).

Additionally, a glycosylphosphatidylinositol (GPI)-anchor can be attached at the C-terminal side, which connects the AGP to the plasma membrane (Silva *et al.*, 2020). There are descriptions of AGPs as periplasmic calcium capacitors proposing AGPs as being important partners in calcium signalling (Lamport and Várnai, 2013; Lamport, 2023). Even if it is not yet fully explained how the signal transmission of AGPs takes place, the periplasmic localization facilitates this process. AGPs of seed plants show many diverse functions, which include cell growth, pattern formation, salt- and drought-tolerance, cell-cell communication or adhesiveness (for review, see Ma *et al.*, 2018; Mareri *et al.*, 2018; Leszczuk *et al.*, 2023; Seifert & Roberts, 2007). Because of these functions, AGPs are ideal candidates for molecules that are essential for life on land and may, therefore, have evolved in the last common ancestor of all streptophytes. Ferns and bryophyte have the same general AGP structure as known from seed plants, but shows unique variations in the carbohydrate part, e.g. the presence of 3-*O*-methylrhamnose as terminal monosaccharide (Bartels *et al.*, 2017; Bartels & Classen, 2017; Fu *et al.*, 2007; Mueller *et al.*, 2023). Whether AGPs (i.e. typical protein backbones with typical glycosylation) are present in the different algae lineages is still questionable. Based on bioinformatics screenings of transcriptomes, protein backbones of AGPs have been identified in brown, red and green algae (Johnson *et al.*, 2017a). Furthermore, AGP glycan epitopes have been detected by monoclonal antibodies in brown (Hervé *et al.* 2016; Raimundo *et al.*, 2016) and green algae, including some streptophyte algae (Eder *et al.*, 2008; Estevez *et al.*, 2008; Estevez *et al.*, 2009; Domozych *et al.*, 2009; Palacio-López *et al.*, 2019; Permann *et al.*, 2021a, 2021b; Přerovská *et al.*, 2021; Ruiz-May *et al.*, 2018; Sørensen *et al.*, 2011). Nevertheless, it remains open whether epitopes are linked to the characteristic protein backbones.

To the best of our knowledge, no AGPs similar to the ones in land plants have been isolated from streptophyte algae to date. Closely related rhamnogalactan-proteins (RGPs) are present in the cell walls of *Spirogyra pratensis*, a member of the Zygnematophyceae (Pfeifer *et al.*, 2022). These RGPs reveal typical AGP features like a Hyp-rich protein moiety covalently bound to 1,3-, 1,6- and 1,3,6-linked galactans and the ability to precipitate with Yariv's reagent. Interestingly, there is a nearly complete replacement of arabinose by rhamnose at the periphery of these RGPs, leading to a less hydrophilic surface, which may be connected with different functions in the freshwater habitat (Pfeifer *et al.*, 2022). To continue the search for evolutionary roots of AGPs or AGP-like molecules in streptophytes, we searched for these glycoproteins in four *Chara* species (Charophyceae). As hydroxylation of proline is the basis for *O*-glycosidic linkage between protein- and carbohydrate moiety in AGPs, we also performed a bioinformatic

search for P4Hs. The work is complemented by sequential extraction of *Chara* cell walls to get insights into the general cell wall polysaccharide composition of this genus. The results broaden our general understanding of cell walls of the higher branching streptophyte algae and further enlighten the process of cell wall evolution from algae to land plants.

RESULTS

Sequential extraction of polysaccharide fractions from *Chara* spp. cell walls

We examined four *Chara* species to investigate their cell wall compositions. Sequential extraction of the plant material with water (AE), ammonium-oxalate ($[\text{NH}_4]_2\text{C}_2\text{O}_4$) and hydrochloric acid (HCl), as well as sodium carbonate (Na_2CO_3) and potassium hydroxide (KOH), resulted in a water-soluble, two pectic and two hemicellulosic fractions. The yields of the different fractions varied between 0.2% and 21.2% of the dry plant material (Table S2). The high yield of the $(\text{NH}_4)_2\text{C}_2\text{O}_4$ fraction of *Chara aspera* (21.2%) was striking and indicated huge amounts of pectins in this species.

Pectic fractions of *Chara* spp. cell walls

The monosaccharide compositions of the pectic fractions are shown in Tables 1, S3A and S3B and Figure 1. As expected, the two pectic fractions showed the highest amounts of uronic acids. In the $(\text{NH}_4)_2\text{C}_2\text{O}_4$ fractions, the content reached 33% to 60% of the dry fraction material and decreased in the HCl fractions of all investigated *Chara* spp. (Table 1). In contrast to the other *Chara* species, the uronic acid content in *C. aspera* was the highest, with over 60% in the $(\text{NH}_4)_2\text{C}_2\text{O}_4$ and almost 40% in the HCl fraction. The dominant neutral monosaccharide in both fractions was Glc, with 25 to 66% (Tables S3A and S3B). In the HCl fractions, the content was approximately doubled in *C. globularis* and *C. subspinoso* compared to the corresponding $(\text{NH}_4)_2\text{C}_2\text{O}_4$ fractions. It cannot be excluded that at least part of the Glc derived from coextracted starch. Other monosaccharides, like Rha, Gal and Ara present in rhamnogalacturonan-I (RG-I) or Xyl part of xylogalacturonan (XG), were also detected in these fractions. High amounts of Xyl, especially in *C. tomentosa* and substantial amounts of Fuc and Man in all fractions indicate that further polysaccharides besides pectins are present in these fractions. A very unusual feature, present mainly in the $(\text{NH}_4)_2\text{C}_2\text{O}_4$ fractions, is 3-*O*-MeGal, especially prominent in *C. aspera*.

To confirm the presence of pectins, the antibody LM19 raised against unesterified HG epitopes (Verhertbruggen *et al.*, 2009b) was tested for binding affinity to the $(\text{NH}_4)_2\text{C}_2\text{O}_4$ fractions (Figure 1), which revealed comparable amounts of unesterified HG in all *Chara* species. The

antibody INRA-RU2, which recognizes the RG-I backbone (Ralet *et al.*, 2010) showed no affinity to the $(\text{NH}_4)_2\text{C}_2\text{O}_4$ and the AE-AP fractions of all *Chara* species (Figure S2).

Table 1. Colorimetric determination of the content of uronic acids in the different cell wall fractions from different *Chara* species in % (w w⁻¹).

	<i>C. aspera</i>	<i>C. globularis</i>	<i>C. subspinoso</i>	<i>C. tomentosa</i>
AE	5.8	3.4	3.6	4.2
$(\text{NH}_4)_2\text{C}_2\text{O}_4$	60.6 ± 1.7	33.1 ± 1.2	50.9 ± 2.5	42.8 ± 4.1
HCl	39.4 ± 8.5	7.1	8.2	11.3
Na_2CO_3	7.6	4.8	6.3	10.0
KOH	6.0	7.1	5.3	6.1

Hemicellulosic fractions of *Chara* spp. cell walls

Glc was dominating the sodium carbonate fractions (Table S3C) with 59% to 80%. All other monosaccharides were present in amounts less than 10% (except 12.7% Xyl in *C. tomentosa*), indicating the occurrence of mainly glucans in these fractions.

The KOH fractions (Table S3d) was dominated by Xyl and Glc, accompanied by Man. In all species, Xyl and Glc accounted for a minimal of 80% of the neutral monosaccharides, while the ratio of Xyl: Glc varied. Again, *C. aspera* was stood out, with a very low Xyl content in this fraction. The occurrence of xylan and xyloglucan was supported by ELISA with the antibodies LM10 and LM15. These antibodies detect the epitopes of the non-reducing end of (1→4)-β-D-xylan (LM10; McCartney *et al.*, 2005; Ruprecht *et al.*, 2017), as well as the XXXG-motif of xyloglucan (LM15; Marcus *et al.*, 2008; Pedersen *et al.*, 2012). The highest absorption with both antibodies was detectable in *C. globularis*, followed by *C. tomentosa* and *C. subspinoso*. *C. aspera* revealed no binding to one of these antibodies.

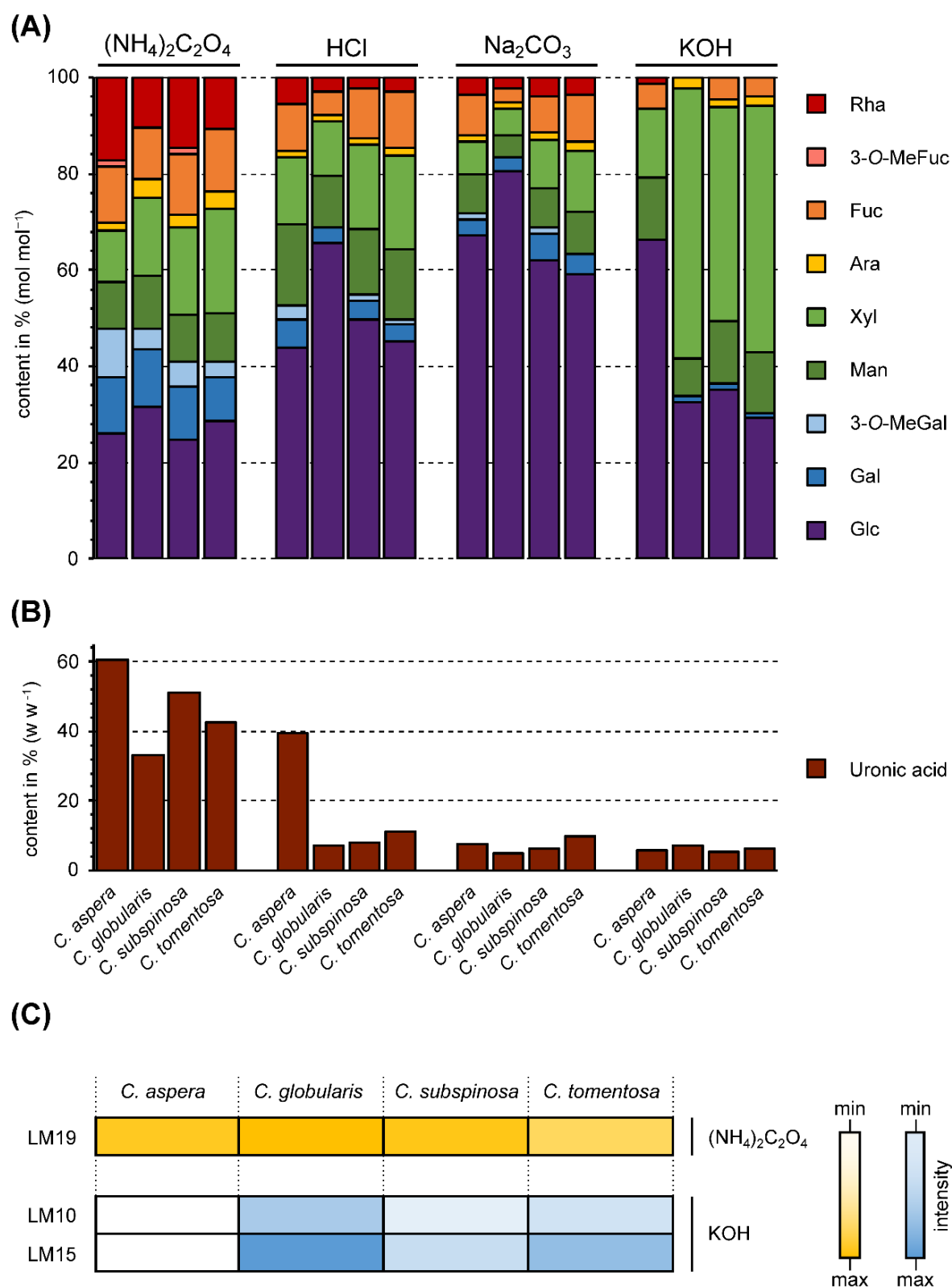


Figure 1. Monosaccharide composition of different cell wall fractions ($(\text{NH}_4)_2\text{C}_2\text{O}_4$, HCl, Na_2CO_3 , KOH) from the streptophyte algae *C. aspera*, *C. globularis*, *C. subspinoso* and *C. tomentosa*. (a) Relative neutral monosaccharide composition determined by gas chromatography (GC; % mol mol⁻¹). (b) Absolute content of uronic acids determined by colorimetric assay (w w⁻¹ of dry fraction weight). (c) Reactivity of *Chara* spp. fractions with antibodies via ELISA after 40 min in the concentration 12.5 $\mu\text{g ml}^{-1}$ ($(\text{NH}_4)_2\text{C}_2\text{O}_4$: LM19; KOH: LM10, LM15).

Search for AGPs in *Chara* spp. cell walls

Water-soluble polysaccharides were precipitated with ethanol 80% (AE) and consisted mainly of Gal (including 3-*O*-MeGal) and Glc (Table S4A). The amounts of uronic acids in AE were quantified photometrically and varied between 3.4% and 5.8% (Table 1). In preliminary experiments, precipitation of AE with Yariv's reagent yielded no AGP-like monosaccharide composition. The precipitate was had a similar composition as AE, with only a slight increase in Gal content (data not shown). Therefore, we used enzymatic treatments to purify putative AGPs, which might be present in AE in very minor amounts. As starch and some pectins might have been coextracted with these AGP-like galactan structures, we treated AE fractions with α -amylase and pectinase, precipitated the remaining polysaccharides with ethanol 80% and dialyzed the precipitates to remove residual mono- or oligosaccharides (Table S4B). These treatments led to a decrease in Glc and an increase in Gal content in all species (compare Tables S4A and S4B). Comparable to the $(\text{NH}_4)_2\text{C}_2\text{O}_4$ fraction, the highest amount of 3-*O*-MeGal, with 19.3%, was found in *C. aspera*. The monosaccharides Rha, Fuc, Xyl and Man were distributed in quite similar quantities, between 7.5% – 16.5%, in all investigated *Chara* species, whereas the amounts of Ara were relatively low (2.2% – 4.0%). Compared to the different *Chara* species, *N. obtusa* was richer in Rha and Ara. To detect uronic acids, samples were carboxy-reduced by the use of sodium borodeuteride. There were only slight increases in Gal and Glc (compare Tables S4B and 2). The mass spectra showed deuterated fragments deriving from GlcA and, to a lesser extent, from GalA.

Table 2. Neutral monosaccharide composition of dialyzed water-soluble polysaccharides, pre-treated with amylase and pectinase after reduction of uronic acids (AE_AP_UR), from different *Chara* species and *Nitellopsis obtusa* in % (mol mol⁻¹; tr: trace value < 1%).

Neutral mono-saccharide	<i>C. aspera</i> AE_AP_UR n=3	<i>C. globularis</i> AE_AP_UR n=3	<i>C. subspinosa</i> AE_AP_UR n=3	<i>C. tomentosa</i> AE_AP_UR n=3	<i>N. obtusa</i> AE _{purified} _AP_UR n=3
Rha	12.6 ± 0.1	10.7 ± 0.2	13.7 ± 0.2	10.0 ± 0.2	18.6 ± 0.3
3- <i>O</i> -MeFuc	-	-	1.9 ± 0.1	-	-
Fuc	8.7 ± 0.0	14.1 ± 0.1	8.7 ± 0.2	11.6 ± 0.1	6.4 ± 0.0
Ara	2.1 ± 0.1	3.7 ± 0.1	2.3 ± 0.1	2.1 ± 0.1	14.4 ± 0.1
Xyl	6.7 ± 0.4	8.6 ± 0.1	9.7 ± 0.0	12.8 ± 0.8	5.1 ± 0.0
Man	9.0 ± 0.1	9.9 ± 0.1	10.7 ± 0.2	12.8 ± 0.2	8.0 ± 0.2
3- <i>O</i> -MeGal	21.3 ± 0.3	8.1 ± 0.2	10.1 ± 0.1	4.7 ± 0.2	2.5 ± 0.0
Gal	18.3 ± 0.2	22.4 ± 0.2	20.2 ± 0.4	16.7 ± 0.1	26.8 ± 0.0
Glc	21.3 ± 0.7	22.5 ± 0.2	22.7 ± 0.2	29.3 ± 0.4	18.2 ± 0.1

Gel diffusion assay

A typical feature of AGPs is the precipitation with Yariv phenyl glycosides, like β -D-glucosyl Yariv-reagent (β GlcY). A gel diffusion assay provides a first hint of whether AGPs are present in the sample. If AGPs are included, a red precipitation line will appear between the sample and the β GlcY (Clarke *et al.*, 1979). The water-soluble fractions (AE) of all *Chara* species showed no Yariv precipitation, but after enzymatic treatment, weak precipitation lines were observed for all *Chara* species but not for *Nitellopsis obtusa*, another member of the Charophyceae (Figure S3).

Structure elucidation

The purified aqueous extracts (AE_AP, see Material and Methods, “Isolation of cell wall fractions”) of all *Chara* species and of *N. obtusa* were subjected to linkage-type analysis (Table 3) to gain insight into the polysaccharides present. Galp as the main monosaccharide was present as terminal residue (1.3% – 4.4%), in 1,3-linkage (6.7% – 13.6%), 1,6-linkage (5.1% – 41.6%) and 1,3,6-linkage (4.5% – 13.2%). Interestingly, these are the typical Gal linkage types present in land plant AGPs. To identify the linkage types of 3-*O*-MeGal, permethylation was carried out by using IM-d₃. Mass spectra (GC-MS after acetylation) clearly revealed that some of the terminal and also 1,6-linked Galp residues are present as 3-*O*-MeGal in the non-reduced samples. Typical AGP linkage types of Araf (terminal and 1,5-linked Ara) in higher amounts were present only in *N. obtusa* AE_AP. All samples and especially that of *N. obtusa* were further characterized by high amounts of 1,4-linked Rhap, accompanied by small amounts of other linkage types of this monosaccharide. Further components of the samples were Glc/GlcA, Fuc and Xyl as terminal residues and further linkage types of desoxyhexoses (Rha and/or Fuc) and hexoses (Man and Glc). The mass spectrum of terminal Glc in the uronic acid reduced sample clearly showed additional *m/z* +2 in the primary fragments containing the original carboxyl group at C6. These deuterated fragments revealed the presence of GlcA in the native sample. The peak of 1,4-Hexp also contained small amounts of deuterated fragments, thus revealing the presence of 1,4-GalA or 1,4-GlcA (same retention time) in the native sample.

Table 3. Linkage type analysis of AE_AP from *Chara* spp. and *N. obtusa* in % (w w⁻¹, n=1).

Mono-saccharide	linkage type	<i>C. aspera</i>	<i>C. globularis</i>	<i>C. subspinoso</i>	<i>C. tomentosa</i>	<i>N. obtusa</i>
		AE_AP	AE_AP	AE_AP	AE_AP	AE_AP
Galp	1,3,6-	7.0	5.7	6.0	4.5	13.2
	1,3-	6.7	9.0	9.7	9.0	13.6
Galp/ 3-O-MeGalp	1,6-	41.6	13.9	11.1	5.1	10.0
	1-	4.2	4.4	2.8	2.7	1.3
Glc p	1,3-	1.0	4.1	3.7	5.9	2.1
	1-	5.1	7.7	8.4	11.8	2.6
Hexp	1,2,4,6-	1.8	2.8	5.0	3.6	-
	1,4,6-	-	2.4	2.2	1.7	1.1
	1,3,4-	-	3.2	2.4	4.9	1.0
	1,2,6-	-	3.4	5.0	7.5	4.3
	1,4-	3.3	7.3	6.2	6.4	4.4
	1,2-	3.1	5.2	4.7	5.5	2.1
Rhap	1,2,4-	-	1.0	tr	tr	1.0
	1,4-	15.5	9.1	12.4	10.7	19.7
	1,2-	1.4	1.8	1.4	1.5	0.0
	1-	1.9	2.3	2.6	2.2	4.0
Fucp	1-	4.4	5.8	9.3	7.2	3.4
Desoxyhexp	1,3,4-	-	3.1	tr	tr	-
	1,3-	-	1.7	1.3	1.8	1.3
Araf	1,5-	-	-	-	-	5.6
	1-	1.2	1.6	1.3	1.2	6.8
Xylp	1-	1.8	4.5	4.5	7.1	2.5

ELISA with antibodies directed against AG glycan epitopes

Four AE fractions were tested for binding affinities to the antibodies JIM13, KM1, LM2 and LM6 (Figure 2) with the aim to detect AG-glycan structures.

For JIM13 (Figure 2A), the exact epitope is still under debate. It is accepted as a typical AGP antibody, and Rha and uronic acids might be part of the epitope (Pfeifer *et al.*, 2022). The trisaccharide β -D-GlcAp-(1 \rightarrow 3)- α -D-GalAp-(1 \rightarrow 2)- α -L-Rha has been shown to bind to JIM13 (Yates *et al.*, 1996). The affinity of JIM13 to AE of all *Chara* species was strong, concentration-dependent and comparable between the species with slightly weaker binding of the AE of *C. tomentosa*.

The antibody KM1 (Figure 2B) detects (1 \rightarrow 6)- β -D-Galp units in AGs type II (Classen *et al.*, 2004; Ruprecht *et al.*, 2017). LM2 (Smallwood *et al.*, 1996, Figure 2C) recognizes (1 \rightarrow 6)- β -D-Galp units with terminal β -D-GlcAp present in AGPs (Ruprecht *et al.*, 2017) and showed moderate binding properties to AE of *C. globularis* and *C. subspinoso*, but very strong reactivity with AE of *C. aspera*. This species contains the highest amounts of 1,6-linked Gal (Table 3). In contrast, the AE of *C. tomentosa* demonstrated a weaker binding. LM6 (Figure 2D) identifies

(1→5)- α -L-Araf oligomers in arabinans or AGPs (Verhertbruggen *et al.*, 2009a). The AE of *C. tomentosa* showed weak binding to LM6, whereas the other *Chara* species showed no reactivity. Low or no affinity to this antibody is in accordance with low Ara content in the AE of these species (Table 3).

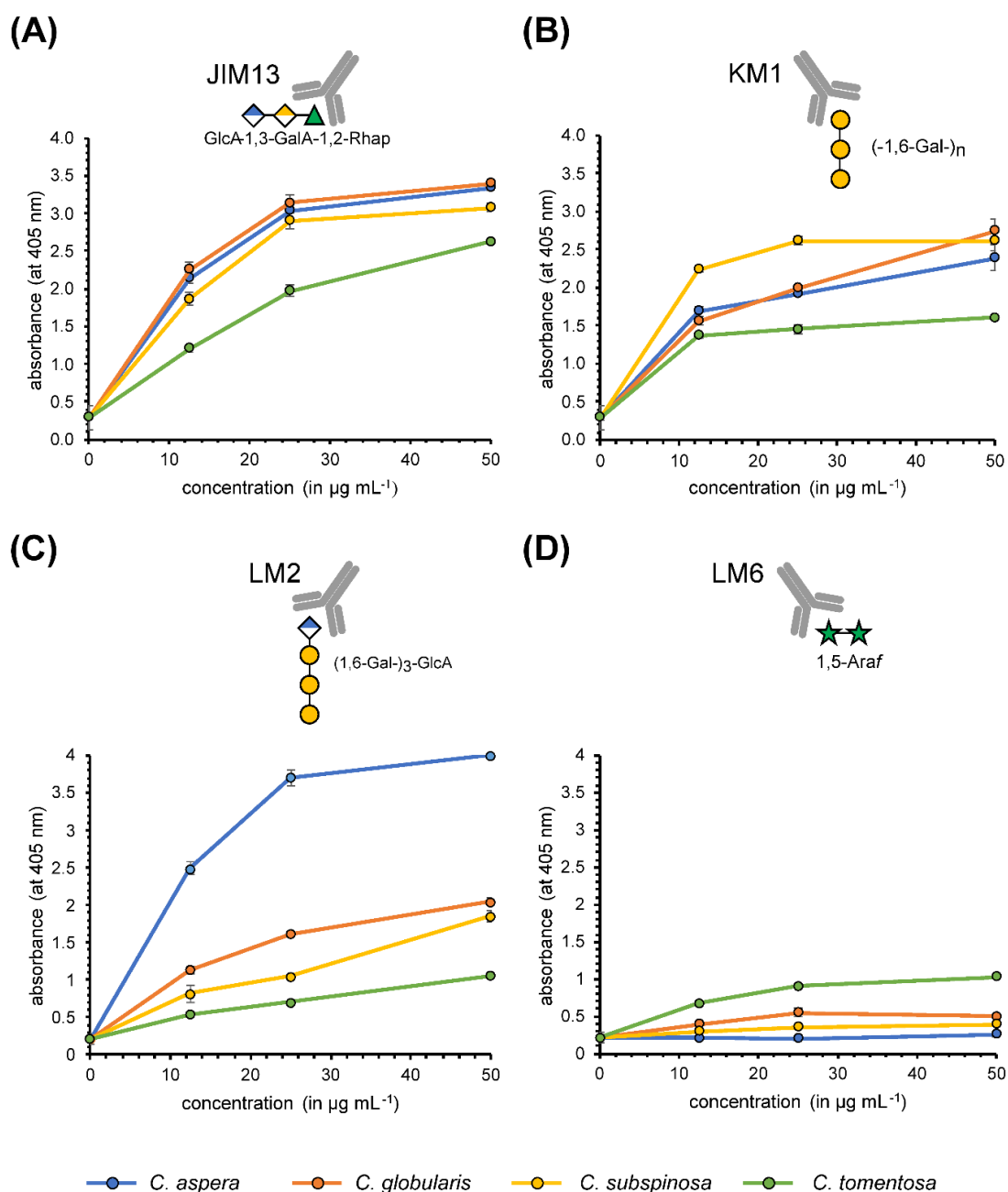


Figure 2. Reactivity of monoclonal antibodies with polysaccharide structures in AEs of different *Chara* species determined *via* ELISA. Antibodies are directed against typical AGP glycan structures, which are briefly symbolized above each diagram. (A) JIM13; (B) KM1; (C) LM2; (D) LM6. For epitopes of the antibodies, see Table S1.

Quantification of hydroxyproline

Most arabinogalactans are covalently linked to a protein backbone *via* the amino acid Hyp. According to Stegemann and Stalder (1967), the Hyp contents of all *Chara* AE samples were quantified photometrically. The results were striking, as Hyp was not detectable in any of the samples. Samples (AE) of *C. globularis*, *C. subspinosus*, *C. tomentosa* (collected in Austria), as well as from *N. obtusa*, showed no detectable Hyp. Therefore, the question of whether P4Hs are present in the genome of *C. braunii* arose.

Bioinformatic search for prolyl-4-hydroxylase

A BLAST search of the available genome data of *C. braunii* revealed the presence of seven putative P4H homologs. In a detailed analysis of the aligned sequences, the absence or presence of relevant amino acids in the oxoglutarate-binding site as well as the iron-binding region (according to Hieta & Myllyharju, 2002; Keskiäho *et al.*, 2007; Koski *et al.*, 2007; Koski *et al.*, 2009) was investigated (Table S5A and S5B; Data S1). Only in two cases, all important residues were found (GBG_70085 and GBG_85197). One of these protein sequences (GBG_70085) lacks Arg⁹³ (nomenclature based on *C. reinhardtii* P4H), which most likely leads to the complete inactivation of P4H activity (Koski *et al.*, 2007). Therefore, only one sequence (GBG_85197) was used for protein structure modelling *via* SWISS-MODEL (Figure 3).

The overlaid protein structures (Figure 3A) revealed overall matching topology in nearly all parts of the molecules but showed diverging structures in the putative substrate binding channel of *C. braunii* P4H in comparison to AtP4H1 and CrP4H (see red and green boxes in Figure 3H). Some of these structural differences (Pro instead of Asp¹⁴⁹; Tyr instead of Asn¹⁵²) are also visible in some of the P4H sequences used for comparison (AtP4H13 and NtP4H1.2). Both substrate channel regions, the β 3- β 4 loop as well as the β II- β III loop, contain flexible parts which show a low degree of alignment (Figure 3B-H) flanked with phylogenetically highly conserved amino acids.

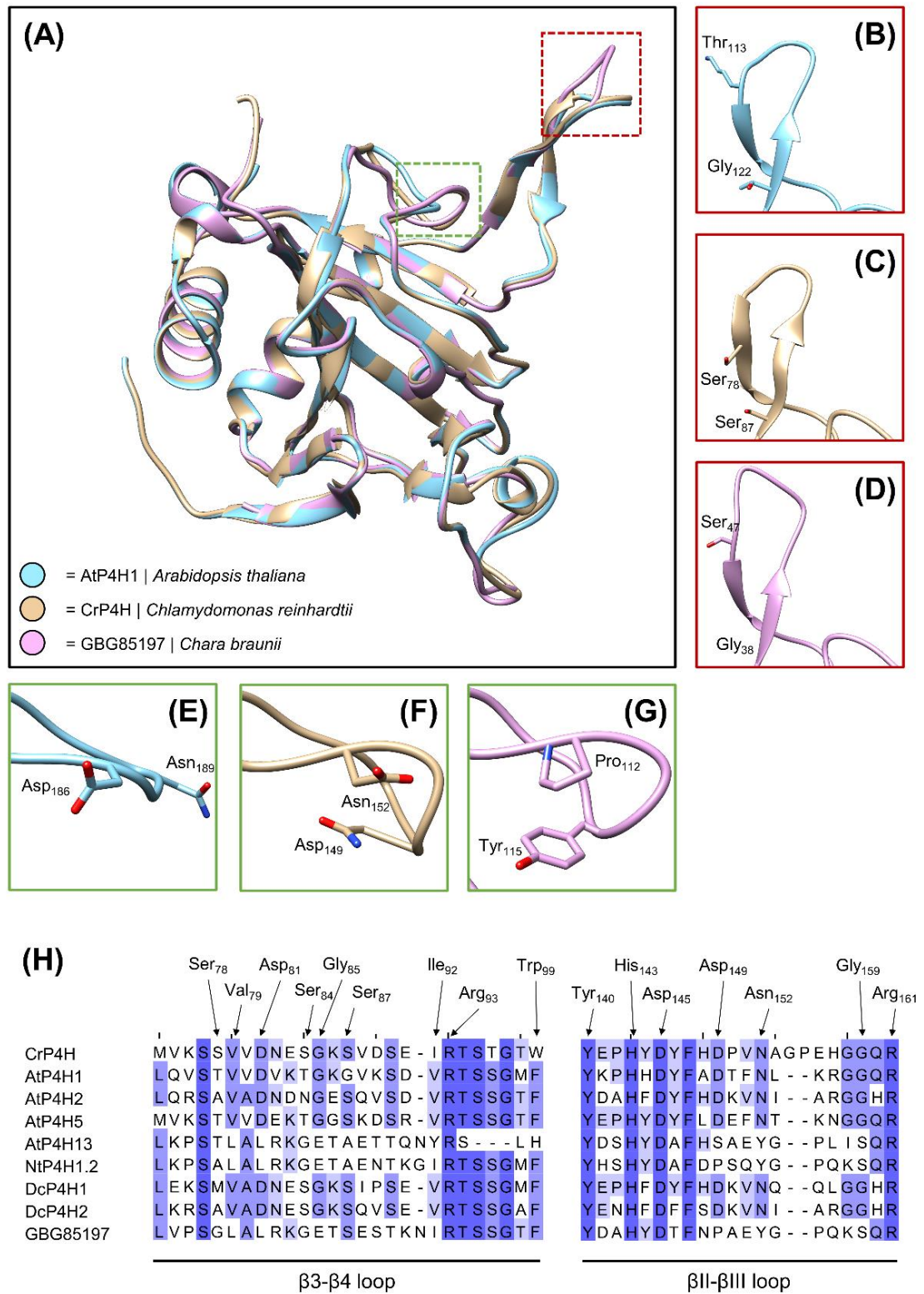


Figure 3. Modelled protein structures of *Chara braunii* prolyl-4-hydroxylase (P4H) and two functionally described P4Hs of *Arabidopsis thaliana* and *Chlamydomonas reinhardtii*. (A) Overlay of the three (modelled) structures with highlighted regions within the substrate binding tunnel (red: β3-β4 loop; green: βII-βIII loop). (B-D) Detailed comparison of the β3-β4 loop. (E-G) Detailed comparison of the βII-βIII loop. (H) Alignment of *C. braunii* P4H with functionally described P4Hs. Only the regions shown in panels A-G are presented and relevant amino acids are highlighted with boxes.

DISCUSSION

Polysaccharides of *Chara* cell walls

Although taxonomically differences in cell wall composition become more and more defined, knowledge on streptophyte algal cell walls is still limited. There is some evidence for the occurrence of nearly all seed plant polysaccharides in streptophyte algae (Domozych & Bagdan, 2022), but recent studies are often based on immunocytochemistry. This approach has limitations as epitopes of antibodies are not always clearly defined. Thus, isolation and analytical characterization of cell wall polysaccharide fractions of streptophyte algae as closest living relatives to land plants help to understand cell wall evolution during plant terrestrialization.

Pectin composition in Charales hints towards presence of (substituted) HGs, but absence of RG-I

For the isolation of pectic fractions, we used standard procedures with chelators and hot acid (Scheller & Ulvskov, 2010). The high amount of the $(\text{NH}_4)_2\text{C}_2\text{O}_4$ fraction in *C. aspera* was striking, compared to the other *Chara* species, which had astonishing low amounts. Since pectins are characterized by a high content of GalA, the high amounts of uronic acids in the two pectic fractions in all *Chara* species were not surprising, but again highest in *C. aspera* with 60% in the $(\text{NH}_4)_2\text{C}_2\text{O}_4$ and 40% in the HCl fraction. As *C. aspera* is the only investigated species which is salt tolerant (Blindow and Schütte, 2007), the involvement of pectins in adaptation to salt water is possible. An increase in pectins in response to this abiotic stress has been shown for several angiosperms (Aquino *et al.*, 2011; Corrêa-Ferreira *et al.*, 2019; Liu *et al.*, 2022). High concentrations of uronic acids were also detected in four other members of the Charophyceae, *Chara corallina*, *C. vulgaris*, *Nitella flexilis* and *N. obtusa* (O'Rourke *et al.*, 2015; Popper & Fry, 2003; Pfeifer *et al.*, 2022) as well as in *Coleochaete scutata* (Coleochaetophyceae). In contrast, the pectic fractions of *S. pratensis* (Zygnematophyceae) contained only low amounts of uronic acids (Pfeifer *et al.*, 2022) and those of two *Klebsormidium* species (Klebsormidiaceae) were completely free of GalA and also GlcA (O'Rourke *et al.*, 2015), thus revealing strong differences in the composition of the pectic fractions of streptophyte cell walls.

Pectins, mainly consisting of non-esterified GalA, have been purified from *Nitella translucens* and *Chara australis* (Anderson & King, 1961a, 1961b). Immunocytochemistry with antibodies directed against HG (LM19, LM20, JIM5, JIM7, 2F4) supported the presence of this pectic polysaccharide in many members of streptophyte algae (Proseus & Boyer, 2006; Eder & Lütz-Meindl, 2008, 2010; Domozych *et al.*, 2014; Herburger *et al.*, 2019; Palacio-López *et al.*, 2019;

Permann *et al.*, 2021a, 2021b; Sørensen *et al.*, 2011), but glycan microarray with HG antibodies JIM5 and 2F4 also revealed strong differences. Whereas there was strong reactivity with CDTA extracts of *Chara*, *Coleochaete*, *Cosmarium*, *Penium* and *Netrium*, no reactivity was detected in *Spirogyra*, *Klebsormidium* and *Chlorokybus* (Sørensen *et al.*, 2011). In contradiction to these results, CDTA extracts of *Spirogyra mirabilis* and *Mougeotia disjuncta* showed strong binding, especially to LM19 and JIM5, which both recognize HG with a low degree of esterification (Permann *et al.*, 2021a, 2021b). To conclude, it seems that the presence of homogalacturonans is an ancient feature of streptophytes, secondarily lost in some species.

In the presence of RG-I, Rha, Gal and Ara should be detectable in the pectic fractions. Rha accounts for over 10% of the neutral monosaccharides in the $(\text{NH}_4)_2\text{C}_2\text{O}_4$ fractions of all *Chara* species investigated in this study, Gal (including 3-*O*-MeGal) is also present in higher amounts, but the content of Ara is low. Low amounts of Ara were also verified for the $(\text{NH}_4)_2\text{C}_2\text{O}_4$ fractions of *C. vulgaris* and *N. flexilis* (O'Rourke *et al.*, 2015). In *C. australis* and several members of the Zygnematophyceae, linkage-types and antibody reactivities typically associated with Ara and Gal sidechains of RG-I were either absent or present at low levels (Sørensen *et al.*, 2011). Isolation of pectins by oxalate followed by paper chromatography suggested the presence of RG I only in the later-diverging CGA *N. flexilis*, *C. vulgaris* and *C. scutata* (O'Rourke *et al.*, 2015). The antibody LM5 directed against an epitope containing 1,4-linked Gal present in RG-I showed weak binding to CDTA extracts from *Mougeotia disjuncta* and *Spirogyra mirabilis* (Permann *et al.*, 2021a, 2021b). To conclude, the presence of RG-I side chains in streptophyte algae is still not finally settled, but is more likely for members of the ZCC grade.

While INRA-RU1 and 2 reactivity (recognition of the RG-I backbone, Ralet *et al.*, 2010) was shown for CDTA extracts of *Mougeotia* and *Spirogyra* (Permann *et al.*, 2021a, 2021b), our $(\text{NH}_4)_2\text{C}_2\text{O}_4$ fractions showed no binding (Figure S3) in any of the *Chara* species investigated. This hints to the absence of RG-I, at least in this genus of the Charophyceae.

A special feature of all pectic fractions of the four *Chara* species was 3-*O*-MeGal, which was also detected in *C. vulgaris* and *C. corallina* (Sørensen *et al.*, 2011). It has been suggested that this methylated monosaccharide might have replaced Ara in RG-I of *Chara* species (O'Rourke *et al.* 2015), which is contradictory to our results that propose the absence of RG-I in *Chara* species.

Investigations on glycosyl linkages revealed none of the characteristic sugars of RG II (2-OMeFuc, 2-OMeXyl, apiose, aceric acid) in streptophyte algae (Sørensen *et al.*, 2011). This is in line with several other publications proposing RG-II as a typical land plant feature (e.g.

Matsunaga *et al.*, 2004; Mikkelsen *et al.*, 2014). Therefore, further investigations are also necessary to clarify the evolutionary roots of RG-II.

Ancestral hemicellulose core structures seem to have diversified after the divergence of Charales and all other streptophytes

Since most hemicelluloses can be extracted under alkaline conditions (Scheller & Ulvskov, 2010), two alkaline fractions (sodium carbonate and KOH) were extracted from the cell walls of the four investigated *Chara* species. Xyl, Man, and Glc were abundant in the hemicellulose fractions of all *Chara* spp., which might be part of xylans, xyloglucans and (gluco)mannans. Striking was the low Xyl content of the KOH fraction of *C. aspera*. This is also demonstrated by the Xyl:Glc ratio. In the other *Chara* species, this ranges from 1.3 – 1.7:1, whereas *C. aspera* shows a ratio of 1:4.6. Presence of xylans and xyloglucans in the cell walls of *C. globularis*, *C. subspinosa* and *C. tomentosa* was supported by ELISA with LM10 (xylans) and LM15 (xyloglucans). As the KOH fraction of *C. aspera* showed no reactivity with the antibodies, this species might be characterized by a lack, or structural modifications, of both hemicelluloses. It has to be mentioned that LM10 only detects not or only slightly substituted xylans (McCartney *et al.*, 2005). Interestingly, the NaOH extract of *C. corallina* also showed no binding to LM10, but bound to LM11 detecting arabinoxylans as well (Sørensen *et al.*, 2011).

In general, there is good evidence for the presence of xylans and xyloglucans in streptophyte algae. This is based on investigations with antibodies directed against xylan and xyloglucan epitopes (Eder & Lütz-Meindl, 2008; Domozych *et al.*, 2009; Sørensen *et al.*, 2011; Ikegaya *et al.*, 2012; Mikkelsen *et al.*, 2021; Permann *et al.*, 2021a, 2021b), but also on structural characterization (Ikegaya *et al.*, 2008; Sørensen *et al.*, 2011; Mikkelsen *et al.*, 2021) and investigations of enzymes involved in the biosynthesis (Del-Bem & Vincentz, 2010; Franková & Fry, 2021; Mikkelsen *et al.*, 2014; Mikkelsen *et al.*, 2021; Nishiyama *et al.*, 2018).

The presence of fucosylated and galactosylated xyloglucans has been shown for *Mesotaenium* (Mikkelsen *et al.*, 2021), underlining that these xyloglucan substitutions known from land plants are also present, at least in some, streptophyte algae. Especially in the sodium carbonate fractions of the *Chara* species investigated here, Gal and Fuc are present in amounts between 2.8% and 9.8%, maybe indicating fucosylated and/or galactosylated xyloglucans.

As far as mannans are concerned, there are convincing data suggesting the presence in most, if not all, charophyte algae. These data range from results of chemical analysis of cell wall fractions of *Chara* and *Nitella* (O'Rourke *et al.*, 2015) to antibody profiling results (Domozych *et al.*, 2009; Sørensen *et al.*, 2011). Our chemical analysis is in support of this conclusion for *Chara* and *Nitellopsis* species by showing relevant amounts of Man in the hemicellulosic and

pectic fractions (Figure 1A). This is in line with the composition data for *Klebsormidium* spp., which also showed widespread occurrence of Man in the different cell wall fractions (O'Rourke *et al.*, 2015). Mannan structures, in general, have to be further investigated for defining the occurrence as homo- or heteromannan, as this is currently unknown for all charophyte algae (Franková and Fry, 2021). Most interestingly, *Chara*, *Nitella* and *Klebsormidium* have been demonstrated to contain unusually high trans- β -mannanase and trans- β -xylanase activities. These have been proposed as hemicellulose remodelling strategies alternative to xyloglucan endotransglucosylase (XET) activity known from land plants (Franková and Fry, 2021).

Purified aqueous extracts include unusual rhamnans and galactans

Gel diffusion assay

Detection of AGPs is possible by precipitation with β GlcY (Yariv *et al.*, 1962). Although the exact precipitation mechanism has not yet been precisely determined, it is certain that a β -1,3-linked galactan is important for this interaction (Kitazawa *et al.*, 2013; Paulsen *et al.*, 2014). In addition, it has been proposed that high concentrations of 1,6-linked galactans can interfere with the precipitation, either directly by steric hindrance (Kiyohara *et al.*, 1989) or relatively by a shifted 1,6-Gal to 1,3-Gal ratio (Kitazawa *et al.*, 2013; Paulsen *et al.*, 2014).

In a radial gel diffusion assay with β GlcY of AE from all *Chara* species showed no precipitation lines, proposing the absence of AGPs in this genus. After purification of AE by treatment with α -amylase and pectinase (AE_AP; deletion of starch and homogalacturonan, which might have been coextracted), thin precipitation lines could be detected (Figure S3), possibly originating from 1,3-linked galactans and not from AGPs, as no Hyp was present (see below).

Analyses of the carbohydrate moiety

Seed plant, fern and bryophyte AGPs have been isolated from aqueous extracts (AE) rich in Ara and Gal by precipitation with β GlcY (Bartels & Classen, 2017; Classen *et al.*, 2004; Happ & Classen, 2019; Mueller *et al.*, 2023). The AE fraction compositions of the cell walls of the investigated *Chara* species differed with high Gal contents but only low amounts of Ara. AE of *Nitellopsis* was slightly different with higher amounts of Rha and Ara. AE of *C. aspera* was striking due to the high content of uronic acids (over 30%). Furthermore, the presence of 3-*O*-MeGal was striking in all AE, especially in *C. aspera*. Methylation of one hydroxyl-group of monosaccharides is a rare modification of different carbohydrates and has been described for some bacteria, fungi, worms, molluscs and also plants (for review see Staudacher, 2012). It offers the possibility to modulate glycan structures, thereby leading to new biological activities. In plants, galactose is the most common methylated hexose (Staudacher, 2012), especially in

algae. 4-*O*-MeGal and 3-*O*-MeGal occur in red algae (Araki *et al.*, 1986; Allsobrook *et al.*, 1974; Navarro & Stortz, 2008). In cell walls of chlorophyte green algae, polysaccharides containing 3-*O*-MeGal, 2-*O*-MeRha and 3-*O*-MeRha (*Chlorella vulgaris*) or 3-*O*-MeRha and 3-*O*-MeFuc (*Botryococcus braunii*) were found (Allard & Casadevall, 1990; Ogawa *et al.*, 1994; Ogawa *et al.*, 1997). For *Chlorella vulgaris*, it was shown that 3-*O*-MeGal is part of a neutral galactan with a ratio of Gal : 3-*O*-MeGal of 7.1:1 (Ogawa *et al.*, 2001). In *S. pratensis*, 3-*O*-MeGal, 2-*O*-MeRha and 3-*O*-MeRha were detected only in trace amounts (Pfeifer *et al.*, 2022). In the streptophyte algae *K. flaccidum*, *C. corallina* and *C. scutate*, 3-*O*-MeRha was also identified in small amounts (Popper & Fry 2003), but 3-*O*-MeGal was not detected at all (Popper *et al.*, 2001). More recently, it was shown that pectins of *C. vulgaris* are characterized by the presence of 3-*O*-MeGal (O'Rourke *et al.*, 2015). Among the land plants, the cell walls of bryophytes and ferns contain 3-*O*-MeRha, especially as part of AGPs (Bartels *et al.*, 2017; Bartels & Classen, 2017; Happ & Classen, 2019, Baumann *et al.*, 2021, Mueller *et al.*, 2023), or RG-II (Matsunaga *et al.*, 2004), whereas higher concentrations of 3-*O*-MeGal were detected in the cell walls of the young leaves of both homosporous (*Lycopodium*, *Huperzia* and *Diphasiastrum*) and heterosporous (*Selaginella*) lycophytes (Popper *et al.*, 2001). Although only rarely, 3-*O*-MeGal was found in some seed plant polysaccharides as well (Barsett & Paulsen, 1992; Hokputsa *et al.*, 2004), even as part of an arabinogalactan-protein (Capek, 2008). To verify the presence of arabinogalactans, antibodies directed against arabinogalactan epitopes present in AGPs are commonly used (e.g. JIM8, JIM13, JIM16, LM2, LM6, LM14, KM1, MAC207). AE of all *Chara* species investigated showed comparable binding profiles in ELISA with JIM13, LM2, LM6 and KM1. There was nearly no binding of *Chara* AE to LM6, indicating lack of detectable 1,5-linked Ara. In contrast, AE of *N. obtusa* bound to LM6 and structure elucidation revealed high amounts of 1,5-linked Ara (Table 3). KM1, which recognizes 1,6-linked Gal, bound to AE of all *Chara* species and also to AE of *N. obtusa* (Pfeifer *et al.*, 2022) thus revealing presence of 1,6-linked Gal. Binding of AE to JIM13 with an epitope probably including Rha and uronic acids was comparable for the *Chara* species but very low for *N. obtusa* (Pfeifer *et al.*, 2022). In ELISA with LM2, *C. aspera* reacted very strongly. According to Ruprecht *et al.* (2017), this antibody recognizes (1→6)-β-D-Galp units with terminal β-D-GlcAp. Probably the high content of 1,6-Gal residues in AE of *C. aspera* is responsible for the higher affinity to this antibody. In ELISA experiments with AE of *S. pratensis* (Pfeifer *et al.*, 2022), no affinity was detected for LM6 and KM1, whereas there was strong binding to JIM13. CDTA extracts of other members of the Zygnematophyceae (*S. mirabilis* and *Mougeotia sp.*) also showed strong interaction with JIM13 (Permann *et al.*, 2021a, 2021b). In a glycan microarray, different antibodies directed against AG epitopes (LM2, LM14,

JIM8, JIM13 and MAC207) have been tested for interaction with different streptophyte algae (Sørensen *et al.*, 2011). All antibodies (except for LM2) and especially JIM13 bound to CDTA extracts of *C. corallina*, but JIM13 was the only antibody binding to *Spirogyra* CDTA extracts, thus hinting at strong structural differences between the Charophyceae and Zygnematophyceae. Several members of the Zygnematophyceae showed positive interaction with JIM13 (Eder *et al.*, 2008; Domozych *et al.*, 2009; Ruiz-May *et al.*, 2018; Palacio-Lopez *et al.*, 2019). Interestingly, *K. flaccidum*, representing the lower-branching KCM-grade, showed no reactivity with antibodies directed against arabinogalactan epitopes (Sørensen *et al.*, 2011, Steiner *et al.*, 2020).

Structural analyses verified the presence of unusual galactans (Figure 4). Galactan linkage-types typical for AGPs were present. These were detected by antibodies directed against AGPs (see above) and weak interaction with Yariv's reagent (Kitazawa *et al.*, 2013; Paulsen *et al.*, 2014). A special feature were high amounts of 3-*O*-MeGal, present in 1,6-linkage or as terminal residue. The ratio of Gal to 3-*O*-MeGal varied (see Table 2) and was highest for *C. aspera* (1:1.2). There was a shifted in the ratio of backbone galactan to side-chain galactans between the species. *C. aspera* shows the longest 1,6-Gal side chains, whereas *N. obtusa* is special due to short 1,6-linked Gal side chains. Similar galactan structures (longer 1,6-linked Gal side chains; lower degree of methylated Gal) have been isolated from *Chlorella vulgaris*, a unicellular member of the Chlorophyta (Ogawa *et al.*, 2001), hinting at a shared evolutionary origin.

Another interesting finding of linkage-type analysis were high amounts of 1,4-linked Rhap in all investigated members of the Charales. To the best of our knowledge, no plant polysaccharide with a substantial amount of 1,4-linked Rhap has been described up to now. Typical linkage types known for Rha in seed plants are 1,2- and 1,2,4-linked Rha residues as part of RG-I. A main component of the fibers extracted from the green algae *Monostroma angicava* and *Monostroma nitidum* (Chlorophyceae) are sulfated rhamnans with 1,3- and 1,2-linked Rha residues (Liu *et al.*, 2018; Suzuki & Terasawa, 2020) and the rhamnogalactan-protein isolated from *Spirogyra pratensis* is rich in 1,3-linked Rhap (Pfeifer *et al.*, 2022).

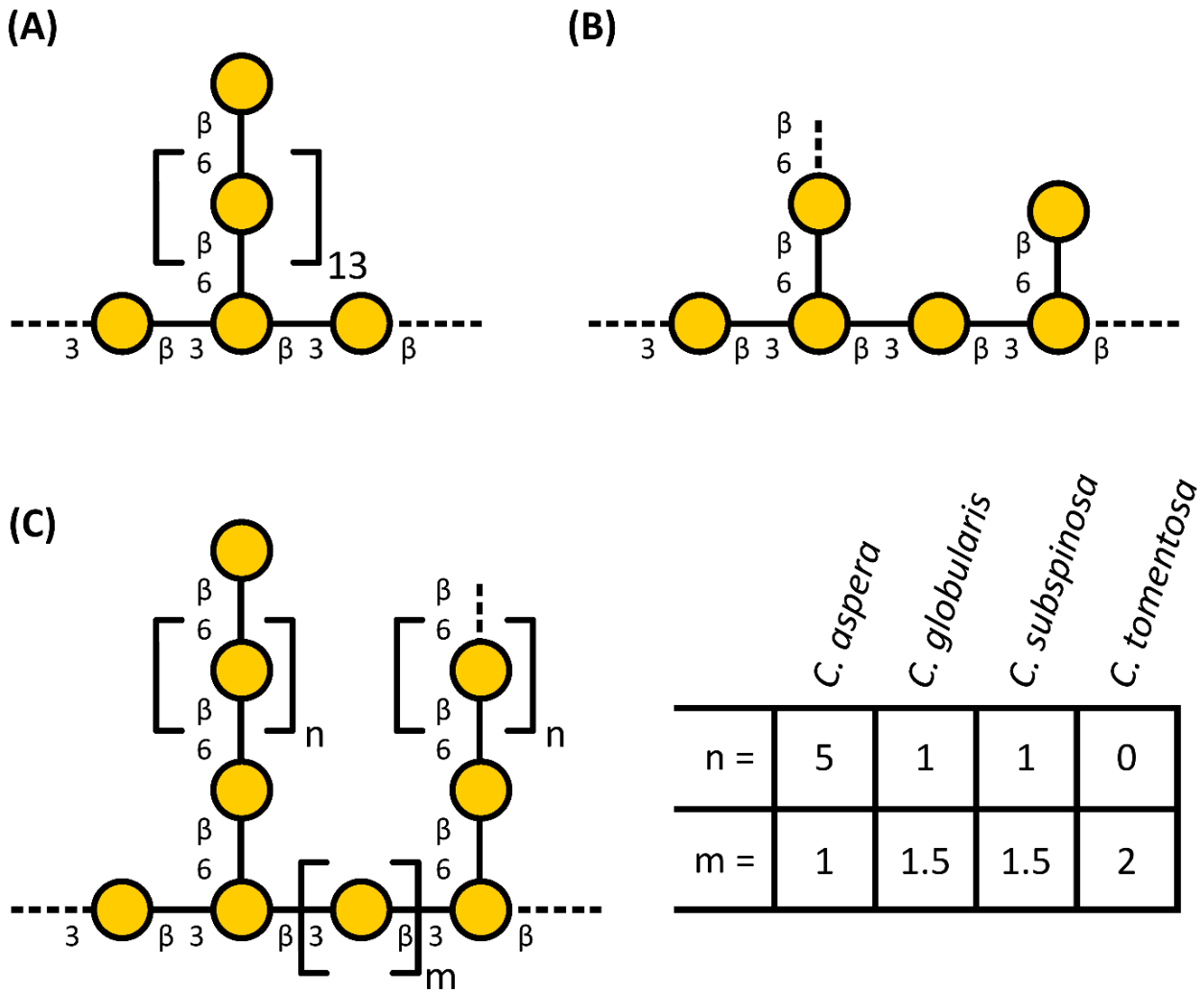


Figure 4. Partial structural proposals for galactans of *Chara* species in the context of other algal galactan structures. (A) Structural proposal of *Chlorella vulgaris* based on the published results of Ogawa *et al.* (2001). Patterns of methylation are not shown. (B) Galactan structures of *Nitellopsis obtusa*. (C) Galactan structures of the investigated four *Chara* species. The structural features were inferred from the linkage-type analysis. The dashed lines symbolize attachment sites for galactoses (main chain) or for other monosaccharides (side chain). Part of the Gal residues are methylated (see Table 2 for amounts of 3-*O*-MeGal).

Hydroxyproline seems to be absent in Charales and AGP-associated P4H activity is questionable

The protein backbone of classical AGPs consists of an *N*-terminal signal peptide, a protein sequence rich in proline (Pro), alanine (Ala), serine (Ser), and threonine (Thr; PAST), and a C-terminal domain (Johnson *et al.*, 2018). The carbohydrate moieties are covalently linked to the protein part *via* Hyp. Hydroxylation of Pro to Hyp is catalyzed by the enzyme P4H (Seifert *et al.*, 2021).

In different studies, the occurrence of Hyp was tested in various chlorophyte algae and the charophyte algae *S. pratensis*, *Nitella* sp. and *N. obtusa*. Hyp was detected in all algae, except of the two algae genera of the Charophyceae family: *Nitella* and *Nitellopsis* (Gotelli & Cleland, 1968; Morrison *et al.*, 1993; Pfeifer *et al.*, 2022; Thompson & Preston, 1967). Our results that

Hyp is missing in all investigated *Chara* species is in support of these previous results and fosters the assumption that Hyp is absent in all members of the Charophyceae.

At the first glimpse, the finding of seven P4H homologs *via* BLAST analysis is in contrast to this statement. With the here presented analysis of the relevant amino acids in both catalytic sites (compare Hieta & Myllyharju, 2002; Keskiäho *et al.*, 2007; Koski *et al.*, 2007; Koski *et al.*, 2009) it is likely that most homologs lost their functionality for prolyl-hydroxylation either in general or with regard to the characteristic HRGP substrates. The substrate specificity is highly dependent on the substrate tunnel being shaped by the β 3- β 4 loop as well as the β II- β III loop, which cover the tripeptide structure of the substrate. In direct comparison with various human P4H α -subunits (C-P4HI-III and HIF-P4H-2), it was shown that both regions have a certain degree of flexibility (Koski *et al.*, 2009). Numerous studies with recombinant enzyme expression underlined the flexibility in utilized substrates (Mócsai *et al.*, 2021; Velasquez *et al.*, 2015; Vlad *et al.*, 2010). Despite of the described activities of P4Hs on different substrates, it is not possible to predict specificity conclusively (see Moussu & Ingram, 2023). The few studies comparing substrate activities (Mócsai *et al.*, 2021; Velasquez *et al.*, 2015; Vlad *et al.*, 2010) have included an AGP peptide in their analyses but also reveal that for *C. reinhardtii* P4H this activity was not determined (Vlad *et al.*, 2010). The selected candidate sequence GBG85197 from *C. braunii* showed overall similarity to the two P4Hs from *A. thaliana* and *C. reinhardtii* (Figure 3) with various structural variations in the two flexible regions. Even though the catalytically relevant amino acids are present (Hieta & Myllyharju, 2002; Keskiäho *et al.*, 2007; Koski *et al.*, 2007; Koski *et al.*, 2009), this could mean extremely different or even lacking activity. Timmins *et al.* (2017) performed excessive mutations (Y140F, Y140G, W243F, W243G, Y140G/W243G) in the two investigated loops and showed inactivity, changed regioselectivity or different substrate activity by mutation of single amino acids. Presence of a putatively functional P4H and lack of hydroxyproline in the biochemical assays is explainable in different ways: (1) The occurrence of the coding gene in the genome is not equivalent to permanent expression of a functional protein. This could be occasionally expressed or not expressed following a distinct (environmental) stimulus. (2) The P4H coding gene could be a remnant of the least common ancestor of all Chloroplastida, which utilized the enzyme for hydroxylation of very specialized substrates. Exemplarily, the cell walls in Chlamydomonales are formed nearly exclusively by (glyco-)proteins showing *O*-glycosylation (Bollig *et al.*, 2007; Ferris *et al.*, 2001; Miller *et al.*, 1972; Voigt *et al.*, 2014; Woessner & Goodenough, 1994;). Whether their glycosylation, showing similarities to land plant extensins (Bollig *et al.*, 2007), is performed (similar to embryophytes) by homologs of carbohydrate-active enzymes from the GT95, GT77 and GT47 families is questionable by looking at the work

of Barolo *et al.* (2020) who detected few, if any, homologs in microalgal genomes. (3) The complex interplay of three different P4Hs (AtP4H2, AtP4H5 and AtP4H13) was shown in *A. thaliana* (Velasquez *et al.*, 2015). The formation of homodimers of AtP4H5 or heterodimers of AtP4H5 with either AtP4H2 or AtP4H13 is required for correct peptidyl-proline hydroxylation. This is the case for at least extensins, but cannot be ruled out for other HRGPs. From these three P4Hs, GBG85197 showed most similarity with AtP4H13 in the β II- β III loop thus hinting potential inactivity in a monomeric state. All these three possible explanations are speculative but highlight the general aim that presence or absence of P4H homologs should not be seen equivalent to presence or absence of AGPs or extensins. The latter has to be individually shown by a combination with analytical methods as shown in this study.

CONCLUSION

Although presence of pectic polysaccharides is unquestionable and especially the cell walls of *C. aspera* contain huge amounts of these polysaccharides possibly involved in salt tolerance of this species, further investigations have to follow to elucidate the exact structural composition and to clarify whether only homogalacturonan or also RG-I or even RG-II have evolutionary roots in algae. The most prominent unusual structural features detected in the aqueous extracts of the investigated Charales were 1,4-linked rhamnans and 1,3-, 1,6- and 1,3,6-linked partially methylated galactans. However, these galactans were not part of AGPs. Although one possible functional sequence of P4H was detected in the genome of *C. braunii*, no Hyp (necessary for linkage of the galactan to the protein moiety in AGPs) was detected in any of the investigated species. The fact that antibodies directed against AGP epitopes showed cross reactivities with the unusual methylated galactans is a reminder that results only based on antibodies are not always reliable. Our work reveals strong differences of the cell walls of members of the Charophyceae compared to those of seed plants and even to those of the other members of the higher-branching ZCC-grade of streptophyte algae, namely the Coleochaetophyceae and the Zygnematophyceae. More detailed investigations of the cell walls of the different streptophyte algal taxa are necessary to understand how these algae met the challenge of cell wall adaptation necessary for life on land.

EXPERIMENTAL PROCEDURES

Plant material and sampling

The streptophyte algae *Chara globularis* THUILL., *Chara subspinoso* RUPR. and *Chara tomentosa* L. were collected in June 2018 in the lake “Lützlöwer See” in Uckermark (53°14'45.9"N, 14°01'54.2"E; Germany). *Chara aspera* WILLD. was collected in July 2021 in the lake in Lalendorf (53°40'33.2"N, 12°26'05.9"E; Germany). All samples were cleaned with water and freeze-dried (Christ Alpha 1-4 LSC, Martin Christ Gefriertrocknungsanlagen GmbH). Preliminary experiments were carried out with *C. subspinoso* from the Lunzer See and *C. tomentosa* and *C. globularis* from the Neusiedler See. The Austrian samples were collected and identified by Prof. Dr Michael Schagerl and Barbara Mähner from the Department for Limnology and Oceanography of the University of Wien. Previously studied samples of *Echinacea purpurea* (Classen *et al.*, 2004) and *Nitellopsis obtusa* (Pfeifer *et al.*, 2022) were additionally used for comparison and were treated similarly to the *Chara* samples for experiments missing in the original publications.

Isolation of cell wall fractions

The freeze-dried and ground plant material was pre-extracted two times (2 h and 21 h) with 70% acetone solution (v/v) in a 1:10 (w/v) ratio. After drying, the plant residue was extracted with double-distilled water (ddH₂O) for 21 h under constant stirring (SM 2484, Edmund Bühler GmbH) at 4°C in a 1:10 (w/v) ratio. The aqueous extract was separated with a tincture press (HAFICO HP 2 H, Fischer Tinkturenpressen GmbH) and the insoluble plant pellet was freeze-dried for further extractions (see below).

After heating the aqueous extract in a water bath (GFL 1002, LAUDA-GFL Gesellschaft für Labortechnik mbH) at 90 – 95°C for 10 min, the denatured proteins were removed by centrifugation (4,122 g, 20 min, 4°C, Heraeus Multifuge X3R, Thermo Scientific Inc.). To precipitate polysaccharides and AGPs, the aqueous extract was first evaporated in a rotary evaporator (40°C, 0,010 mbar; Laborota 4000, Heidolph Instruments GmbH & CO.) to approximately one-tenth of its volume and subsequently added to cooled ethanol resulting in a final concentration of 80% (v/v). After incubation overnight at 4°C, the precipitate was isolated by centrifugation (4°C, 19,000 g, 20 min) and finally freeze-dried (AE).

To remove starch, approximately 100 mg of AE were treated with α -amylase + amyloglucosidase (α -amylase from *Aspergillus oryzae*, EC number 3.2.1.1., 15 U mg⁻¹ polysaccharide; amyloglucosidase from *Aspergillus niger*, EC number 3.2.1.3., 7 U mg⁻¹ polysaccharide; both from Sigma-Aldrich Chemie GmbH; in 50 mmol L⁻¹ acetate buffer at pH 5.2, 50°C for 20 h). Subsequently, the samples were treated with pectinase (Sigma-Aldrich

Chemie GmbH, from *A. niger*, EC number 3.2.1.15., 1 $\mu\text{L mg}^{-1}$, for 5h, in 50 mmol L^{-1} acetate buffer at pH 5.2, 37.5°C) to cleave homogalacturonan parts. The enzymes were removed by heating in a boiling water bath for 10 min with the following centrifugation at 19,000 g for 20 min. Afterwards, the samples were dialyzed against demineralized water (4°C; 4d; MWCO 12 – 14 kDa, Visking®, Medicell International Ltd) and freeze-dried (AE_AP).

According to a modified method of O'Rourke *et al.* (2015) and Raimundo *et al.* (2016), the insoluble plant pellet after water extraction (see above) was used for the isolation of four additional polysaccharide fractions.

The pellet was subsequently extracted with ammonium oxalate ($(\text{NH}_4)_2\text{C}_2\text{O}_4$, 0.2 mol L^{-1}), hydrochloric acid (HCl, 0.01 mol L^{-1}), sodium carbonate (Na_2CO_3 , 3% (w/v)) and potassium hydroxide (KOH, 2 mol L^{-1}), each in a ratio of 1:100 (w/v) at 70°C under constant stirring for 21 h (RET basic, ETS D5, IKA Labortechnik, Staufen, Germany). The pellet and the supernatant were separated after each extraction by centrifugation (4°C, 19,000 g , 20 min, Heraeus Multifuge X3, Thermo Fisher Scientific Corp.).

To precipitate the Na_2CO_3 fraction, the supernatant was added to acetone in a 1:4 (V/V) ratio. After incubation overnight at 4°C, the precipitated material was re-dissolved in ddH₂O in a 1:100 (w/V) ratio. The KOH extract was neutralized (761 Calimatic, Knick Elektronische Messgeräte GmbH & Co. KG). All fractions were dialyzed against demineralized water (4°C, 4 d, MWCO 12 – 14 kDa, Visking®) and freeze-dried. The whole workflow is schematically represented in Figure S1.

Analysis of monosaccharides

The neutral monosaccharide composition was determined by the method of Blakeney *et al.* (1983) with slight modifications (see Mueller *et al.*, 2023). Gas chromatography (GC) with flame ionization detection (FID) and mass spectrometry (MS) detection were used to identify and quantify the neutral monosaccharides: GC + FID: 7890B; Agilent Technologies Inc.; MS: 5977B MSD; Agilent Technologies, USA; column: Optima-225; Macherey-Nagel GmbH & Co. KG; 25 m, 250 μm , 0.25 μm ; helium flow rate: 1 mL min^{-1} ; split ratio 30:1. A temperature gradient was performed to achieve peak separation (initial temperature 200°C, subsequent holding time of 3 min; final temperature 243°C with a gradient of 2°C min^{-1}). The methylated monosaccharide 3-*O*-MeRha was identified by retention time and mass spectrum (see Happ & Classen, 2019), 3-*O*-MeFuc was determined using the mass spectrum and the deviating retention time to 3-*O*-MeRha. 3-*O*-MeGal was also quantified by mass spectrum, but additionally, the validated method of Pfeifer *et al.* (2020) was used to distinguish 3-*O*-MeGal from 4-*O*-MeGal.

The uronic acid (UA) compounds were determined photometrically at 525 nm (UVmini-1240, Shimadzu AG) according to the method of Blumenkrantz & Asboe-Hansen (1973), for modifications, see Mueller *et al.* (2023).

Carboxy-reduction of uronic acids

The method of Taylor and Conrad (1972), with slight modifications, was used to perform a carboxy-reduction of the uronic acids of the AE_{AP} fractions. Firstly, 20 – 30 mg AE_{AP} were dissolved in 20 mL ddH₂O and 216 mg of *N*-cyclohexyl-*N'*-[2-(*N*-methylmorpholino)-ethyl]-carbodiimide-4-toluenesulfonate was added slowly under constant stirring. An autotitrator (Metrohm 719 S-Titrino, Deutsche METHROM GmbH & Co. KG) adjusted the pH to 4.75 with 0.01 M HCl for 2 h. One to two drops of 1-octanol were added to avoid strong foaming. Sodium borodeuteride solutions (in ddH₂O) were added in increasing concentrations (4.0 mL of 1 mol L⁻¹; 5 mL of 2 mol L⁻¹; 5 mL of 4 mol L⁻¹) to carboxy-reduce the uronic acids. The autotitrator adjusted the pH to 7.00 with 2 M HCl for another 2 h. After pH setting to 6.5 with glacial acetic acid, the solutions were dialyzed for three days at 4°C against demineralized water (MWCO 12 – 14 kDa, Visking®) and freeze-dried.

Structural characterization of water-soluble polysaccharides

Following the method of Harris *et al.* (1984; see Mueller *et al.*, 2023 for modifications), structural characterization of the polysaccharides was performed. Potassium methylsulfinyl carbanion (KCA) and iodomethane-d₃ (IM-d₃) were added to the samples in a defined scheme to methylate the samples (1) 100 µL KCA for 10 min; (2) 80 µL IM-d₃ for 5 min; (3) 200 µL KCA for 30 min; (4) 150 µL IM-d₃ for 60 min). After following hydrolysis, reduction, and acetylation, the samples were modified to permethylated alditol acetates (PMAA). These were identified by GC-MS (instrumentation see above: "Analysis of monosaccharides"; column: Optima-1701, 25 m, 250 µm, 0.25 µm; helium flow rate: 1 mL min⁻¹; initial temperature: 170°C; hold time 2 min; rate 1°C min⁻¹ until 210°C was achieved; rate: 30°C min⁻¹ until 250°C was achieved; final hold time 10 min) by their retention times and comparison to a PMAA library established in the working group.

Determination of hydroxyproline content

For Hyp quantification, the methodology of Stegemann & Stalder (1967) was used in a modified version (see Mueller *et al.*, 2023). The Hyp content was measured colourimetrically at 558 nm and quantified *via* a linear regression analysis with a Hyp standard.

Indirect enzyme-linked immunosorbent assay (ELISA)

First, 96-well plates (Nunc-Immuno® Plates, Thermo Scientific) were coated with 100 µl per well of the sample in triplicate (concentrations in ddH₂O: 12.5 µg mL⁻¹ for [NH₄]₂C₂O₄ and KOH; 12.5 µg mL⁻¹, 25 µg mL⁻¹ 50 µg mL⁻¹ for AE). Afterwards, these were incubated at 37.5°C for 3 days. A negative control of ddH₂O was used and treated likewise. The plates were washed three times with 100 µl phosphate buffered saline (PBS)-T (pH 7.4, 0.05% Tween® 20) per well and blocked with 200 µl of BSA (bovine serum albumin, 1%, w/v) in PBS per well. After incubation at 37.5°C for 1 h, the plates were washed again three times. Following the addition of 100 µl of primary antibody solution (INRA-RU2, 1:200 dilution; JIM13, 1:40 dilution; KM1, LM2, LM6, LM10, LM15, LM19, 1:20 dilution) per well in PBS 7.4 dilution, the plates were incubated again (1 h at 37.5°C). After washing three times again, the procedure was repeated for the secondary antibody (anti-mouse-IgG for INRA-RU2 and KM1; anti-rat-IgG for all other antibodies; both produced in goat and conjugated with alkaline phosphatase, Sigma-Aldrich Chemie GmbH) in a ratio of 1:500 (v/v) in PBS 7.4. Subsequently, the substrate solution of *p*-nitro-phenylphosphate was added (100 µl well⁻¹). The plates were incubated at room temperature in the dark, and the absorbance was determined at 405 nm with a plate reader (Infinite F50 Plus, Tecan Group Ltd.) after 40 min. For visualization purposes, the absorbance of the control was set to 0 and the highest signal in the dataset was set to 1.0. Epitopes of the antibodies and key references are listed in Table S1.

Gel diffusion assay

For the gel diffusion assay, an agarose gel (Tris-HCl, 10 mmol L⁻¹; CaCl₂, 1 mmol L⁻¹; NaCl, 0.9% w/v; agarose, 1% w/v) was used, in which several cavities were stamped in. The cavities in the first and third rows were filled with dilutions (100 mg mL⁻¹) of the samples. In the second line, the cavities left and right were filled with the positive control, AGP from *Echinacea purpurea* (10 mg mL⁻¹), and the middle cavities with the βGlcY solution (1 mg mL⁻¹). The assay was incubated for 22 h in the dark. If AGPs are present in the samples, a red precipitation line appears, as in the positive control.

Bioinformatic search for prolyl-4-hydroxylase (P4H)

Candidate sequences for P4Hs were obtained from the translated proteome of *Chara braunii* (Nishiyama *et al.*, 2018; https://plants.ensembl.org/Chara_braunii/Info/Index, v1.0) under the use of the R package rBLAST (Hahsler & Nagar, 2019) with the *Arabidopsis thaliana* P4Hs as query sequences. An E-value of 1e⁻⁷ was used and the resulting candidates were aligned with functionally described P4H sequences (Hieta & Myllyharju, 2002; Keskiäho *et al.*, 2007; Vlad

et al., 2010; Velasquez *et al.*, 2014; Yuasa *et al.*, 2005) by the use of MAFFT in L-INS-i mode (Kato & Standley, 2013). The occurrence of relevant amino acids was evaluated in comparison to *Chlamydomonas reinhardtii* P4H1. Afterwards, some sequences were modelled with the SWISS-MODEL web server (Waterhouse *et al.*, 2018) with default settings on the JIG2/A crystal structure of *C. reinhardtii* P4H (Koski *et al.*, 2007).

ACKNOWLEDGEMENTS

The authors thank Prof. Dr. Michael Schagerl and Barbara Mähner from the Department for Limnology and Oceanography of the University of Wien for collection of *Chara* species used in preliminary experiments. Funding: LP and BC (project-number 440046237) are grateful for funding within the framework of MAdLand (<http://madland.science>), priority programme 2237 of the German Research Foundation (DFG). HS also thanks the DFG for funding (project SCHU 983/23-1).

AUTHORS CONTRIBUTIONS and CONFLICT OF INTEREST

BC and LP planned and designed the research. HS collected and identified the plant material. FE, KM, LP and JU performed the extractions as well as carbohydrate and ELISA experiments. JBJZ performed preliminary analytical work on *Chara* species from Austria. LP performed bioinformatic searches. LP and KM created all main text figures. All authors analysed the data (BC, FE, KM, LP: carbohydrate analysis; LP bioinformatics search for P4Hs). BC, KM and LP wrote the draft manuscript; all authors revised the manuscript, read and approved the final manuscript. The authors declare that they have no competing interests.

DATA AVAILABILITY STATEMENT

All relevant data can be found within the manuscript and its supporting materials.

SUPPORTING INFORMATION

Table S1. Antibodies tested for binding to *Chara* species cell wall fractions AE, (NH₄)₂C₂O₄ or KOH.

Antibody	Epitope	Key References
INRA-RU2	[(4)- α -D-GalA-(1,2)- α -L-Rha] ₄ of RG-I	Ralet <i>et al.</i> (2010)
JIM13	AGP glycan, e.g. β -D-GlcAp-(1 \rightarrow 3)- α -D-GalAp-(1 \rightarrow 2)- α -L-Rha	Pfeifer <i>et al.</i> (2022); Yates <i>et al.</i> (1996)
KM1	(1 \rightarrow 6)- β -D-Galp units in AGs type II	Classen <i>et al.</i> (2004); Ruprecht <i>et al.</i> (2017)
LM2	(1 \rightarrow 6)- β -D-Galp units with terminal β -D-GlcAp in AGP	Ruprecht <i>et al.</i> (2017); Smallwood <i>et al.</i> (1996);
LM6	(1 \rightarrow 5)- α -L-Araf oligomers in arabinan or AGP	Verhertbruggen <i>et al.</i> (2009a)
LM10	Non-reducing end of (1 \rightarrow 4)- β -D-xylan	McCartney <i>et al.</i> (2005); Ruprecht <i>et al.</i> (2017)
LM15	XXXG-motif of xyloglucan	Marcus <i>et al.</i> (2008); Pedersen <i>et al.</i> (2012)
LM19	Unesterified HG	Verhertbruggen <i>et al.</i> (2009b)

Table S2. Yields of the different extracts from different *Chara* species in % of dry plant material (w w⁻¹).

	<i>C. aspera</i>	<i>C. globularis</i>	<i>C. subspinososa</i>	<i>C. tomentosa</i>
AE	2.5	0.6	1.6	1.3
(NH ₄) ₂ C ₂ O ₄	21.2	2.3	5.9	5.0
HCl	1.9	0.3	0.2	0.7
Na ₂ CO ₃	2.9	0.7	1.2	1.0
KOH	6.1	6.3	3.5	2.8

Table S3a. Neutral monosaccharide composition of the ammonium oxalate fraction ((NH₄)₂C₂O₄) from different *Chara* species in % (mol mol⁻¹; tr: trace value < 1%).

Neutral monosaccharide	<i>C. aspera</i> (NH ₄) ₂ C ₂ O ₄ n=3	<i>C. globularis</i> (NH ₄) ₂ C ₂ O ₄ n=3	<i>C. subspinososa</i> (NH ₄) ₂ C ₂ O ₄ n=3	<i>C. tomentosa</i> (NH ₄) ₂ C ₂ O ₄ n=3
3- <i>O</i> -MeRha	tr	tr	tr	tr
Rha	17.2 \pm 0.3	10.4 \pm 0.1	14.7 \pm 0.2	10.8 \pm 0.5
3- <i>O</i> -MeFuc	1.2 \pm 0.1	tr	1.1 \pm 0.0	tr
Fuc	11.9 \pm 0.1	10.8 \pm 0.1	12.7 \pm 0.1	12.9 \pm 0.1
Ara	1.4 \pm 0.0	3.9 \pm 0.2	2.7 \pm 0.1	3.5 \pm 0.0
Xyl	10.7 \pm 0.3	16.2 \pm 0.2	18.0 \pm 0.3	21.8 \pm 0.2
Man	9.9 \pm 0.4	10.8 \pm 0.1	9.7 \pm 0.1	9.9 \pm 0.2
3- <i>O</i> -MeGal	9.9 \pm 0.3	4.2 \pm 0.2	5.4 \pm 0.1	3.5 \pm 0.1
Gal	11.6 \pm 0.1	12.1 \pm 0.2	11.0 \pm 0.2	8.9 \pm 0.2
Glc	26.2 \pm 0.7	31.6 \pm 0.7	24.7 \pm 0.3	28.7 \pm 0.9

Table S3b. Neutral monosaccharide composition of the hydrochloric acid fraction (HCl) from different *Chara* species in % (mol mol⁻¹; tr: trace value < 1%).

Neutral monosaccharide	<i>C. aspera</i> HCl n=3	<i>C. globularis</i> HCl n=1	<i>C. subspinoso</i> HCl n=1	<i>C. tomentosa</i> HCl n=3
3- <i>O</i> -MeRha	tr	-	-	-
Rha	5.6 ± 0.1	2.9	2.5	2.9 ± 0.1
3- <i>O</i> -MeFuc	tr	-	-	-
Fuc	9.7 ± 0.2	4.9	10.2	11.8 ± 0.1
Ara	1.2 ± 0.0	1.4	1.4	1.6 ± 0.0
Xyl	14.0 ± 0.3	11.2	17.3	19.3 ± 0.9
Man	16.9 ± 0.2	10.7	13.7	14.6 ± 0.5
3- <i>O</i> -MeGal	2.8 ± 0.1	tr	1.2	1.0 ± 0.1
Gal	5.9 ± 0.1	3.3	4.1	3.7 ± 0.1
Glc	43.9 ± 0.7	65.6	49.6	45.1 ± 0.7

Table S3c. Neutral monosaccharide composition of the sodium carbonate fraction (Na₂CO₃) from different *Chara* species in % (mol mol⁻¹; tr: trace value < 1%).

Neutral monosaccharide	<i>C. aspera</i> Na ₂ CO ₃ n=3	<i>C. globularis</i> Na ₂ CO ₃ n=1	<i>C. subspinoso</i> Na ₂ CO ₃ n=3	<i>C. tomentosa</i> Na ₂ CO ₃ n=3
3- <i>O</i> -MeRha	-	tr	-	tr
Rha	3.5 ± 0.1	2.4	3.9 ± 0.1	3.6 ± 0.1
3- <i>O</i> -MeFuc	-	tr	-	tr
Fuc	8.9 ± 0.1	2.8	7.6 ± 0.0	9.8 ± 0.2
Ara	1.1 ± 0.1	1.4	1.6 ± 0.0	1.9 ± 0.1
Xyl	7.1 ± 0.3	5.3	9.9 ± 0.4	12.7 ± 0.2
Man	8.1 ± 0.1	4.6	8.3 ± 0.2	8.7 ± 0.3
3- <i>O</i> -MeGal	1.3 ± 0.0	tr	1.3 ± 0.0	tr
Gal	3.1 ± 0.2	3.0	5.4 ± 0.1	4.1 ± 0.1
Glc	67.2 ± 0.7	80.5	62.0 ± 0.6	59.2 ± 0.4

Table S3d. Neutral monosaccharide composition of the potassium hydroxide fraction (KOH) from different *Chara* species in % (mol mol⁻¹; tr: trace value < 1%).

Neutral monosaccharide	<i>C. aspera</i> KOH n=3	<i>C. globularis</i> KOH n=1	<i>C. subspinoso</i> KOH n=3	<i>C. tomentosa</i> KOH n=3
3- <i>O</i> -MeRha	-	-	-	-
Rha	1.4 ± 0.1	tr	tr	tr
3- <i>O</i> -MeFuc	tr	-	-	-
Fuc	5.1 ± 0.1	tr	4.5 ± 2.4	3.9 ± 0.3
Ara	tr	2.3 ± 0.4	1.7 ± 0.4	2.1 ± 0.1
Xyl	14.3 ± 0.3	56.2 ± 12.5	44.5 ± 14.4	51.2 ± 2.2
Man	12.9 ± 0.4	7.7 ± 3.3	12.8 ± 7.3	12.4 ± 0.8
3- <i>O</i> -MeGal	tr	-	-	-
Gal	tr	1.4 ± 0.5	1.4 ± 0.7	1.0 ± 0.1
Glc	66.3 ± 0.9	32.4 ± 9.1	35.1 ± 4.4	29.4 ± 1.1

Table S4a. Neutral monosaccharide composition of water-soluble polysaccharides (AE) from different *Chara* species and *Nitellopsis obtusa* (Pfeifer *et al.*, 2022) in % (mol mol⁻¹; tr: trace value < 1%).

Neutral mono-saccharide	<i>C. aspera</i> AE n=3	<i>C. globularis</i> AE n=3	<i>C. subspinosa</i> AE n=3	<i>C. tomentosa</i> AE n=3	<i>N. obtusa</i> AE n=3
3- <i>O</i> -MeRha	tr	-	-	-	-
Rha	11.8 ± 0.2	10.7 ± 0.9	11.9 ± 0.4	10.3 ± 0.8	18.0 ± 0.4
3- <i>O</i> -MeFuc	tr	tr	1.9 ± 0.1	1.1 ± 0.2	-
Fuc	7.0 ± 0.7	12.1 ± 2.4	7.2 ± 0.1	11.0 ± 1.1	5.8 ± 0.0
Rib	tr	1.4 ± 0.2	tr	tr	-
Ara	3.0 ± 0.1	6.9 ± 1.9	3.4 ± 0.1	6.4 ± 2.8	20.8 ± 0.7
Xyl	6.1 ± 0.3	9.6 ± 1.3	16.4 ± 0.5	12.8 ± 1.5	3.7 ± 0.5
Man	8.7 ± 0.4	9.1 ± 0.3	7.2 ± 0.4	12.3 ± 5.0	7.3 ± 0.4
3- <i>O</i> -MeGal	18.8 ± 0.3	5.8 ± 1.6	7.4 ± 0.2	3.7 ± 0.7	-
Gal	13.7 ± 0.4	22.9 ± 2.8	13.5 ± 0.3	12.7 ± 1.6	18.6 ± 0.2
Glc	30.9 ± 1.4	21.5 ± 1.6	31.1 ± 0.6	29.7 ± 2.4	25.8 ± 0.9

Table S4b. Neutral monosaccharide composition of dialyzed water-soluble polysaccharides, pre-treated with amylase and pectinase (AE_AP), from different *Chara* species and *Nitellopsis obtusa* in % (mol mol⁻¹; tr: trace value < 1%).

Neutral mono-saccharide	<i>C. aspera</i> AE_AP n=3	<i>C. globularis</i> AE_AP n=3	<i>C. subspinosa</i> AE_AP n=3	<i>C. tomentosa</i> AE_AP n=3	<i>N. obtusa</i> AE_AP n=3
Rha	15.5 ± 0.2	12.2 ± 0.2	14.5 ± 0.2	10.0 ± 0.1	21.8 ± 0.3
3- <i>O</i> -MeFuc	tr	tr	1.8 ± 0.1	1.0 ± 0.1	-
Fuc	9.7 ± 0.2	16.5 ± 0.3	9.8 ± 0.2	14.3 ± 0.1	7.4 ± 0.3
Ara	2.4 ± 0.2	4.0 ± 0.1	2.5 ± 0.0	2.2 ± 0.0	12.5 ± 0.1
Xyl	7.5 ± 0.4	9.5 ± 0.4	10.1 ± 0.2	14.3 ± 0.5	5.2 ± 0.2
Man	8.5 ± 0.2	9.0 ± 0.2	10.1 ± 0.1	12.0 ± 0.3	8.0 ± 0.2
3- <i>O</i> -MeGal	19.3 ± 0.2	6.6 ± 0.3	9.9 ± 0.2	4.2 ± 0.0	3.4 ± 0.1
Gal	16.8 ± 0.2	22.4 ± 0.2	20.3 ± 0.2	14.5 ± 0.1	27.2 ± 0.4
Glc	20.3 ± 0.5	19.8 ± 0.4	21.0 ± 0.1	27.5 ± 0.4	14.5 ± 0.7

Table S5a. Detailed comparison of the oxoglutarate-binding region of putative *Chara braunii* P4Hs. Amino acid positions refer to P4H from *Chlamydomonas reinhardtii* according to Koski *et al.* (2007).

	Tyr ₁₃₄	Thr ₁₇₈	Lys ₂₃₇	Ser ₂₃₉	Thr ₂₄₁	Trp ₂₄₃
GBG60506	✓	× (Gln)	✓	× (Lys)	× (Lys)	× (Leu)
GBG60917	×	×	×	×	×	×
GBG70085	✓	✓	✓	✓	✓	✓
GBG70087	✓	× (Met)	✓	× (Lys)	× (Lys)	× (Leu)
GBG72676	×	✓	✓	✓	✓	✓
GBG72677	×	✓	✓	✓	✓	✓
GBG85197	✓	✓	✓	✓ (Val)	✓	✓

Table S5b. Detailed comparison of the iron-binding region of putative *Chara braunii* P4Hs. Amino acid positions refer to P4H from *Chlamydomonas reinhardtii* according to Koski *et al.* (2007).

	His ₁₄₃	Asp ₁₄₅	His ₂₂₇
GBG60506	✓	✓	✓
GBG60917	×	×	×
GBG70085	✓	✓	✓
GBG70087	×	×	×
GBG72676	×	×	✓
GBG72677	×	×	✓
GBG85197	✓	✓	✓

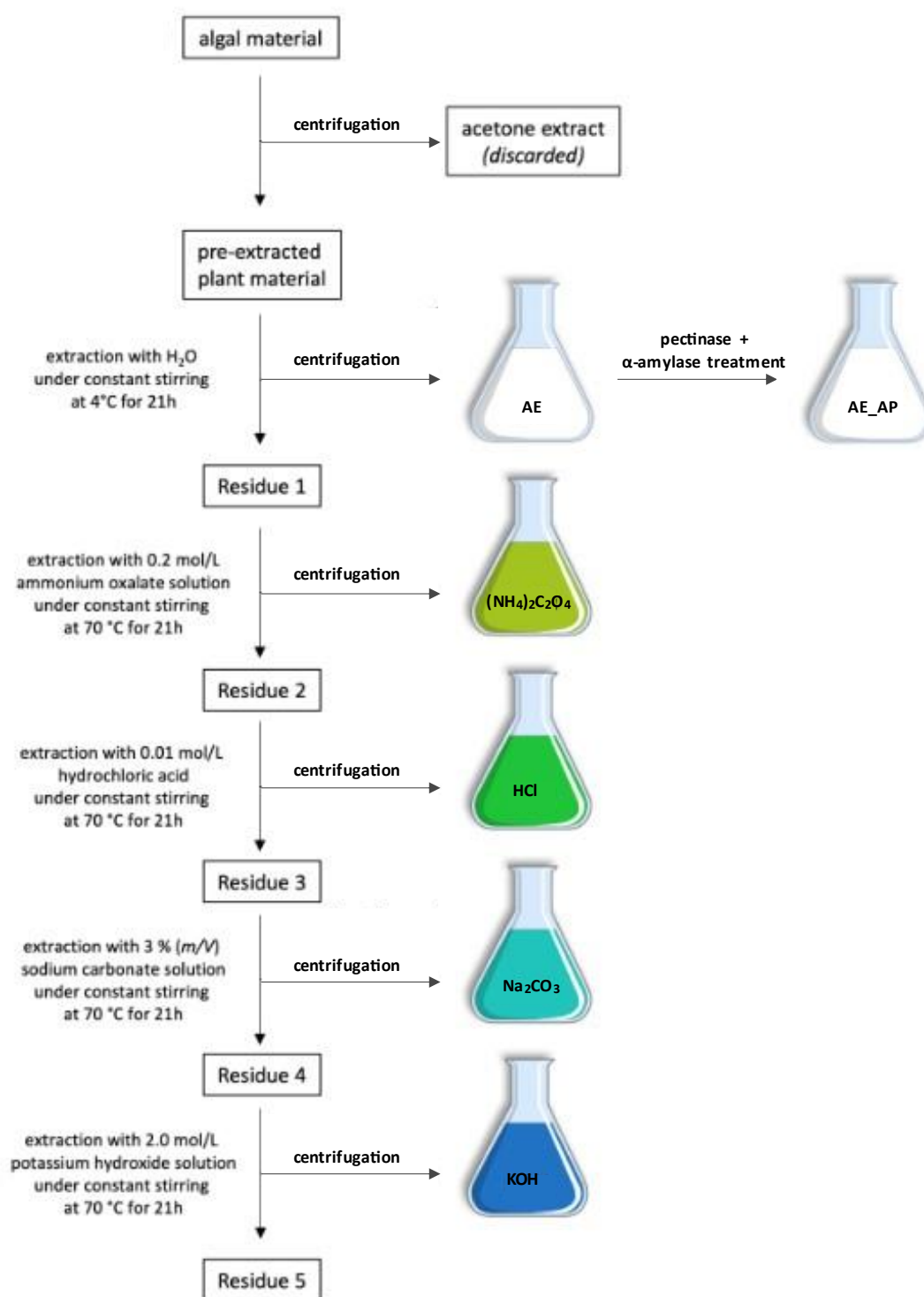


Figure S1. Schematic representation of the extraction and purification workflow. The figure is adapted modified from Pfeifer *et al.* (2022).

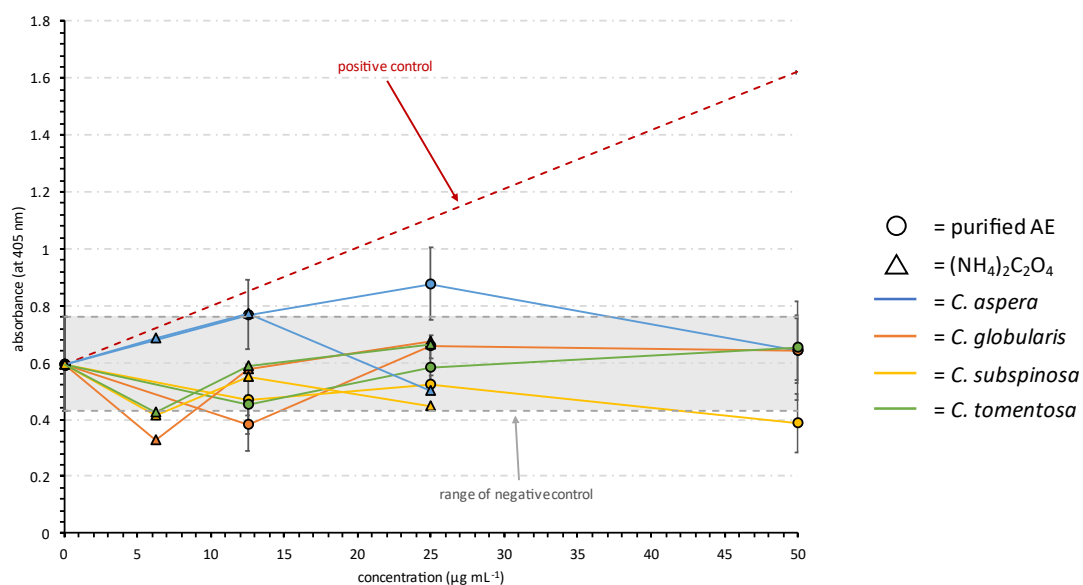


Figure S2. ELISA results of purified aqueous (AE, circles) and $(\text{NH}_4)_2\text{C}_2\text{O}_4$ extracts (triangles) with the antibody INRA-RU2 for the four *Chara* species. Positive (citrus pectin) and negative controls are highlighted in the diagram with arrows. The measured sample values are not significantly outside the range of negative control values.

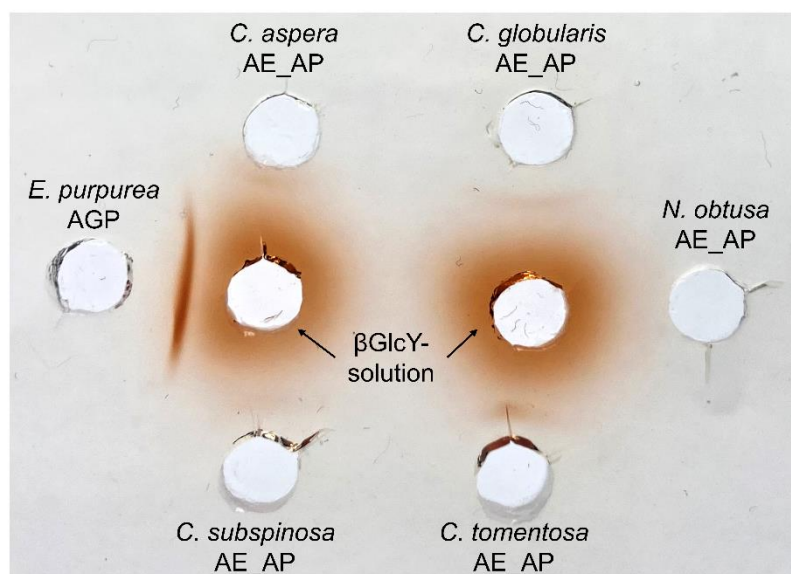


Figure S3. Gel diffusion assay with aqueous fractions after enzymatic treatment from *C. globularis*, *C. subspinoso*, *C. tomentosa* and *C. aspera* and *N. obtusa* (100 mg mL^{-1}) and βGlcY (1 mg mL^{-1}). The red precipitation line indicates presence of AGPs. As positive control, AGP from *Echinacea purpurea* (10 mg mL^{-1}) was used.

2. The cell wall of hornworts and liverworts: Innovations in early land plant evolution?

Lukas Pfeifer¹, Kim-Kristine Mueller¹ and Birgit Classen¹

¹ Pharmaceutical Institute, Department of Pharmaceutical Biology, Christian-Albrecht-University of Kiel, Gutenbergstr. 76, 24118 Kiel, Germany

ABSTRACT

An important step for plant diversification was the transition from freshwater to terrestrial habitats. The bryophytes and all vascular plants share a common ancestor that was probably the first to adapt to life on land. A polysaccharide-rich cell wall was necessary to cope with newly faced environmental conditions. Therefore, some pre-requisites for terrestrial life have to be shared in the lineages of modern bryophytes and vascular plants. This review focuses on hornwort and liverwort cell walls and aims to provide an overview on shared and divergent polysaccharide features between these two groups of bryophytes and vascular plants. Analytical, immunocytochemical and bioinformatic data were analysed. The major classes of polysaccharides, cellulose, hemicelluloses and pectins, seem to be present but have structurally diversified during evolution. Some polysaccharide groups show structural characteristics, which separate hornworts from the other bryophytes or are poorly studied in detail to give absolute statements. Hydroxyproline-rich glycoprotein backbones are found in horn- and liverworts and show differences in e.g. the occurrence of GPI-anchored arabinogalactan-proteins while glycosylation is nearly unstudied. Overall, the data appeal to researchers in the field to gain more knowledge on cell wall structures in order to understand the changes with regard to bryophyte evolution.

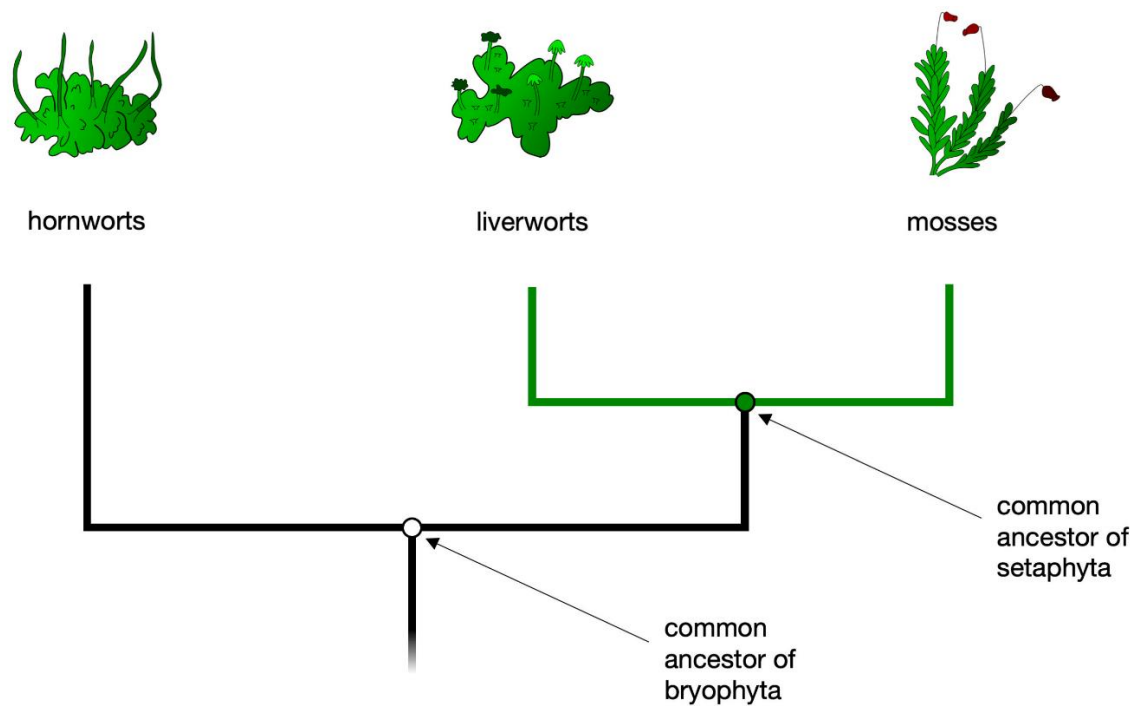


Fig. 1. Illustration of the monophyletic bryophytes and the setaphyte clade of liverworts and mosses.

INTRODUCTION

Plant terrestrialization was one of the most fundamental events in the history of life on Earth. Around 500 million years ago (mya) or even earlier (Su *et al.*, 2021), land plants evolved from streptophyte algae, which are most closely related to extant Zygnematophyceae (Wodniok *et al.*, 2011; Timme *et al.*, 2012; Ruhfel *et al.*, 2014; Wickett *et al.*, 2014; De Vries and Archibald, 2018; Leebens-Mack *et al.*, 2019). Transformation of the terrestrial biosphere resulted in today's extant lineages of land plants: bryophytes, lycophytes, ferns and spermatophytes (Delwiche and Cooper, 2015; Bowman *et al.*, 2017; Harrison, 2017; De Vries and Archibald, 2018). The bryophytes (hornworts, liverworts and mosses) are the closest living relatives of early land plants and comprise around 13,000 species, with about 9000 liverworts and 250 hornworts among them, distributed in nearly all terrestrial habitats. They contribute to critical ecological functions, including water storage, nutrient flows, interaction with other organisms, soil-building and carbon storage (Deane-Coe and Stanton, 2017; Hodgetts *et al.*, 2019). Bryophyte phylogenetic relationships are essential for an understanding of the evolution of land plant-specific traits. The relationship of hornworts, liverworts and mosses to the monophyletic vascular plant group has been discussed controversially with up to seven alternative hypotheses (Harrison, 2017; Morris *et al.*, 2018; Puttick *et al.*, 2018) of which three are well supported: bryophyte monophyletic; mosses and liverworts monophyletic with hornworts sister to tracheophytes; mosses and liverworts monophyletic with hornworts sister to all land plants (Delaux *et al.*, 2019). In conclusion, the position of hornworts was the only uncertainty and the

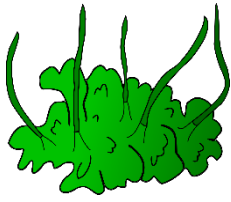
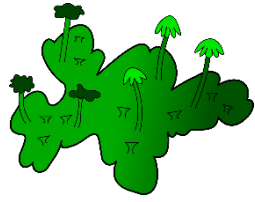
key aspect for resolving bryophyte phylogeny. To date, different studies strongly support the monophyly of the three bryophyte groups (Nishiyama *et al.*, 2004; Cox *et al.*, 2014; Puttick *et al.*, 2018; Renzaglia *et al.*, 2018; De Sousa *et al.*, 2019; Leebens-Mack, 2019; Zhang *et al.*, 2020; De Vries *et al.*, 2021; Donoghue *et al.*, 2021; Su *et al.*, 2021; see Fig. 1). Genome assemblies of bryophytes, which are rare at the moment (Marks *et al.*, 2021), will further enlighten this question. Besides these phylogenetic discrepancies, all bryophytes have in common that their life cycle is dominated by a vegetative haploid gametophyte. The unbranched sporophyte is always attached to the maternal gametophyte and develops a single sporangium. Although they share common attributes, hornworts possess a series of distinct features, e.g. a chloroplast with pyrenoids not present in other land plants but typical for many green algae. Table 1 offers a comparison of morphological features of horn- and liverworts.

The transition from water to land exposed plants to new conditions that required key physiological and structural changes. Genome sequencing of *Physcomitrium* (Rensing *et al.*, 2008), *Marchantia* (Bowman *et al.*, 2017) and *Anthoceros* (Li *et al.*, 2020; Zhang *et al.*, 2020) offers first evolutionary insights into the origin of some fundamental plant properties, e.g. new phytohormone (e.g. auxin) signaling pathways (Bowman *et al.*, 2017). These are involved in regulation of key processes of land plants like growth, development and response to terrestrial stresses.

It is obvious that the conquest of land also required major changes in cell wall composition (Sarkar *et al.*, 2009; Sørensen *et al.*, 2010). Cell walls of spermatophytes are composed of distinct chemical polymers including polysaccharides (see Fig. 2), glycoproteins and proteins arranged in a specific 3D architectural organization. Beside structural functions, biochemical properties allow re-organization of components and signalling processes during development or in response to biotic or abiotic stress (Carpita and Gibeaut, 1993; Somerville *et al.*, 2004; Cosgrove, 2018). Typical polysaccharides known from spermatophytes comprise cellulose, hemicelluloses and pectins (Fig. 2) and are accompanied by different members of hydroxyproline-rich glycoproteins (HRGPs). Search for glycosyltransferases responsible for cell wall biosynthesis in transcriptomes revealed evidence that many of these cell wall polysaccharides already existed in the common ancestor of charophytes and embryophytes (Mikkelsen *et al.*, 2014). It has been proposed that there was no substantial innovation in cell wall composition following terrestrial colonization, but rather an elaboration of a pre-existing set of polysaccharides (Sørensen *et al.*, 2010). In contrast, Harholt *et al.* (2016) proposed indeed an influence of the terrestrialization process on charophyte cell walls and dated the terrestrialization prior to the diversification of all clades of streptophyta. In this light, the multicellular freshwater charophytes evolved in a lineage that re-colonized water and kept the

“terrestrial cell wall”. Analysis of cell walls of extant bryophytes as early divergent clades of land plants sheds light on the possible cell wall composition of their common ancestor, which succeeded to perform the water-to-land transition. This review offers a detailed summary and discussion of literature on cell walls of horn- and liverworts. Moss cell walls are not included as they are reviewed in another contribution of this special issue (Ye *et al.*, 2022). The question whether there were really no innovations of cell wall composition during terrestrialisation will be discussed. Elucidation of common features but also differences between horn- and liverworts are summarized and (as far as possible) discussed in the evolutionary context. The structures of the main polysaccharides of vascular plants are shown in Fig. 2. An overview of investigations with regard to cell walls of horn- and liverworts is given in Table 2.

Table 1. Morphological differences between hornworts and liverworts*.

Generation	Feature	 hornwort	 liverwort
gametophyte	habitus	thalloid	thalloid or leafy
	gametangia	immersed	superficial
	placental interface	transfer cells with wall ingrowths	transfer cells with wall ingrowths
	chloroplast/cell	monoplastidy, with pyrenoids	polyplastidy in vegetative cells, monoplastidy in spermatogenous cells
sporophyte	special tissue	mucilage cavities	oil bodies
	habitus	elongated, with chlorophyll	small, without chlorophyll
	persistence	persistent (presence of a basal meristem)	ephemeral
	seta	×	✓
	columella	✓	×
	placental interface	haustorial cells without wall ingrowths	transfer cells with wall ingrowths
	dispersion of spores	pseudo elaters	elaters
	gas exchange	(inactive) stomata (not present in all hornworts) ⁶	respiration cavity

*This table was elaborated from the information extracted in Renzaglia *et al.*, 2000; Ligrone *et al.*, 2012; Shimamura M, 2016; Merced and Renzaglia, 2019; Frangedakis *et al.*, 2020; Henry *et al.*, 2020; Zhang *et al.*, 2020

Cellulose

Cellulose is the most abundant polysaccharide of plant cell walls and the main structural component. It is exceptionally stable under tension and hard to digest (Niklas, 2004). The linear and unbranched (1→4)-β-D-glucan structure is mostly assembled in form of parallel layers into microfibrils/nanofibrils together with a variety of structural proteins, pectins and hemicelluloses (Niklas, 2004; Lampugnani *et al.*, 2018; Seddiqi *et al.*, 2021). Each fibril consists of a large crystalline domain and a small amorphous domain (Seddiqi *et al.*, 2021). The glucan chains and the crystalline domains can vary in length, number and organisation depending on the different sources (Brown *et al.*, 1996; Seddiqi *et al.*, 2021). Just to illustrate variation, the degree of polymerization is described to range from 1,000 in *Sorghum* species to 15,000 in *Gossypium* (for an in-depth review please refer to Seddiqi *et al.*, 2021).

Biosynthesis of cellulose is performed directly at the plasma membrane by members of the cellulose synthase (CesA) family, which are described to have deep roots in eukaryotes (Popper and Tuohy, 2010; Yin *et al.*, 2014). Therefore, presence of CesA homologs in the sequenced genomes of hornworts and liverworts is not surprising (Bowman *et al.*, 2017; Li *et al.*, 2020; Zhang *et al.*, 2020). A common method for labelling cellulose is the Calcofluor white staining, a fluorescing dye for (1→4)- and (1→3)-β-glucans (Maeda and Ishida, 1967). In many cell wall research studies, this staining was positive in horn- and liverwort cell walls (Kremer *et al.*, 2004; Henry *et al.*, 2020; Renzaglia *et al.*, 2020; Henry *et al.*, 2021) thus supporting the general assumption that cellulose is present in all land plants (Brown, 1985; Popper and Tuohy, 2010). Surprisingly, only the primary cell wall of the mature pseudo elaters of the hornwort *Megaceros gracilis* and the elators of the liverwort *Radula buccinifera* gave a positive response to the dye, the secondary cell wall did not react. The authors admit that absence of staining in mature secondary walls may be due to pigmentation of the wall that masks Calcofluor staining (Kremer *et al.*, 2004).

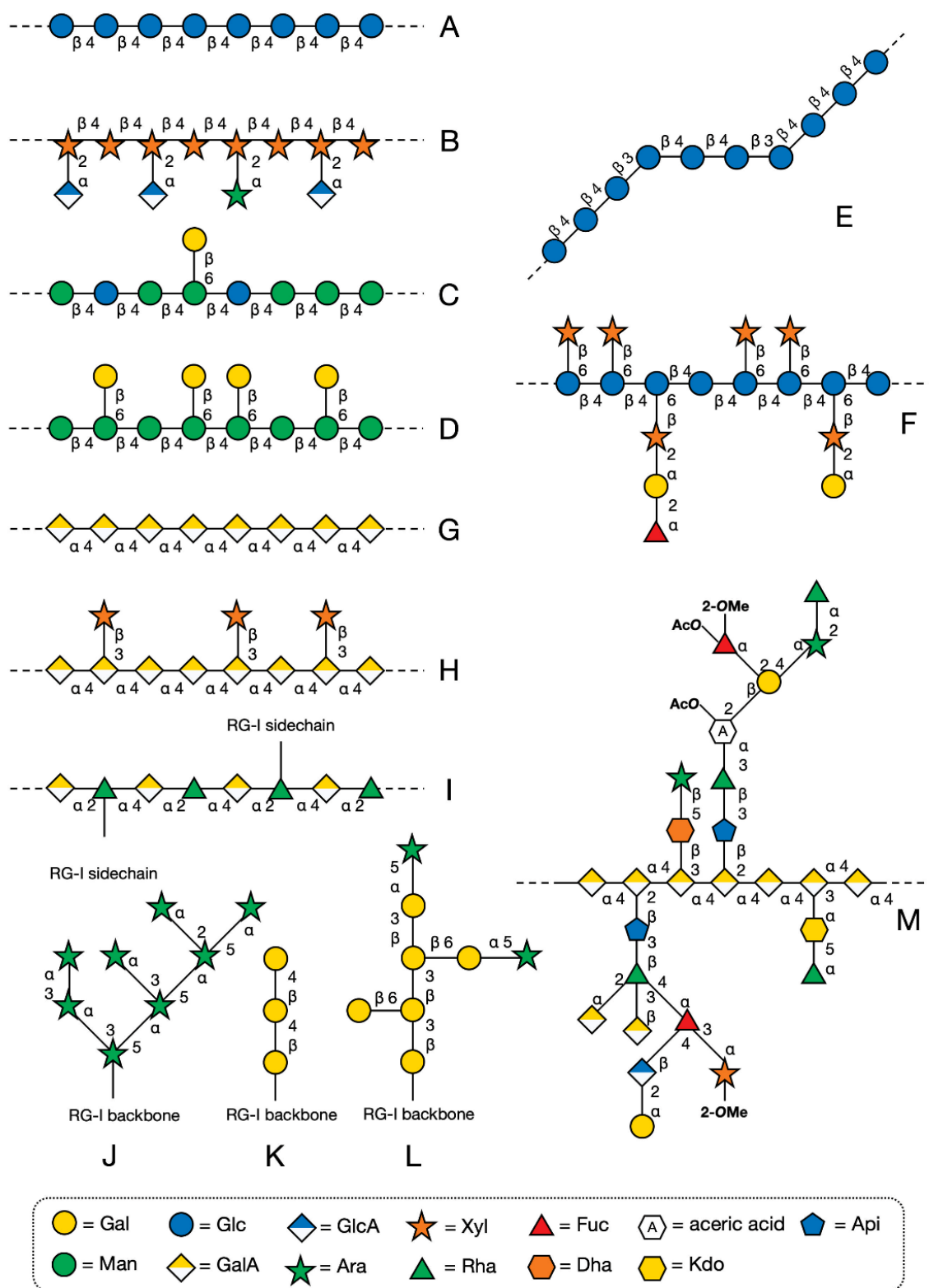


Fig. 2. Structures of the main polysaccharide components of vascular plants according to Mohnen *et al.* (2008), Peña *et al.* (2008), Scheller and Ulvskov (2010) and Atmodjo *et al.* (2013). The structures can be classified into the groups cellulose (A), hemicelluloses (B-F) and pectins (G-M). (A) cellulose, (B) glucuronoxylan, (C) (galacto-) glucomannan, (D) galactomannan, (E) mixed-linkage glucan (restricted to Poales), (F) xyloglucan, (G) homogalacturonan, (H) xylogalacturonan, (I) rhamnogalacturonan I with a selection of possible sidechains (J-L, arabinan, galactan, arabinogalactan type II) and (M) rhamnogalacturonan II. In case of RG-II, the acetylation and methylation pattern is shown (OMe and OAc) because it is conserved in most plants (Atmodjo *et al.*, 2013).

Hemicelluloses

The cellulose framework is further interwoven with different hemicelluloses (Popper and Fry, 2003; Scheller and Ulvskov, 2010). This group consists of xylans, xyloglucans, (gluco-) mannans and mixed-linkage glucans (MLGs) and contributes to the biomechanical stability of the cell wall, especially by interaction with cellulose fibrils and during growth (Hayashi *et al.*, 1989; Scheller and Ulvskov, 2010; Lampugnani *et al.*, 2018). In the past, hemicelluloses were often classified according to their alkali-solubility (Doner and Hicks, 1997). Scheller and Ulvskov (2010) revised this classification and defined hemicelluloses as polysaccharides that have a β -1,4-linked core structure with the ether group between C1 and C4 in equatorial position (for a detailed explanation of the chemical background, please refer to that review article). Several studies contributed to the elucidation of hemicelluloses in the cell wall of horn- and liverworts (see below).

Xylans

Xylans have a backbone consisting of (1 \rightarrow 4)- β -xylose with a high degree of substitution (York and O'Neill, 2008; Hatfield *et al.*, 2016; Peña *et al.*, 2016; Tryfona *et al.*, 2019) and play an important role in crosslinking with other structural components, especially cellulose (Lampugnani *et al.*, 2018). In grasses and other commelinid monocots, (glucuronoarabino-) xylans are dominating (Carpita and McCann, 2002). Especially in grasses, arabinoxylans are known to be decorated with ferulic acid, which contributes firstly to their interaction with other cell wall components but secondly to other functions like pathogen resistance and growth cessation (De O. Buanafina, 2009). Taking the near ground lifestyle of bryophytes into account, both functions are sensible. Synthesis of ferulic acid in bryophytes seems to be enzymatically possible (see section “lignin”, De Vries *et al.*, 2021).

Carafa *et al.* (2005) investigated the occurrence of xylans in all bryophyte lineages and tracheophytes with the monoclonal antibodies LM10 and LM11. Both antibodies recognize unsubstituted xylans, but LM11 can also bind to substituted arabinoxylans (McCartney *et al.*, 2005). According to Ruprecht *et al.* (2017), LM10 specifically tracks the nonreducing ends of xylan polymers. Microscopic investigations detected LM10 and LM11 xylan epitopes in all extant tracheophyte lineages and proposed a deep connection between occurrence of xylans and the evolution of mechanical and vascular tissues (Carafa *et al.*, 2005). Accordingly, LM10 epitopes were not present in liverworts, hornworts and mosses. Interestingly, LM11 binding was heterogeneous in the different bryophytes. Whereas no binding of LM11 was detected in liverworts and mosses, this antibody detected xylan epitopes in pseudo elaters and spores of

hornworts. This is an indication that at least some tissues of the hornwort sporophyte produce arabinoxylan. Presence of arabinoxylan in the hornwort *Anthoceros* has also been suggested by O'Rourke *et al.* (2015). It is important to mention, that due to specificity of the antibodies LM10 and LM11, Carafa *et al.* (2005) did not exclude occurrence of highly substituted xylans in all bryophyte groups. Presence of glucuronoxylans in *Physcomitrium* as a model organism for mosses has been shown (Kulkarni *et al.*, 2012). Up to now, no xylan has been isolated and characterized from a horn- or a liverwort.

Mannans

Mannans have a (1→4)-β-D-backbone of mannose, whereas glucomannans combine mannose and glucose in a nonrepeating pattern. These backbones can be decorated with a (1→6)-α-D-galactose to form galactomannans and galactoglucomannans (Scheller and Ulvskov, 2010; Dehorst *et al.*, 2019). These complex heteroglycans have storage functions (especially in seeds, Buckeridge *et al.*, 2000) and contribute to embryogenesis (Goubet *et al.*, 2009), as well as growth and developmental processes (Benova-Kakosova *et al.*, 2006, Liepman *et al.*, 2007) *via* signalling functions *in planta*. Responsible for the mannan backbone (Dhugga *et al.*, 2004; Liepman *et al.*, 2005) as well as the glucomannan (Goubet *et al.*, 2009) biosynthesis is the CSLA gene family. Verhertbruggen *et al.* (2011) showed mannan synthase activity also in the CSLD gene family. Members of these gene families were annotated in the genomes of *Marchantia polymorpha* (Yin *et al.*, 2014; Bowman *et al.*, 2017) and *Anthoceros angustus* (Zhang *et al.*, 2020). Mannans are the main hemicellulosic components in many genera of green algae (Rodriguez-Gacio *et al.*, 2012), thus supporting deep roots of these polysaccharides in plant evolution.

Up to now, no purified mannans have been isolated from liverworts and hornworts. Popper and Fry (2003) accounted the mannose content they detected with paper chromatography in TFA hydrolysates of primary cell walls of eleven liverworts and one hornwort to the presence of mannans. The results showed that the yield of mannose was much higher in the primary cell wall of liverworts and mosses than in hornworts. This could be a hint that mosses and liverworts may be more closely related to each other than to hornworts. Happ and Classen (2019) investigated *Marchantia polymorpha* extracts and showed mannose contents of 6 – 10 % in different cell wall fractions. A pectic subfraction from *Marchantia* cell walls (Konno *et al.*, 1987) consisted of equal amounts of mannose, glucose, galactose and galacturonic acid, maybe indicating the presence of an acidic galactoglucomannan. As mentioned above, most studies accounted the mannose content after cell wall hydrolysis to occurrence of mannans. To strengthen that hypothesis, degrading enzymes for mannans (for review see Malgas *et al.*,

2015), e.g. β -mannanase (EC 3.2.1.78) and β -mannosidase (EC 3.2.1.25) could be used to specifically cleave mannan-derived oligosaccharides which could then be further characterized with chromatographic (e.g. Popper and Fry, 2003) or electrophoretic (e.g. Goubet *et al.*, 2002) methods.

Additionally, the presence of mannan and (1 \rightarrow 4)- β -manno-oligosaccharide can be detected with the antibody LM21 (Marcus *et al.*, 2010). Henry *et al.* (2020 and 2021) tested this antibody in placental cell walls at the interface of sporophyte and gametophyte in the hornwort *Phaeroceros carolinianus* and the liverwort *Marchantia polymorpha*. Interestingly, the antibody reaction was only positive in the placental cells of the liverwort but not in that of the hornwort. It has to be taken into account that in this work only the placental cells were investigated, which are locally restricted specialized cells. Furthermore, the epitopes of the available anti-mannan antibodies tend to be masked *in situ* by other cell wall components, e.g. homogalacturonans (Marcus *et al.*, 2010). Therefore, presence of mannans in hornworts should be further verified by pre-treatments with pectate lyase, which was shown to be effective to elevate mannan detection levels (Marcus *et al.*, 2010).

Mixed-linkage glucans

MLGs consist of an unsubstituted linear chain of (1 \rightarrow 3),(1 \rightarrow 4)- β -D-glucans that show distinct ratios of (1 \rightarrow 3) to (1 \rightarrow 4) linkages in connection to their physicochemical properties (Burton and Fincher, 2009). Additionally, they seem to have physiological functions in pathogen defense where they can be active as microbe-associated molecular patterns (MAMPs, Rebaque *et al.*, 2021). Search for MLGs in different embryophytes revealed restricted presence in the Poales order (Popper and Fry, 2003) since their levels of xyloglucans are very low (Carpita and McCann, 2002). Surprisingly, in the eusporangiate fern *Equisetum arvense* (Sørensen *et al.*, 2008) and other *Equisetum* species (Fry *et al.*, 2008) as well as in the charophyte green algae species *Micrasterias denticulata* (Eder *et al.*, 2008), MLGs are also present.

Popper and Fry (2003) investigated numerous embryophytes to determine the absence or presence of MLGs in the different evolutionary lineages of embryophytes by using lichenase digestion in combination with paper-chromatographic detection of hydrolysis products. The hornwort *Anthoceros caucasicus* as well as 10 liverwort species completely lacked presence of characteristic lichenase-digestion products of MLGs. Only the liverwort *Lophocolea bidentata* showed presence or absence of MLG-like molecules at different collection dates (Popper and Fry, 2003). A seasonal or lifecycle-dependent change of MLGs can be possibly connected with an intermediate storage function as hypothesized by Burton and Fincher (2014) based on cereal grain MLG levels. The MLG-like molecules detected in *Lophocolea* differed from

homopolymeric MLGs (like e.g. from barley) by presence of relevant Ara contents (Popper and Fry, 2003). In the cell wall of *Physcomitrium patens*, (1→3),(1→4)-β-D-arabinoglucans have been detected. Compared to MLGs, 1,3-Glcp is replaced by 1,3-Araf in this unusual polysaccharide (Roberts *et al.*, 2018).

The cellulose synthase-like (CSL) gene families CSLF and CSLH were characterized from rice and barley and contain the responsible enzymes of MLG biosynthesis (Burton *et al.*, 2006; Doblin *et al.*, 2009). Nucleotide sequences annotated as members of these gene families were absent in the genome of the liverwort *Marchantia polymorpha* (Yin *et al.*, 2014; Bowman *et al.*, 2017), as well as in the genome of the hornwort *Anthoceros angustus* (Zhang *et al.*, 2020). Interestingly, bioinformatic investigations revealed that the biosynthetic machinery for arabinoglucans isolated from *Physcomitrium* might also be present in horn- and liverworts (Roberts *et al.*, 2018).

To conclude, proof of MLGs in hornworts and liverworts was not given, but presence of arabinoglucans, showing structural and putatively functional similarities but lacking lichenase-digestibility. Further studies should be performed to support the knowledge on that novel polysaccharide group. Furthermore, more knowledge would help to understand the evolutionary relations of MLGs, occurring in very distinct lineages (like cereals and horsetails).

Xyloglucans

Xyloglucans are the most abundant cellulose cross-linking polysaccharides in the primary cell wall of eudicots and non-commelinid monocots. In contrast to that in grasses and other commelinid monocots (glucuronoarabino-) xylans are dominating (Penning *et al.*, 2019). Xyloglucans consist of a (1→4)-β-D-glucose (G) main chain, substituted with (1→6)-α-D-xylose (X) side chains. The core of the (1→4)-chain is biosynthesized by the CSLC gene family (Cocuron *et al.*, 2007) and then further modified by the xyloglucan endotransglycosylase/hydrolase (XET/XTH) class of enzymes (Popper, 2008; Sarkar *et al.*, 2009; Lampugnani *et al.*, 2018). Xyloglucans interact with cellulose microfibrils and regulate cell wall strengthening (Dehors *et al.*, 2019). They can be further decorated with other sugars, usually galactose, arabinose and fucose (Scheller and Ulvskov, 2010). In *Arabidopsis*, seven different GTs (glycosyltransferases) are necessary to accomplish the biosynthesis of a completely branched xyloglucan (Zabotina *et al.*, 2021).

In the liverwort and hornwort genomes of *M. polymorpha* and *A. angustus* CSLC and XET sequences are annotated, thus supporting presence of xyloglucans in both bryophyte lineages (Yin *et al.*, 2014; Bowman *et al.*, 2017; Zhang *et al.*, 2020).

The classification of xyloglucans based on X and G nomenclature is well explained in Fry *et al.* (1993) and Peña *et al.* (2008). Most seed-bearing plants and ferns possess an XXXG-type, Lamiids have an XXGG-type and grasses an XXGGG-type. Interestingly, the xyloglucan types of hornworts and liverworts differ (Fig. 3). The thalloid liverwort *Marchantia polymorpha* has an XXGG-type with atypical residues like 2,4-linked α -D-Xylp and β -D-GalpA (Peña *et al.*, 2008). The hornworts *Anthoceros agrestis*, *Phaeoceros sp.* and *Megaceros sp.* possess an XXXG-type, like the most seed-bearing plants and ferns (Peña *et al.*, 2008). Remarkably, Peña *et al.* (2008) found some fucosylated side chains in *Megaceros sp.* using MALDI-TOF-MS analysis and 2D-NMR spectra. At that time, this fucosylation pattern was only known for tracheophytes thus suggesting a closer relationship of hornworts to tracheophytes than to liverworts and mosses.

Recent investigations revealed the presence of fucosylated and galactosylated xyloglucans in the charophyte algae species *Mesotaenium* (Mikkelsen *et al.*, 2021), proposing that these changes of the basic xyloglucan structure already occurred in the most recent common ancestor of CGA and embryophytes. A complex xyloglucan genetic machinery has been found in most groups of charophyte algae excluding *Mesostigma* (Mesostigmatophyceae) and *Chlorokybus* (Chlorokybophyceae) which belong to the earliest diverging groups of the streptophytes (Del Bem, 2018).

Popper and Fry (2003) studied the primary cell wall of one hornwort, two thalloid liverwort and nine leafy liverwort species. Xyloglucan was detected in all of them with a methodology combining Driselase digestion and chromatography. The yields of the digestion analysis were lower compared to those of angiosperms, which can be a result of lower concentrations or differences in digestibility due to different structures of xyloglucans in bryophytes. It is important to mention that also methods based on antibodies (see below) have this possible pitfall due to masked or slightly modified epitopes.

Various xyloglucan epitopes are detectable with several monoclonal antibodies, including CCRC-M1, recognizing α -Fuc-(1 \rightarrow 2)- β -Gal-epitopes at xyloglucans or rhamnogalacturonan I (Puhlmann *et al.*, 1994), LM25 for galactosylated xyloglucans (Pedersen *et al.*, 2012) and LM15, detecting XXXG motifs of xyloglucan with only slight galactose substitutions (Marcus *et al.*, 2008).

The monoclonal antibody CCRC-M1 was used in two studies (Ligrone *et al.*, 2002; Kremer *et al.*, 2004) and detected fucosylated side groups of xyloglucan in the cortical parenchyma cells of two leafy (*Haplomitrium gibbsiae* and *H. ovalifolium*) and two thalloid (*Hymenophyton flabellatum* and *Symphyogyna undulata*) liverworts (Ligrone *et al.*, 2002). This xyloglucan epitope was also present in water-conducting cells, but only in those of the leafy liverworts, and

in the secondary cell walls of mature elaters of the leafy liverwort *Radula buccinifera*, but not in the cell walls of mature pseudo elaters of the hornwort *Megaceros gracilis* (Kremer *et al.*, 2004). This is in contrast to the identification of fucosylated xyloglucans in *Megaceros* by Peña *et al.* (2008). Additionally, placental cells of the thalloid liverwort *Marchantia polymorpha* and the hornworts *Phaeroceros carolinianus* and *Phaeroceros laevis* were stained positively with LM15 (Henry *et al.*, 2020; Henry *et al.*, 2021). Again, this is in contrast to the finding that only hornworts possess the XXXG type (see above, Peña *et al.*, 2008). Both discrepancies might be related to the use of different tissues in the different studies.

Galactosylated xyloglucans (LM25) were shown to be present in the spore wall of various hornworts (Renzaglia *et al.*, 2020) and in the placental cells of the thalloid liverwort *Marchantia polymorpha* and the hornwort *Phaeroceros carolinianus* (Henry *et al.*, 2020; Henry *et al.*, 2021). With the same antibody (LM25), galactosylated xyloglucans were identified as the main polysaccharides in the rhizoids of the thalloid liverworts *Blasia pusilla*, *Lunularia cruciata* and *Marchantia polymorpha* (Galloway *et al.*, 2018). Xyloglucan was secreted by the rhizoids of these liverworts and it was assumed that the secretion of xyloglucan plays an important role in the aggregation of the soil and is a stimulating factor for the interaction with the environment. The occurrence of a rhizospheric environment was proposed to be an influential factor in the colonization of land. Additionally, xyloglucan deficient *Arabidopsis* mutants showed lack of cell wall stiffness (Cavalier *et al.*, 2008).

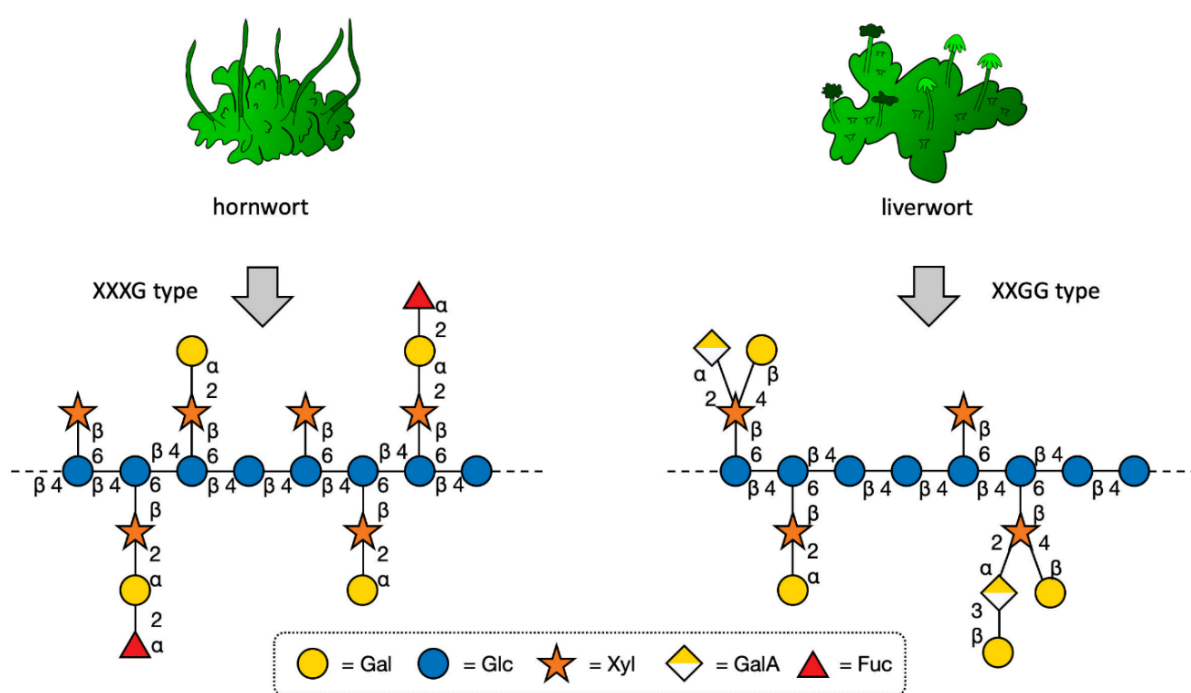


Fig. 3. Xyloglucan structures of hornworts (left) and liverworts (right) according to Peña *et al.* (2008).

Pectic polysaccharides

From a structural point of view, pectins are the most complex group of plant cell wall polysaccharides. This complexity most likely reflects their diverse functions in processes like growth, morphogenesis, development, cell expansion, cell adhesion and interaction with the environment, e.g. in defense (for review see Mohnen, 2008; Caffall and Mohnen, 2009). Generally, pectins can be subdivided into (substituted) homogalacturonan (HG), rhamnogalacturonan-I (RG-I) and rhamnogalacturonan-II (RG-II). Even though the latter mentioned sound similar, their main and side chains differ remarkably. While the backbone of RG-II resembles that of HG, (a linear α -1,4-linked galacturonic acid chain), RG-I contains the repetitive core-disaccharide of α -1,4-GalA and α -1,2-Rha. Within the group of substituted HGs, apio- and xylogalacturonans are the most common derivatives.

Most publications on bryophyte pectic polysaccharides used monoclonal antibodies raised against pectic epitopes of embryophytes. Antibody collections (e.g., from Professor Hahn, Complex Carbohydrate Research Center, University of Georgia, Athens and Professor Knox, University of Leeds), offer numerous antibodies against HG structures (either methyl-esterified or de-esterified) and RG-I side chains (namely 1,4-galactan and 1,5-arabinan).

Evidence for presence of homogalacturonans in horn- and liverworts has been shown by numerous studies (Ligrone *et al.*, 2002; Kremer *et al.*, 2004; Merced and Renzaglia, 2019; Renzaglia *et al.*, 2020; Henry and Renzaglia, 2021; Henry *et al.*, 2021). This is not surprising, as occurrence of HGs with different degrees of methyl-esterification has also been proven for charophyte green algae, thus supporting deep roots in streptophyta (Sørensen *et al.*, 2010; Sørensen *et al.*, 2011). Identification of pectin methyltransferases in the genome of *M. polymorpha* is another proof of presence of HG in bryophytes (Bowman *et al.*, 2017).

The core RG-I backbone, consisting of repetitions of α -1,4-GalA and α -1,2-Rha, was indirectly described to be present in the liverwort *Marchantia polymorpha* by the heterologous expression of RG-I rhamnosyltransferases MpRRT1 and MpRRT3 in *Nicotiana benthamiana* followed by biochemical characterization (Wachananawat *et al.*, 2020). It was shown that these rhamnosyltransferases (RRT) extend an existing RG-I chain by addition of UDP-Rha, which is consistent with the RRT activities in *Arabidopsis thaliana* (Takenaka *et al.*, 2018). To the best of our knowledge, no study used the antibodies INRA-RU1/RU2 (Ralet *et al.*, 2010) directed against the repetitive disaccharide unit of RG-I to investigate hornworts and liverworts. This tool seems to be a straightforward approach to complement the biochemical data. In a comparative study based on their own recent works on placental walls of *Marchantia polymorpha* (Henry *et al.*, 2020) and two species of *Phaeoceros* (Henry *et al.*, 2021), Henry and Renzaglia (2021) showed potential differences in RG-I side chain structures. While the

liverwort completely lacked reactivity with LM5 (1,4-galactan side chains) and LM13 (1,5-arabinan side-chains) in the placental interface between sporophyte and gametophyte, the hornworts showed only reactivity of LM5 (supported also by Merced and Renzaglia, 2019). Presence of RG-I epitopes recognized by LM5 in hornworts and their absence in liverworts was confirmed by Kremer *et al.* (2004). Here, the authors detected restricted presence of the LM5 epitope in the primary walls of *Megaceros pseudo elaters*, while elaters of *Radula buccinifera* (liverwort) lacked reactivity. The antibody CCRC-M7 (Puhlman *et al.*, 1994; Steffan *et al.*, 1995) detects arabinosylated 1,6-linked galactans present as side chains of RG I (and also of arabinogalactan-proteins, AGPs) and was shown to bind to liverwort and hornwort tissues, especially to water-conducting cells of liverworts (Ligrone *et al.*, 2002; Kremer *et al.*, 2004). As CCRC-M7 was generated against RG-I purified from suspension-cultured *Acer pseudoplatanus*, we assume that this antibody indicates the presence of RG-I rather than AGP. A recently described antibody against RG-II epitopes (Zhou *et al.*, 2018) could contribute to our current understanding of RG-II in bryophytes (De Vree *et al.*, 2021). To-date, this antibody has not yet been tested for binding to bryophyte tissues. As RG-II contains four conserved side-chains with 12 very unusual glycoses (D-apiose, L-aceric acid, 2-*O*-methyl L-fucose, 2-*O*-methyl D-xylose, L-galactose, 2-keto-3-deoxy-D-lyxo-heptulosaric acid and 2-keto-3-deoxy-D-manno-octulosonic acid, see O'Neill *et al.*, 2004) an antibody directed against these side-chains is likely to be very specific and to lack cross-reactivities with other (pectic) polysaccharides. An innovative approach of Matsunaga *et al.* (2004) made use of boron crosslinking properties of RG-II and quantified boron by ICP-MS analysis in different taxonomic groups of land plants (including hornworts, liverworts and mosses). The authors detected only very low amounts of boron in bryophytes (including four liverwort and one hornwort species), thus concluding that bryophyte walls contain less than 1 % of the amount of RG-II that is present in the walls of tracheophytes. The study failed in isolation of RG-II from bryophytes due to the low amount. Smith *et al.* (2016) reported identification and functional characterization of a homolog of UDP-Api synthase (UAS) from the hornwort *Megaceros vicentianus* and the liverwort *Marchantia palacea* and detected apiose in aqueous methanolic extracts of bryophytes but not in their cell walls. The authors concluded that bryophytes lack some of the GT machinery for synthesis of apiose-containing cell wall glycans, although they may have the ability to synthesize apiosylated secondary metabolites. Therefore, it has to be elucidated in more detail whether RG-II is present in the cell walls of bryophytes (Bar-Peled *et al.*, 2012).

Different pectic fractions have been isolated from the liverwort *M. polymorpha* (Konno *et al.* 1987; Happ and Classen, 2019) and proposed the presence of homogalacturonan and rhamnogalacturonan in lower amounts. Furthermore, hydrolysis of *Anthoceros* pectins with

Driselase released Rha and Gal, suggesting RG-I (O'Rourke *et al.*, 2015). Up to now, no pure pectic polysaccharide has been isolated and characterized from a hornwort or a liverwort. Current knowledge is mainly based on binding of antibodies generated against polysaccharides of spermatophytes, which show more or less cross-reactivities (see Pattathil *et al.*, 2010). A methodology for estimation of cellulose, hemicellulose and pectin content in mosses has been published (Roig-Oliver *et al.*, 2021). An alcohol insoluble residue (AIR) reflecting the total cell wall material was prepared, destarched and fractionated by trifluoroacetic acid hydrolysis. The fractions were further analyzed by colorimetric assays (Dubois *et al.*, 1956; Blumenkrantz and Asboe-Hansen, 1973) in order to quantify cellulose, hemicelluloses and pectin. This methodology would be a rapid possibility to get a quantitative overview of these main polysaccharide groups in horn- and liverworts.

Callose

Callose is a linear (1→3)-β-D-glucan homopolysaccharide with some (1→6)-β-D-glucose side branches. The biosynthesis is performed by callose synthase (CalS)/glucan synthase-like (GLS) complexes at the plasma membrane (Verma and Hong, 2001; Li *et al.*, 2003; Dehors *et al.*, 2019) and the degradation and recycling of callose takes place through (1→3)-glucan hydrolase genes (Dehors *et al.*, 2019). Callose plays a crucial role in many plant growth and development processes, such as pollen wall formation and patterning, pollen tube growth, plasmodesmata regulation, cell plate formation, sieve pore development, sporogenesis and spore wall development (Chen and Kim, 2009; Schuette *et al.*, 2009; Renzaglia *et al.*, 2015; Dehors *et al.*, 2019; Henry *et al.*, 2021). In addition, callose is involved in wound healing and in response to biotic and abiotic stress (Chen and Kim, 2009; Schuette *et al.*, 2009; Berry *et al.*, 2016; Lampugnani *et al.*, 2018; Henry *et al.*, 2020). Callose is often synthesized in particular cells and tissues only at specific stages of development and forms local depositions of temporal character. Due to this transient nature, callose is sometimes difficult to detect (Renzaglia *et al.*, 2015).

Aniline blue fluorescence staining is often used to identify callose in plant tissues. Since this dye also detects other glucan structures (Smith and McCully, 1978), the monoclonal antibody BS 400-2 (also called “anti-callose antibody”, Meikle *et al.*, 1991) is a more specific tool which can be combined with fluorescence or electron microscopy. This antibody recognizes only (1→3)-β-linked glucan structures including at least with five glucopyranose residues (Meikle *et al.*, 1991).

Using anilin blue fluorescence, no callose could be detected in sporophyte seta cells of the leafy liverwort *Lophocolea heterophylla* (Thomas, 1977) and in cell walls of mature elaters/pseudo

elaters of the leafy liverwort *Radula buccinifera* and the hornwort *Megaceros gracilis* (Kremer *et al.*, 2004). The absence of callose in these tissue types is not surprising because callose deposition is often connected with changing or transforming tissues and cells (e.g. cell plates, plasmodesmata, tip growing cells, pollen tubes or stomata, Schneider *et al.*, 2016).

Several studies showed presence of callose in cell walls of horn- and liverworts, e.g., in regenerated cell walls of protoplasts of the thalloid liverwort *Marchantia polymorpha* (Shibaya and Sugawara, 2007). Ligrone *et al.* (2002) detected callose in water-conducting cells and cortical parenchyma cells of two leafy liverworts, *Haplomitrium gibbsiae* and *Haplomitrium ovalifolium*, and two thalloid liverworts, *Symphyogyna undulata* and *Hymenophyton flabellatum*, by using the anti-callose antibody. Callose labelling was especially strong in the water-conducting cells of the thalloid liverworts, while the two leafy liverworts showed no reaction.

Anilin blue and the antibody BS 400-2 were used to search for callose at the placental interface of different bryophytes (Henry *et al.*, 2020; Henry *et al.*, 2021). Liverworts contain transfer cells on the gametophyte and the sporophyte side of the placenta, whereas hornworts have transfer cells only on the gametophyte side. The sporophyte side consists of smooth-walled haustorial cells that intermingle with the transfer cells of the gametophyte. In these studies, callose could only be detected in the gametophyte transfer cells of the hornworts.

Sporogenesis is one of the key processes that require callose. Cell walls of various hornworts and one thalloid liverwort were screened for callose to elucidate its involvement in sporogenesis and spore wall development (Renzaglia *et al.*, 2015; Renzaglia *et al.*, 2020). Callose was detectable in the spore walls of the hornworts *Anthoceros agrestis*, *Leiosporoceros dussii*, *Megaceros flagellaris*, *Notothylas orbicularis*, *Phaeoceros carolinianus* but not in the derived hornwort *Dendroceros crispatus*, an epiphyte that produces multicellular endosporic spores. Comparable to the liverwort *Pellia epiphylla*, callose only appears in developing cell walls of the multicellular spores as cell plates are formed (Renzaglia *et al.*, 2020). In *Sphaerocarpos* spore wall development, high amounts of callose are deposited outside of the sporocyte plasmalemma prior to formation of the exine (Renzaglia *et al.*, 2015).

Involvement of callose synthases (CalS) in pollen development (CalS5, CalS11, CalS12) and gametogenesis (CalS9, CalS10) underlines the important roles of callose in these processes (Piršelová and Matušíková, 2013). Interestingly, sequences similar to CalS10 and 12 from *A. thaliana* were annotated in the genome of *Anthoceros angustus* (Zhang *et al.*, 2020). By reviewing all the data presented in this paragraph there is good evidence to conclude general presence of callose in horn- and liverworts when looking at specialized tissues.

Hydroxyproline-rich glycoproteins (HRGPs)

HRGPs are a major group of cell wall proteins which comprise the three categories arabinogalactan-proteins (AGPs), proline-rich proteins (PRPs) and extensins (Johnson *et al.*, 2018). In AGPs, the polysaccharide part is dominating (around 90 %) with the main monosaccharides arabinose (Ara) and galactose (Gal). The glycan part of extensins is around 50 % whereas the proline-rich proteins are only minimally glycosylated. As the different groups of HRGPs are highly diverse also with regard to functions, these are mentioned in the subsections below.

AGPs

The protein backbones of AGPs are rich in hydroxyproline/proline (Hyp/Pro), alanine (Ala), serine (Ser) and threonine (Thr), and these amino acids are regularly arranged as Ala–Pro, Ser–Pro, and Thr–Pro. The arabinogalactan moieties are covalently linked to the protein moiety *via* hydroxyproline and are characterized by a typical galactan core structure consisting of a backbone of 1,3-linked β -D-Galp, branched at position 6 to 1,6-linked β -D-Galp side chains, which are substituted with α -L-Araf and often also terminal GlcpA (for review see Strasser *et al.*, 2021). Especially for angiosperms, functions of AGPs in different processes like cell growth, cell proliferation, pattern formation, programmed cell death, plant microbe interactions and sexual reproduction have been shown (for review see Seifert and Roberts, 2007; Ma *et al.*, 2018). Some AGPs are linked to the plasma membrane by a glycosylphosphatidylinositol (GPI)-anchor (Youl *et al.*, 1998), which makes them ideal candidates for communication between the cytoplasm and the extracellular matrix.

Hybrid AGPs combine features of different classes of HRGPs, e.g. AGPs and extensins, whereas chimeric AGPs combine AGP motifs with a non-HRGP domain (Ma *et al.*, 2017). One subclass of the chimeric AGPs, the fasciclin-like AGPs (FLAs) consist of both fasciclin domains and AGP regions. The fasciclin domain has been described as capable of binding multiple ligands and being involved in cell adhesion (for review, see Seifert, 2018).

Occurrence of AGPs in spore-producing land plants has been already shown in the 1970s by gel-diffusion assays with the β -glucosyl Yariv reagent (β GlcY, Clarke *et al.*, 1978) and included the liverwort *Lunularia cruciata* (Marchantiaceae). Although the specific interaction of AGPs with these artificial reagents is still not fully understood, it is known that mainly the galactan part of AGPs is responsible for binding and especially 1,3-linked Gal oligosaccharides are essential (Kitazawa *et al.*, 2013, Paulsen *et al.*, 2014). Due to the red colour of the reagent, the formation of a red precipitation line with AGPs in gel diffusion offers the opportunity to detect AGPs even in crude plant extracts. In the 1980s, the presence of AGPs was shown in a great

number of liverwort species from different families and orders by staining plant tissue with β GlcY and the authors concluded that AGPs are common for liverwort cell walls (Basile and Basile, 1987). Staining of elaters/pseudo elaters of the liverwort *Radula* and the hornwort *Megaceros* with β GlcY revealed presence of AGPs in *Megaceros* pseudoelaters, but not in *Radula* elaters (Kremer *et al.*, 2004). These results were confirmed by staining with the antibodies JIM8 and LIM13, two monoclonal antibodies directed against glycan epitopes of AGPs (Kremer *et al.*, 2004). No binding to *Radula* elaters was observed, but both antibodies bound to the central secondary wall layer of *Megaceros* pseudoelaters (Kremer *et al.*, 2004). Immunocytochemical differences in liverwort elaters and hornwort pseudoelaters (Kremer *et al.*, 2004; Carafa *et al.*, 2005), underline that these cells are not homologous (Renzaglia *et al.*, 2000).

Water-conducting cells of different liverworts were also not labelled with JIM8, indicating absence of AGPs (Ligrone *et al.*, 2002). In contrast, JIM8 labelling indicated occurrence of AGPs in the cortical parenchyma of these liverwort species (Ligrone *et al.*, 2002). Results for LM6, an arabinan antibody detecting also Ara-sidechains of AGPs, supported these findings (very weak binding to WCC, good binding to CP; Ligrone *et al.*, 2002). JIM8, JIM13, LM2 and LM6 have been used to detect AGPs in the placenta at the gametophyte-sporophyte interface of *Marchantia* and the hornwort *Phaeoceros* (Henry *et al.*, 2020; Henry *et al.*, 2021). Whereas JIM13 and LM2 bound to this tissue in both species, JIM8 exclusively labelled the liverwort- and LM6 the hornwort placenta (Henry *et al.*, 2020; Henry *et al.*, 2021). To the best of our knowledge, no AGP from a hornwort and only one AGP from a liverwort (*Marchantia polymorpha*, Happ and Classen, 2019) has been isolated and structurally characterized up to now. Precipitation with β GlcY yielded 0.18 % AGP in relation to the dry weight of the liverwort, which is comparable to AGP content in the mosses *Sphagnum* and *Physcomitrium*, but 3-fold higher compared to *Polytrichastrum* (Bartels *et al.*, 2017). The carbohydrate moiety of the *Marchantia* AGP reflected the typical composition known from seed plant AGPs with the main components 1,3,6-linked Galp, 1,3-linked Galp and terminal Araf. This is in line with the finding that members of glycosyltransferase families involved in AGP synthesis (e.g. GT14, GT29, GT31; Showalter and Basu, 2016; Strasser *et al.*, 2021) are present in the *Marchantia* genome (Bowman *et al.*, 2017). Low amounts of 1,6-linked Galp indicate a highly branched structure of *Marchantia* AGP. JIM13 reacted strongly with the isolated AGP, whereas KM1 and LM2 showed weaker interaction. Binding of LM6, an antibody directed against 1,5-linked Ara, was missing due to absence of this epitope in *Marchantia* AGP (Happ and Classen, 2019). The unusual monosaccharide acofriose (3-*O*-Me-Rhap) was also part of *Marchantia* AGP. 3-*O*-Me-Rhap was also purified and identified by NMR from the alcohol insoluble cell wall

residues of the hornwort *Anthoceros caucasicus*, the thalloid liverwort *Pellia epiphylla* and the leafy liverworts *Trichocolea tomentella*, *Marsupella emarginata* and *Porella cordaeana* (Popper and Fry, 2003). Furthermore, acofriose appears in cell walls of some charophyte green algae (Popper *et al.*, 2004), is part of the unusual rhamnogalactan-protein of *Spirogyra* (Pfeifer *et al.*, 2021) and is also present in AGPs from different mosses and some gymnosperm genera (Fu *et al.*, 2007; Bartels *et al.*, 2017; Baumann *et al.*, 2021), but is absent in angiosperms.

Protein content of *Marchantia* AGP was found to be nearly 25 % of the molecule (Happ and Classen, 2019). High levels of protein in AGPs have also been reported for the moss *Polytrichastrum* (Bartels *et al.*, 2017) and the lycophyte *Lycopodium* (Bartels and Classen, 2017). In contrast to seed plants, where Hyp is often up to 10 % of the protein, Hyp content in *Marchantia* AGP was only 1.25 % (Happ and Classen, 2019).

Bioinformatic search for AGP protein backbones in plant transcriptomes revealed the origin of glycosylphosphatidylinositol (GPI)-anchored AGPs in green algae and a 3-to 4-fold increase of these AGPs in liverworts and mosses, but a strong decrease in hornworts (Johnson *et al.*, 2017a). GPI-anchoring of AGPs is proposed to facilitate co-location of signalling partners in lipid microdomains (Konrad and Ott, 2015). It has to be taken into account, that only a low number of hornwort species were included in the study. AGPs without GPI anchor were much more abundant in bryophytes, with comparable amounts in hornworts, liverworts and mosses. Bioinformatic searches for hybrid AGPs revealed their presence in all bryophyte classes in comparable amounts (Johnson *et al.*, 2017a), and 14 genes encoding FLAs have been identified in *Marchantia polymorpha* (He *et al.*, 2019).

As mentioned above, functions of AGPs in seed plants are strongly diverse. First information on functions of AGPs in liverworts was obtained by blocking AGPs through addition of the β -glucosyl-Yariv's reagent to protoplast suspension cultures of *M. polymorpha*. The results indicate a role of AGPs in protonemata differentiation (Shibaya *et al.*, 2005), cell plate formation (Shibaya and Sugawara, 2009) and cell wall regeneration of cultured protoplasts (Shibaya and Sugawara, 2007). According to Kremer *et al.* (2004), presence of AGPs in the pseudoelaters of the hornwort *Megaceros* might be connected to water-absorbing capabilities of AGPs. Occurrence of AGPs in placental cells of horn- and liverwort might be a hint of a role in calcium binding and release associated with signal transduction and solute movement across generations (Henry *et al.*, 2021). Fu *et al.* (2007) speculated that presence of 3-*O*-Me-Rha residues occurring at the surface of bryophyte AGPs might influence the overall polarity and enable hydrophobic interactions essential in bryophytes but not in angiosperms.

Extensins and Proline-rich proteins

Extensins contain repetitive SO₃₋₅ motifs which are responsible for moderate glycosylation with arabinose-oligosaccharides attached to hydroxyproline. Furthermore, single galactose residues are linked to serine. Cross-linking of extensins in the cell wall provides structural support and is important for inhibiting cell expansion (Dehors *et al.*, 2019). According to bioinformatic data based on transcriptomes, cross-linking extensins (CL-EXTs) are present in liverworts and mosses, but much more abundant in hornworts with amounts comparable to tracheophytes (Johnson *et al.*, 2017a). In hornworts, CL-EXTs were present in all investigated species, whereas in liverworts, only approximately one third of the investigated species contained CL-EXTs (Johnson *et al.*, 2017a). Due to low numbers of hornworts included in this study, these results must be verified by future investigations. GPI-anchored extensins were found only in small amounts in eudicots and were missing in all bryophytes and also in all other plant lineages (Johnson *et al.*, 2017a).

PRPs are enriched in Pro, often arranged in repeating blocks of KPPVY(K) (Johnson *et al.*, 2018) with minimal glycosylation. They are responsive to different phytohormones (e.g. gibberellins, Rodríguez-Concepción *et al.*, 2001) and stress like wounding (Chen and Varner, 1985) and are upregulated e.g. in early fruit development (Rodríguez-Concepción *et al.*, 2001). Bioinformatic searches detected no PRPs in bryophytes (Johnson *et al.*, 2017a).

Lignin

In the secondary cell walls of vascular plants, lignin is integrated into the cell wall polysaccharide network and provides structural rigidity mainly to sclerenchyma and xylem cells. The water-conducting tracheids and vessels need high stability of the wall to withstand the negative pressure caused by surface tension during water transport (Ralph *et al.*, 2004; Renault *et al.*, 2019). Lignin is a complex heteropolymer of three phenylpropanoid alcohols: *p*-coumaryl alcohol, coniferyl alcohol and sinapyl alcohol, which are polymerized to *p*-hydroxyphenyl (H), guaianyl (G) and syringyl (S) units (Lewis and Yamamoto, 1990; Ralph *et al.*, 2004). H- and G-lignin monomers are present in all vascular plants, whereas the S-lignin monomer is taxonomically restricted to lycophytes, gnetophytes and angiosperms (Rencoret *et al.*, 2021) due to the limited occurrence of the ferulate 5-hydroxylase (F5H, e.g. Boerjan *et al.*, 2003; Weng *et al.*, 2008; Wagner *et al.*, 2015). For example, the lignin of angiosperms consists of G-S-copolymers with lower proportions of H-units. Most coniferous gymnosperms as well as ferns deposit lignin mainly build of G-units with a minority of H-units (Ligrone *et al.*, 2008; Weng *et al.*, 2008; Espiñeira *et al.*, 2011). Classical histochemical tests for presence of lignin in bryophytes detected no lignin (Thomas, 1977; Lewis and Yamamoto, 1990; Popper and Fry,

2003; Kremer *et al.*, 2004; Ligrone *et al.*, 2008; Espiñeira *et al.*, 2011). Ligrone *et al.* (2008) used polyclonal antibodies directed against epitopes of homoguaiacyl (G) and guaiacyl/syringyl (GS) lignin-like polymers to study four liverworts and two hornworts. Weak binding of both antibodies was observed in all species with a stronger reactivity of the antibody directed against GS. Whereas antibody binding in liverworts was not tissue-specific, the hornworts showed stronger labelling in the pseudo elaters and spores compared to other cell types. It has to be mentioned that antibodies were raised against synthetic reaction products of monolignols (Ruel *et al.*, 1994). Epitopes of the polyclonal sera are not clearly defined (Joseleau and Ruel, 1997) and might also detect monomers in other phenolic macromolecules. Function of these phenolic lignin-like monomers may involve protection against microbial attack and/or UV radiation instead of a specific structural function (Ligrone *et al.*, 2008). Similarly, the study by Espiñeira *et al.* (2011) on *Marchantia polymorpha* cell walls provides evidence only for the monolignols and not the entire macromolecule. Diversification of the biosynthetic machinery for lignin has likely been performed in the tracheophyta (Renault *et al.*, 2019), although different phenylpropanoid biosynthetic genes are also present in charophyte green algae (De Vries *et al.*, 2021) and even in red algae (Martone *et al.*, 2009). All lignin biosynthesis genes were found in the thalloid liverwort *Marchantia polymorpha* and the moss *Physcomitrium patens*, except of the ferulate 5-hydrolase. As lignin polymers have not been found, it has been suggested that these enzymes may function in a “pre-lignin” pathway (Xu *et al.*, 2009; Bowman *et al.*, 2017) arising in early non-vascular plants during the first stages of the transition from water to land (Renault *et al.*, 2017). It is assumed that phylogenetic-specific expansions in the responsible enzyme families are related to the diversity of phenylpropanoid structures in embryophyta (De Vries *et al.*, 2021).

Table 2. Overview of studies on cell wall polysaccharides from hornworts and liverworts.

Species	Microscopy/ Immunolabelling (histochemistry / antibodies)				Biochemical investigations			References
	Bioinformatics	Hemicellulose	Pectin	HRGP	Lignin-like	Composition	Structure	Methods
Hornworts								
<i>Anthoceros caucasicus</i>						✓		HPAEC-PAD; NMR; PC; TLC; PE Popper & Fry, 2003 Popper <i>et al.</i> , 2003 Popper <i>et al.</i> , 2004
<i>Anthoceros agrestis</i>	✓	✓	✓			✓	✓	HPAEC-PAD; MALDI-TOF-MS; 2D-NMR De Vries <i>et al.</i> 2021 Li <i>et al.</i> , 2020 O'Rourke <i>et al.</i> , 2015 Peña <i>et al.</i> , 2008 Renzaglia <i>et al.</i> , 2020
<i>Anthoceros angustus</i>	✓							Zhang <i>et al.</i> , 2020
<i>Anthoceros punctatus</i>	✓							De Vries <i>et al.</i> , 2021 Li <i>et al.</i> , 2020
<i>Dendroceros crispatus</i>		✓	✓					Renzaglia <i>et al.</i> , 2020
<i>Leiosporoceros dussii</i>		✓	✓					Renzaglia <i>et al.</i> , 2020
<i>Megaceros flagellaris</i>		✓	✓		✓			Carafa <i>et al.</i> , 2005 Ligrone <i>et al.</i> , 2008 Renzaglia <i>et al.</i> , 2020
<i>Megaceros fuegiensis</i>		✓			✓			Carafa <i>et al.</i> , 2005 Ligrone <i>et al.</i> , 2008
<i>Megaceros gracilis</i>		×	✓	✓	×			Kremer <i>et al.</i> , 2004
<i>Megaceros sp.</i>		✓					✓	MALDI-TOF-MS; 2D-NMR Peña <i>et al.</i> , 2008
<i>Notothylas orbicularis</i>		✓	✓					Renzaglia <i>et al.</i> , 2020
<i>Phaeoceros carolinianus</i>		✓	✓	✓		✓		SEC/ICP-MS Matsunaga <i>et al.</i> , 2004 Merced & Renzaglia, 2019 Renzaglia <i>et al.</i> , 2020 Henry <i>et al.</i> , 2021
<i>Phaeoceros laevis</i>		✓	✓	✓				Carafa <i>et al.</i> , 2005 Henry <i>et al.</i> , 2021
<i>Phaeoceros sp.</i>		✓					✓	MALDI-TOF-MS; 2D-NMR Peña <i>et al.</i> , 2008
<i>Phaeoceros sp. nov.</i>		✓						Carafa <i>et al.</i> , 2005
Liverworts (thalloid)								
<i>Blasia pusilla</i>		✓						Galloway <i>et al.</i> , 2018
<i>Conocephalum conicum</i>					✓	✓		SEC/ICP-MS Ligrone <i>et al.</i> , 2008 Matsunaga <i>et al.</i> , 2004
<i>Fossombronia foveolata</i>				✓				Basile & Basile, 1987
<i>Hymenophyton flabellatum</i>		✓	✓	✓				Ligrone <i>et al.</i> , 2002
<i>Lunularia cruciata</i>		✓		✓		✓		HPAEC-PAD; PC; TLC; PE Clarke <i>et al.</i> , 1978 Galloway <i>et al.</i> , 2018 Popper and Fry, 2003 Bowman <i>et al.</i> , 2017 De Vries <i>et al.</i> , 2021
<i>Marchantia polymorpha</i>	✓	✓	✓	✓	✓	✓	✓	GLC/FID/MS; ELISA; MALDI-TOF-MS; 2D-NMR Espiñeira <i>et al.</i> , 2010 Galloway <i>et al.</i> , 2018 Happ & Classen, 2019 Henry <i>et al.</i> , 2020 Honkanen <i>et al.</i> , 2016

						Konno <i>et al.</i> , 1987 Ligrone <i>et al.</i> , 2008 Matsunaga <i>et al.</i> , 2004 Peña <i>et al.</i> , 2008 Shibaya <i>et al.</i> , 2005 Shibaya & Sugawaran, 2007 Shibaya & Sugawaran, 2009 Wachananawat <i>et al.</i> , 2020 Yin <i>et al.</i> , 2014
<i>Pallavicinia subciliata</i>				✓	SEC/ICP-MS	Matsunaga <i>et al.</i> , 2004
<i>Pellia epiphylla</i>				✓	HPAEC-PAD; PC; TLC; PE	Popper & Fry, 2003 Renzaglia <i>et al.</i> , 2020
<i>Riccardia sinuate</i>			✓			Basile & Basile, 1987
<i>Riccia duplex</i>			✓			Basile & Basile, 1987
<i>Symphyogyna undulata</i>	✓	✓	✓	✓		Ligrone <i>et al.</i> , 2002 Ligrone <i>et al.</i> , 2008
Liverworts (leafy)						
<i>Bazzania pompeana</i>				✓	SEC/ICP-MS	Matsunaga <i>et al.</i> , 2004
<i>Gymnocolea inflata</i>			✓			Basile & Basile, 1987 Basile <i>et al.</i> , 2000
<i>Haplomitrium gibbsiae</i>	✓	✓	✓	✓		Ligrone <i>et al.</i> , 2002 Ligrone <i>et al.</i> , 2008
<i>Haplomitrium mnioides</i>			✓			Basile & Basile, 1987
<i>Haplomitrium ovalifolium</i>	✓	✓	✓			Ligrone <i>et al.</i> , 2002
<i>Jungermannia leiantha</i>			✓			Basile & Basile, 1987
<i>Lepidozia reptans</i>				✓	HPAEC-PAD; PC; TLC; PE	Popper & Fry, 2003
<i>Lophocolea bidentata</i>				✓	HPAEC-PAD; PC; TLC; PE	Popper & Fry, 2003
<i>Lophocolea heterophylla</i>		×		×	GLC/FID	Thomas <i>et al.</i> , 1977
<i>Marsupella emarginata</i>				✓	HPAEC-PAD; PC; TLC; PE	Popper & Fry, 2003
<i>Nardia scalaris</i>				✓	HPAEC-PAD; PC; TLC; PE	Popper & Fry, 2003
<i>Nowellia curvifolia</i>			✓			Basile & Basile, 1987
<i>Plagiochila asplenoides</i>				✓	HPAEC-PAD; PC; TLC; PE	Popper & Fry, 2003
<i>Pleurozia purpurea</i>				✓	HPAEC-PAD; PC; TLC; PE	Popper & Fry, 2003
<i>Porella cordaeana</i>				✓	HPAEC-PAD; PC; TLC; PE	Popper & Fry, 2003
<i>Radula buccinifera</i>	✓	✓	×	×		Kremer <i>et al.</i> , 2004
<i>Scapania nemorosa</i>			✓			Basile & Basile, 1987
<i>Scapania undulata</i>				✓	HPAEC-PAD; PC; TLC; PE	Popper & Fry, 2003
<i>Trichocolea tomentella</i>				✓	HPAEC-PAD; PC; TLC; PE	Popper & Fry, 2003

CONCLUDING REMARKS


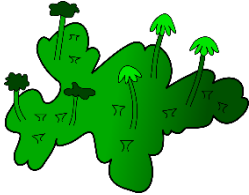
To date, knowledge on cell walls of bryophytes and especially of horn- and liverworts is limited. Some interesting cell wall differences have been elucidated (Table 3), sometimes underlining the different phylogenetic positions of horn- and liverworts (Fig. 1).

Arabinoxylans, detectable with the antibody LM11, were not present in liverworts and mosses, but in pseudo elaters and spores of hornworts. Xyloglucans were studied in detail and found to be of XXXG type in hornworts, whereas liverworts contained XXGG type xyloglucans (Peña *et al.*, 2008, Fig. 3). Furthermore, genes for GPI-anchored AGPs were much more abundant in liverworts whereas genes for extensins dominate in hornworts (Johnson *et al.*, 2017a). Although more species have to be investigated, the existing data on cell wall composition suggest a closer relationship between liverworts and mosses compared to liverworts and hornworts, thus supporting current taxonomy.

Identification of polysaccharides is mainly based on studies with antibodies directed against carbohydrate epitopes or bioinformatics search for glycosyltransferases involved in biosynthesis of the different polymers. Both methodologies have limitations. Epitopes of antibodies are not always clearly defined (Pfeifer *et al.*, 2021) and knowledge on biosynthetic pathways is still incomplete (Strasser *et al.*, 2021). The existing data suggests that beside cellulose, major classes of polysaccharides are present in horn- and liverworts. There is good evidence that mannans, xyloglucans, the pectic polysaccharides HG and RG I and callose are present in both groups as well as AGPs and extensins as members of the HRGPs. Further studies are needed to elucidate the structures of the side chains of RG I and to answer the question, whether RG II is present, as current evidence for RG II is mainly based on boron content (Matsunaga *et al.*, 2004). There seems to be consensus that lignin is missing but bryophytes possess the biosynthetic potential to synthesize some kind of “pre-lignin”.

As land plants evolved from streptophyte algae most closely related to extant Zygnematophyceae (e.g. Leebens-Mack *et al.*, 2019), further investigations on cell walls of charophytes and bryophytes are urgently needed to better understand early land plant evolution.

Table 3. Summary of cell wall components of horn- and liverworts.

Cell wall component			comments
	hornwort	liverwort	
Cellulose	✓	✓	
Xylan	✓	×	Based only on LM11 epitope detection
Mannan	✓	✓	Content maybe lower in hornworts
MLG	×	×	
Xyloglucan	✓	✓	Different types. XXXG and XXGG type for hornworts and liverworts, respectively
HG	✓	✓	
RG-I backbone	✓	✓	Based on detection of RG-I with antibodies against side-chains
RG-II	(✓)	(✓)	Based only on detection of small amounts of boron
Callose	✓	✓	
“true” lignin	×	×	Some monolignols are found, but the whole lignin molecule was not isolated
AGP-carbohydrate	✓	✓	For hornworts based only on detection with antibodies
GPI-AGPs	✓ (few)	✓ (many)	Based on bioinformatics searches
CL-EXTs	✓ (many)	✓ (few)	Based on bioinformatics searches
PRPs	×	×	Based on bioinformatics searches

ACKNOWLEDGEMENTS

This project was carried out in the framework of MAdLand (<http://madland.science>, DFG priority programme 2237); LP, KM and BC are grateful for funding by the DFG (project-number 440046237).

AUTHORS CONTRIBUTIONS and CONFLICT OF INTEREST

LP, KM and BC contributed equally to this review. The authors have no conflicts to declare.

3. The model organisms *Anthoceros agrestis* and *Physcomitrium patens*: Insights into their cell walls and arabinogalactan-proteins

Kim-Kristine Mueller¹ and Birgit Classen¹

¹Pharmaceutical Institute, Department of Pharmaceutical Biology, Christian-Albrechts-University of Kiel, Gutenbergstr. 76, 24118 Kiel, Germany

ABSTRACT

About more than 470 million years ago, the first land plants, the bryophytes, evolved and today are classified into hornworts, liverworts and mosses. While the latest common ancestor of all land plants colonised land, it had to cope with enormous environmental changes, which made adaptations of the cell wall necessary. To extend the limited knowledge on bryophyte cell walls and to gain better understanding of the cell wall of the common ancestor, two model organisms, *Anthoceros agrestis* and *Physcomitrium patens*, were analysed for their cell wall composition in this study. The main polysaccharide classes, cellulose, hemicelluloses and pectins, are present but reveal in some cases structural differences to angiosperm cell walls. Analytical data indicate presence of pectins, probably mainly homogalacturonan in both species. Immunocytochemical experiments demonstrated that the backbone of rhamnogalacturonan-I (RG-I) was absent, while the response of several antibodies raised against highly branched RG-I side chain epitopes was detectable in the cell wall of both species. Antibodies directed against xylans and the XXXG-motif of xyloglucans indicated low amounts of xylans in the hemicellulose fractions of both bryophytes. On the other hand, high amounts of xyloglucans possessing a XXXG type were only identified in those of *Anthoceros*. Cell wall glycoproteins, the arabinogalactan-protein (AGPs), were isolated, characterized and compared with other land plant AGPs. The highly branched galactan core structure was similar to those of other bryophyte and fern AGPs, but different to angiosperm AGPs, as 1,6-linked galactose was more or less absent. The terminal residues were dominated by furanosidic arabinose (Araf) and pyranosidic rhamnose (Rhap). In the *Physcomitrium* AGP, the Araf linkages were mainly terminal or 1,5-linked, while in the *Anthoceros* AGP, t-Araf dominated and was accompanied by low amounts of 1,3-Araf and terminal pyranosidic Ara. The unusual 3-O-methylated Rhap was also detectable in both bryophyte AGPs comparable to other spore producing land plant AGPs.

INTRODUCTION

Although they have no “true” leaves, no “true” roots and no vascular systems, they display nowadays the second largest biodiversity after the angiosperms: the bryophytes. About more than 470 million years ago (mya) the bryophytes evolved as the first land plant clade and contain more than 20,000 extant species (Morris *et al.*, 2018; Wang *et al.*, 2022). Bryophytes can be divided into hornworts, liverworts and mosses, with liverworts and mosses belonging to the setaphytes due to the formation of seta. Recent phylogenetic studies confirm that hornworts evolved monophyletically to the setaphytes (Zhang *et al.*, 2020; Wang *et al.*, 2022; Bechteler *et al.*, 2023). The latest common ancestor of the bryophytes represents thus a sister lineage to all tracheophytes (Yadav *et al.*, 2023). One of the most important differences between bryophytes and tracheophytes is the dominant stage of the life cycle. Among the bryophytes, this is the haploid gametophyte, while the diploid sporophyte is partially or completely dependent on the gametophyte (Wang *et al.*, 2022). This is exactly the opposite of the tracheophytes, where the sporophyte dominates.

Modern model organisms have been established for all three bryophyte clades: the moss *Physcomitrium patens*, the liverwort *Marchantia polymorpha* and the hornwort *Anthoceros agrestis*. Bryophytes have been successfully used as model organisms to study various biological processes, such as gametogenesis, evolutionary developmental biology or phylogenetic studies (Yadav *et al.*, 2023). For the latter, the decoding of the genomes of bryophyte species have been a considerable support (Rensing *et al.*, 2008, Bowman *et al.*, 2017; Li *et al.*, 2020; Zhang *et al.*, 2020).

It is particularly important because all three bryophyte lineages have very special characteristics. While most mosses develop multicellular protonemata and rhizoids (Frangedakis *et al.*, 2021; Yadav *et al.*, 2023), in hornworts the sporophyte grows from a basal meristem. Most hornworts have only one chloroplast per cell with pyrenoids (Frangedakis *et al.*, 2021); most liverworts, on the other hand, have unique oil bodies (Shimamura, 2016).

What all bryophytes have in common is that they are survivalists. They have the ability to grow in almost all habitats, including the wet tropical forest or even the arctic, for example (Hodgetts *et al.*, 2019; Wang *et al.*, 2022). This is mainly due to the fact that they are extremely adaptable as they have an extreme abiotic stress tolerance. These stressors include above all UV radiation, temperature fluctuations, desiccation and drought (de Vries & Archibalt, 2018; Fürst-Jansen *et al.*, 2020; Bowles *et al.*, 2021; Yadav *et al.*, 2023).

The latest common ancestor of all land plants had to cope with these enormous environmental changes as it colonized the land (de Vries & Archibalt, 2018, McCourt *et al.*, 2023).

Today, it is generally agreed that this latest common ancestor of extant land plants belonged to the streptophyte algae of the Zygnematophyceae-Coleochaetophyceae-Charophyceae-grade, the ZCC-grade (de Vries & Archibalt, 2018; Domozych & Bagdan, 2022).

In order to survive under these altered conditions, one of the most important adaptations was the modification of the plant's cell wall (Harholt *et al.*, 2016).

In general, the cell wall is a highly complex and dynamic system designed to protect the cell from abiotic and biotic stress factors, but also to strengthen the cell and thereby the whole plant. The main components of the cell wall are polysaccharides and cell wall proteins, which can be further classified. The most important groups of polysaccharides are cellulose, hemicelluloses and pectins. Cellulose comprises most of the mass of the cell wall of plants, is organized in microfibrils that are cross-linked with hemicelluloses. This construct is embedded in a matrix of pectins (Popper, 2008).

Pectins are rich in GalA and can be further subdivided into homogalacturonan (HG), rhamnogalacturonan-I (RG-I) and rhamnogalacturonan-II (RG-II), whereby RG-II offers a special feature. It exists as a dimer *via* a borate diester linkage by apiose residues (Matsunaga *et al.*, 2004; Atmodjo *et al.*, 2013). Hemicelluloses are defined as polysaccharides with a β -1,4-linked core structure with an ether group between C1 and C4 positioned in an equatorial configuration (Scheller & Ulvskov, 2010). Common representatives of this class are xylans, xyloglucans, (1 \rightarrow 3),(1 \rightarrow 4)- β -D-glucans, also called the mixed-linkage glucans (MLGs), and (gluco)mannans.

Cellulose, hemicelluloses and pectins have been detected and partly isolated in various bryophytes (Geddes & Wilkie, 1971; Kremer *et al.*, 2004; Carafa *et al.*, 2005; Berry *et al.*, 2016; Pfeifer, Mueller, Classen, 2022). In addition to many similarities with the cell wall of tracheophytes, differences were also discovered, e.g. acidic xyloglucans with an altered basic motif in mosses and liverworts (Peña *et al.*, 2008). Furthermore, unusual arabinoglucans have been isolated from *P. patens* (Roberts *et al.*, 2018). Additionally, it is still unclear whether bryophytes contain RG-II, as so far only traces of the compound element boron have been detected, which could possibly also indicate contamination (Matsunaga *et al.*, 2004).

Besides polysaccharides, (glyco)proteins are important components of plant cell walls. One of the largest groups of cell wall proteins are the hydroxyproline-rich glycoproteins (HRGPs), which can be subdivided into arabinogalactan-proteins (AGPs), extensins (EXT) and proline-rich proteins (PRPs). These differ primarily in their degree of glycosylation. This is up to 90 % for AGPs, 50 % for EXT and only found to a low degree in PRPs (Johnson *et al.*, 2018). The protein part of AGPs is covalently linked to its carbohydrate part *via* the amino acid hydroxyproline (Hyp). This polysaccharide moiety consists of type II arabinogalactans and is

characterized by a (1→3)-β-D-galactan core chain that is often linked to (1→6)-β-D-galactan side chains at position O-6. These side chains are further decorated with α-L-Araf and other monosaccharides in minor amounts, such as L-Rha, L-Fuc or D-GlcAp (Kitazawa *et al.*, 2013; Strasser *et al.*, 2021).

AGPs are widely distributed among land plants and were first described in bryophyte samples in the 1970s by Clarke *et al.* (1978) using a special precipitation reaction. This precipitation reaction is performed with a specific reagent, the β-glucosyl Yariv reagent (βGlcY; Yariv *et al.*, 1962). When AGPs interact with the Yariv reagent, precipitation results and a red precipitate is formed, which can be used for isolation of AGPs. In addition to AGPs from cell walls of ferns, gymnosperms as well as monocot and dicot angiosperms (Classen *et al.*, 2004; Göllner *et al.*, 2011, Bartels & Classen, 2017; Baumann *et al.*, 2021, Mueller *et al.*, 2023), AGPs have been also isolated from bryophyte cell walls (Lee *et al.*, 2005; Fu *et al.*, 2007; Bartels *et al.*, 2017; Happ & Classen, 2019).

The most significant difference between the AGPs of spore plants and those of embryophytes is the presence of methylated rhamnose (3-O-MeRha; acofriose; Fu *et al.*, 2007; Bartels *et al.*, 2017; Bartels & Classen, 2017; Happ & Classen, 2019; Mueller *et al.*, 2023).

Functions of AGPs in seed plants are extremely diverse and numerous. These include xylem differentiation, cell proliferation, growth, salt and drought tolerance as well as interaction with plant microbes (Seifert & Roberts, 2007; Ma *et al.*, 2018; Mareri *et al.*, 2018). Up to now, little is known about functions of AGPs in bryophytes: AGPs are involved in the apical cell extension of protonemata in the moss *P. patens* (Lee *et al.*, 2005) and play a role in the water balance in mosses (Kobayashi *et al.*, 2011; Cui *et al.*, 2012; Ligrone *et al.*, 2002).

In this study, AGPs were isolated from the two model organisms *Physcomitrium patens* and *Anthoceros agrestis* in order to expand structural elucidation and further clarify the evolution of AGPs within the land plants. To the best of our knowledge, no AGP of a hornwort has been isolated before. As the knowledge about the cell walls of bryophytes is still limited, a sequential cell wall extraction was performed to gain insight into polysaccharide composition and distribution. Furthermore, this provides information about the evolution of the plant cell wall during the conquest of land.

RESULTS

Sequential extraction of polysaccharide fractions from bryophyte cell walls

To investigate the cell wall composition of *Anthoceros* and *Physcomitrium*, the dried plant material was subjected to sequential extraction with water (AE), ammonium-oxalate $[(\text{NH}_4)_2\text{C}_2\text{O}_4]$ and hydrochloric acid (HCl) as well as sodium carbonate (Na_2CO_3) and potassium hydroxide (KOH). In this way, five fractions were obtained: one water-soluble, two pectic and two hemicellulose fractions.

The yields of the AE fractions were $12.0 \% \pm 3.1 \%$ for *Anthoceros* (n=2) and 2.1 % of the dry plant material for *Physcomitrium*. The extraction yields of the other fractions (Tab. S1) also varied between the two species. In *Anthoceros*, the dominant fraction was the $(\text{NH}_4)_2\text{C}_2\text{O}_4$ fraction with a yield of 28.4 %, whereas in *Physcomitrium*, the KOH fraction dominated with 20.2 %.

Pectic fractions of bryophyte cell walls

The monosaccharide compositions of the two pectic fractions are shown in Tables S2a and S2b and Figure 1. As expected, the two pectic fractions were rich in uronic acids with highest amounts in the $(\text{NH}_4)_2\text{C}_2\text{O}_4$ fractions of both bryophytes. *Anthoceros* was outstanding with 49.1 % of uronic acids in the $(\text{NH}_4)_2\text{C}_2\text{O}_4$ fraction and 17.3 % of uronic acids in the HCl-fraction (Tab. S3).

The common neutral monosaccharides of pectic polysaccharides are mostly Rha, Gal and Ara of rhamnogalacturonan-I (RG-I) or Xyl and Gal of xylogalacturonans (XG). These neutral monosaccharides were also present in the pectic fractions of both bryophytes.

The amount of Gal, Glc and Xyl were greatest in both pectic fractions of *Anthoceros*, reaching values from 5.8 % to 77.2 %, in those of *Physcomitrium* the highest monosaccharide contents were Glc, Gal and Rha (8.6 % – 53.0 %).

The monosaccharides Gal, Xyl and Rha, as well as Ara (with amounts of 2.1 % – 8.6 %) in all pectic fractions could be a hint for pectic polysaccharides such as RG-I and XG, and the contained Glc, Fuc and Man could be indicative of other polysaccharides or, in case of Glc, of co-extracted starch.

In addition, the methylated monosaccharide 3-*O*-methyl-rhamnose (=Acofriose; 3-*O*-MeRha) could be detected in pectic fractions of both species.

To confirm presence of RG-I, the antibodies INRA RU2, LM5, LM6, LM16 and LM26 were used for binding affinity to $(\text{NH}_4)_2\text{C}_2\text{O}_4$ fractions (see Fig. 2A and Tab. S4 for references). INRA RU2 detects epitopes of the RG-I backbone, LM5 and LM16 are directed against RG-I galactan side chains, LM6 and LM26 against RG-I arabinan side chains, whereas LM16 and

LM 26 are directed against branched RG-I side chains (see Fig. 2B for epitopes of all antibodies). The $(\text{NH}_4)_2\text{C}_2\text{O}_4$ fraction of *Arabidopsis thaliana* was tested as a positive control (fraction data unpublished) and showed strong interaction with all antibodies directed against RG-I epitopes. In contrast, the RG-I backbone antibody INRA RU2 indicated no affinity to the $(\text{NH}_4)_2\text{C}_2\text{O}_4$ fractions of both bryophytes.

The $(\text{NH}_4)_2\text{C}_2\text{O}_4$ fraction of *Anthoceros* showed only a weak binding affinity to LM16 and a very weak affinity to LM26. That of *Physcomitrium*, on the other hand, has a great affinity to the arabinan antibody LM5 and moderate binding affinity to the others.

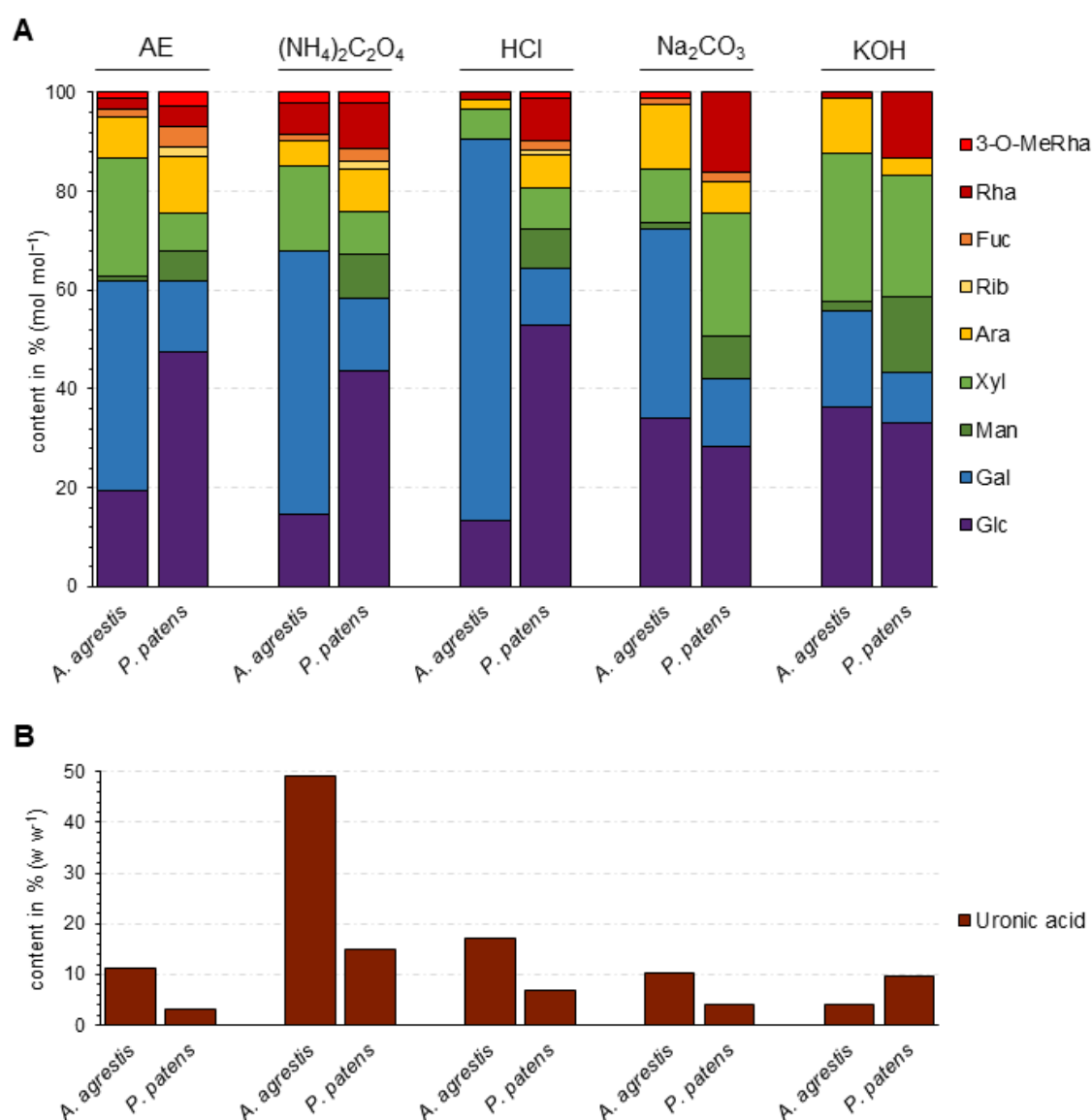


Figure 1. Monosaccharide composition of different cell wall fractions [$(\text{NH}_4)_2\text{C}_2\text{O}_4$, HCl, Na_2CO_3 , KOH] from the hornwort *Anthoceros agrestis* and the moss *Physcomitrium patens*. **A:** Relative neutral monosaccharide composition determined by gas chromatography (GC; % mol mol⁻¹). **B:** Absolute content of uronic acids determined by colorimetric assay (% w w⁻¹ of dry fraction weight).

Hemicellulose fractions of bryophyte cell walls

In the alkaline fractions of *Anthoceros* (Fig. 1 and Tab. S2a, S3), the monosaccharides Gal, Glc, Ara and Xyl were present in amounts between 10.9 % – 38.2 %.

In *Physcomitrium*, Glc and Xyl were dominant in both alkaline fractions and accounted for together 54 % – 57 % of the neutral monosaccharides (Fig. 1 and Tab. S2b, S3). The contents of the other monosaccharides Rha, Man, Gal and Ara were varied from 3.7 % to 16.2 %. This could indicate the presence of distinct xylans, glucans and mannans in these bryophyte cell walls.

The same was the case for the KOH fraction of *Anthoceros* with 66 % of summarized Glc and Xyl. The Na₂CO₃ fraction of *Anthoceros* differed with dominance of Gal.

The content of the uronic acids of the KOH fraction of *Physcomitrium* was 9.8 % and thus higher than that of the HCl fraction. This suggest that the hemicelluloses of *Physcomitrium* might contain uronic acids.

Because of the high contents of Glc and Xyl in the KOH fractions of both species, the factions were tested against epitopes of xylan and xyloglucan *via* ELISA (see Fig. 2).

A 4 M NaOH fraction of *Arabidopsis thaliana* were used as a positive control (fraction data unpublished).

The antibody LM10 detects the epitope of the non-reducing end of (1→4)-β-D-xylan (McCartney *et al.*, 2005; Ruprecht *et al.*, 2017) and LM15 the XXXG-motif of xyloglucan (Marcus *et al.*, 2008; Pedersen *et al.*, 2012).

The KOH fraction of *Anthoceros* showed a moderate binding to the epitope of LM10 (xylan) and a strong affinity to the XXXG-motif of LM15, whereas that of *Physcomitrium* presented only a weak affinity to both antibodies.

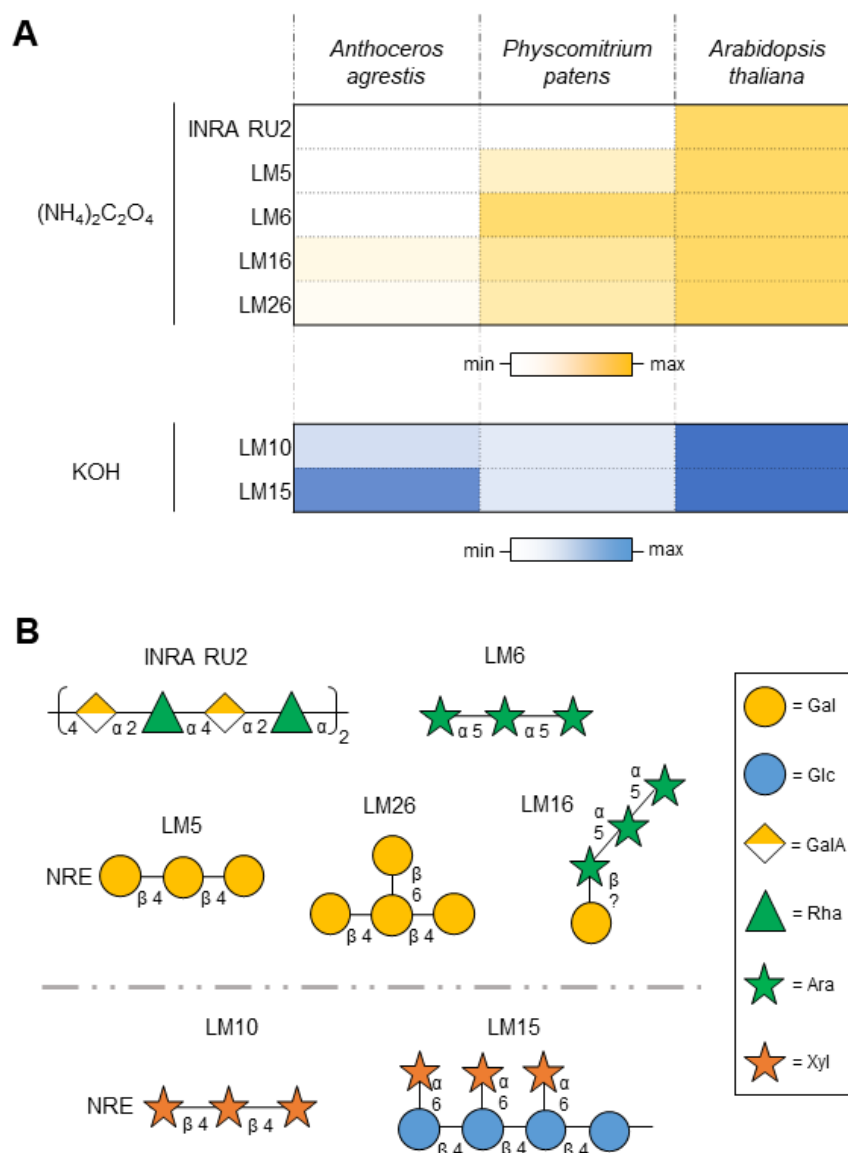


Figure 2. Reactivity of different fraction of *Anthoceros agrestis*, *Physcomitrium patens* and *Arabidopsis thaliana* as positive control after 40 min via ELISA at the concentration $12.5 \mu\text{g mL}^{-1}$. **A:** Yellow heat map of reactivity of $(\text{NH}_4)_2\text{C}_2\text{O}_4$ fractions tested with antibodies against epitopes of RG-I (INRA RU2; LM5; LM6; LM16; LM26); blue heat map of reactivity of alkaline fractions tested with antibodies against epitopes of xylan (LM10) and of xyloglucan (LM15). **B:** Epitopes of the antibodies used, for references see also Table S4.

Search for AGPs in the cell walls of *Anthoceros* and *Physcomitrium*

The extraction of the water-soluble fractions from *Anthoceros* and *Physcomitrium* yielded two fractions with different monosaccharide composition, although Glc, Gal, Xyl and Ara were dominant in both fractions (Fig. 1 and Tab. S2a, S2b, S3).

For the extraction of the AE of *Anthoceros*, a 2.5-fold higher amount of water was used than for that of *Physcomitrium*, in order to provide a complete extraction of the water-soluble polysaccharides, since the AE exhibited a very viscous consistency.

This is also reflected in the quantified uronic acid content in the AE fractions, which was higher in the AE of *Anthoceros* with 11.1 % compared to the AE of *Physcomitrium* with 3.1 %.

Considering the neutral monosaccharides, high amounts of Gal were found in the AE of *Anthoceros*, followed by similar contents of Glc and Xyl as well as Ara with 8.4 %. In that of *Physcomitrium*, Glc was most abundant, followed by Gal and Ara in approximately equal amounts.

Ara and Gal are the main monosaccharides of the carbohydrate moiety of AGPs, which could indicate their presence.

The high Glc content in both AEs and the Xyl content in that of *Anthoceros* could indicate co-extraction of starch due to the lack of amylase treatment or also water-soluble hemicelluloses such as glucans, xylans or xyloglucans.

Other neutral monosaccharides were detected in amounts less than 9.0 %, including the unusual 3-*O*-MeRha.

Gel diffusion assay

A gel diffusion assay was used to search for AGPs in the bryophyte AE samples. AGPs contain 1,3-galactan structures, that precipitate with Yariv phenyl glycosides, such as β -D-glucosyl Yariv-reagent (β GlcY; Kitazawa *et al.*, 2013; Paulsen *et al.*, 2014). This reaction produces a red precipitate that can be perceived as a red line in a gel diffusion assay (Clarke *et al.*, 1979). The gel diffusion test was positive for both *Anthoceros* and *Physcomitrium* AEs (Fig. S1) and compared to AE from *Marchantia polymorpha*, which has been investigated in a previous study (Happ & Classen, 2019).

Isolation and identification of AGPs

Based on the Ara and Gal amounts as well as the positive gel diffusion assay (see Fig. S1), the AE fractions were treated with β GlcY-reagent to gain AGP fractions. After purification, the yield of the *Anthoceros* AGP fraction was 0.31 % \pm 0.08 % (n=2) and that of *Physcomitrium* 0.09 % of the dry plant material.

The monosaccharide compositions of the bryophyte AGPs are shown in Table 1.

The neutral monosaccharides Ara and Gal were dominant in both bryophyte AGP fractions. The Ara : Gal ratio was in both AGPs quite similar with 1:1.7 in the *Anthoceros* AGP and 1:1.6 in the *Physcomitrium* AGP. In *Physcomitrium* AGP, high amounts of Glc were present additionally, which might at least partly be due to unseparated β GlcY.

Besides other minor monosaccharides, the content of 3-*O*-MeRha is quite high, 5.6 % in *Anthoceros* AGP and 10.0 % in *Physcomitrium* AGP.

The uronic acid content of the AGPs of both bryophytes was determined photometrically and was in the same range, 6.5 % (*Anthoceros*) and 7.3 % (*Physcomitrium*). For uronic acid

identification, the AGPs were subjected to uronic acid reduction with sodium borodeuteride (AGP_{UR}). In the mass spectrum analysis, deuterated fragments were detected only in the Glc peak. This, together with the increase of Glc in the neutral monosaccharide analysis (Tab. 1) indicate that in both AGPs the uronic acids were GlcA.

Since AGPs consist of a protein moiety covalently linked *via* Hyp in addition to the carbohydrate part, the protein and the Hyp content of these AGPs were also determined.

From the nitrogen content measured by elemental analysis (2.6 % for *Anthoceros* and 2.7 % for *Physcomitrium* AGP) the amount of protein in the AGPs was calculated using the Kjeldahl constant ($\times 6.25$) and determined to be 16.3 % and 16.9 %, respectively.

The Hyp amount of the *Anthoceros* AGP was slightly higher (0.31 %) compared to that of *Physcomitrium* (0.25 %).

This results in a Hyp proportion of 1.9 % of the protein in *Anthoceros* AGP and 1.5 % for that of *Physcomitrium*.

Table 1. Neutral monosaccharide composition of AGPs and AGP_{UR}s from *Anthoceros agrestis* and *Physcomitrium patens* in % (mol mol⁻¹; tr: trace value < 1 %).

Neutral monosaccharide	<i>A. agrestis</i>		<i>P. patens</i>	
	AGP (n=1)	AGP _{UR} (n=3)	AGP (n=1)	AGP _{UR} (n=2)
3- <i>O</i> -Me-Rha	5.6	4.3 \pm 0.1	10.0	10.6 \pm 0.4
Rha	tr	tr	3.4	2.8 \pm 0.1
Fuc	tr	tr	2.0	1.5 \pm 0.1
Ara	31.8	35.6 \pm 0.7	21.8	21.1 \pm 0.0
Xyl	4.0	3.3 \pm 0.4	2.8	2.7 \pm 0.3
Man	1.6	1.9 \pm 0.3	3.0	2.4 \pm 0.0
Gal	53.9	50.3 \pm 0.8	35.2	35.6 \pm 0.0
Glc	3.1	4.6 \pm 1.0	21.8	23.3 \pm 0.0
Ara : Gal	1 : 1.7	1 : 1.7 \pm 0.0	1 : 1.6	1 : 1.7 \pm 0.0

AG structure elucidation of bryophyte AGPs

For structural characterization, the AGPs and the uronic acid-reduced AGPs (AGP_{UR}) were subjected to linkage analysis (Tab. 2). In all samples, Galp was the main monosaccharide and present as terminal residue (1.0 % – 1.8 %), in 1,3-linkage (10.4 % – 20.1 %), 1,6-linkage (traces to 1.4 %), 1,3,4-linkage (only *Anthoceros* about 6.4 %) and 1,3,6-linkage (18.1 % – 27.7 %).

Terminal Glcp was characterized in amounts of 1.4 % to 3.5 %. The increase of this terminal residue in the AGP_{UR} samples to approximately double was due to the presence of GlcA in the native AGP.

Further hexose linkage types were 1,4-Hexp, 1,6-Manp and 1,3,4,6-Hexp. In the *Physcomitrium* AGP, the 1,4-Hexp peak was in both samples the highest (20.0 % – 23.4 %). When comparing

the detected monosaccharides from the methylation analysis with those from the acetylation, most of the Glc content is lacking. This hexose is thus Glc.

An 1,4-Hexp peak was only found in traces in the *Anthoceros* AGP, but in the uronic acid-reduced sample it was up to 2 %. The additional deuterated fragments found indicate that it is a pyranosidic uronic acid-containing hexose. It could be assumed that it is more likely to be Glc, as approximately 2 % of the Glc was not recovered in both samples. However, this is only speculative.

Additionally, a 1,3,4,6-Hexp peak was identified in both AGP samples of *Anthoceros*. Since it cannot be clearly determined whether this is an artificial peak due to undermethylation, it was not taken into account in the structural proposal (see below, chapter *Discussion*).

The AGP linkage types of Ara differ in the two investigated bryophytes. In *Anthoceros* AGP, terminal Araf was strongly dominant (23.7 % – 25.7 %) and only low amounts of additional 1,3-Araf were found. In *Physcomitrium* AGP, the 1,5-Araf was slightly dominant and was accompanied by almost similar amounts of terminal Araf. The main terminal monosaccharide of *Physcomitrium* AGP was t-Rhap with up to 18.0 %. In addition to t-Rhap, pyranosidic Ara and Xyl were identified as terminal residues in the AGP of *Anthoceros*, while t-Fucp was only detected in that of *Physcomitrium*.

Table 2. Linkage type analysis of AGP and AGP_{UR} from *Anthoceros agrestis* and *Physcomitrium patens* in % (mol mol⁻¹, n=1; tr: trace value < 1 %; * including deuterated fragments).

Mono-saccharide	linkage type	<i>Anthoceros</i>		<i>Physcomitrium</i>	
		AGP	AGP _{UR}	AGP	AGP _{UR}
Galp	1,3,6-	27.7	23.8	22.3	18.1
	1,3,4-	6.5	6.3	-	-
	1,6-	tr	1.1	1.4	1.4
	1,3-	20.1	18.3	11.0	10.4
	1-	1.4	1.0	1.6	1.8
GlcP	1,3,4-	-	-	tr	tr
	1,4-	-	-	23.4	20.0
	1-	1.4	2.4*	1.8	3.5*
Manp	1,6-	tr	tr	tr	2.1
Hexp	1,3,4,6-	6.7	7.4	-	-
	1,4,6-	-	-	tr	tr
	1,2,3-	tr	tr	-	tr
HexAp	1,4-	tr	1.9*	-	-
Rhap	1,2,4-	tr	tr	-	tr
	1,4-	-	tr	tr	tr
	1,2-	-	-	tr	tr
	1-	8.4	7.3	16.7	18.0
Fucp	1-	-	-	1.4	1.4
Araf	1,5-	tr	tr	11.0	13.2
	1,3-	2.4	2.0	tr	tr
	1,2-	tr	tr	tr	tr
	1-	23.7	25.7	9.4	10.1
Arap	1-	1.7	1.6	tr	tr
Xylp	1,2-/1,4-	tr	tr	-	-
	1-	tr	1.2	tr	tr

ELISA experiment with antibodies directed against AG glycan epitopes

To obtain more information about the structure of the AG moiety of the two bryophyte AGPs, these AGPs were tested for their binding affinity with different antibodies against arabinogalactan-protein glycan epitopes: KM1, JIM13, LM2 and LM6 (Fig. 3).

The antibody JIM13 (Fig. 3A) is generally considered to be an AGP antibody, although the epitope has not been fully clarified to date. Yates *et al.* (1996) showed binding of the trisaccharide structure β -D-GlcAp-(1 \rightarrow 3)- α -D-GalAp-(1 \rightarrow 2)- α -L-Rha. Additionally, Pfeifer *et al.* (2022) also demonstrated that Rha and uronic acids contribute to the binding. The results of the ELISA showed a strong reactivity of the *Physcomitrium* AGP and a moderate of that of *Anthoceros*.

To detect the (1 \rightarrow 6)- β -D-Galp units in AGs type II, the antibody KM1 (Fig.3B) was used (Classen *et al.*, 2004; Ruprecht *et al.*, 2017) and showed no affinity to the *Anthoceros* AGP and very weak reaction to the *Physcomitrium* AGP.

The LM2 antibody (Smallwood *et al.*, 1996, Fig. 3C) identifies (1→6)- β -D-Galp units with terminal β -D-GlcAp in AGPs (Ruprecht *et al.*, 2017) and reacted very strong with the *Anthoceros* AGP and also strong with the *Physcomitrium* AGP.

To recognized oligomers with (1→5)- α -L-Araf linkages in arabinans or AGPs, the antibody LM6 (Fig. 3D) was applied (Verhertbruggen *et al.*, 2009a). Only the AGP of *Physcomitrium* showed a moderate binding.

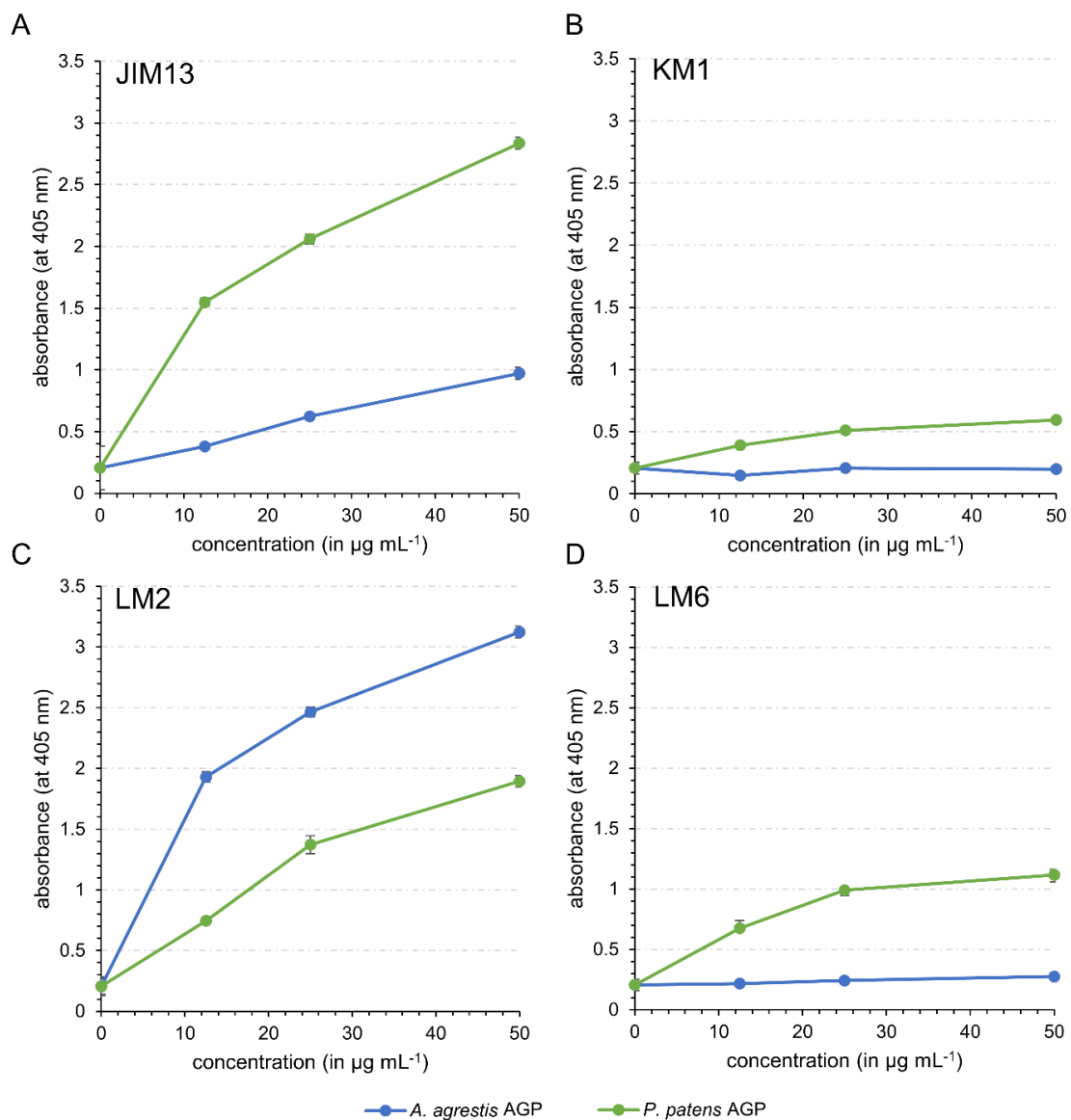


Figure 3. Reactivity of *Anthoceros agrestis* and *Physcomitrium patens* AGP by ELISA. Antibodies against epitopes of AGP glycans. **A:** JIM13; **B:** KM1; **C:** LM2; **D:** LM6. For epitopes of the antibodies, see Table S4.

DISCUSSION

Polysaccharides of *Anthoceros* und *Physcomitrium* cell walls

About 500 mya, terrestrialization was one of the most significant earth events for life on land. This led to enormous adaptations of plants to the changed environmental conditions (Domozych & Bagdan, 2022). In order to cope with these stressors, varieties of adaptations were needed, including those involving the cell wall. Since bryophytes are classified as the first land plants, they are of particular importance in the research of cell wall modification during land plant evolution (Bechteler *et al.*, 2023). Additionally, the study of extant bryophytes can provide insights into the cell wall composition of the common ancestor. Because knowledge on cell wall composition of bryophytes is limited and often based on immunocytochemistry and not on isolation and analytical characterization, the model organisms *Anthoceros* and *Physcomitrium* were chosen to fill this gap.

Pectic polysaccharides in the cell walls of bryophytes

Pectins consist mainly of uronic acids and the neutral monosaccharides Rha, Gal, and Ara, which were found in the $(\text{NH}_4)_2\text{C}_2\text{O}_4$ and the HCl fraction of *Anthoceros* and *Physcomitrium*. Due to the high content of Xyl, substituted homogalacturonans, the xylogalacturonans, might be present in the pectic fractions of *Anthoceros*. This composition of pectic fractions of *Anthoceros* corresponds to that determined by O'Rourke *et al.* (2015). Xylogalacturonan epitopes were not detectable in the cell walls of *Physcomitrium* (Moller *et al.*, 2007).

In addition, the unusual monosaccharide 3-*O*-MeRha was found in the pectic fractions of both bryophytes, this was also the case in those of the liverwort *Marchantia polymorpha*, indicating that 3-*O*-MeRha is a component of pectins in bryophytes (Happ & Classen, 2019). According to Matsunaga *et al.* (2004), 3-*O*-MeRha might also be part of RG-II of a lycophyte and some ferns.

Presence of HG with low or high degree of esterification in cell walls of hornworts and mosses were confirmed in several studies with monoclonal antibodies including different tissues of *Physcomitrium* cell walls and spore walls of *Anthoceros* (Ligrone *et al.* 2002; Kremer *et al.*, 2004; Lee *et al.*, 2005; Moller *et al.*, 2007; Berry *et al.*, 2016; Merced & Renzaglia, 2019; Renzaglia *et al.*, 2020). Additionally, the typical backbone linkage types for HG (1,4-GalAp) and for RG-I (1,4-GalAp and 1,2-Rhap) were found in a linkage type analysis of protonemal cell walls of *Physcomitrium* (Moller *et al.*, 2007).

To identify RG-I epitopes several antibodies were tested in this study. The negative result of the INRA RU2 antibody suggests that both bryophytes either do not produce RG-I or the RG-I

backbones have increased branching because the epitope is directed against a linear backbone of [(4)- α -D-GalA-(1,2)- α -L-Rha]₄.

The increased branching is also reflected in the positive response of LM16 and LM26 directed against branched arabinan and galactan side chains present in RG-I of the (NH₄)₂C₂O₄ fraction of *Anthoceros*. The RG-I in the (NH₄)₂C₂O₄ fraction of *Physcomitrium* contained epitopes of linear and branched arabinan and galactan side chains with the highest affinity for linear arabinan side chains, demonstrated by the antibody LM6. This result was also confirmed in two further antibody studies of *Physcomitrium* cell walls (Moller *et al.*, 2007; Berry *et al.*, 2016).

The LM5 epitope of (1→4)- β -galactans was also labelled in primary walls of the hornwort *Megaceros*, whereas the hyaline cells of *Sphagnum* were labelled by the antibody CCRC-M7, which is raised against (1→6)- β -galactans, also present in AGPs (Puhlmann *et al.*, 1994; Kremer *et al.*, 2004). Ligrone *et al.* (2002) detected epitopes of LM5, LM6 and CCRC-M7 in water conducting cells and cortical parenchyma cells of several mosses and liverworts.

The presence of RG-II in the cell wall of bryophyte gametophytes has not yet been fully clarified. In a study by Matsunaga *et al.* (2004), the boron content of RG-II was detected in very low quantities. Since RG-II contains 12 different unusual monosaccharides in angiosperms (O'Neill *et al.*, 2004), it is also useful to search for them. However, O'Rourke *et al.* (2015) only found 2-*O*-MeXyl in the cell wall of *Anthoceros agrestis*.

The high proportions of uronic acids, especially in the (NH₄)₂C₂O₄ fraction of *Anthoceros*, might be a release of the unusual disaccharide α -D-GalA-(1→3)-L-Gal, which was found in *Anthoceros caucasicus* by NMR (Popper *et al.*, 2003). This disaccharide was mainly detected in an acidic aqueous buffer and a Na₂CO₃ fraction and only in minor amounts in a mild NaOH fraction. Cell walls of various plants above the *green lineage* were analysed for this disaccharide, but it could only be detected in the cell wall of this hornwort (Popper *et al.*, 2003). This indicates that *Anthoceros agrestis* may also contain this unusual disaccharide due to the high contents of uronic acids and Gal in the first three fractions.

Different types of hemicelluloses with special features within the bryophytes

Xylans and Xyloglucans. Common members of hemicelluloses are xylans and xyloglucans (XyG) (Anderson & Kieber, 2020). These representatives are mainly composed of the monosaccharides Gal, Glc, Man and Xyl, which were found in the alkaline fractions of *Anthoceros* and *Physcomitrium*, except of the monosaccharide Man in those of *Anthoceros*, in which Ara was increased. A high amount of Rha was also detected in the fractions of *Physcomitrium*.

O'Rourke *et al.* (2015) also investigated the cell wall of *Anthoceros* and gained a hemicellulose fraction by extraction with 6 M NaOH. In this study, a similar monosaccharide composition and distribution was detected. The high Ara, Glc and Xyl amounts might be a hint for xylans, arabinoxylans and xyloglucans, which can be confirmed using antibodies directed against epitopes of those. The antibody LM10 is raised against epitopes of the non-reducing end of (1→4)-β-D-xylan. The moderate response of the alkaline fraction of *Anthoceros* and the very weak binding of that of *Physcomitrium* to LM10 were not corresponding to the results of the antibody study by Carafa *et al.* (2005). In this study, all tested hornworts, liverworts and mosses did not bind to LM10. Only the four investigated hornworts were positive for LM11, which is raised against substituted xylans, such as arabinoxylans. This confirms the suggestion of arabinoxylans also in *Anthoceros*. The weak binding of the *Physcomitrium* fraction to LM10 was also observed by labelling other alkaline fractions of *Physcomitrium* cell walls and by binding restricted to *Physcomitrium* gametophores (Moller *et al.*, 2007; Berry *et al.*, 2016). The binding of the antibody LM11 was detected only in axillary hair cells (Kulkarni *et al.*, 2012). The reason of this could be the absence of the non-reducing end of xylans in *Physcomitrium* as proposed by Kulkarni *et al.* (2012). There, it was demonstrated, that glucuronylated xylans, which are common in land plants, differ structurally in cell walls of *Physcomitrium* from those in secondary cell walls of seed plants. Glucuronoxylans of seed plants consist of 4-*O*-Me-α-D-GlcAp and α-D-GlcAp side chains, whereas xylans of *Physcomitrium* lack the methylated GlcAp side chains (Kulkarni *et al.*, 2012).

Popper and Fry (2003) identified the presence of XyGs in various bryophyte species by Driselase digestion, although the yields of XyG in the bryophytes were lower than those in angiosperms (Popper & Fry, 2003). This could indicate that bryophytes generally contain less XyG in the cell wall or that they are more difficult to digest due to altered side chains (Pfeifer, Mueller, Classen, 2022). Epitopes of motifs and side chains of XyGs can be verified with various antibodies. LM15 is raised against the XXXG-motif of XyG (Marcus *et al.*, 2008). The antibody interacted only weakly with the KOH fraction of *Physcomitrium*, indicating that there are limited XyGs with the XXXG-motif. The binding was also restricted to the protoplast and protonemal cells and was only weakly recognised in other alkaline fractions of *Physcomitrium* (Moller *et al.*, 2007; Berry *et al.*, 2016).

In contrast, the alkaline fraction of *Anthoceros* showed strong binding to LM15, which implies that *Anthoceros* cell walls contain high amounts of XyGs with XXXG-motifs. This motif is common in XyGs of tracheophytes and was also found in three hornwort species by NMR analysis, including *Anthoceros agrestis* (Peña *et al.*, 2008). Galactosylated side chain epitopes can be detected with the antibody LM25 and were found in spore cell walls of *Anthoceros* and

other hornworts (Pedersen *et al.*, 2012; Renzaglia *et al.*, 2020). The detailed structural analysis of Peña *et al.* (2008) detected fucosylated side chains only in the XyGs of the hornwort *Megaceros*, which, however, contrasts with the negative results of the antibody test with CCRC-M1, directed against Fuc containing side chains, on cell walls of *Megaceros* (Puhlmann *et al.*, 1994; Kremer *et al.*, 2004). This antibody reacted positive in cell walls of some liverworts and only weakly in mature *Sphagnum* cell walls (Ligrone *et al.*, 2002; Kremer *et al.*, 2004). Other tested moss cell wall fractions did not bind to this antibody, including *Physcomitrium* (Ligrone *et al.*, 2002; Moller *et al.*, 2007).

Instead, galactosylated side chains were found in XyGs in cell walls of *Physcomitrium* (LM25; Galloway *et al.*, 2018). The lack of the Fuc side chains and the presence of the Gal side chains in *Physcomitrium* XyGs were confirmed by Peña *et al.* (2008). The general branching pattern was determined to be a XXGGG-motif, which also explains the weak response of the LM15 antibody in this study. This motif is the common motif for XyGs of grasses. In addition, four unusual side chains, P and Q as well as M and N, were detected in the moss XyG. These are characterized by a 2,4-linked Xylp residues with β -D-Galp, which are substituted with β -D-GalAp (P and Q) or α -L-Araf (M and N). The side chains Q and N are characterized by an additional β -D-Galp residue. The galacturonic acid side chains P and Q were only found in XyGs of the liverwort *Marchantia* and the GalAp residue in XyGs in root hair cells walls of *Arabidopsis* (Peña *et al.*, 2008, 2012). These side chains could also be the cause for the increased content of uronic acids in the KOH fraction of *Physcomitrium*.

Mannans and Glucans. The alkaline fractions of *Anthoceros* and *Physcomitrium* are rich in Man and Glc, especially those of *Physcomitrium*. This indicates the presence of mannans and glucans. Mannose was found to be abundant in bryophyte cell walls, whereas the only hornwort cell wall tested, *Anthoceros caucasicus*, contained less than the most investigated mosses (Popper & Fry, 2003). Epitopes of mannans and glucomannans can be detected with the antibody BS 400-4 (Pettolino *et al.*, 2001) and were abundant in alkaline fractions of cell walls as well as rhizoids, protoplasts, protonema cells and gametophores of *Physcomitrium* (Moller *et al.*, 2007; Berry *et al.*, 2016). In addition, a galactoglucomannan was isolated from an alkaline fraction of the aquatic moss *Fontinalis antipyretica* (Geddes & Wilkie, 1971).

Roberts *et al.* (2018) identified a special arabinoglucan with both (1 \rightarrow 3)-Araf and (1 \rightarrow 4)-Glc p chains. The linkage types of the arabinoglucan are similar to that of mixed-linkage glucans (MLGs), which were previously only detected in horsetails and Poales within the land plants (Popper & Fry, 2004; Sørensen *et al.*, 2008).

AGPs in bryophytes are similar but with characteristic differences

In the past, AGPs have been detected in different bryophytes, but mostly on the basis of gel diffusion assays or antibody reaction (Clarke *et al.*, 1978; Basile & Basile, 1987; Ligrone *et al.*, 2002; Kremer *et al.*, 2004; Lee *et al.*, 2005; Berry *et al.*, 2016). However, only a few bryophyte AGPs have been isolated (Lee *et al.*, 2005; Fu *et al.*, 2007; Bartels *et al.*, 2017; Happ & Classen, 2019). As a result of this study, two further bryophyte AGPs can be added to this list.

The AGP yield of *Physcomitrium* (0.09 %) is in the same range as isolated AGPs from other bryophytes and ferns (0.06 % – 0.19 %; Bartels & Classen, 2017; Bartels *et al.*, 2017; Happ & Classen, 2019; Mueller *et al.*, 2023), while the AGP yield of *Anthoceros* is higher (0.31 %). This could be due to the fact that *Anthoceros* was cultivated on medium and not on soil. This is also reflected in a *Physcomitrium* AGP yield of 0.23 % when *Physcomitrium* was grown in cell culture (Bartels *et al.*, 2017).

Protein moiety of AGPs. The moss and the hornwort AGPs contain a similar protein content of around 16 % – 17 %. This is comparable to the protein content of another moss, *Polytrichastrum* (Bartels *et al.*, 2017). Other studies revealed a high variety of the protein amount in bryophyte AGPs ranging from 4.6 % (*Sphagnum*; Bartels & Classen, 2017) to 24.9 % (*Marchantia*, Happ & Classen, 2019). The protein parts of fern AGPs are slightly lower (6.4 % – 12.3 %; Bartels & Classen, 2017). Only the protein content of two water ferns, *Azolla* and *Salvinia*, was in the same range (14.6 % and 19.4 %; Mueller *et al.*, 2023). In addition, the Hyp amount in relation to the total protein of *Physcomitrium* and *Anthoceros* was in the same range as that of the bryophytes and aquatic ferns mentioned above (0.9 % – 2.5%; Bartels *et al.*, 2017; Happ & Classen, 2019; Mueller *et al.*, 2023). The only exception was again *Sphagnum* with 5.8 %, which corresponds to the proportion that also occurs in terrestrial leptosporangiate ferns (Bartels & Classen, 2017; Bartels *et al.*, 2017).

Carbohydrate part of AGPs. The polysaccharide part of the AGP of *Anthoceros* consists mainly of Ara, Gal and 3-*O*-MeRha, which make up over 90 %. This part of the *Physcomitrium* AGP also contains a high content of Glc, although it cannot be excluded that this could also be starch or Glc contamination of the β GlcY. *Physcomitrium* AGPs of three different fractions, a soluble fraction, a membrane fraction and a cell wall fraction were also isolated by a study of Fu *et al.* (2007). The soluble fraction is more comparable to the AGP fraction of this work than the other fractions, despite the fact that no solvent extraction was performed in this soluble AGP fraction. The monosaccharide amounts are comparable to our results, except of the contents of Glc and GlcA. Glc was represented by 1.3 %, while GlcA accounted for 12.3 %. This could not be

confirmed in the AGP_{UR}, instead it was almost the other way round. The amount difference of Glc might also be due to the type of cultivation, as in Fu *et al.* (2007) *Physcomitrium* was grown under aseptic conditions and not on soil as in our study. This is supported by another study by Bartels *et al.* (2017), in which AGPs of *Physcomitrium*, grown in cell culture, also contained only a low amount of Glc (GlcA was not tested).

The unusual 3-*O*-MeRha has never been detected in any cell wall component of an angiosperm, but it has been found in cell walls and also AGPs of algae, bryophytes, ferns and gymnosperms (Ogawa *et al.*, 1997; Popper & Fry, 2003; Pfeifer *et al.*, 2022; Bartels & Classen, 2017; Bartels *et al.*, 2017; Happ & Classen 2019; Baumann *et al.*, 2021; Mueller *et al.*, 2023).

To obtain further information about the AGPs of these two bryophytes, a linkage type analysis was performed. The typical galactan core of angiosperms consists of 1,3-, 1,6- and 1,3,6-linked Galp. These were also found in those of the bryophytes except for low amounts of the 1,6-Galp (less than 2 %). Low amounts of 1,6-Galp linkages were also characteristic for other AGPs of spore producing land plants and indicate a high degree of branching of these AGPs (Lee *et al.*, 2005; Bartels & Classen, 2017; Bartels *et al.*, 2017; Happ & Classen, 2019; Mueller *et al.*, 2023). Only the AG structure of *Sphagnum* is again an exception, whose content of 1,6-Galp linkages is in the range of seed plants (Bartels *et al.*, 2017; Thude & Classen, 2005). Instead, a further branching structure, the 1,3,4-Galp, was only detected in the AGP of the hornwort *Anthoceros*. However, this linkage was also found in traces in the AGP of *Physcomitrium*, cultivated in cell cultures, and in some fern AGPs (Lee *et al.*, 2005; Bartels & Classen, 2017). In the AGPs of the mosses *Polytrichastrum* and *Sphagnum*, the unique branching point 1,2,3-Galp was identified, which was detectable only in traces in both bryophyte AGPs.

A high content of 1,4-Glcp was also determined in the AGP of *Physcomitrium*. This linkage type was not reported previously as part of an AGP and only detected at 1 % in the AGP of *Physcomitrium*, which was grown under aseptic conditions (Lee *et al.*, 2005). However, this *Physcomitrium* AGP contained high amounts of 1,4-GlcAp, which could not be detected in our study.

In contrast, 1,4-Galp has often been described as part of AGPs, including those of the mosses *Sphagnum* and *Polytrichastrum* and the liverwort *Marchantia* (Bartels & Classen, 2017; Bartels *et al.*, 2017; Happ & Classen, 2019; Baumann *et al.*, 2021).

An additional acidic hexose linkage type, the 1,4-HexAp, was found in the AGP_{UR} of *Anthoceros*. Since only 1,4-GlcAp linkages have been described in AGPs to date, it is likely that this is also GlcA (Pfeifer *et al.*, 2020).

The other main component of the carbohydrate structure of AGPs are the terminal residues, which consist mainly of Ara. The Ara linkages of angiosperm AGPs are mostly furanosidic,

either terminal or 1,5-linked (Classen *et al.*, 2000; Thude & Classen, 2005). This is also the case for the *Physcomitrium* AGP in our study and in correspondence to the work of Lee *et al.* (2005). The 1,5-linkage was also determined in the peat moss *Sphagnum* and the eusporangiate fern *Equisetum* (Bartels & Classen, 2017; Bartels *et al.*, 2017). In contrast, the AGP of *Anthoceros* showed a 1,3-Araf linkage. This 1,3-Araf linkage was also the main Ara linkage in the lycophyte *Lycopodium* (Bartels & Classen, 2017). Most of the terminal Ara was also found there in pyranosidic form, which could also be detected in the AGP of *Anthoceros*, but only in low amounts. The majority of the terminal Ara was also furanosidic, as in *Physcomitrium*. The liverwort *Marchantia* and the other moss *Polytrichastrum* contain both, 1,3-Araf and 1,5-Araf, in similar quantities (Bartels *et al.*, 2017; Happ & Classen, 2019). The 1,2-linkage type of Araf, which occurs mainly in leptosporangiate ferns, was detected only in traces in both bryophyte species (Bartels & Classen, 2017; Mueller *et al.*, 2023).

In addition, high proportions of terminal 3-*O*-MeRhap were determined in the AGPs of both bryophytes, but these were about twice as high in *Physcomitrium* compared to *Anthoceros*. Comparable high amounts of this methylated monosaccharide were found in the AGP of *Physcomitrium* which was cultivated in cell culture (Lee *et al.*, 2005). It seems that this unusual 3-*O*-MeRhap is a typical feature of AGPs of bryophytes, ferns and gymnosperms (Akiyama *et al.*, 1987; Bartels & Classen, 2017; Bartels *et al.*, 2017; Happ & Classen, 2019; Baumann *et al.*, 2021), but is not part of angiosperm AGPs.

To provide further information on structural elucidation, the binding affinity of the AG moieties of the two bryophyte AGPs was tested with several antibodies raised against epitopes of AGP-glycans (Fig. 3). The epitope of JIM13 is not fully elucidated, but the trisaccharide β -D-GlcAp-(1 \rightarrow 3)- α -D-GalAp-(1 \rightarrow 2)- α -L-Rha has been shown to interact with this antibody (Yates *et al.*, 1996). Since the AGP of *Physcomitrium* showed a stronger binding affinity than the AGP of *Anthoceros*, it was confirmed that Rha in particular is involved in binding. Berry *et al.* (2016) also detected epitopes of JIM13 at *Physcomitrium* protoplasts and gametophores. In addition, JIM13 epitopes were identified in secondary wall layers of the hornwort *Megaceros* and in hyaline cells, water retaining cells, of the peat moss *Sphagnum* (Kremer *et al.*, 2004). These cells of *Megaceros* and *Sphagnum* were also labelled with the AGP antibody JIM8, of which the epitope is still unknown (Pennell *et al.*, 1991; Kremer *et al.*, 2004).

Ligrone *et al.* (2002) used JIM8 and two other antibodies raised against AGPs in the investigation of water conducting cells of several mosses. While JIM8 epitopes showed no affinity to these cells, the presence of AGPs was detected by the binding of the antibody CCRC-M7, directed against arabinosylated 1,6-linked galactans, and LM6, raised against 1,5-Araf side chains of AGPs (Puhlman *et al.*, 1994; Verherbruggen *et al.*, 2009a).

These side chains of 1,5-Araf in *Physcomitrium* were also confirmed by the antibody LM6 in this study. The binding to this antibody was negative for the AGP of *Anthoceros*, confirming that other Araf linkage types are present in this AGP. Both antibodies were also used in the study of Lee *et al.* (2005). There, LM6 had a higher affinity to protonemal cells of *Physcomitrium* than JIM13. In particular, LM6 showed binding to the plasma membrane and cell wall surfaces at the tip of the growing protonemata, indicating that AGPs are involved in apical cell expansion.

The low amounts of 1,6-Galp linkages were verified by the result with the antibody KM1, which did not bind to the *Anthoceros* AGP and showed only weak interaction with *Physcomitrium* AGP. The epitope of this antibody was developed against 1,6-Galp linkages of the angiosperm AGP of *Echinacea purpurea* (Classen *et al.*, 2004).

The antibody LM2 recognizes a carbohydrate epitope of an AGP from rice rich in Ara and Gal and minor amounts of GlcA and GlcA was effective at inhibiting LM2 binding (Smallwood *et al.*, 1996). According to Ruprecht *et al.* (2017), an oligosaccharide with 1,6-linked Gal with a terminal GlcA was an effective epitope of the LM2 antibody. Due to lack of 1,6-linked Gal in both bryophyte AGPs, it would have been expected that reactivity with LM2 should be weak. However, since the binding profile of both bryophyte AGPs showed a strong affinity, GlcA probably plays a more decisive role in the epitope. Detection of the epitope of LM2 was also verified by Berry *et al.* (2016) at *Physcomitrium* protoplasts, protonemata, rhizoids and gametophores.

Based on the data from the linkages type analysis and the ELISA results, a proposed structure of the AGP of *Anthoceros* was illustrated (Fig. 4). This was not carried out for the AGP of *Physcomitrium*, as it is not certain whether the high amounts of 1,4-Glcp are part of the AGP or might be due to contaminations.

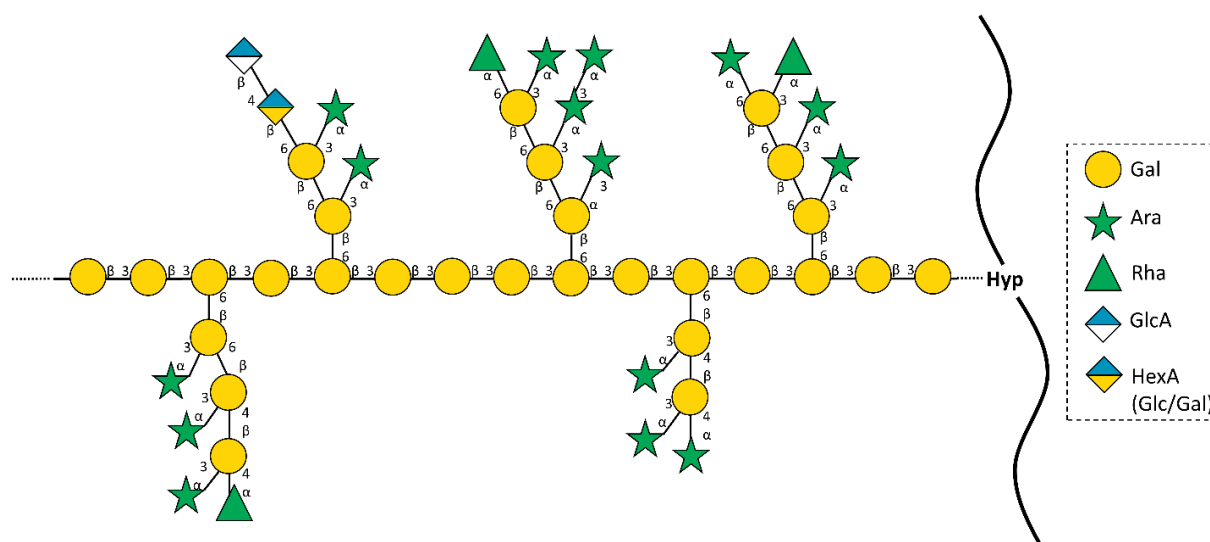


Figure 4. Structural proposal for the carbohydrate moiety of the AGP from *Anthoceros agrestis*. The proposal was derived from the compositional, immunochemical and linkage-type analyses of the AGP and the reduced AGP_{UR}.

CONCLUSION

The knowledge of cell wall composition of bryophytes is still very limited and often based only on immunocytochemical detection. In this study, the isolation and characterization of the cell walls of the two model organisms *Anthoceros* and *Physcomitrium* enriches this knowledge.

The main cell wall components of seed plant cell walls are found in the cell walls of both bryophytes. Within the pectins, presence of HG in both species is reasonable due to high amounts of uronic acids in both pectic fractions, especially in *Anthoceros*. Although the RG-I backbone was not detectable by the antibody INRA RU2, RG-I side chains could be detected in *Physcomitrium*, but only to lower extent in *Anthoceros*. Up to now, no RG-I and RG-II has been isolated from a bryophyte wall. The question, whether these pectic polysaccharides are part of bryophyte cell walls is therefore still unsolved and an interesting task for future research. Different hemicelluloses are also part of the bryophyte walls. For long time, it was thought that among the bryophytes, only hornworts have xylans, which are all substituted (Carafa *et al.*, 2005), but in this work, it could be demonstrated immunocytochemically that the hornwort and the moss contain low amounts of epitopes of unsubstituted xylans.

To date, only a few AGPs have been isolated from bryophyte cell walls and now, for the first time, a hornwort AGP. The general features of the galactan core structure of seed plant AGPs can be identified in both bryophyte AGPs. The 1,3-Galp and the 1,3,6-Galp linkages were present in similar amounts, with only low contents of 1,6-Galp found, demonstrating a highly branched galactan core structure. This characteristic has been also found in AGPs of other spore producing plants.

There are additional differences in the Ara linkages in the side chains. The *Anthoceros* AGP contained 1,3-Araf, t-Araf and low amounts of t-Arap, comparable to the linkage types of AGP of the lycophyte *Lycopodium*. The AGP of *Physcomitrium* showed mainly 1,5-Araf linkages and t-Araf residues, similar to those of angiosperm AGPs. On the other hand, both bryophyte AGPs contained the unusual 3-O-MeRhap residues, which were not detectable in any cell wall component of angiosperms.

Based on these findings, differences of the AGP structures of the three phylogenetic bryophyte groups cannot yet be precisely defined. Further species need to be investigated in order to obtain a clearer picture of bryophyte AGPs.

EXPERIMENTAL PROCEDURES

Plant material and sampling

The hornwort *Anthoceros agrestis* PATON (*Anthoceros*) was cultivated on plates in the Pharmaceutical Institute of Kiel University (Germany) and collected in the years 2021 to 2023. Spores and fresh gametophyte material of *Anthoceros* “Bonn” strain were kind gifts of Péter Szövényi (University of Zurich). For spore germination and gametophyte culture on BCD medium, the protocol of Cove *et al.* (2009) was used.

The moss *Physcomitrium patens* (HEDW.) BRUCH & SCHIMP (*Physcomitrium*) was grown and collected in April and July 2022 in the greenhouse of the garden of the Pharmaceutical Institute. Fresh gametophyte materials of *Physcomitrium* “Reute” strain were kind gifts of Stefan A. Rensing (University of Freiburg).

All samples were cleaned with water and freeze-dried (Christ Alpha 1-4 LSC, Martin Christ Gefriertrocknungsanlagen GmbH, Osterode, Germany).

Isolation of cell wall fractions and arabinogalactan-proteins (AGPs)

After freeze-drying and grounding of the plant material, it was pre-extracted two times (2 h and 21 h) with 70 % acetone solution (V/V) in a ratio of 1:10 (w/V) for *Anthoceros* and 1:20 (w/V) for *Physcomitrium*. The air-dried plant residue was extracted with double-distilled water (ddH₂O) under constant stirring (SM 2484, Edmund Bühler GmbH, Bodelshausen, Germany) for 21 h at 4°C in a 1:50 (w/V) ratio for *Anthoceros* and 1:20 (w/V) for *Physcomitrium*. Afterwards, the aqueous extract was separated from the insoluble plant material in case of *Anthoceros* by centrifuge (19,000 g, 4 °C, 20 min; Haraeus Multifuge X3R, Thermo Scientific Waltham, USA) or through a tincture press (HAFICO HP 2 H, Fischer Tinkturenpressen GmbH, Mönchengladbach, Germany; *Physcomitrium*). The insoluble plant pellet was freeze-dried and used for further extractions (see below).

After incubating the aqueous extract in a water bath (GFL 1002, LAUDA-GFL Gesellschaft für Labortechnik mbH, Burgwedel, Germany) at 90 – 95°C for ten minutes, the denatured proteins were removed by centrifugation (20 min, 4°C, for *Anthoceros* 4,122 g and for *Physcomitrium* 19,000 g). The aqueous extract was then evaporated in a rotary evaporator (40°C, 0,010 mbar; Laborota 4000, Heidolph Instruments GmbH & CO. KG, Schwabach, Germany) to approximately one-tenth of its volume. After adding this extract to cooled ethanol resulting in a final concentration of 80 % ethanol (V/V), it was incubated overnight at 4°C. The precipitate was isolated by centrifugation (4°C, 19,000 g, 20 min) and finally freeze-dried (AE).

AGPs were isolated from the AE with the β -Glc-Yariv reagent (β GlcY) according to the procedure of Classen *et al.* (2005) and Mueller *et al.* (2023).

The insoluble plant pellet, mentioned above, was used to gain two pectic and two hemicellulose fractions. The two pectic fractions were represented by the $(\text{NH}_4)_2\text{C}_2\text{O}_4$ and HCl fraction, extracted by 0.2 mol L⁻¹ ammonium oxalate and 0.01 mol L⁻¹ hydrochloric acid. The two hemicellulose fractions were extracted by sodium carbonate [Na_2CO_3 fraction, 3 % (w/V)] and potassium hydroxide (KOH fraction, 2 mol L⁻¹). The extraction of the four fractions followed the method of O'Rourke *et al.* (2015) and Raimundo *et al.* (2016) with modifications described in Pfeifer *et al.* (2023).

Analysis of monosaccharides

The determination of the neutral monosaccharide compositions was performed by the method of Blakeney *et al.* (1983), and uronic acid (UA) compounds were identified photometrically by the method of Blumenkrantz & Asboe-Hansen (1973); both with modifications described in Mueller *et al.* (2023).

The neutral monosaccharides were identified and quantified *via* gas chromatography (GC) with flame ionization detection (FID) and mass spectrometry detection (MSD): GC + FID: 7890B; Agilent Technologies, USA; MS: 5977B MSD; Agilent Technologies, USA; column: Optima-225; Macherey-Nagel, Germany; 25 m, 250 μm , 0.25 μm ; helium flow rate: 1 mL min⁻¹; split ratio 30:1. A temperature gradient was performed to achieve peak separation (initial temperature 200 °C, subsequent holding time of 3 min; final temperature 243 °C with a gradient of 2 °C min⁻¹).

To identify the methylated monosaccharide 3-*O*-MeRha, the retention time and mass spectrum described in Happ & Classen (2019) were used.

Reduction of uronic acids of AGPs and structural characterization of AGPs

Using a modified method of Taylor & Conrad (1972) with modifications described in Mueller *et al.* (2023), a carboxy reduction of the uronic acids of 10 – 20 mg isolated AGP was performed (AGP_{UR}). Following the method of Harris *et al.* (1984; see Mueller *et al.*, 2023 for modifications), linkage type analyses of the AGPs and the AGP_{URS} were performed. The produced permethylated alditol acetates (PMAA) were identified by gas-liquid chromatography-mass spectroscopy (instrumentation see above: "Analysis of monosaccharides"; column: Optima-1701, 25 m, 250 μ m, 0.25 μ m; helium flow rate: 1 mL min⁻¹; initial temperature: 170 °C; hold time 2 min; rate 1°C min⁻¹ until 210°C was reached; rate: 30 °C min⁻¹ until 250 °C was achieved; final hold time 10 min) by their retention times and comparison of the mass spectra to a PMAA library established in the working group.

Determination of protein and hydroxyproline content

The protein content was calculated based on the nitrogen content with the factor 6.25 (Kjeldahl, 1883), which was determined by elemental analysis in the Chemistry Department of Kiel University, Kiel, Germany (HEKAtech CHNS Analyzer, Wegberg, Germany).

The measurement of hydroxyproline (Hyp) was performed photometrically at 558 nm according to Stegemann & Stalder (1967) with slight modification (see Mueller *et al.*, 2023). The Hyp content was quantified *via* a linear regression analysis.

Indirect enzyme-linked immunosorbent assay (ELISA)

The ELIS-assays were performed as described in Mueller *et al.* (2023). The (NH₄)₂C₂O₄ and KOH fractions were used in the concentration 12.5 μ g mL⁻¹, the aqueous AGP solutions in the concentrations 12.5 μ g mL⁻¹, 25 μ g mL⁻¹ and 50 μ g mL⁻¹. The (NH₄)₂C₂O₄ and 4 M NaOH fractions were generated according to Jander, 2021 (data not published). The primary antibodies (INRA RU2, JIM13, KM1, LM2, LM5; LM6; LM16; LM26; Institut national de la recherche agronomique, France; Kerafast, Inc., Boston; USA) were diluted in a ratio of 1:20 (V/V), only INRA RU2 in 1:200 (V/V) and the secondary antibodies (SA), anti-rat-IgG or anti-mouse-IgG (only for INRA RU2 and KM1) in a ratio of 1:500 (V/V) in phosphate-buffered saline (PBS; pH 7.4). The SA were conjugated with alkaline phosphatase, produced in goat (Sigma-Aldrich Chemie GmbH, Taufkirchen, Germany). Epitopes of the antibodies and key references are listed in Table S4.

Gel diffusion assay

An agarose gel (Tris-HCl, 10 mmol L⁻¹; CaCl₂, 1 mmol L⁻¹; NaCl, 0.9 % w/V; agarose, 1 % w/V) was used for a gel diffusion assay. Several cavities were stamped in the gel and filled with dilutions (100 mg mL⁻¹) of the AE samples or with βGlcY solution (1 mg mL⁻¹). The gel was incubated in the dark overnight. If AGPs are present in the samples, a red precipitation line appears.

ACKNOWLEDGEMENTS

Funding: BC (project-number 440046237) is grateful for funding within the framework of MAdLand (<http://madland.science>), priority programme 2237 of the German Research Foundation (DFG). We thank Péter Szövényi for spore and fresh gametophyte delivering of *Anthoceros*, and Stefan A. Rensing for fresh gametophytes of *Physcomitrium* as well as Lukas Pfeifer for cultivating the plant material and helping with the linkage type analysis.

AUTHORS CONTRIBUTION and CONFLICT OF INTEREST

BC and KM planned and designed the research. KM performed the extractions as well as the carbohydrate and ELISA experiments. KM created all main text figures. All authors analysed the data. KM wrote the draft manuscript with the help of BC. BC and KM revised the manuscript, read and approved the final manuscript.

DATA AVAILABILITY STATEMENT

All relevant data can be found within the manuscript and its supporting materials.

SUPPORTING INFORMATION

Table S1. Yields of the different extracts from *Anthoceros agrestis* and *Physcomitrium patens* in % of dry fraction (w w⁻¹).

	<i>A. agrestis</i>	<i>P. patens</i>
(NH ₄) ₂ C ₂ O ₄	28.4	4.3
HCl	5.9	1.2
Na ₂ CO ₃	7.9	6.5
KOH	11.7	20.2

Table S2a. Neutral monosaccharide composition of different cell wall fractions from *Anthoceros agrestis* in % (mol mol⁻¹; n=3; tr: trace value < 1 %).

Neutral monosaccharide	<i>A. agrestis</i> AE	<i>A. agrestis</i> (NH ₄) ₂ C ₂ O ₄	<i>A. agrestis</i> HCl	<i>A. agrestis</i> Na ₂ CO ₃	<i>A. agrestis</i> KOH
3- <i>O</i> -MeRha	1.3 ± 0.1	2.2 ± 0.1	tr	1.2 ± 0.1	tr
Rha	2.2 ± 0.1	6.2 ± 0.2	1.4 ± 0.3	tr	1.1 ± 0.0
Fuc	1.4 ± 0.1	1.2 ± 0.1	tr	1.3 ± 0.1	tr
Rib	tr	tr	-	-	tr
Ara	8.4 ± 0.1	5.2 ± 0.1	2.1 ± 0.2	13.1 ± 1.0	11.1 ± 0.5
Xyl	23.8 ± 0.1	17.2 ± 0.4	5.8 ± 1.6	10.9 ± 1.1	30.1 ± 2.2
Man	1.2 ± 0.0	tr	tr	1.1 ± 0.1	2.0 ± 0.1
Gal	42.2 ± 0.3	52.8 ± 1.2	77.2 ± 2.8	38.2 ± 5.2	19.4 ± 1.4
Glc	19.5 ± 0.2	14.3 ± 0.6	13.5 ± 0.7	34.2 ± 3.0	36.3 ± 2.9

Table S2b. Neutral monosaccharide composition of different cell wall fractions from *Physcomitrium patens* in % (mol mol⁻¹; n=3; tr: trace value < 1 %).

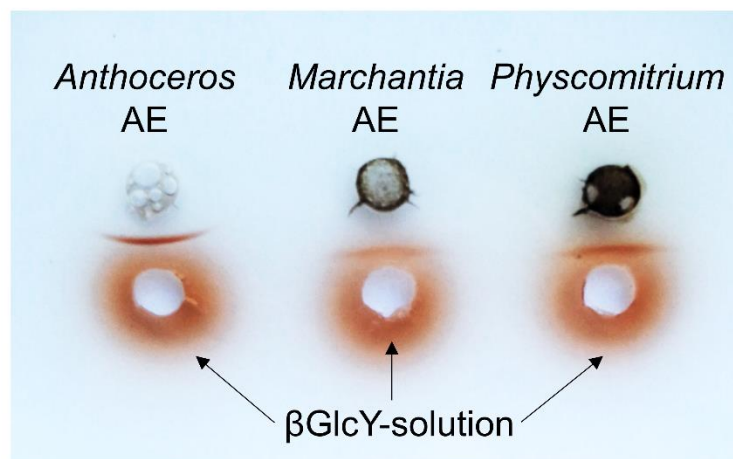
Neutral monosaccharide	<i>P. patens</i> AE	<i>P. patens</i> (NH ₄) ₂ C ₂ O ₄	<i>P. patens</i> HCl	<i>P. patens</i> Na ₂ CO ₃	<i>P. patens</i> KOH
3- <i>O</i> -MeRha	2.7 ± 0.0	2.0 ± 0.1	1.2 ± 0.1	tr	tr
Rha	4.2 ± 0.0	9.2 ± 0.7	8.6 ± 0.2	16.2 ± 1.0	13.2 ± 1.3
Fuc	4.0 ± 0.1	2.8 ± 0.1	1.9 ± 0.0	1.8 ± 0.2	tr
Rib	2.1 ± 0.2	1.5 ± 0.3	1.0 ± 0.1	-	-
Ara	11.5 ± 0.2	8.6 ± 0.5	6.5 ± 0.1	6.3 ± 0.0	3.7 ± 0.1
Xyl	7.7 ± 0.1	8.7 ± 0.5	8.4 ± 0.1	25.0 ± 2.6	24.3 ± 0.3
Man	6.0 ± 0.2	8.7 ± 0.1	8.1 ± 0.1	8.6 ± 0.2	15.4 ± 0.5
Gal	14.2 ± 0.3	14.8 ± 0.4	11.3 ± 0.1	13.8 ± 0.3	10.2 ± 0.0
Glc	47.6 ± 0.8	43.7 ± 2.3	53.0 ± 0.1	28.3 ± 1.5	33.2 ± 0.4

Table S3. Content of uronic acids in the different cell wall fractions from *Anthoceros agrestis* and *Physcomitrium patens* in % (w w⁻¹).

	<i>A. agrestis</i>	<i>P. patens</i>
AE	11.1	3.1
AGP	7.3	6.5
(NH ₄) ₂ C ₂ O ₄	49.1	14.9
HCl	17.3	6.9
Na ₂ CO ₃	10.2	4.1
KOH	4.2	9.8

Table S4. Antibodies tested for binding to bryophyte cell wall fractions AGPs.

Antibody	Epitope	Key References
INRA RU2	[(4)- α -D-GalA-(1,2)- α -L-Rha] ₄ of RG-I	Ralet <i>et al.</i> (2010)
JIM13	AGP glycan, e.g. β -D-GlcAp-(1 \rightarrow 3)- α -D-GalAp-(1 \rightarrow 2)- α -L-Rha	Pfeifer <i>et al.</i> (2022); Yates <i>et al.</i> (1996)
KM1	(1 \rightarrow 6)- β -D-Galp units in AGs type II	Classen <i>et al.</i> (2004); Ruprecht <i>et al.</i> (2017)
LM2	(1 \rightarrow 6)- β -D-Galp units with terminal β -D-GlcAp in AGP	Ruprecht <i>et al.</i> (2017); Smallwood <i>et al.</i> (1996);
LM5	Non-reducing end of (1 \rightarrow 4)- β -D-galactan	Torode <i>et al.</i> (2018)
LM6	(1 \rightarrow 5)- α -L-Araf oligomers in arabinan or AGP	Verhertbruggen <i>et al.</i> (2009a)
LM10	Non-reducing end of (1 \rightarrow 4)- β -D-xylan	McCartney <i>et al.</i> (2005); Ruprecht <i>et al.</i> (2017)
LM15	XXXG-motif of xyloglucan	Marcus <i>et al.</i> (2008); Pedersen <i>et al.</i> (2012)
LM16	Processed arabinan/ putativ galactan stub	Verhertbruggen <i>et al.</i> (2009a)
LM26	Branched (1 \rightarrow 6)- β -D-Galp-(1 \rightarrow 4)- β -D-galactan	Torode <i>et al.</i> (2018)

**Fig S1.** Gel diffusion assay with aqueous extracts from *Anthoceros agrestis*, *Marchantia polymorpha* and *Physcomitrium patens* (100 mg mL⁻¹) and β GlcY (1 mg mL⁻¹). The red precipitation line indicates presence of AGPs.

4. Sequential extraction of fern cell walls and characterization of arabinogalactan-proteins from the “living fossil”

Psilotum nudum

Kim-Kristine Mueller¹, Lukas Pfeifer¹, Lina Schuldt¹ and Birgit Classen¹

¹Pharmaceutical Institute, Department of Pharmaceutical Biology, Christian-Albrechts-University of Kiel, Gutenbergstr. 76, 24118 Kiel, Germany

ABSTRACT

During the colonization of land about more than 500 million years ago, abiotic and biotic changes induced extreme adaptation in plants, including the cell wall. While a lot is already known about seed plant cell walls, much is still unknown about those of spore-bearing plants. As ferns are sister to seed plants, studying their cell wall is key for solving the evolutionary development of the cell wall. To shed light on the evolution of fern cell walls, different cell wall fractions of one eusporangiate fern, *Psilotum nudum*, and three leptosporangiate ferns, *Azolla filiculoides*, *Salvinia x molesta* and *Ceratopteris richardii* were investigated. The main polysaccharides of seed plant cell walls cellulose, hemicelluloses and pectins were also found in the cell walls of ferns, however in varying quantities and compositions. The pectic fractions of *Ceratopteris* contained more homogalacturonan than those of *Azolla* and *Salvinia*. A hemicellulose fraction of *Azolla* was rich in xylans, that of *Salvinia* contained a high proportion of XXXG-xyloglucans, and high amounts of mannose could be detected in the fractions of *Psilotum*.

In addition, the arabinogalactan proteins (AGPs) of *Psilotum* were isolated, characterized and compared to those of other ferns. The pyranosidic 1,3- and 1,3,6-linked galactose of the carbohydrate backbone was comparable, but a special feature of fern AGPs, the pyranosidic 3-*O*-methyl rhamnose, was not detectable. Instead, terminal furanosidic and pyranosidic arabinose (Ara) as well as furanosidic 1,3-linked Ara were found in amounts and ratios only comparable to an AGP of the lycophyte *Lycopodium*. This underlines the special evolutionary position of the whisk ferns.

INTRODUCTION

The cell wall of plants is a highly dynamic, complex structure, which is ubiquitous in the plant kingdom. It consists mainly of polysaccharides, cell wall glycoproteins and sometimes polyphenols, mainly lignin. The three main classes of polysaccharides comprise cellulose, hemicelluloses and pectins (Popper, 2008). Cellulose is the most abundant polysaccharide and consists of linear and unbranched (1→4)-β-D-glucan chains. These glucan chains form microfibrils, which are cross-linked with hemicelluloses (Sediqqi *et al.*, 2021). The class of hemicelluloses also possesses a β-1,4-linked core structure, but is also composed of monosaccharides other than only Glc, such as xylans, xyloglucans or mannans. These have in common, that all of them are characterized by an ether group between C1 and C4 in an equatorial configuration (Scheller & Ulvskov, 2010). The third main group are pectins, acidic polysaccharides that form a matrix in which cellulose and hemicelluloses are embedded. Pectins can be divided into homogalacturonan (HG), rhamnogalacturonan-I (RG-I) and rhamnogalacturonan-II (RG-II; Mohnen, 2008). The framework of (substituted) HG consists of a linear α-1,4-linked GalA chain, which is also present in the backbone of RG-II (Barnes *et al.*, 2021). This backbone of RG-II is linked to up to six conserved side chains, which are illustrated in Barnes *et al.* (2021). A special feature of RG-II is the dimerization of two RG-II molecules *via* a boron ester linkage by Apiose residues (Mohnen, 2008). In contrast, RG-I possesses a core structure of repeating disaccharide units of α-1,4-GalA and α-1,2-Rha units (Avci *et al.*, 2018).

In addition to the high proportion of polysaccharides, there are also cell wall glycoproteins, mostly hydroxyproline-rich-glycoproteins (HRGPs). The HRGPs with the highest degree of glycosylation of up to 90 % are the arabinogalactan-proteins (AGPs; Ellis *et al.*, 2010). The carbohydrate part consists mainly of Ara and Gal and contains minor amounts of other monosaccharides in its side chains. The core structure is a (1→3)-β-D-galactan chain which is often linked to (1→6)-β-D-galactan side chains (Ma *et al.*, 2018). In addition, this core structure is responsible for one of the special features of AGPs: the precipitation with the β-glucosyl Yariv reagent (βGlcY), which can be used to isolate AGPs (Yariv *et al.*, 1962; Paulsen *et al.*, 2014; Ma *et al.*, 2018). The high polysaccharide part is covalently linked to the protein part *via* the amino acid hydroxyproline (Hyp; Ellis *et al.*, 2010). AGPs are involved in a variety of functions in seed plants, including cell proliferation and division, growth, pattern formation, xylem differentiation, programmed cell death or the regulation of salt stress (Seifert & Roberts, 2007; Lamport *et al.*, 2014; Ma *et al.*, 2018; Pfeifer *et al.*, 2020).

A high proportion of another polymer, the lignin, is preferably found in secondary walls of sclerenchyma cells and vascular tissue. It is produced by the condensation of three

phenylpropanoid alcohols (*p*-coumaryl, coniferyl and sinapyl alcohol), which are polymerized to *p*-hydroxyphenyl (H), guaianyl (G) and syringyl (S) units (Lewis & Yamamoto, 1990).

Based on their occurrence of vascular tissue, land plants can be divided into two groups: the non-vascular bryophytes and the vascular tracheophytes. The tracheophytes evolved around 440 million years ago (mya) and comprise lycophytes, ferns and seed plants (Delaux *et al.*, 2019; Pires & Dolan, 2012).

The main polysaccharides, cell wall glycoproteins and lignin have been found in different fern cell walls (Popper, 2006; Wang *et al.*, 2008; Mueller *et al.*, 2023). At first glance, the fern cell wall components appear to be very similar in comparison to those of seed plants, but they differ in quantity and composition of the components (Popper, 2006). Immunocytochemical studies on fern cell walls detected various epitopes of pectins, hemicelluloses and the arabinogalactan part of AGPs (Carafa *et al.*, 2005; Eeckhout *et al.*, 2014; Leroux *et al.*, 2015; Chernova *et al.*, 2020). Isolation of different cell wall fractions and further characterization shed light on those compositions (Matsunaga *et al.*, 2004; Popper & Fry, 2004; Silva *et al.*, 2011; Hsieh & Harris, 2012). Hemicelluloses, like xylans and xyloglucans contain many variations in their side chains (Carafa *et al.*, 2005; Peña *et al.*, 2008). Mannans and glucomannans seem to be abundant in some fern cell walls, especially in eusporangiate ferns (Popper & Fry, 2004; Silva *et al.*, 2011; Leroux *et al.*, 2013). The pectin RG-II occurs in the same quantities as in seed plants but has the specific feature that Rha is methylated (3-*O*-MeRha; Matsunaga *et al.*, 2004). This unusual 3-*O*-MeRha has not been found in any cell wall component of angiosperms to date. However, it was identified in AGPs of ferns and bryophytes (Bartels & Classen, 2017; Bartels *et al.*, Mueller *et al.*, 2023). It is discussed that this more hydrophobic character of the AGPs was an advantage in adapting to desiccation during land plant evolution (Bartels *et al.*, 2017; Mueller *et al.*, 2023). That AGPs have an influence on desiccation tolerance was demonstrated in the fern *Mohria caffrorum* (Moore *et al.*, 2013). In addition, a special AGP gene called xylogen has been detected in the moss *Physcomitrium* and in the lycophyte *Selaginella*. Originally, it was found in *Zinnia* cell cultures and shown to be responsible for xylem differentiation (Kobayashi *et al.*, 2011).

Another cell wall innovation against water loss is the incorporation of the hydrophobic lignin into secondary cell walls. Lignins of lycophytes and angiosperms consists primarily of S-unit, while lignins of ferns and gymnosperms contain mainly the G-unit (Weng *et al.*, 2008).

To enhance knowledge on fern cell walls, different cell wall fractions of four ferns were isolated and characterized in this work. We have chosen one eusporangiate fern *Psilotum nudum* and three leptosporangiate ferns *Azolla filiculoides*, *Salvinia molesta* and *Ceratopteris richardii* to

receive a broad overview. Additionally, the AGP of the eusporangiate fern was isolated and characterized. We chose *Psilotum*, as it is known as a “living fossil” with reduced morphological structure (Chernova *et al.*, 2020) and its AGP might therefore display special features different to other fern AGPs (Bartels & Classen, 2017). To the best of our knowledge, only one eusporangiate fern AGP has been isolated and characterized up to now (Bartels & Classen, 2017), so this work provides additional information about the evolution of AGPs in ferns.

RESULTS

Sequential extraction of pectic and hemicellulose fractions of fern cell walls

Sequential extraction resulted in two pectic fractions isolated with ammonium-oxalate $[(\text{NH}_4)_2\text{C}_2\text{O}_4]$ and hydrochloric acid (HCl) as well as three hemicellulose fractions gained by extraction with sodium carbonate (Na_2CO_3) and potassium hydroxide in two concentrations (2 M KOH; 8 M KOH). The yields of the pectic and hemicellulose fractions vary between 0.4 % and 23.4 % of the dry fraction material (w w⁻¹), see Table S1. The monosaccharide compositions are shown in Figure 1A and 1B, Tables S2a – S2e as well as Table S3. Furthermore, the pectic and two hemicellulose fractions were tested for interactions with antibodies directed against pectin (LM19, LM20), xylan (LM10) and xyloglucan (LM15, LM25) epitopes (Fig. 1C, Tab. S6).

The composition of the $[(\text{NH}_4)_2\text{C}_2\text{O}_4]$ fractions (Fig. 1, Tab. S2a and S3) reflected the typical composition of pectic polysaccharides with uronic acids and the neutral monosaccharides Gal, Ara and Rha, although the amounts of uronic acids in *Psilotum* and *Ceratopteris* were lower compared to the floating aquatic ferns, *Azolla* and *Salvinia*. Reactivity with antibodies directed against HG epitopes confirmed presence of this pectic polysaccharide in all investigated species. LM19 directed against nonesterified HG and LM20 against methyl-esterified HG showed strongest interaction with this fraction of *Ceratopteris*. The content of esterified HG in *Azolla* as indicated by reactivity with LM20 seems to be very low. Furthermore, Glc was present in these fractions and was even the dominant monosaccharide in *Psilotum* and *Salvinia*, which might be due to occurrence of starch.

The fractions isolated by HCl (Fig. 1, Tab. S2b and S3) were similar to a certain extent indicating also the presence of pectic polysaccharides. As confirmed by ELISA with LM19, all tested species and especially *Ceratopteris* contained unesterified HG in this fraction. LM20 showed no reactivity with this fraction in case of *Salvinia* and *Azolla*, but strong reactivity with

this fraction of *Ceratopteris*. In all species, Glc was the dominant monosaccharide of these fractions. As fractions were not treated with amylase, starch might have been co-extracted with pectins.

The extraction with sodium carbonate (Fig. 1, Tab. S2c and S3) yielded a fraction mainly composed of Glc, Gal, Ara, Rha and uronic acids. The amounts of uronic acids of *Psilotum* were found in the same range as in the pectic HCl fraction. In *Ceratopteris*, these were unusually high for a hemicellulose fraction. This was in correspondence with the results from ELISA. Antibodies directed against xylan (LM10) and xyloglucans (LM15, LM25) showed only low or no binding to these fractions.

The hemicellulose fraction, extracted with 2 M KOH (Fig. 1, Tab. S2d and S3), revealed a typical composition with mainly Glc and Xyl. In all species except of those of *Psilotum*, Xyl and Glc comprised over 80 % of the neutral monosaccharides, but the ratio of Xyl:Glc varied strongly with 1:6.7 for *Salvinia*, 1:0.6 for *Azolla* and 1:1.7 for *Ceratopteris*. The Xyl and Glc contents of the 2 M KOH fraction of *Psilotum* were also the highest and had the same ratio as in *Ceratopteris*, but the amounts of Ara and Man were also high. Binding of the antibody LM10 directed against the non-reducing end of xylans was restricted to the *Azolla* fraction (*Psilotum* not tested), which was in correspondence to the high Xyl content in this fraction of *Azolla*. LM15 and LM25 directed against xyloglucans showed strong reactivity with this fraction from all investigated species.

The 8 M KOH fractions consisted mainly of Xyl, Glc, and Man (Fig. 1A and 1B, Tab. S2e and S3). The highest amount of Xyl was detected in *Ceratopteris* at 57.6 %, the greatest content of Man was found in *Psilotum* (39.1 %), and of Glc in *Salvinia* (36.1 %). The uronic acid contents of both KOH fractions of all species were lower compared to the other fractions in all species.

Three additional *Salvinia* species (*S. auriculata*, *S. cucullata*, *S. natans*) were cultivated in lower amounts and analysed additionally (except of the 8 M KOH fraction). Compositions of the different fractions were comparable between species, indicating a similar cell wall composition within the genus *Salvinia* (see Fig. S1 and Tab. S5a-S5e). Therefore, these species were not investigated further. Variations in the content of Glc might be due to different amounts of glucans or differences in accumulation of starch depending on the harvest time.

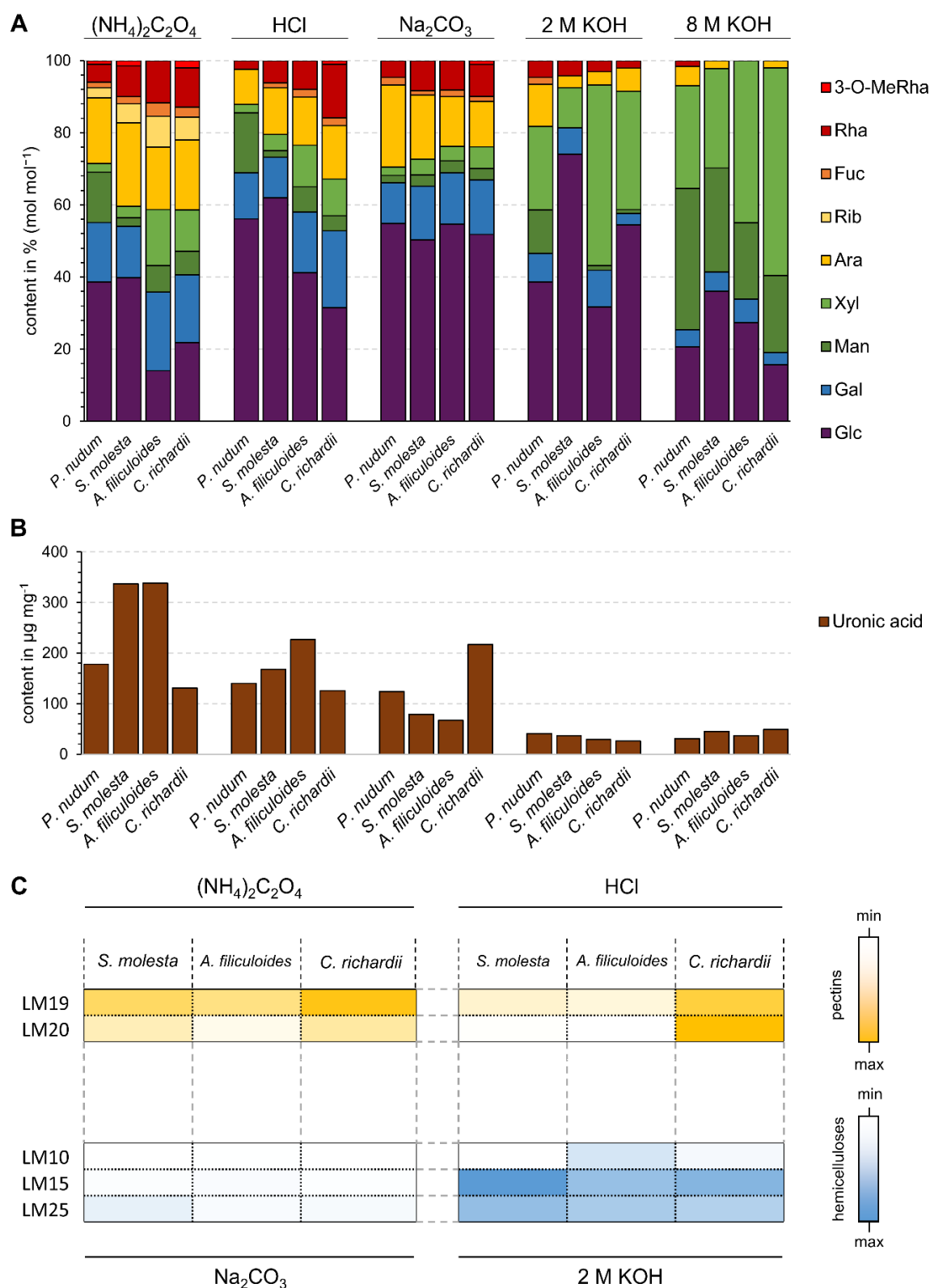


Figure 1. Monosaccharide composition of different cell wall fractions [(NH₄)₂C₂O₄, HCl, Na₂CO₃, 2 M KOH, 8 M KOH] of the ferns *Psilotum nudum*, *Salvinia molesta*, *Azolla filiculoides* and *Ceratopteris richardii*. **A:** Relative neutral monosaccharide composition determined by gas chromatography (GC; % mol mol⁻¹). **B:** Absolute content of uronic acids determined by colorimetric assay (% w w⁻¹ of dry fraction weight). **C:** Reactivity of *S. molesta*, *A. filiculoides* and *C. richardii* fractions with antibodies via ELISA after 10 min in the concentration 25 µg mL⁻¹ [(NH₄)₂C₂O₄, HCl: LM19, LM20; Na₂CO₃, 2 M KOH: LM10, LM15, LM25].

Water-soluble polysaccharides and arabinogalactan-proteins present in the cell wall of *Psilotum*

The dried fern material of *Psilotum* was extracted with water to obtain a water-soluble fraction (AE) possibly containing AGPs. The yield of the AE of *Psilotum* amounted to 2.2 % of dry plant material (w w⁻¹) and the neutral monosaccharide composition is shown in Figure 2A and Table S1.

In the aqueous extract of *Psilotum* (Tab. S4), Gal, Ara and Glc were present in high amounts (19.4 % – 34.9 %), followed by Man (10.6 %). The detected Rha, Fuc and Xyl amounts as well as the absolute uronic acid content were less than 5 %. The AE yields and compositions of the other three ferns are not described here, as these were published in Mueller *et al.* (2023).

Due to the high proportions of Ara and Gal, the AE was used for isolation of water soluble AGPs. Therefore, a precipitation reaction with the β GlcY was performed and yielded an AGP fraction of 0.08 % of dry plant material (w w⁻¹). The neutral monosaccharide composition of the *Psilotum* AGP is shown in Figure 2A and Table S4. The Ara content was 36.6 % and that of Gal was 54.7 %, which corresponds to a ratio of 1:1.5. In addition, 4.7 % Rha and less than 5 % of Glc were present. A content of 6.9 % was measured photometrically for the uronic acids. It has to be taken into account, that low amounts of Glc might be derived from the β GlcY.

In order to provide additional insight into the protein part of the AGP, both the protein and the hydroxyproline content were determined. The protein amount was calculated using the measured nitrogen content of 0.86 % (w/w) multiplied by the Kjeldahl constant (x 6.25). This resulted in a protein moiety of 5.4 %. As the amino acid Hyp covalently links the protein and carbohydrate part of AGPs, this was also analyzed. The absolute Hyp content was 0.33 %. In relation to the whole protein, the Hyp amount results in 6.1 %.

Reduction of uronic acids and partial degradation of the *Psilotum* AGP

To detect uronic acids, the carboxy groups of the uronic acids were reduced (AGP_{UR}). The neutral monosaccharide composition is shown in Figure 2A and Table S4. Compared to the monosaccharides of the native AGP, this reduction results in a low increase of the Glc content indicating the presence of GlcA in the native AGP. In addition, the mass spectrum and the fragmentation pattern of the monosaccharides were analyzed. Deuterated fragments were only found in the Glc peak, which confirms presence of low amounts of GlcA.

The oxalic acid partial hydrolysis was performed to separate labile Ara residues from the galactan core structure (AGP_{UROX}). To confirm that the reaction was successful, the neutral monosaccharide composition was determined again (see Fig. 2A and Tab. S4). This showed a 25 % decrease of Ara residues but also a slight decrease of Rha.

Elucidation of the AG-structure of the *Psilotum* AGP

The native AGP, the AGP_{UR} and the AGP_{UROX} were used for structural elucidation. Therefore, a linkage type analysis was performed (Tab. 1). The FID chromatogram of partially methylated alditol acetates (PMAAs) of AGP_{UR} is shown in Figure 2B.

The main linkage types the AGP and the AGP_{UR} were 1,3,6-Galp, 1,3-Galp and 1,3-Araf in amounts ranging between 10.3 % and 34.4 %. The dominant terminal residues were t-Araf and t-Arap with up to 9.9 %. Other linkage types and terminal residues were found in lower amounts below 5 %. The 1,4-linked Hexp represents Glc or Gal due to the overlapping retention time of both monosaccharides. In addition, the terminal residue 1-GlcAp and the 1,4-HexAp were detected in the linkage types of AGP_{UR}.

In the linkage type analysis of AGP_{UROX}, Galp linkages were together more than 80 % of all linkage types of this molecule. An increase of 1-Galp and 1,6-Galp in particular and a decrease of all Ara linkage types was determined.

Table 1. Linkage type analysis of AGP, AGP_{UR}, and AGP_{UROX} of *Psilotum nudum* in % (mol mol⁻¹, n=1; * containing deuterated fragments).

Mono-saccharide	linkage type	AGP	AGP _{UR}	AGP _{UROX}
Galp	1,3,6-	34.4	33.5	31.5
	1,6-	3.4	2.9	17.7
	1,3-	21.9	20.5	18.6
	1-	3.5	4.2	14.3
Glc p	1-	tr	1.0*	1.9*
Manp	1,6-	1.1	1.1	tr
Hexp	1,4-	3.4	4.9*	4.4*
Rhap	1-	3.6	3.4	3.0
Araf	1,5-	1.4	1.1	-
	1,3-	10.3	10.8	3.6
	1-	7.1	7.1	1.5
Arap	1-	9.9	9.5	3.5

tr: trace value 0.4 % – 1 %; linkage types < 0.4 % not listed

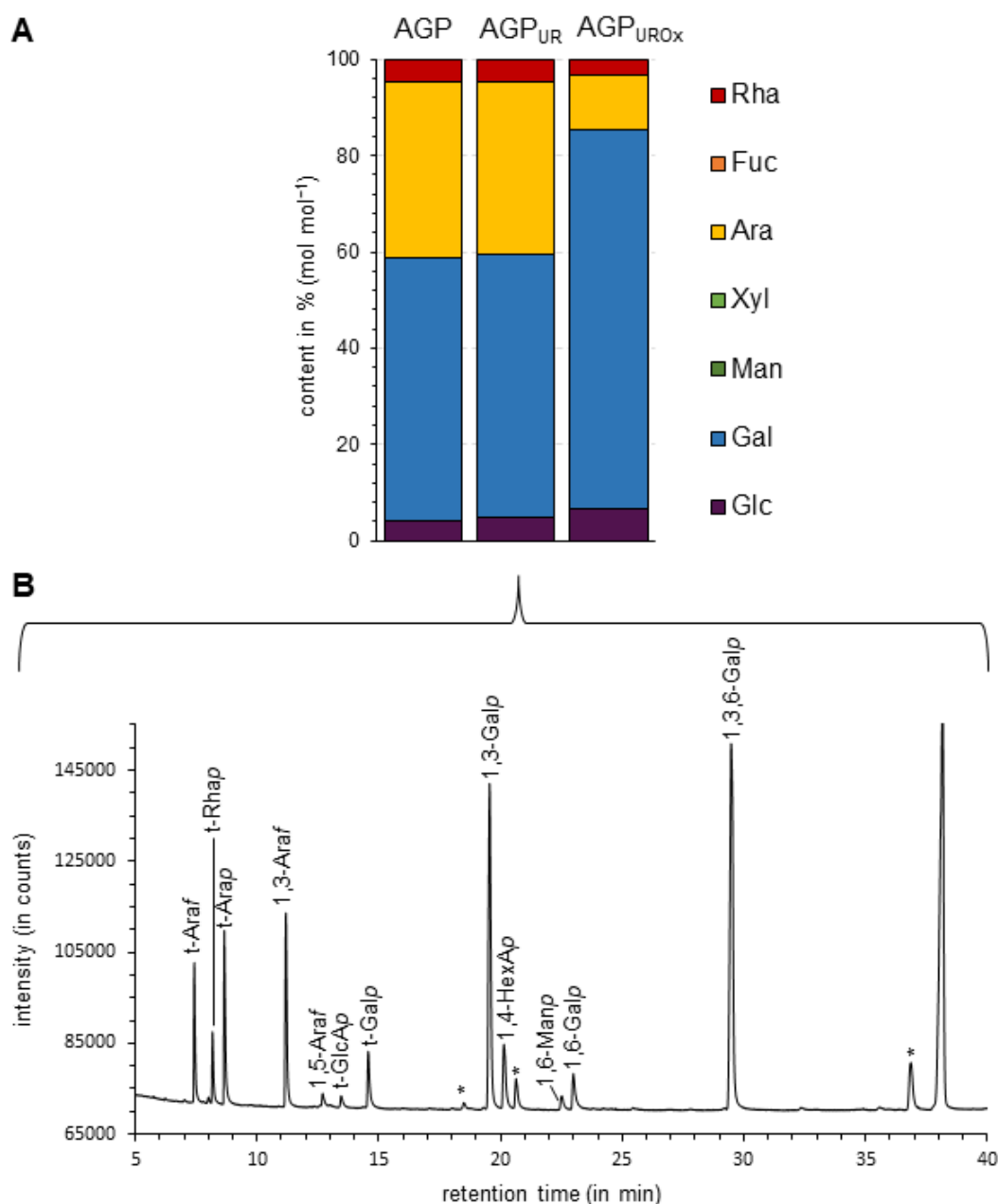


Figure 2. Features of the isolated and chemically treated AGPs of *Psilotum nudum*. **A:** Neutral monosaccharide composition of the aqueous extract (AE), the native AGP, after reduction of uronic acids (AGP_{UR}) and subsequent partial hydrolysis with oxalic acid (AGP_{URox}) determined by gas chromatography (GC; % mol mol⁻¹). **B:** FID chromatogram of partially methylated alditol acetates (PMAAs) of AGP_{UR} after GLC analysis (*incompletely methylated constituents).

Microscopic detection of AGPs in *Psilotum* stems

Cross sections of *Psilotum* stems were incubated in a β -glucosyl Yariv reagent solution (β GlcY) and in α -galactosyl Yariv reagent solution (α GalY), as well as in water (Figure 3). The α GalY solution was used as a negative control (Clarke *et al.*, 1975; Pfeifer *et al.*, 2022). The β GlcY staining showed a slight orange staining of the cell walls of the parenchyma cells, but no difference to the negative control in the area of the vascular bundle.

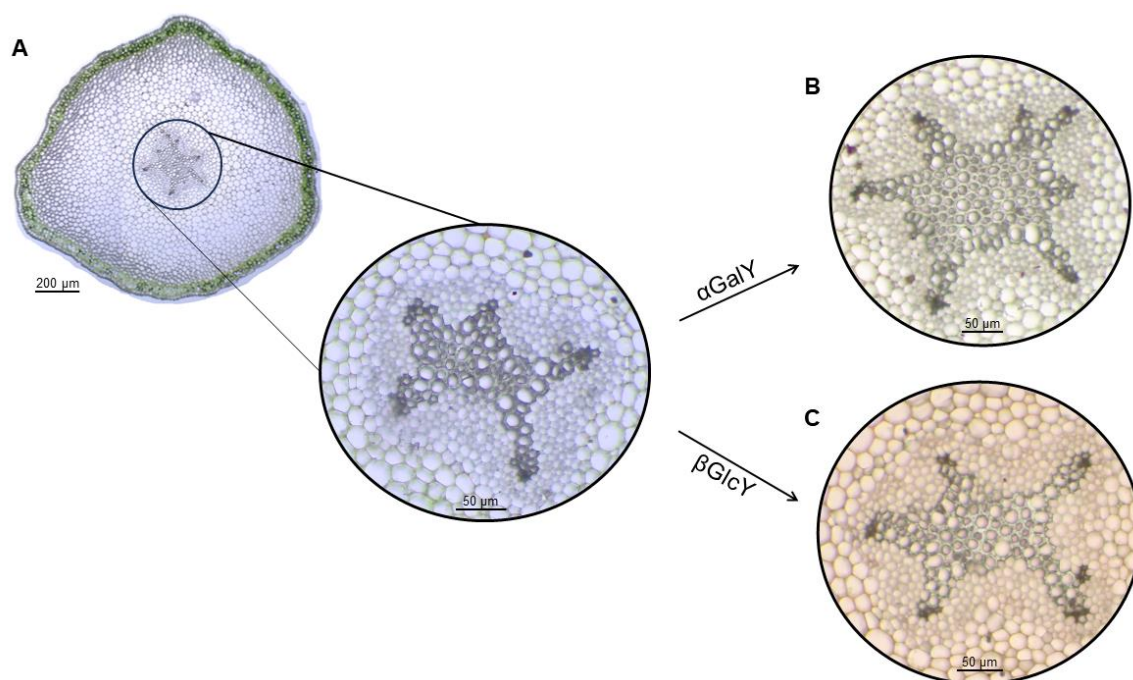


Figure 3. Cross sections of *Psilotum nudum* stems. **A:** Water preparations with focus on the vascular bundle. **B:** Vascular bundle stained with α GalY (negative control). **C:** Vascular bundle stained with β GlcY.

DISCUSSION

Polysaccharides of fern cell walls

Because of the limited knowledge about fern cell walls, four fern species were investigated in this work with regard to their cell wall composition. As ferns are sister to seed plants, they have main cell wall characteristics in common with those of seed plants, including cellulose, hemicelluloses, pectins, cell wall glycoproteins and lignin (Bartels & Classen, 2017; Leroux *et al.*, 2013a; Matsunaga *et al.*, 2004; Popper & Fry, 2004; Popper, 2008; Weng *et al.*, 2008). However, a closer look into these studies reveals structural differences of fern to seed plant cell walls. The main reason of this difference is supposedly reflected in plant colonization of land. During this process, plants had to cope with various abiotic stressors, such as drought or UV-radiation (Harholt *et al.*, 2016). To manage all these stress factors, innovations like vascular tissues or a cuticle surrounding the cell wall were developed (de Vries *et al.*, 2016; de Vries & Archibald, 2018). This also involved modifications in the composition of the cell wall (de Vries & Archibald, 2018).

Pectic polysaccharides. The two pectic fractions isolated with ammonium oxalate and hydrochloric acid reflected a typical composition with uronic acids and the neutral monosaccharides Gal, Ara and Rha. Reactivity with LM19 confirmed presence of unesterified HG in both fractions and in all investigated species, with highest amounts in *Ceratopteris*.

LM20 against methyl-esterified HG showed strongest interaction with *Ceratopteris*, weaker binding to *Salvinia* and low or no binding to *Azolla* pectic fractions in the tested concentrations. Our results for *S. molesta* and the other *Salvinia* species (see Figure S1) corresponded well with investigations on a $(\text{NH}_4)_2\text{C}_2\text{O}_4$ fraction from *Salvinia auriculata* (Silva *et al.*, 2011) where Gal, Ara and Glc were also identified as the main neutral monosaccharides. Glycan microarray with CDTA extracts and antibodies LM19 and LM20 supported presence of high amounts of HG in the *Ceratopteris* sporophyte (Eeckhout *et al.*, 2014) and a high number of other tracheophytes including *S. auriculata* with LM19 epitope being generally more abundant than the LM20 epitope (Leroux *et al.*, 2015).

Immunocytochemical labelling of *Ceratopteris* (Eeckhout *et al.*, 2014) and *Asplenium* (Leroux *et al.*, 2015) with LM19 and LM20 confirmed presence of HG epitopes in primary walls of nearly all organs and tissues, whereas labelling of the lycophyte *Huperzia* stem was only weak (Leroux *et al.*, 2015). JIM5 and JIM6 are two further antibodies raised against partially Me-HG and de-esterified HG (only JIM5). Strong labelling was shown in several tissues of the stem of *Psilotum* (Chernova *et al.*, 2020).

High abundance of Gal and Ara in the pectic fractions of the four ferns investigated indicate the presence of RG-I. This has also been proposed for $(\text{NH}_4)_2\text{C}_2\text{O}_4$ fractions from various other fern species (Silva *et al.*, 2011). This was confirmed by the labelling of the antibody LM5 (directed against 1,4-linked Gal side chains of RG-I) of *Equisetum* and *Psilotum* stems (Popper, 2006; Chernova *et al.*, 2020). On the other hand, LM5 showed only weak binding to the CDTA extract of *Ceratopteris* in glycan microarray which was restricted to phloem cells in immunocytochemistry (Eeckhout *et al.*, 2014).

RG-II is part of fern sporophyte cell walls in amounts comparable to angiosperms, whereas gametophytes of bryophytes only 1 % of the RG II amount of angiosperms (Matsunaga *et al.*, 2004). However, it cannot be excluded that this was not a case of contamination. The glycosyl sequence of RG-II seems to be conserved in vascular plants with the special feature that one Rha is replaced by 3-*O*-MeRha, at least in the lycophyte *Lycopodium* and the ferns *Psilotum*, *Salvinia*, *Platycerium* and *Ceratopteris* (Matsunaga *et al.*, 2004).

Glucans. The sodium carbonate fractions of the four species were very similar with over 50 % Glc and comparable to a fraction isolated from *Salvinia auriculata* by weak sodium hydroxide (Silva *et al.*, 2011), indicating the presence of glucans of unknown structure. Mixed-linkage glucans (MLGs) are known from the Poales order (Popper & Fry, 2003) and are also present in different *Equisetum* species (Soerensen *et al.*, 2008; Fry *et al.*, 2008). Xue & Fry (2012) explored the occurrence of MLG by TLC analysis of lichenase digests in a selection of ferns.

In this study, MLG oligosaccharides were detected in different *Equisetum* species but there was no evidence for the presence of MLGs in the other eusporangiate or leptosporangiate ferns studied, thus confirming results of Hsieh & Harris (2012). Studies based on use of the antibody BS-400-3 raised against a (1→3,1→4)-β-glucan-bovine serum albumin conjugate (Meikle *et al.*, 1994) are somehow contradictory. On the one hand, this BS-400-3 antibody showed no binding to the cell walls of the stem of *Psilotum* (Chernova *et al.*, 2020), but the MLG epitope was detected in the lycophyte *Selaginella* (Harholt *et al.*, 2012) as well as in the lycophyte *Huperzia* and different eusporangiate and leptosporangiate ferns including *Salvinia auriculata* (Leroux *et al.*, 2015). This indicates that MLGs or MLG-like glucans might also be present in the three ferns investigated here. As the cell wall of the moss *Physcomitrium* contains unusual (1→3,1→4)-arabinoglucans (Roberts *et al.*, 2018) and Ara is a substantial monosaccharide in this fraction in all four ferns investigated, arabinoglucans might be hemicelluloses present also in fern cell walls. The assumption that other algae and spore bearing plants synthesize arabinoglucans is supported by the finding, that sequences similar to the *Physcomitrium* arabinoglucan synthase have been identified in algae, bryophytes, lycophytes and ferns (Roberts *et al.*, 2018).

The sodium carbonate fractions of *Psilotum*, *Salvinia*, *Azolla* and *Ceratopteris* also contained appreciable amounts of Gal and Rha. Especially in *Ceratopteris*, the content of uronic acids was highest compared to the other fractions of this species. In *Psilotum*, the uronic acid amount was in the same range as in the HCl fraction. Thus, it might be assumed that pectins with unusual solubility are also present.

Xylans. The 2 M and 8 M KOH fractions revealed a composition with strong dominance of Glc, Man and Xyl indicating the presence of xylans, xyloglucans, and mannans. However, the Glc:Xyl ratios differed greatly within the ferns.

LM10, an antibody directed against the non-reducing end of unsubstituted xylans (McCartney *et al.*, 2005), reacted only with the 2 M KOH fraction of *Azolla*, which was also highest in Xyl content, indicating that unsubstituted xylans in high amounts were present only in *Azolla*. Investigations of different plant parts of *Ceratopteris* revealed presence of LM10 epitope in high amounts in the petioles (Eeckhout *et al.*, 2014). In another glycan microarray study, LM10 epitopes were not detected in a high number of lycophytes and ferns (Leroux *et al.*, 2015).

In contrast, Carafa *et al.*, (2005) detected LM10 epitopes in secondary walls of extant tracheophyte lineages by immunolabelling, but the xylan epitope was lacking in liverworts, hornworts and mosses. It was concluded that occurrence of xylans might be related to the evolution of mechanical and vascular tissue (Carafa *et al.*, 2005). If this assumption is correct,

it might be the reason for the lower xylan content in the studied ferns, as these are adapted to an aquatic habitat.

The occurrence of substituted xylans cannot be excluded as LM11 directed against substituted xylans was not included in our study. In glycan microarray of 80 lycophyte and fern species, the LM11 epitope was detected only in eleven species, but not in *Salvinia auriculata* (Leroux *et al.*, 2015), indicating that substituted xylans are not a common feature for all lycophytes and ferns. In *Psilotum*, substituted xylans were present in secondary walls of sclerenchyma cells and tracheids (Chernova *et al.*, 2020), which there also found in *Ceratopteris* petioles, roots and fertile laminae (Eeckhout *et al.*, 2014).

Xyloglucans. The 2 M KOH fractions of the investigated species reacted strongly with the antibodies LM15 and LM25 directed against xyloglucan epitopes. LM15 detects a XXXG motif of xyloglucans (Marcus *et al.*, 2008; for classification of xyloglucans based on X and G see Fry *et al.*, 1993; Peña *et al.*, 2008), which is typical for seed plants, ferns and also some hornworts, but not for liverworts and mosses (Peña *et al.*, 2008). Fragmentation of xyloglucan from *Ceratopteris* by xyloglucan-specific endo-glucanase gave rise to different xyloglucan oligosaccharides with dominance of the XXXG followed by XLSG motif (Peña *et al.*, 2008). The letter G and X denote an unbranched Glc residue and the Xyl-(1→6)-Glc motif, respectively. The letter L and S describe further substitution of X with Gal or Ara, and F is the fucosylated L motif.

As we also detected Gal and Ara in the 2 M KOH fractions of *Psilotum*, *Salvinia*, *Azolla* and *Ceratopteris*, presence of the L and S motif besides X and G is likely.

Glycan microarray detected the LM15 epitope in many lycophyte and fern species including *Salvinia auriculata* and *Psilotum* (Leroux *et al.*, 2015) and *Ceratopteris*, where it mainly labelled phloem tissue in the primary cell walls (Eeckhout *et al.*, 2014). The LM15 epitope was also detected in phloem tissue of *Equisetum* (Leroux *et al.*, 2011) and *Adiantum* (Leroux *et al.*, 2013b).

In our investigation, LM25, which shares the XXXG-specificity with LM15 but also recognizes galactosylated xyloglucan (Pedersen *et al.*, 2012), reacted weaker with the 2 M KOH extracts of the three species compared to LM15. In another study on *Ceratopteris*, LM25 bound more extensively compared to LM15 and labelled many different tissues but not the xylem (Eeckhout *et al.*, 2014). The antibody CCRC-M1 detects an epitope of fucosylated xyloglucan (Puhlmann *et al.*, 1994) and reacted with NaOH extracts of many fern species including *Salvinia auriculata* and *Psilotum* (Leroux *et al.*, 2015). Therefore, fucogalactoxyloglucans might be present in very

small amounts in the four investigated, as Fuc was detected only in traces or in amounts less than 2 % in *Psilotum*.

It was suggested that xyloglucan might have been important for the evolution of phloem tissue (Leroux *et al.*, 2015). However, only two out of 36 species of the family Aspleniaceae showed weak interaction with this antibody (Leroux *et al.*, 2015), indicating strong differences between cell walls of different monilophyte families. This was confirmed by studies of Hsieh & Harris (2012). Thirteen species from ten families of monilophytes were compared with regard to the structure of xyloglucans. In six species, XXXG and XLFG oligosaccharides were most abundant comparable to the xyloglucans of gymnosperms, eudicotyledons and non-commelinid monocotyledons, whereas the other species varied in their xyloglucan structures. The dominant xyloglucan oligosaccharides of *Psilotum* were XXXG, XLFG and XXLG. This means that galactoxyloglucans (L motif) and the fucogalactoxyloglucans (F motif) are present, which is in accordance with our analytical results. In addition, the results for *Azolla* confirm our analytical data, which contain dominant oligosaccharides with XXXG and XLLG motifs. In the *Ceratopteris* 2 M KOH fraction, Ara was more abundant compared to Gal, thus confirming occurrence of arabinoxyloglucans (S motif), which have been detected in *Ceratopteris* (Hsieh & Harris, 2012).

As mentioned above, we detected strong differences in the Xyl:Glc ratio of the 2 M KOH fractions of the four species: 1:6.7 for *Salvinia*, 1:0.6 for *Azolla* and 1:1.7 for *Psilotum* and also for *Ceratopteris*. In a pure XXXG type xyloglucan, the ratio would be 1:1.3, which is close to the amounts in *Psilotum* and *Ceratopteris*. *Azolla* contains much more Xyl, a further hint for presence of xylans (see above) beside xyloglucans, whereas in *Salvinia*, Glc is more dominant, raising the question whether the G motif is more abundant in this species.

Mannans. In angiosperms, mannans and glucomannans mainly appear in storage tissues such as seed endosperm, particularly in the Fabaceae (Buckeridge, 2010), but they also fulfil structural functions (Scheller & Ulvskov, 2010; Voiniciuc, 2022). It has been proposed that mannan und glucomannan are abundant in ferns (Leroux *et al.*, 2013a; Popper & Fry, 2004; Silva *et al.*, 2011; Frankova & Fry, 2011; Wee *et al.*, 2014) with higher amounts of mannans in primary walls of eusporangiate ferns compared to leptosporangiate ferns (Popper & Fry, 2004; Popper, 2006). Especially the eusporangiate fern *Psilotum* has been shown to contain high amounts of Man (Popper & Fry, 2004). This could be confirmed in our study. A high Man content was only found in the 2 M KOH fraction of *Psilotum*. After treating the cell wall with a higher alkali concentration, fractions with high amounts of Man were obtained in all investigated ferns. But also in this case, the Man content of *Psilotum* was the highest compared

to the other three 8 M KOH fractions. These results were supported by the study of Silva *et al.* (2020), in which a sequential extraction of fern cell walls with 4 M and 8 M NaOH was also performed. In half of the species investigated Man was abundant, while Glc or Xyl dominated in the other species (Silva *et al.*, 2011).

In addition, the LM21 antibody can be used for detecting epitopes of gluco- and galactomannan (Marcus *et al.*, 2010). Labelling with this antibody was found in the stem of *Psilotum* especially in the epidermis and the cortex (Chernova *et al.*, 2020). In glycan microarray, the LM21 epitope was detected in the CDTA and NaOH fractions of many lycophytes and ferns, including *Psilotum* and *Salvinia auriculata* (Leroux *et al.*, 2015). These results indicate strong differences in the hemicelluloses among different fern families.

AGPs present in *Psilotum*

Isolation of AGPs yielded 0.08 % of dry plant weight, which is comparable to *Ceratopteris* and *Salvinia* AGP (Mueller *et al.*, 2023) but lower compared to another eusporangiate fern (*Equisetum*) and four leptosporangiates (Bartels & Classen, 2017; Mueller *et al.*, 2023). However, it should be taken into account that the ferns were not all harvested at the same time.

Protein moiety of AGP. The content of the protein part of the *Psilotum* AGP (5.4 %) is comparable to the most other fern and seed plant AGPs (5 % – 12.3 %; Classen *et al.*, 2000; Bartels & Classen, 2017; Baumann *et al.*, 2021). In contrast, the aquatic ferns *Azolla* and *Salvinia* as well as the bryophytes and the lycophyte *Lycopodium* contain a higher protein content (15 % – 25 %). The moss *Sphagnum* sp. is an exception with 4.6 %. (Bartels *et al.*, 2017; Bartels & Classen, 2017; Happ & Classen, 2019; Mueller *et al.*, 2023).

However, the Hyp content of the whole protein of the eusporangiate *Psilotum* AGP (6.1 %) is more similar to those of the leptosporangiates (1.5 % – 5.3 %) than to the high proportion of that found in the *Equisetum* AGP (15.9 %; Bartels & Classen, 2017; Mueller *et al.*, 2023).

Carbohydrate moiety of AGP. The arabinogalactan part of the *Psilotum* AGP shows the typical galactan core structure known from seed plants (Seifert & Roberts, 2007). The 1,3,6-Galp linkage was determined in high amounts in the same range as in the angiosperms, the 1,3-Galp linkage was slightly higher and the 1,6-Galp lower than in several dicots (Classen *et al.*, 2000; Thude & Classen, 2005). The lower amount of the Galp in 1,6-linkage was also found in the other fern and one lycophyte AGP (Bartels & Classen, 2017; Mueller *et al.*, 2023).

The partial oxalic acid hydrolysis of AGP of *Psilotum* increased these 1,6-Galp linkages as well as the terminal 1-Galp linkages. It can be concluded that the Ara or acid labile Rha residues,

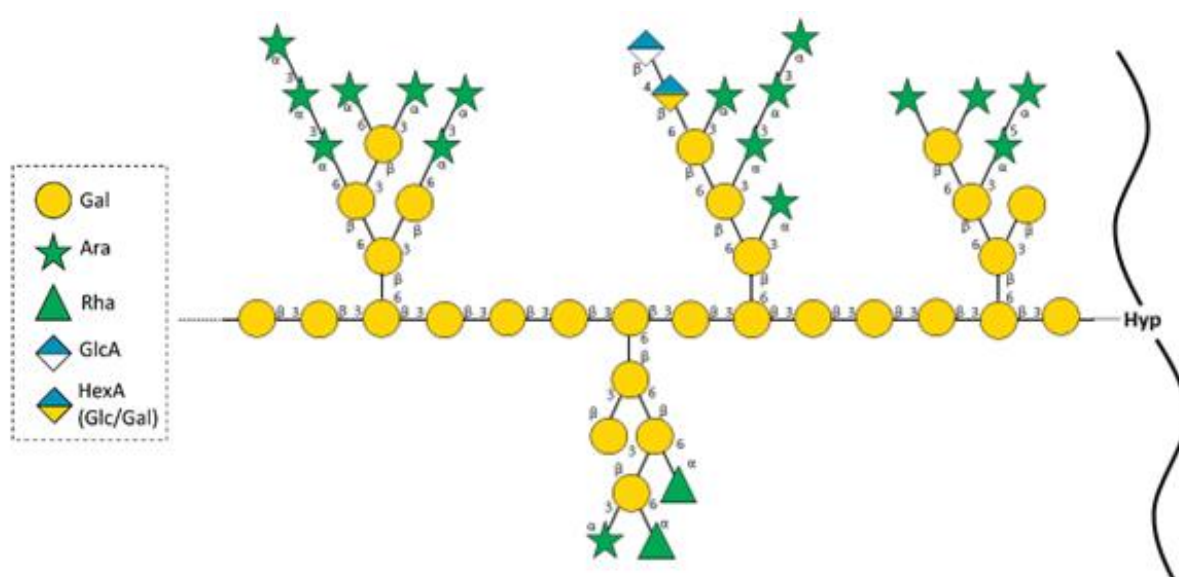
removed by this reaction, were attached to C3 and C6 of the 1,3,6-Galp linkages. This results in a high degree of branching, which was also found in other fern AGPs (Mueller *et al.*, 2023). Additionally, a further hexose with a 1,4-linkage was found. Based on the retention time, this will be either Gal or Glc. Due to the detection of deuterated fragments in the AGP_{UR}, there is also 1,4-HexAp in addition to 1,4-Hexp. The 1,4-Galp linkage was detected in other bryophytes, one lycophyte, ferns and gymnosperms (Bartels & Classen, 2017; Bartels *et al.*, 2017; Happ & Classen, 2019; Baumann *et al.*, 2021). The 1,4-Glcp linkage was found in only 1 % of the carbohydrate part of the AGP of *Physcomitrium patens* (Lee *et al.*, 2005). However, high amounts of 1,4-GlcAp were also detected in this *Physcomitrium* AGP and have also been reported in the AGP of *Zostera marina* (Lee *et al.*, 2005; Pfeifer *et al.*, 2020).

The galactan core structure of seed plants is mainly decorated with Ara side chains (Ma *et al.*, 2018), but the linkage of these chains differs within the land plant AGPs. In angiosperm AGP, the 1,5-Araf is most abundant (Classen *et al.*, 2000; Goellner *et al.*, 2010), this is also the case for the AGP of *Equisetum* (Bartels & Classen, 2017). In addition to these 1,5-linkages, most leptosporangiate ferns also contain high amounts of 1,2-Araf (Bartels & Classen, 2017; Mueller *et al.*, 2023). Bryophytes, on the other hand, possess 1,5- and 1,3-Araf in different ratios (Bartels *et al.*, 2017; Happ & Classen, 2019). Only the lycophyte AGP of *Lycopodium* is decorated with mostly 1,3-Araf linkages, which were also detected in high amounts in the AGP of *Psilotum*. In addition, high contents of terminal Ara were also found in both pyranosidic and furanosidic form. The fact that both forms were present in abundant quantities is only the case in the AGP of *Lycopodium* (Bartels & Classen, 2017).

A further difference of the *Psilotum* AGP to the AGPs of the most bryophytes, ferns and gymnosperms is the lack of terminal 3-O-MeRhap (Akiyama *et al.*, 1987; Fu *et al.*, 2007; Bartels & Classen, 2017; Bartels *et al.*, 2017; Happ & Classen, 2019; Baumann *et al.*, 2021). This methylated monosaccharide was only detectable in the AE fraction, but not in the AGP fraction (Tab. S4). However, also in the *Psilotum* AGP, the terminal unmethylated Rhap was found. *Lycopodium* AGP is characterized by complete lack of Rha (Bartels & Classen, 2017). Based on these findings, a structural proposal of the *Psilotum* AGP was formed and illustrated in Figure 4.

When classifying the AGP of *Psilotum* in the evolutionary context, the structure of the galactan core protein is similar to that of the lycophyte and most ferns. Considering the Ara side chains and end groups, *Psilotum* AGP is more comparable to that of *Lycopodium* with the exception that Rhap is not part of the lycophyte AGP. This occurs in the most land plant AGPs, including ferns and bryophytes (Wack *et al.*, 2005; Bartels & Classen, 2017; Bartels *et al.*, 2017; Happ & Classen, 2019; Baumann *et al.*, 2021; Mueller *et al.*, 2023). Phylogenetic studies have also

shown that *Psilotum* is more closely related to *Equisetum* than to lycophytes (Ruhfel *et al.*, 2014).



CONCLUSION

The conquest of land required a stable and resistant cell wall against external influences. The cell wall had to change constantly in course of evolution. In order to understand this evolution, it is important to study the cell walls of spore producing plants like ferns in comparison to the seed plant cell walls.

This work shows that cell wall fractions of the four fern species contain pectins and different hemicelluloses, especially xyloglucans, which are probably XXXG-type with additional F-, L-, and S-motifs. Xylans seem to be more abundant in *Azolla* compared to *Salvinia* and *Ceratopteris*. Mannans occur in the highest alkaline fractions in all species and were most abundant in *Psilotum*. This supports the finding that mannans are more abundant in eusporangiate ferns compared to the leptosporangiates. The nature of glucans has to be elucidated further.

The isolation of AGPs from the cell wall of *Psilotum* provides further insights into the evolution of AGPs. Structure elucidation revealed that general features known from seed plant AGPs are present. The unusual monosaccharide 3-*O*-MeRha (acofriose), common for most fern AGPs, could not be detected in the *Psilotum* AGP. Instead, the Ara linkage types t-Arap and 1,3-Araf, also present in the lycophyte *Lycopodium*, were found in high amounts.

As to date AGPs from only one other eusporangiate fern and only one lycophyte have been isolated and characterized, AGPs from further species of this group should be investigated to get a more accurate insight into the evolution of AGPs in the tracheophytes. In addition, further functional analyses of fern AGPs should be established in order to gain more knowledge in this area as well.

EXPERIMENTAL PROCEDURES

Plant material, growth conditions and sampling

The floating ferns *Azolla filiculoides* LAM. (*Azolla*, *A. filiculoides*), *Salvinia × molesta* D. S. MITCHELL (*Salvinia*, *S. molesta*), *Salvinia auriculata* AUBL., *Salvinia cucullata* ROXB. and *Salvinia natans* (L.) ALL., as well as *Ceratopteris richardii* BRONGN. (*Ceratopteris*, *C. richardii*) were cultivated in the greenhouse in the Garden of the Pharmaceutical Institute, *Psilotum nudum* (L.) BEAUV. (*Psilotum*, *P. nudum*) in the greenhouse of the Botanical Garden of the Christian-Albrechts-University of Kiel. The sporophytes of all ferns were used in this study (for *Psilotum* and *Ceratopteris* only the aerial part). The harvest times were between August and October 2018 (*S. molesta*), between July and October 2020 (*Salvinia* spp.), in September and in January 2019/2020 (*Azolla*), in August 2020 (*Psilotum*) and in July and in August 2021 (*Ceratopteris*). The *Ceratopteris* RN3 strain spores were a kind gift of Péter

Szövényi (University of Zurich). For culturing of those, the protocol of Plackett *et al.* (2015) was used. The plant material was cleaned with water and freeze-dried.

Isolation of the cell wall fractions

The cell wall was isolated by sequential extraction, in which up to six fractions were obtained. The preparation of the aqueous extract (AE) for *Psilotum* in a ratio of 1:20 (w/V) has been performed according to Mueller *et al.* (2023). Isolation of the two pectic fractions, here the ammonium oxalate fraction $[(\text{NH}_4)_2\text{C}_2\text{O}_4]$ and the hydrochloric acid fraction (HCl), as well as the hemicellulose fractions, extracted with sodium carbonate (Na_2CO_3) and potassium hydroxide (2 M KOH), are described in Pfeifer *et al.* (2023). Additionally, a third hemicellulose fraction for *Azolla*, *Ceratopteris*, *Psilotum* and *Salvinia* was extracted by using 8 mol L⁻¹ potassium hydroxide (8 M KOH) at the same conditions as for the 2 M KOH.

Analysis of monosaccharides

The method of Blakeney *et al.* (1983) with slight modifications, described in Mueller *et al.* (2023) was used to determine the neutral monosaccharide compositions of the fractions. The quantification was performed by gas chromatography (GC) with flame ionization detection (FID) and mass spectrometry detection (MSD): GC + FID: 7890B; Agilent Technologies, USA; MS: 5977B MSD; Agilent Technologies, USA; column: Optima-225; Macherey-Nagel, Germany; 25 m, 250 μm , 0.25 μm ; helium flow rate: 1 ml min⁻¹; split ratio 30:1. A temperature gradient was performed to achieve peak separation (initial temperature 200 °C, subsequent holding time of 3 min; final temperature 243 °C with a gradient of 2 °C min⁻¹). For identification of 3-*O*-MeRha, the retention time and the mass spectrum were used (according to Happ & Classen, 2019).

The content of uronic acids in the fractions was determined by a modified method of Blumenkrantz and Asboe-Hansen (1973; see Mueller *et al.*, 2023).

Reduction of uronic acids and partial degradation of arabinogalactan-proteins (AGPs)

The AGPs of *Psilotum* were isolated according to Classen *et al.* (2005). As uronic acids are not detectable by the method described above (“Analysis of monosaccharides”), these were reduced to the corresponding neutral monosaccharides following a modified method of Taylor and Conrad (1972) to gain the AGP_{UR} fraction. The AGP_{UR} fraction was partial degraded by oxalic acid hydrolysis according to Gleeson and Clarke (1979), to get further structural information (AGP_{UROX} fraction). The procedures are described in detail in Mueller *et al.* (2023).

Structural characterization of arabinogalactan moiety of *Psilotum* AGP

The AGP, the AGP_{UR} and the AGP_{UROX} fractions of *Psilotum* were used for structure elucidation. Therefore, a modified method of Harris *et al.* (1983), described in Mueller *et al.* (2023) was applied. Quantification was performed by GLC-mass spectroscopy (see above "Analysis of monosaccharides"; column: Optima-1701, 25 m, 250 μ m, 0.25 μ m; helium flow rate: 1 mL min⁻¹; initial temperature: 170 °C; hold time 2 min; rate 1 °C min⁻¹ until 210 °C was reached; rate: 30 °C min⁻¹ until 250 °C was reached; final hold time 10 min).

Determination of the protein and hydroxyproline (Hyp) content

The protein content was calculated *via* the nitrogen content determined by elemental analysis with multiplication of the factor 6.25 (Kjeldahl, 1883). For elemental analysis, the vario MICRO cube elemental analyzer (Elementar Analysensysteme GmbH, Langenselbold, Germany) was used, which was determined in the Chemistry Department of Kiel University, Kiel, Germany. The Hyp content was measured and quantified photometrically at 558 nm by a linear regression analysis according to Stegeman and Stalder (1967).

Microscopy

Cross sections of stems of *Psilotum* were prepared and stored in water. A part of these sections was incubated in a solution of α -Gal-Yariv and another part in a β GlcY solution (both 1 mg mL⁻¹ in 0.15 mol L⁻¹ sodium chloride) overnight at 4 °C. The sections were washed with 0.15 mol L⁻¹ sodium chloride solution until the red colour disappeared. Those as well as the water sections were investigated by light microscopy (Primostar 3, Carl Zeiss Microscopy Deutschland GmbH, Oberkochen, Germany) and the images taken by a digital camera (AxioCam 208 color, Carl Zeiss Microscopy Deutschland GmbH).

Indirect enzyme-linked immunosorbent assay (ELISA)

The samples of the fractions were dissolved in the concentration 25 μ g mL⁻¹ in ddH₂O. The test performance is described in Pfeifer *et al.* (2023).

The primary antibodies LM10 and LM15 were used for the hemicellulose fractions (Kerafast, Inc., Boston, MA, USA); LM19, LM20, and LM25 (Kerafast, Inc.) for the pectic fractions, all in a dilution of 1:20 (V/V). The secondary antibody (anti-rat-IgG conjugated with alkaline phosphatase, produced in goat, Sigma-Aldrich Chemie GmbH, Taufkirchen, Germany) was dissolved in a dilution of 1:500 (V/V). The samples were analyzed in triplicate. For presentation, the absorbance of the control was set to zero and the highest signal in the dataset was set to 1.0. Epitopes of the antibodies and key references are listed in Table S6.

ACKNOWLEDGEMENTS

Funding: LP and BC (project-number 440046237; CL448/3-1) are grateful for funding within the framework of MADLand (<http://madland.science>), priority programme 2237 of the German Research Foundation (DFG). All authors thank Péter Szövényi for delivering the spores of *Ceratopteris*.

AUTHORS CONTRIBUTION and CONFLICT OF INTEREST

BC, KM and LP planned and designed the research. KM, LP and LS cultivated the plant material and performed the extractions as well as carbohydrate and ELISA experiments. KM created all main text figures with the help of LP (Figure 1). All authors analysed the data. KM and BC wrote the manuscript. The authors declare that they have no competing interests.

DATA AVAILABILITY STATEMENT

All relevant experimental data can be found within the manuscript and its supporting materials.

SUPPORTING INFORMATION

Table S1. Yields of different cell wall fractions of *Psilotum nudum*, *Salvinia molesta*, *Azolla filiculoides*, and *Ceratopteris richardii* in % of dry fraction material (w w⁻¹).

Yields	<i>P. nudum</i>	<i>S. molesta</i>	<i>A. filiculoides</i>	<i>C. richardii</i>
(NH ₄) ₂ C ₂ O ₄	4.0	8.9	8.7	11.3
HCl	0.4	1.4	3.3	3.7
Na ₂ CO ₃	2.0	4.0	8.6	3.7
2 M KOH	14.6	22.6	23.4	10.9
8 M KOH	3.2	0.9	0.7	0.3

Table S2a. Neutral monosaccharide composition of the ammonium oxalate fraction of *Psilotum nudum*, *Salvinia molesta*, *Azolla filiculoides*, and *Ceratopteris richardii* in % (mol mol⁻¹; n=3).

Neutral monosaccharide	<i>P. nudum</i> (NH ₄) ₂ C ₂ O ₄	<i>S. molesta</i> (NH ₄) ₂ C ₂ O ₄	<i>A. filiculoides</i> (NH ₄) ₂ C ₂ O ₄	<i>C. richardii</i> (NH ₄) ₂ C ₂ O ₄
3- <i>O</i> -Me-Rha	1.0 ± 0.1	1.5 ± 0.1	tr	2.1 ± 0.2
Rha	5.0 ± 0.2	8.5 ± 0.3	11.7 ± 0.1	10.8 ± 0.6
Fuc	1.5 ± 0.0	2.0 ± 0.0	3.7 ± 0.1	2.8 ± 0.3
Rib	2.8 ± 0.4	5.3 ± 0.2	8.6 ± 0.7	6.3 ± 0.2
Ara	18.3 ± 0.7	23.1 ± 0.4	17.3 ± 0.1	19.4 ± 1.8
Xyl	2.4 ± 0.1	3.1 ± 0.1	15.5 ± 0.4	11.5 ± 0.5
Man	13.9 ± 0.5	2.5 ± 0.0	7.4 ± 0.3	6.5 ± 1.6
Gal	16.5 ± 0.6	14.2 ± 0.1	21.8 ± 0.8	18.8 ± 1.2
Glc	38.6 ± 1.4	39.8 ± 0.9	14.0 ± 0.2	21.8 ± 2.4

tr: trace value < 1 %

Table S2b. Neutral monosaccharide composition of the hydrochloric acid fraction of *Psilotum nudum*, *Salvinia molesta*, *Azolla filiculoides*, and *Ceratopteris richardii* in % (mol mol⁻¹).

Neutral monosaccharide	<i>P. nudum</i> HCl n=1	<i>S. molesta</i> HCl n=3	<i>A. filiculoides</i> HCl n=3	<i>C. richardii</i> HCl n=3
3- <i>O</i> -Me-Rha	tr	tr	tr	tr
Rha	2.4	6.2 ± 0.5	8.0 ± 0.3	15.0 ± 0.2
Fuc	tr	1.3 ± 0.2	2.1 ± 0.1	2.2 ± 0.1
Rib	tr	tr	tr	-
Ara	9.8	13.0 ± 0.3	13.4 ± 0.2	14.9 ± 0.6
Xyl	2.3	4.5 ± 0.6	11.5 ± 0.6	10.4 ± 0.7
Man	16.6	1.8 ± 0.2	7.0 ± 0.5	4.1 ± 0.2
Gal	12.8	11.3 ± 0.4	16.8 ± 0.3	21.5 ± 0.4
Glc	56.1	61.9 ± 1.6	41.2 ± 1.1	31.9 ± 1.2

tr: trace value < 1 %

Table S2c. Neutral monosaccharide composition of the sodium carbonate fraction of *Psilotum nudum*, *Salvinia molesta*, *Azolla filiculoides*, and *Ceratopteris richardii* in % (mol mol⁻¹).

Neutral monosaccharide	<i>P. nudum</i> Na ₂ CO ₃ n=1	<i>S. molesta</i> Na ₂ CO ₃ n=3	<i>A. filiculoides</i> Na ₂ CO ₃ n=3	<i>C. richardii</i> Na ₂ CO ₃ n=3
3- <i>O</i> -Me-Rha	tr	tr	tr	1.1 ± 0.7
Rha	4.7	8.3 ± 1.1	8.2 ± 0.4	8.8 ± 1.5
Fuc	2.1	1.3 ± 0.1	1.8 ± 0.1	1.4 ± 0.3
Rib	-	tr	tr	tr
Ara	22.7	17.7 ± 1.6	13.8 ± 0.2	12.6 ± 1.5
Xyl	2.3	4.4 ± 2.7	4.0 ± 0.1	6.0 ± 2.2
Man	2.1	3.1 ± 0.8	3.1 ± 0.1	3.2 ± 1.0
Gal	11.2	14.9 ± 1.6	14.3 ± 0.1	15.1 ± 3.0
Glc	54.9	50.3 ± 1.2	54.6 ± 0.9	51.8 ± 9.8

tr: trace value < 1 %

Table S2d. Neutral monosaccharide composition of the 2 M potassium hydroxide fraction of *Psilotum nudum*, *Salvinia molesta*, *Azolla filiculoides*, and *Ceratopteris richardii* in % (mol mol⁻¹; n=3).

Neutral monosaccharide	<i>P. nudum</i> 2 M KOH	<i>S. molesta</i> 2 M KOH	<i>A. filiculoides</i> 2 M KOH	<i>C. richardii</i> 2 M KOH
3- <i>O</i> -Me-Rha	tr	-	-	-
Rha	4.7 ± 0.1	4.3 ± 0.1	3.1 ± 0.1	2.0 ± 0.4
Fuc	1.9 ± 0.0	tr	tr	tr
Rib	-	tr	-	tr
Ara	11.7 ± 0.3	3.2 ± 0.2	3.7 ± 0.1	6.3 ± 0.1
Xyl	23.1 ± 1.5	11.1 ± 0.4	50.0 ± 0.9	32.8 ± 0.6
Man	12.1 ± 0.4	tr	1.3 ± 0.1	1.1 ± 0.0
Gal	7.9 ± 0.1	7.4 ± 0.1	10.2 ± 0.1	3.2 ± 0.3
Glc	38.6 ± 0.9	74.0 ± 0.6	31.8 ± 0.7	54.6 ± 1.2

tr: trace value < 1 %

Table S2e. Neutral monosaccharide composition of the 8 M potassium hydroxide fraction of *P. nudum*, *S. molesta*, *A. filiculoides* and *C. richardii* in % (mol mol⁻¹; n=3).

Neutral monosaccharide	<i>P. nudum</i> 8 M KOH	<i>S. molesta</i> 8 M KOH	<i>A. filiculoides</i> 8 M KOH	<i>C. richardii</i> 8 M KOH
3- <i>O</i> -Me-Rha	-	-	-	-
Rha	1.6 ± 0.1	-	-	-
Fuc	tr	tr	-	-
Rib	-	-	-	-
Ara	5.4 ± 0.1	2.3 ± 0.1	-	2.0 ± 0.3
Xyl	28.5 ± 2.5	27.5 ± 0.4	45.0 ± 0.1	57.6 ± 0.8
Man	39.1 ± 1.7	28.8 ± 0.2	21.1 ± 0.1	21.3 ± 0.4
Gal	4.7 ± 0.2	5.3 ± 0.1	6.6 ± 0.2	3.4 ± 0.3
Glc	20.7 ± 0.6	36.1 ± 0.2	27.3 ± 0.2	15.7 ± 0.2

tr: trace value < 1 %

Table S3. Colorimetric determination of the content of uronic acids in the different cell wall fractions of *Psilotum nudum*, *Salvinia molesta*, *Azolla filiculoides*, and *Ceratopteris richardii* in % (w w⁻¹).

Uronic acids	<i>P. nudum</i>	<i>S. molesta</i>	<i>A. filiculoides</i>	<i>C. richardii</i>
AE	3.0	1.8*	8.4*	4.4*
(NH ₄) ₂ C ₂ O ₄	17.8	33.7	33.8	13.1
HCl	14.0	16.8	22.7	12.6
Na ₂ CO ₃	12.4	7.9	6.7	21.6
2 M KOH	4.1	3.7	2.9	2.6
8 M KOH	3.1	4.5	3.7	4.9

*: published in Mueller *et al.* (2023)

Table S4. Neutral monosaccharide composition of AE, AGP, AGP_{Ur} and AGP_{UrOx} of *Psilotum nudum* in % (mol mol⁻¹; n=3).

Neutral monosaccharide	AE	AGP	AGP _{Ur}	AGP _{UrOx}
3- <i>O</i> -Me-Rha	-	-	-	-
Rha	4.0 ± 0.1	4.7 ± 0.1	4.5 ± 0.2	3.3 ± 0.2
Fuc	1.2 ± 0.1	tr	-	-
Ara	26.7 ± 0.8	36.6 ± 0.8	36.0 ± 0.6	11.2 ± 0.1
Xyl	3.2 ± 0.2	-	-	-
Man	10.6 ± 1.0	tr	tr	-
Gal	34.9 ± 1.6	54.7 ± 0.5	54.6 ± 0.3	78.8 ± 0.4
Glc	19.4 ± 1.1	4.0 ± 0.3	4.9 ± 0.3	6.7 ± 0.3
Ara : Gal	1 : 1.3 ± 0.0	1 : 1.5 ± 0.0	1 : 1.5 ± 0.0	1 : 7.0 ± 0.1

tr: trace value < 1 %

Table S5a. Neutral monosaccharide composition of the water-soluble polysaccharides from *Salvinia* spp. in % (mol mol⁻¹; n=3).

Neutral monosaccharide	<i>S. auriculata</i> AE	<i>S. cucullata</i> AE	<i>S. natans</i> AE
3- <i>O</i> -Me-Rha	2.8 ± 0.1	1.3 ± 0.2	1.7 ± 0.1
Rha	4.7 ± 0.1	6.7 ± 0.6	7.1 ± 0.2
Fuc	1.9 ± 0.0	4.8 ± 0.6	3.1 ± 0.0
Rib	1.4 ± 0.0	1.1 ± 0.1	2.0 ± 0.1
Ara	33.8 ± 1.1	30.5 ± 0.3	34.5 ± 0.5
Xyl	5.3 ± 0.2	7.9 ± 0.6	6.8 ± 0.1
Man	4.3 ± 0.1	7.4 ± 0.0	4.5 ± 0.1
Gal	25.7 ± 0.3	25.3 ± 1.6	25.6 ± 0.4
Glc	20.1 ± 0.7	15.0 ± 0.3	14.6 ± 0.4

tr: trace value < 1 %

Table S5b. Neutral monosaccharide composition of the ammonium oxalate fraction from *Salvinia* spp. in % (mol mol⁻¹; n=1).

Neutral monosaccharide	<i>S. auriculata</i> (NH ₄) ₂ C ₂ O ₄	<i>S. cucullata</i> (NH ₄) ₂ C ₂ O ₄	<i>S. natans</i> (NH ₄) ₂ C ₂ O ₄
3- <i>O</i> -Me-Rha	1.7	1.0	tr
Rha	11.2	15.2	5.2
Fuc	2.1	4.7	tr
Rib	7.5	9.2	2.8
Ara	27.7	23.3	9.6
Xyl	3.1	5.7	3.2
Man	2.7	5.0	tr
Gal	16.8	19.3	7.0
Glc	27.2	16.6	72.2

tr: trace value < 1 %

Table S5c. Neutral monosaccharide composition of the hydrochloric acid fraction from *Salvinia* spp. in % (mol mol⁻¹; n=1).

Neutral monosaccharide	<i>S. auriculata</i> HCl	<i>S. cucullata</i> HCl	<i>S. natans</i> HCl
3- <i>O</i> -Me-Rha	tr	tr	tr
Rha	7.7	11.7	2.7
Fuc	1.1	4.3	tr
Rib	tr	1.9	tr
Ara	12.8	21.1	4.2
Xyl	4.7	9.1	6.0
Man	1.3	4.9	tr
Gal	10.7	19.5	4.1
Glc	61.7	27.5	83.0

tr: trace value < 1 %

Table S5d. Neutral monosaccharide composition of the sodium carbonate fraction from *Salvinia* spp. in % (mol mol⁻¹; n=1).

Neutral monosaccharide	<i>S. auriculata</i> Na ₂ CO ₃	<i>S. cucullata</i> Na ₂ CO ₃	<i>S. natans</i> Na ₂ CO ₃
3-O-Me-Rha	1.1	tr	-
Rha	7.8	8.3	3.0
Fuc	1.2	3.4	tr
Rib	-	-	tr
Ara	21.3	16.1	8.4
Xyl	2.4	5.9	2.5
Man	2.2	5.2	1.2
Gal	12.3	16.3	6.7
Glc	51.7	44.8	78.2

tr: trace value < 1 %

Table S5e. Neutral monosaccharide composition of the 2 M potassium hydroxide fraction from *Salvinia* spp. in % (mol mol⁻¹; n=1).

Neutral monosaccharide	<i>S. auriculata</i> 2 M KOH	<i>S. cucullata</i> 2 M KOH	<i>S. natans</i> 2 M KOH
3-O-Me-Rha	tr	tr	-
Rha	4.2	12.9	2.5
Fuc	tr	1.3	tr
Rib	tr	-	tr
Ara	4.0	6.2	2.1
Xyl	15.4	13.9	3.9
Man	1.0	8.1	tr
Gal	8.1	15.8	4.4
Glc	67.3	41.8	87.1

tr: trace value < 1 %

Table S6. Antibodies tested for binding to fern cell wall components.

Antibody	Epitope	Key References
LM10	Non-reducing end of (1→4)-β-D-xylan	McCartney <i>et al.</i> (2005); Ruprecht <i>et al.</i> (2017)
LM15	XXXG-motif of xyloglucan	Marcus <i>et al.</i> (2008)
LM19	Unesterified HG	Verhertbruggen <i>et al</i> (2009b)
LM20	Methyl-esterified HG	Verhertbruggen <i>et al</i> (2009b)
LM25	XXXG / galactosylated xyloglucan	Pedersen <i>et al.</i> (2012)

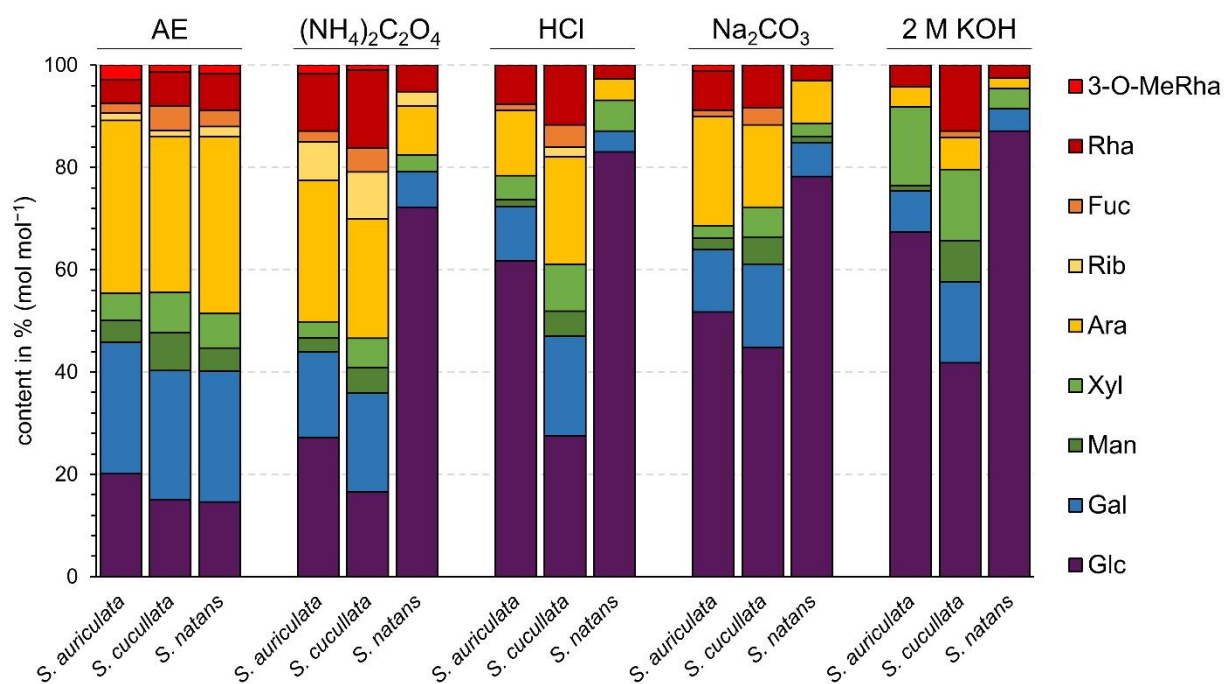


Figure S1. Neutral monosaccharide composition of different cell wall fractions (AE, $(\text{NH}_4)_2\text{C}_2\text{O}_4$, HCl, Na_2CO_3 , 2 M KOH) from further species of the genus *Salvinia* (*S. auriculata*, *S. cucullata*, *S. natans*) determined by gas chromatography (GC; % mol mol⁻¹).

5. Fern cell walls and the evolution of arabinogalactan-proteins in streptophytes

Kim-Kristine Mueller^{1†}, Lukas Pfeifer^{1†}, Lina Schuldt¹, Péter Szövényi^{2,3}, Sophie de Vries⁴, Jan de Vries^{4,5,6}, Kim L. Johnson⁷ and Birgit Classen¹

¹*Pharmaceutical Institute, Department of Pharmaceutical Biology, Christian-Albrechts-University of Kiel, Gutenbergstr. 76, 24118 Kiel, Germany*

²*Dept. of Systematic and Evolutionary Botany, University of Zurich, Zollikerstr. 107, 8008 Zurich, Switzerland*

³*Zurich-Basel Plant Science Center (PSC), ETH Zürich, Tannenstrasse 1, 8092 Zürich, Switzerland*

⁴*University of Goettingen, Department of Applied Bioinformatics, Institute of Microbiology and Genetics, Goldschmidtstr. 1, 37077 Goettingen, Germany*

⁵*University of Goettingen, Goettingen Center for Molecular Biosciences (GZMB), Department of Applied Bioinformatics, Goldschmidtstr. 1, 37077 Goettingen, Germany*

⁶*University of Goettingen, Campus Institute Data Science (CIDAS), Goldschmidtstr. 1, 37077 Goettingen, Germany*

⁷*Department of Animal, Plant and Soil Science, La Trobe Institute for Agriculture & Food, La Trobe University, AgriBio Building, Bundoora, Victoria 3086, Australia*

[†]Authors contributed equally to the publication.

ABSTRACT

Significant changes have occurred in plant cell wall composition during evolution and diversification of tracheophytes. As the sister lineage to seed plants, knowledge on the cell wall of ferns is key to track evolutionary changes across tracheophytes and to understand seed plant-specific evolutionary innovations. Fern cell wall composition is not fully understood, including limited knowledge of glycoproteins such as the fern arabinogalactan-proteins (AGPs). Here, we characterize the AGPs from the leptosporangiate fern genera *Azolla*, *Salvinia* and *Ceratopteris*. The carbohydrate moiety of seed plant AGPs consists of a galactan backbone including mainly 1,3- and 1,3,6-linked pyranosidic galactose, which is conserved across the investigated fern

AGPs. Yet, unlike AGPs of angiosperms, those of ferns contained the unusual sugar 3-*O*-methylrhamnose. Besides terminal furanosidic Ara (Araf), the main linkage type of Araf in the ferns was 1,2-linked Araf, whereas in seed plants 1,5-linked Araf is often dominating. Antibodies directed against carbohydrate epitopes of AGPs supported the structural differences between AGPs of ferns and seed plants. Comparison of AGP linkage types across the streptophyte lineage showed that angiosperms have rather conserved monosaccharide linkage types; by contrast bryophytes, ferns and gymnosperms showed more variability.

Phylogenetic analyses of glycosyltransferases involved in AGP biosynthesis and bioinformatic search for AGP protein backbones revealed a versatile genetic toolkit for AGP complexity in ferns. Our data reveal important differences across AGP diversity which functional significance is unknown. This diversity sheds light on the evolution of the hallmark feature of tracheophytes: their elaborate cell walls.

INTRODUCTION

One of the most important steps in the evolution of life on Earth happened around 500 million years ago (mya), when descendents of streptophyte algae colonized the terrestrial habitat (e.g. Kenrick and Crane, 1997; Becker and Marin, 2009; Delwiche and Cooper, 2015; Bowman *et al.*, 2017; Harrison, 2017; de Vries and Archibald, 2018). By the end of the Devonian (360 mya), the extant lineages of land plants comprising bryophytes, lycophytes, monilophytes (=ferns), and spermatophytes have evolved and the major organ and tissue types known from extant plants (e.g. vasculature, roots, leaves, seeds, wood, secondary growth) were already present (Bowman, 2013). Vascular plants (tracheophytes) comprise lycophytes, ferns and seed plants, and are characterized by features like tracheids and sieve elements for water and nutrient transport and a highly structured and dominant sporophyte. Lycophytes separated from all other living vascular plant lineages already in the nearly-mid Devonian (approx. 400 mya; Banks *et al.*, 2011; Pryer *et al.*, 2004), ferns first appeared in the early Carboniferous (Galtier and Scott, 1985). They comprise around 12,000 extant species belonging to the five lineages Equisetales, Psilotales, Ophioglossales, Marattiales and the dominant group of leptosporangiate ferns (Pryer *et al.*, 2004; PPG 2016; Nitta *et al.*, 2022). Ferns form the sister lineage to seed plants; to understand the evolutionary history of innovations specific to seed-plants, knowledge of this group is necessary to infer (i) the characteristics of the last common ancestor (LCA) shared by ferns and seed-plants and (ii) define the evolutionary trajectory of seed-plant specific characteristics (Rensing, 2017).

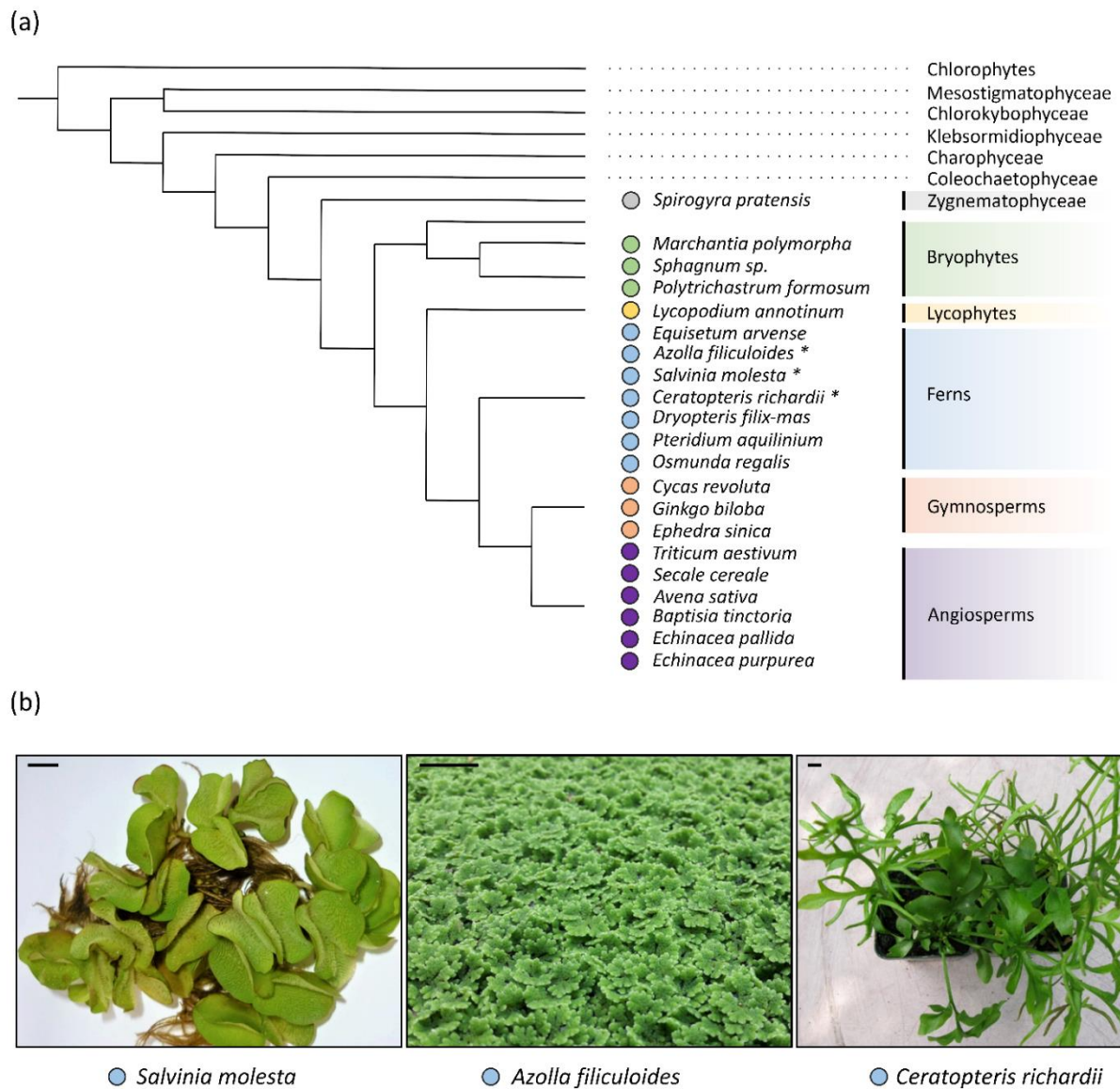


Figure 1. Overview of the investigated plant species. (a) Phylogenetic position of the analyzed plants according to de Vries and Archibald (2018) and Puttick *et al.* (2018). The colored dots indicate inclusion in the PCA (see Figure 3). The fern species which were cultured for this study are marked by asterisks. (b) Cultivation of the ferns *S. molesta*, *A. filiculoides* and *C. richardii* in the greenhouse of the Pharmaceutical Institute of Kiel University. Scale bars = 1 cm.

Ferns are known for possessing large genomes with numerous chromosomes. To date, genome sequence of the heterosporous ferns *Azolla filiculoides* and *Salvinia cucullata*, the homosporous ferns *Ceratopteris richardii*, *Adiantum capillus-veneris*, as well as the tree fern *Alsophila spinulosa* are publicly available (Li *et al.*, 2018; Marchant *et al.*, 2022; Fang *et al.*, 2022; Huang *et al.*, 2022). *Azolla* and *Salvinia* are floating aquatic ferns with high growth rates and the potential to be significant carbon sinks. Data from the Arctic Ocean revealed that around 50 mya, an abundance of *Azolla* characterized an 800,000-year interval called the “*Azolla* event” which possibly had a role in global cooling by sequestering atmospheric carbon dioxide (Brinkhuis *et al.*, 2006; Speelman *et al.*, 2009). *Azolla* is further remarkable due to its obligate

symbiosis with the N-fixing cyanobacterium *Nostoc azollae* in specialized leaf cavities (Li *et al.*, 2018; de Vries *et al.*, 2018; de Vries and de Vries, 2022). *Ceratopteris richardii* is also adapted to water and is known as the genetically tractable fern model organism („C-Fern“ Plackett *et al.*, 2015) and as a teaching tool in biology (Renzaglia and Warne, 1995). *Azolla*, *Salvinia* and *Ceratopteris* all belong to the leptosporangiate ferns, which account for approximately 80 % of non-flowering vascular plant species (Plackett *et al.*, 2015). Among them *Ceratopteris* was suggested as the model for research on adaptive cell wall modification in vascular plants (Leroux *et al.*, 2013a).

Plant cell walls are important at various levels of plant morphology and as such are expected to have changed during evolution (Sørensen *et al.*, 2011). According to current knowledge, fern cell walls share basic features with those of seed plants, e.g. the occurrence of cellulose, hemicelluloses and pectic polysaccharides (Leroux *et al.*, 2013a; Matsunaga *et al.*, 2004; Popper and Fry, 2004; Popper, 2008). However, differences exist, e.g. in lignin structures: Whereas secondary cell walls of lycophytes and angiosperms are reinforced with lignin containing mainly syringyl monomers, lignin of ferns and gymnosperms is derived primarily from guaiacyl monomers (Weng *et al.*, 2008). Besides polysaccharides and lignin, hydroxyproline-rich-glycoproteins (HRGPs) are also important components of plant cell walls. They are broadly classified into the three groups arabinogalactan-proteins (AGPs), extensins and proline-rich proteins (PRPs) however in reality a continuum exists (Johnson *et al.*, 2018). PRPs are only minimally glycosylated, extensins possess a glycan part of around 50 % and AGPs consist of up to 90 % polysaccharides. In AGPs, several arabinogalactan (AG) moieties are covalently linked to the protein *via* hydroxyproline. The characteristic structure of the AG in angiosperms is a backbone of 1,3-linked β -D-Galp, branched at position 6 to 1,6-linked β -D-Galp side chains, which are substituted with α -L-Araf and often also terminal β -D-GlcpA (for review see Ma *et al.*, 2018; Strasser *et al.*, 2021). AGPs are key constituents of seed plants extracellular matrix and are involved in several processes such as cell growth, cell proliferation, pattern formation, sexual reproduction and plant-microbe interactions (for review see Seifert and Roberts, 2007; Ma *et al.*, 2018).

A unique feature of AGPs is their ability to precipitate with red-coloured Yariv phenylglycosides, e.g. the β -glucosyl Yariv reagent (β GlcY). Already in the 1970s, the occurrence of AGPs in extracts of different bryophytes and ferns was shown by precipitation in gel-diffusion assays with Yariv's reagent (Clarke *et al.*, 1978). Additionally, AGPs in plant tissue or extracts can be detected using monoclonal antibodies directed against AG motifs. Using these antibodies in microscopy or ELISA revealed AGP glycan epitopes in different bryophytes (Berry *et al.*, 2016; Kremer *et al.*, 2004; Ligrone *et al.*, 2002; Bartels *et al.*, 2017;

Happ and Classen, 2019) and ferns (Eeckhout *et al.*, 2014; Lopez and Renzaglia, 2014; Bartels and Classen, 2017).

Up to now, fine structures of AGPs from bryophytes (Bartels *et al.*, 2017; Fu *et al.*, 2007, Happ and Classen, 2019) and ferns (Akiyama *et al.*, 1987, Bartels and Classen, 2017) were only sparsely investigated. To systematically assess cell wall characteristics of the emerging model ferns, we isolated and characterized AGPs from the leptosporangiate ferns *Azolla filiculoides*, *Salvinia molesta* and *Ceratopteris richardii*. To obtain broader insight into AGP biosynthesis in ferns, we searched for members of the glycosyltransferase family 31 (GT31) involved in AG glycan biosynthesis as well as identified sequences encoding AGP and other HRGP protein backbones. Knowledge of cell wall diversity contributes to our understanding of plant evolution. Due to their crucial phylogenetic position as sister to land plants, ferns are key for understanding cell wall evolution of land plants.

RESULTS

We used *Salvinia molesta*, *Azolla filiculoides*, and *Ceratopteris richardii* to investigate the diversity and conservation of AGPs in cell walls of ferns. The three species were cultivated under greenhouse conditions, harvested, and dried (see Figure 1 for appearance of cultivated ferns and phylogeny of the green plant lineage). In the water soluble fractions (AE) of all species (Tables S1-S3), Gal and Glc were present in high amounts. The content of Ara differed between the investigated species with around 30 % in *Salvinia*, 20 % in *Ceratopteris*, and only 10 % in *Azolla*. AE of *Azolla* further differed by higher amounts of Man, uronic acids and Fuc as well as lack of 3-*O*-methylrhamnose (3-*O*-MeRha; trivial name acofriose). The content of Xyl was another striking difference between the species with low amounts in *Salvinia* but over 20 % in *Ceratopteris* and *Azolla*.

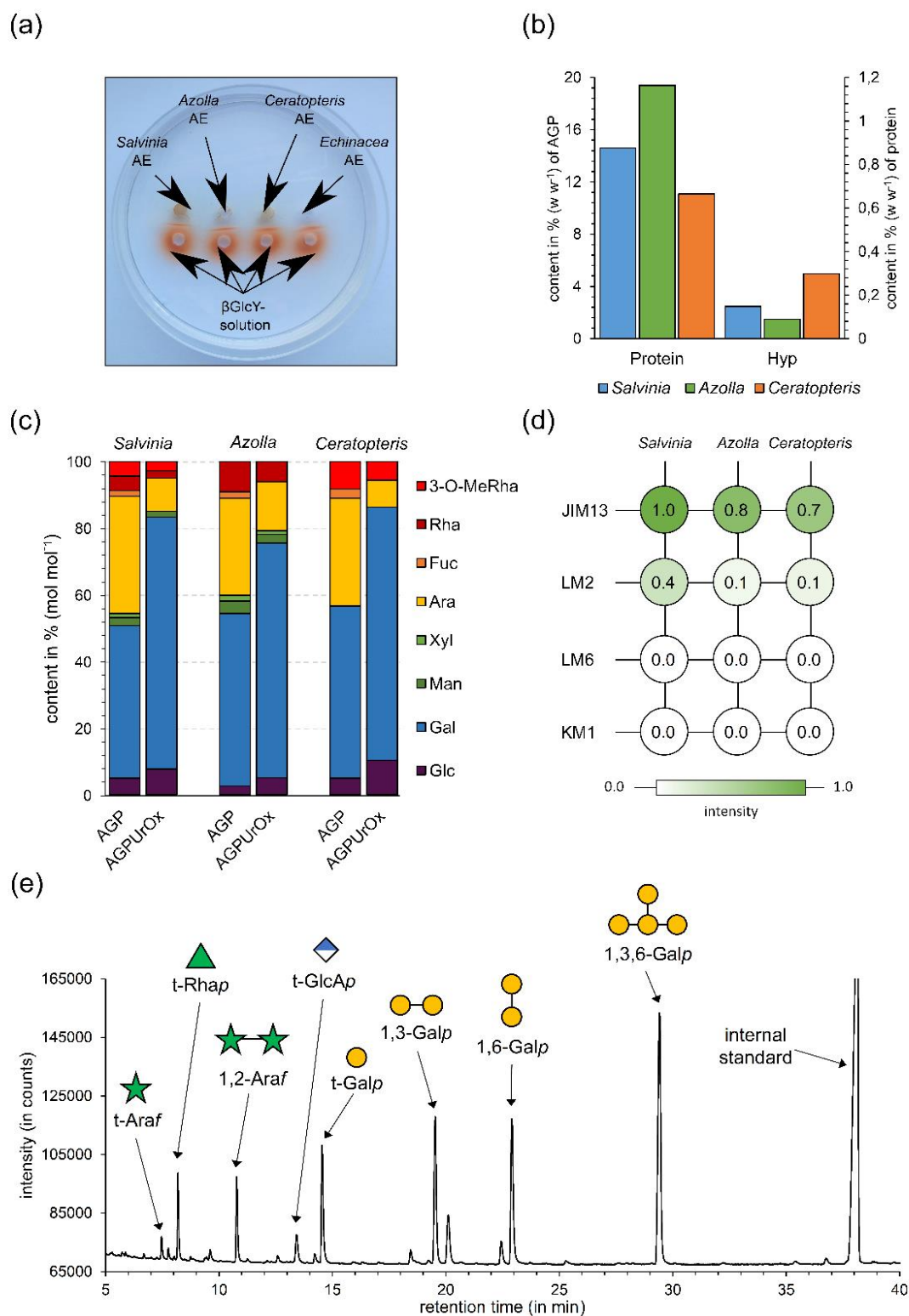


Figure 2. Features of AGPs from *S. molesta*, *A. filiculoides* and *C. richardii*. (a) Gel diffusion assay with β GlcY and fractions AE from the three ferns (100 mg mL^{-1}) compared to *Echinacea purpurea* AGP (10 mg mL^{-1}). The red precipitation line indicates presence of AGPs. (b) Protein (% w w⁻¹ of AGP) and hydroxyproline content (% w w⁻¹ of protein) in AGPs from the three species. (c) Relative monosaccharide composition of AGPs from the three ferns in the native state (AGP) and after reduction of uronic acids and partial hydrolysis with oxalic acid (AGP_{UrOx}) determined by gas chromatography (GC) (% mol mol⁻¹). (d) Results of ELISA experiments with AGPs and antibodies directed against epitopes present in AGPs (JIM13, LM2, LM6, KM1) after 10 min. For epitopes of the antibodies see Table S6. (e) FID chromatogram of partially methylated alditol acetates (PMAAs) from *Salvinia* AGP_{UrOx} after GLC analysis.

(Glyco)diversity in fern AGPs

In a gel diffusion assay with the water-soluble fractions (AE) of the three ferns and β GlcY, red precipitation lines occurred after 22 h of incubation in the dark at room temperature, indicating the presence of AGPs (Figure 2a). Presence of AGPs was further confirmed by isolation with β GlcY in amounts of 0.08 % (*Salvinia*, n=3), 0.18 % (*Azolla*, n=2) and 0.07 % (*Ceratopteris*, n=1) in relation to the dry weight of the ferns.

The amounts of nitrogen in the AGP samples were determined by elemental analyses and used to estimate the protein content of the AGPs according to Kjeldahl (factor 6.25, Figure 2b). The protein amounts of AGPs were 14.6 % for *Salvinia*, 19.4 % for *Azolla*, and 11.1 % for *Ceratopteris*. In AGPs, the amino acid hydroxyproline is responsible for *O*-glycosidic linkage of the arabinogalactan moieties to the protein. Photometric quantification of this amino acid (Stegemann and Stalder, 1967) revealed amounts of 0.36 % for *Salvinia*, 0.29 % for *Azolla*, and 0.55 % for *Ceratopteris* AGP. This means that Hyp accounts for 2.5 % of the protein moiety in *Salvinia*, 1.5 % of the protein moiety in *Azolla*, and 5.0 % of the protein moiety in *Ceratopteris* AGP (Figure 2b).

As expected, Gal and Ara were the dominant monosaccharides of the Yariv-precipitated AGPs and accounted for slightly over 80 % of the neutral monosaccharides in all species (Figure 2c, Table S4) with an Ara : Gal ratio comparable to other AGPs of ferns (Bartels and Classen, 2017) and seed plants (Clarke *et al.*, 1978). These monosaccharides were accompanied by Rha / 3-*O*-MeRha in substantial amounts between 8.3 % and 9.2 % (counted together). Interestingly, the ratio between both deoxyhexoses varied strongly. In *Salvinia* AGP, both were present in nearly equal amounts, whereas in *Azolla* AGP, 3-*O*-MeRha was present only in traces and in *Ceratopteris* AGP, the methylated Rha is strongly dominating (Figure 2c, Table S4). The monosaccharides Glc, Man, Xyl and Fuc were present in smaller amounts, but it cannot be fully excluded that they might be part of other polysaccharides not completely separated during Yariv precipitation. Some Glc might also be the residue of the precipitating agent β GlcY. Photometric quantification of uronic acids revealed a content of 11.0 % for *Salvinia*, 5.6 % for *Azolla* and 11.1 % for *Ceratopteris* AGPs (Table S3).

To gain further information, uronic acids were carboxy-reduced to the corresponding neutral monosaccharides with sodium borodeuteride. Afterwards, deuterated Glc was detected, thus revealing that GlcA has been part of the native AGP. Furthermore, the samples were partially hydrolysed with oxalic acid, a treatment known to hydrolyse mainly furanosidic arabinose residues. This led to strong decrease of the Ara content (Figure 2c, Table S4) and also to further decrease of the minor monosaccharides Rha, Fuc, Xyl and Man.

Fern AGPs structural characteristics appear evolutionarily more flexible compared to angiosperms

Linkage types of monosaccharides were determined by methylation analyses before and after partial acid hydrolysis and uronic acid reduction (Table 1, Figure 2e, compare Figure S1a and b). In the native AGPs, the typical galactan backbone known from seed plant AGPs was present with pyranosidic Gal in 1-, 1,3- 1,6- and 1,3,6-linkage. According to the retention time and the mass spectra, a further peak represented a mixture of pyranosidic, 1,2- and 1,4-linked hexoses (Figure S1). 1,2 and/or 1,4-linked Galp have also been detected in some moss and other fern AGPs (Bartels *et al.*, 2017; Bartels and Classen, 2017). Furanosidic Ara, which is typically located at the periphery of the AGP molecule, was 1-, 1,2- and 1,5-linked with dominance of 1,2-linkage type. After partial acid hydrolysis, there was nearly complete loss of 1,5-linked Ara_f, strong reduction of terminal Ara_f and moderate reduction of 1,2-Ara_f. Furthermore, acid hydrolysis strongly increased the amount of 1,6-linked Galp, which is an indication that Ara is mainly bound to Gal at C-3 of 1,3,6-linked Gal. The increase in terminal Gal is a hint that some Ara or acid-labile Rha or Fuc is bound to C-6 of Gal in the native AGP. Comparable to other fern AGPs, Rhap (including 3-*O*-Me-Rhap) is localized terminally (Bartels and Classen, 2017). After carboxy-reduction of uronic acids to the corresponding deuterium-labeled neutral monosaccharides, only GlcA was detected as a terminal monosaccharide (AGP_{UrOx}).

Antibodies directed against epitopes of the glycan part of angiosperm AGPs (see Experimental section) were tested for their binding capacities to the different fern AGPs to gain further information on AGP structures (Figure 2d, Figure S2). In the tested concentrations, there was no binding of the fern AGPs to KM1 and LM6, thus supporting structural differences to angiosperm AGPs. For KM1 (Classen *et al.*, 2004), it has been shown that β -D-1,6-Galp is part of the epitope (Ruprecht *et al.*, 2017), which is present in the fern AGPs only in small amounts. LM6 is directed against α -L-1,5-linked Ara_f (Verhertbruggen *et al.*, 2009a) present in arabinans but also in some AGPs. Although this Ara linkage type is present in the investigated fern AGPs, the amounts are lower compared to the 1,2-linkage type. Weak binding of LM6 to *Ceratopteris* AGP was observed after longer times of incubation (data not shown), thus confirming higher amounts of 1,5-Ara_f in *Ceratopteris* compared to *Salvinia* and *Azolla* AGP. LM2 showed moderate binding to the fern AGPs, probably due to presence of terminal GlcAp, which has been described as part of the epitope (Ruprecht *et al.*, 2017). JIM13 strongly binds to the three fern AGPs, especially to *Salvinia* AGP. JIM13 is known to recognize many AGPs but the exact epitope is under debate. The trisaccharide β -D-GlcAp(1 \rightarrow 3)- α -D-GalAp-(1 \rightarrow 2)- α -L-Rhaf isolated from hydrolysate of gum karaya binds to this antibody (Yates *et al.*, 1996). Strong binding of JIM13 to a rhamnogalactan-protein from *Spirogyra* (Pfeifer *et al.*, 2022) further

suggests that terminal Rha must be an important part of the epitope of JIM13 and is possibly responsible for binding to the investigated fern AGPs. An exemplary structural proposal for AGP of *Azolla* based on the results above is given in Figure S3.

Table 1. Linkage type analysis of AGPs and hydrolysed AGPs (AGP_{UrOx}) from *S. molesta*, *A. filiculoides* and *C. richardii* in % (mol mol⁻¹, n=1).

Mono-saccharide	linkage type	<i>S. molesta</i>		<i>A. filiculoides</i>		<i>C. richardii</i>	
		AGP	AGP _{UrOx}	AGP	AGP _{UrOx}	AGP	AGP _{UrOx}
Galp	1,3,6-	30.7	33.8	27.0	30.8	35.9	37.8
	1,6-	2.1	15.8	2.6	11.5	2.2	12.4
	1,3-	15.2	14.4	15.5	18.7	16.4	15.0
	1-	2.1	12.0	3.4	5.1	6.0	9.4
Araf	1,5-	3.9	-	4.4	-	7.3	-
	1,2-	17.2	6.7	16.9	10.7	11.5	3.9
	1-	9.6	1.8	8.5	2.6	6.4	1.8
Rhap	1-	11.0	5.9	9.5	6.1	7.8	8.2
Fucp	1-	-	-	1.4	-	2.2	-
GlcAp	1-	nd	3.6	nd	2.9	nd	3.2
Manp	1,6-	2.9	-	2.9	1.2	1.3	2.7
Hexp	1,4-/1,2-	5.3	6.0	7.9	9.2	3.0	5.6

nd: not detectable due to the method

21 different species representing the streptophyte lineage (a streptophyte alga, three bryophytes, a lycophyte, seven ferns, three gymno- and six angiosperms) were compared with regard to AGP linkage types (Table 2). Here, we only used data from our working group to ensure a comparable methodology for isolation and structural characterization (see Figure 3 for references). The comparison of AGP fine structures over the streptophyte lineage by PCA (Figure 3) revealed first hints on lineage-specific structural features of AGPs. The streptophyte alga *Spirogyra pratensis* and the lycophyte *Lycopodium annotinum* were clearly separated from all other species due to high amounts of terminal and unique 1,3-linked Rhap in *Spirogyra* AGP and unusual terminal Arap accompanied by 1,3-linked Araf in *Lycopodium* AGP. Yet, a broader sampling is needed to clarify how common these features are in the respective lineages, or whether these are species-specific characteristics. PCA reveals clustering of angiosperm AGPs due to the common structure with a Galp backbone in 1,3,6- and 1,6- linkage decorated with 1,5-linked and terminal Araf. In contrast, gymnosperms linkage types of AGPs seem to be less conserved, although it needs to be considered that only three species from three lineages, *Ginkgo*, *Cycas* and *Ephedra*, and no representatives from conifers were included in the analyses. For fern AGPs a clear separation to angiosperm AGPs is visible in line with their evolutionary distance. There is an overlap of fern AGPs with those of mosses and gymnosperms. A common feature of AGPs from mosses, ferns and gymnosperms is the presence of the unusual monosaccharide 3-O-Me-Rhap not observed in any angiosperm AGP

or any other angiosperm cell wall polysaccharide. Within the ferns, the only eusporangiate fern AGP from *Equisetum* is separated from the leptosporangiate AGPs. The leptosporangiate *Osmunda* AGP is located in between *Equisetum* AGP and the other leptosporangiate AGPs. This is in accordance with the phylogeny of ferns, where *Osmunda* is sister to the rest of the leptosporangiates. *Azolla* and *Salvinia* are members of the same family (Salviniaceae) and the similarities in their AGPs reflect their close phylogenetic relationship or the similarity of their aquatic lifestyle. Indeed, *Pteridium* and *Ceratopteris* belong to the same family (Pteridaceae), yet *Pteridium* AGPs cluster with those from *Dryopteris*, while those of the aquatic fern *Ceratopteris* is more similar to AGPs from *Salvinia* and *Azolla*.

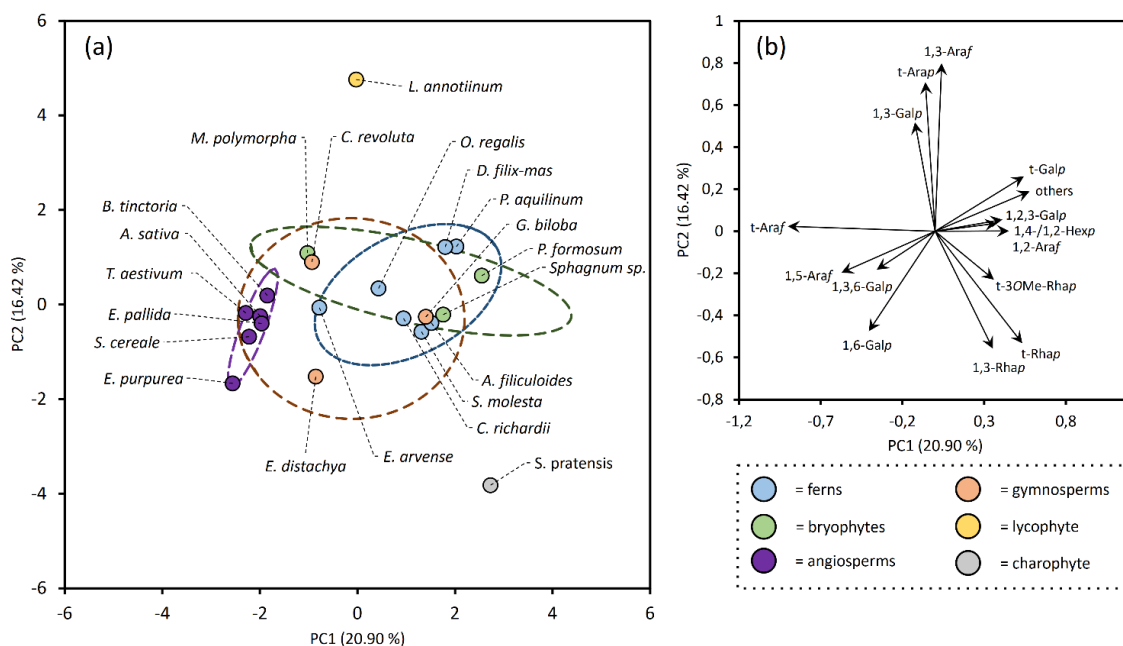


Figure 3. Results of the PCA analysis of linkage-types in AGPs throughout the streptophyte lineage. (a) Scatter plot of PC1 (20.90%) against PC2 (16.42%). Different colors were used for each evolutionary group. Ellipses represent 90 % confidence intervals. For full plant names refer to Bartels and Classen (2017), Bartels *et al.*, (2017), Baumann *et al.* (2021), Classen *et al.* (2000), Goellner *et al.* (2010, 2011, 2013), Happ and Classen (2019), Pfeifer *et al.* (2022), Thude and Classen (2005) and Wack *et al.* (2005). (b) Loading plot for the PCA with influences of the different input variables.

Table 2. Linkage type analysis of AGPs throughout the streptophyte lineage in % (mol mol⁻¹).

		1,3,6-Galp	1,2,3-Galp	1,3-Galp	1,6-Galp	t-Galp	1,2-Araf	1,3-Araf	1,5-Araf	t-Araf	t-Arap	t-Rhap	t-3-O-	MeRhap	1,3-Rhap	1,4-/1,2-Hexp	others
Charophyte alga	<i>S. pratensis</i>	30.7	0	9.8	5.8	0	0	0	0	1.1	0	24.7	2.0	20.0	0	5.9	
Bryophytes	<i>M. polymorpha</i>	27.1	0	19.2	0	0	0	4.3	2.7	36.3	0	1.1	1.1	0	4.3	3.9	
	<i>Sphagnum</i> sp.	27.5	4.8	17.8	7.3	7.0	0	0.5	5.3	3.9	0	1.9	7.2	0	11.1	5.7	
	<i>P. formosum</i>	28.2	6.6	14.5	2.6	14.2	0.6	3.4	1.8	9.2	0	7.4	2.5	0	6.8	2.2	
Lycophyte	<i>L. annotinum</i>	29.2	0	19.5	1.1	1.3	0.2	15.2	1.0	11.8	13.4	0	0	0	3.1	4.2	
Ferns	<i>E. arvense</i>	26.4	0	16.3	1.8	2.4	0.5	0.2	14.3	23.1	0	0	3.4	0	5.2	6.4	
	<i>O. regalis</i>	35.5	0	19.7	1.3	3.4	2.9	0.8	2.4	15.9	0	1.1	5.1	0	6.3	5.6	
	<i>S. molesta</i>	30.7	0	15.2	2.1	2.1	17.2	0	3.9	9.6	0	5.4	5.6	0	5.3	2.9	
	<i>A. filiculoides</i>	27.0	0	15.5	2.6	3.4	16.9	0	4.4	8.5	0	9.5	0	0	7.9	4.3	
	<i>C. richardii</i>	35.9	0	16.4	2.2	6.0	11.5	0	7.3	6.4	0	0	7.8	0	3.0	3.5	
	<i>P. aquilinum</i>	29.7	0	20.6	2.2	10.6	9.6	1.7	2.5	4.6	0	0.5	1.3	0	7.6	9.1	
	<i>D. filix-mas</i>	23.7	0	18.5	2.9	9.0	5.0	1.7	2.9	15.2	0	0.7	1.3	0	4.8	14.3	
Gymnosperms	<i>C. revoluta</i>	32.4	0	13.2	3.8	2.1	1.5	7.1	6.9	21.7	3.7	4.4	0	0	1.1	2.1	
	<i>G. biloba</i>	12.6	0	2.8	1.3	2.3	1.0	2.3	13	8.4	1.0	2.1	1.2	0	47.3	4.7	
	<i>E. distachya</i>	39.2	0	7.3	4.0	0.9	0.7	0	3.7	27.4	0.5	2.4	8.7	0	5.2	0	
Angiosperms	<i>T. aestivum</i>	37.7	0	19.0	3.0	1.2	0	0	9.0	30.1	0	0	0	0	0	0	
	<i>S. cereale</i>	36.3	0	14.2	6.4	3.3	0	0	7.7	32.1	0	0	0	0	0	0	
	<i>A. sativa</i>	36.8	0	19.6	6.1	3.6	0	0	7.3	26.6	0	0	0	0	0	0	
	<i>B. tinctoria</i>	24.2	0	16.7	5.8	3.6	0	1.7	9.4	33.2	1.9	1.7	0	0	1.8	0	
	<i>E. pallida</i>	26.9	0	16.5	6.3	2.5	0	0	14.2	29.4	0	0	0	0	0	4.2	
	<i>E. purpurea</i>	31.8	0	12.7	15.4	0	0	0	11.7	24.8	0	0	0	0	0	3.6	

A genetic framework for AGP glycosylation in ferns

Glycosylation of AGPs is very complex and involves addition of large arabinogalactan (AG) moieties to hydroxyproline residues often arranged in characteristic dipeptide repeats: Ala-Hyp, Ser-Hyp, Thr-Hyp. The AGs consist of β -1,3-Galp backbones with β -1,6-linked Galp side chains that are further decorated with mainly Ara but also GlcA, Rha, Fuc or Xyl (for review, see Showalter and Basu, 2016; Silva *et al.*, 2020, Strasser *et al.*, 2021). The responsible glycosyltransferases (GTs) belong to different GT families that have been classified in the carbohydrate active enzymes (CAZy) database (<http://www.cazy.org>). Although several GTs responsible for AGP glycosylation have been identified in *Arabidopsis*, many enzymes are still unknown, e.g. most arabinosyl- and all rhamnosyltransferases (Silva *et al.*, 2020). Responsible for galactosylation of AGPs are enzymes of the family GT31. A phylogeny of the *Arabidopsis thaliana* sequences in this family divides into three distinct groups which were subdivided into 9 subgroups I-IX (group A with clades I-IV, group B with clades V and VI, group C with clades VII-IX, Qu *et al.*, 2008). Eleven of these enzymes belonging to clades II, III, V and VI have already been characterized and are involved in AGP galactosylation in *Arabidopsis thaliana* (Silva *et al.*, 2020).

To elucidate whether homologs of these enzymes are present in ferns, *Arabidopsis* sequences from group A and B were used to search for GT31 sequences in the genomes of *Salvinia*, *Azolla* and *Ceratopteris* as well as in transcriptomic data from other ferns (Carpenter *et al.*, 2019; Leebens-Mack *et al.*, 2019, Figure 4, Table S5 and Figure S4). The first step of AGP galactosylation is the transfer of the first Gal onto Hyp by a hydroxyproline *O*- β -galactosyltransferase. In *Arabidopsis*, GALT 2-6 (Basu *et al.*, 2015a; Basu *et al.*, 2015b) belonging to clade VI as well as HPGT1, HPGT2 and HPGT3 from clade III within GT31 (Ogawa-Ohnishi and Matsubayashi, 2015) have been identified to be responsible for this step of the biosynthesis. Whereas GALT2-6 contain a galectin domain, this domain is absent in HPGT1-3 (Showalter and Basu, 2016). Genomes of *Azolla*, *Salvinia* and *Ceratopteris* and transcriptomes of all ferns contain at least one corresponding sequence in one of these GT31 families, thus supporting that the transfer of Gal onto Hyp is possible in all fern AGPs.

The *Arabidopsis* genes At1G77810 (Qu *et al.*, 2008), At1G33430 (called UPEX1 or KNS4; Suzuki *et al.*, 2017) as well as GALT8 (Narciso *et al.*, 2021) belonging to clade II and possibly CAGE1 and CAGE2 (clade I, Nibbering *et al.*, 2022) encode β -1,3-galactosyltransferases which function in AGP β -1,3-galactan backbone synthesis. Galactan side chains of AGPs consisting of β -1,6-linked Gal are synthesized by β -1,6-galactosyltransferases of family GALT31A (clade II, Geshi *et al.*, 2013), although in a recent study GALT31A was found to galactosylate substituted and unsubstituted β -1,3-galactan oligosaccharides rather than β -1,6-

linked galactan oligosaccharides (Ruprecht *et al.*, 2020). Homologs to sequences from all *Arabidopsis* enzymes from group A and B responsible for synthesis of the galactan structure are present in *Azolla*, *Salvinia*, *Ceratopteris* and all investigated fern transcriptomes. Clades I and II could not be phylogenetically separated (Figure S4; although clade II had also no support as an independent group in Qu *et al.* 2008, where the groups were originally defined). On balance, the evolution of GT31 group I and II is characterized by lineage-specific diversification (Figure 4): *Arabidopsis* appeared to have slightly more homologs (eight sequences) compared to leptosporangiate (on average 4.8 per species) and eusporangiate ferns (on average 1.8 per species). That said, the investigated fern genomes contain similar numbers of homologs as *Arabidopsis* (eight in *Azolla*, six in *Salvinia* and ten in *Ceratopteris*, see Table S5), indicating that the overall lower number of homologs in transcriptomes of ferns is likely an underestimate caused by technical limitations or other reasons like e.g. low expression or differential regulation. To summarize, the genetic toolkit necessary for galactosylation of Hyp and the biosynthesis of the typical AGP galactan scaffold known from seed plants is present in the fern lineage, corroborating our analytical findings (Figure S3). Overall, this suggests that Hyp galactosylation and the synthesis of typical AGP galactan is conserved and was already present in the LCA of ferns and seed plants.

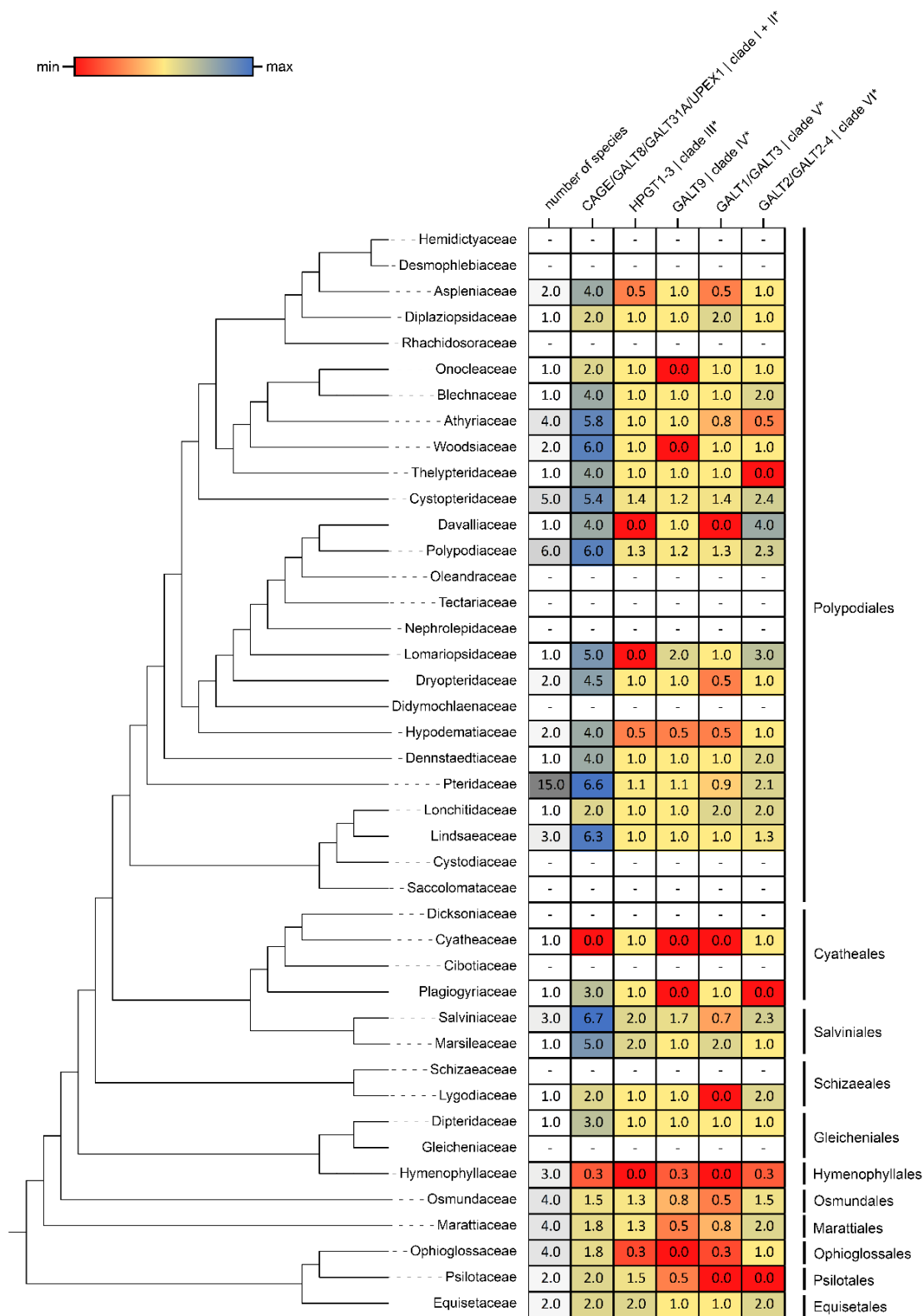


Figure 4. Overview of GT31 homologs from fern transcriptomes and genomes. The fern phylogeny on the left side is based on the dataset of Nitta *et al.* (2022) and was visualized with iTOL (v6.6, Letunic and Bork, 2021). The heatmap on the right side is based on the average homolog number in the respective clades of the phylogenetic tree (Figure S4). White fields with dashes were not covered by the dataset. Clade annotations marked with asterisks are used according to Qu *et al.* (2008).

Identification of AGP and other HRGP protein sequences in fern genomes

Sequences for classical AGPs and other HRGPs (extensins and PRPs) as well as hybrid sequences with motifs from different HRGPs were identified (Figure 5) using the established motif and amino acid bias ‘MAAB’ classification system (Johnson *et al.*, 2017a,b). Class 1 and 4 comprise classical AGPs with and without GPI anchor respectively, class 2 and 9 are extensins (cross-linking or with GPI-anchor) and class 3 contain PRPs. All other classes consist of hybrid HRGP sequences. For the heterosporous ferns *Azolla* and *Salvinia*, AGP sequences identified were similar in number with six for *Azolla* (none with GPI-anchor) and seven for *Salvinia* (three with GPI-anchor), whereas for homosporous ferns *Adiantum*, *Alsophila* and *Ceratopteris*, numbers were much higher with 19 - 41 AGP sequences (two to seven with GPI-anchor). The same trend was found for extensins with no sequence identified in *Azolla*, only one sequence in *Salvinia* and higher numbers of sequences in *Adiantum* and *Ceratopteris*. PRPs were absent in all investigated species and only one sequence was detected in the *Ceratopteris* genome. In *Azolla* and *Salvinia* only one or two hybrid HRGPs were present, whereas in the homosporous ferns, numerous sequences were found, especially in classes 6 (AGP bias), 10 and 12 (extension bias) and 18 (PRP bias). Sequences belonging to class 24 have been detected in all species with the exception of *Alsophila* but have low percentages of HRGP motifs and possibly comprise likely either non-HRGPs or unknown HRGPs (Johnson *et al.*, 2017a)

Chimeric AGPs are characterized by AGP-motifs, a signal peptide and one or more known functional protein domains. They were identified by screening the translated genome for sequences which meet the criteria (i) signal peptide (SignalP 5.0), (ii) predicted AG regions, and (iii) at least one detectable protein domain (Pfam). 108 chimeric AGPs were present in *Adiantum*, 257 in *Alsophila*, 75 in *Azolla*, 184 in *Ceratopteris*, and 71 in *Salvinia* (Figure S5 and Figure 5b).

By evaluation of the intersections between chimeric AGPs from all five species, shared domains were detected (highlighted in Figure S5 and Figure 5b). Ten domains were present in all ferns. Interestingly, they comprise between 47.1 % and 54.9 % of all chimeric AGPs in ferns (Figure S5). The most dominant members are protein kinase-like AGPs, plastocyanin-like AGPs (Cu bind-like domain, pfam02298) and fasciclin-like AGPs. Another shared group of all ferns are xylogen-like AGPs (containing the LTP-2 domain, pfam14368) which occurs in lower numbers in the small aquatic ferns (each two for *Azolla* and *Salvinia*) but higher numbers in *Adiantum* (three sequences), *Alsophila* (four sequences) and *Ceratopteris* (seven sequences).

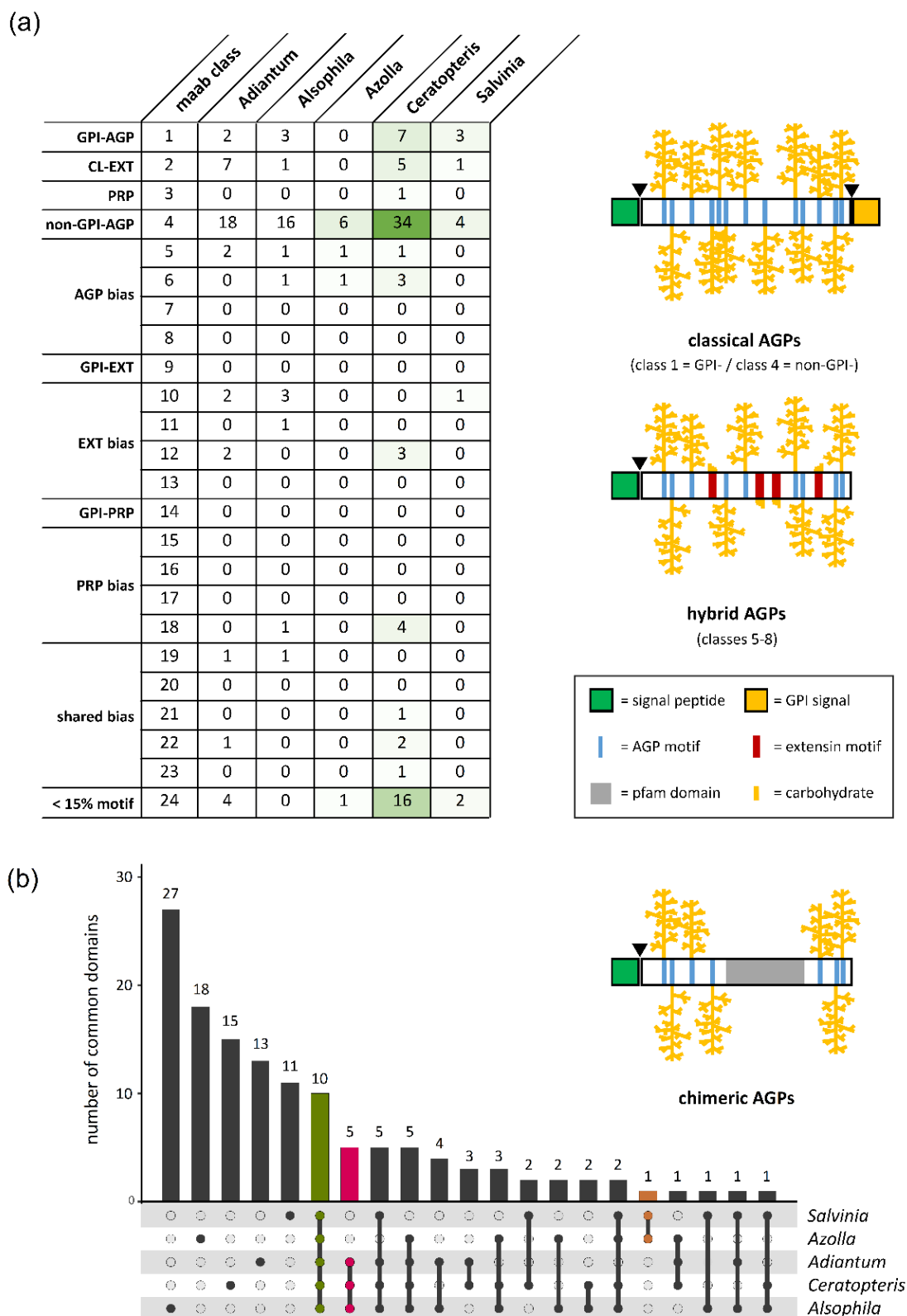


Figure 5. Results of the bioinformatic analyses on AGP backbone sequences from the five fern genomes. (a) MAAB classification of all HRGPs within a possible 24 distinct classes. The schematics on the right side highlight the predicted post-translational modifications on classical, hybrid and chimeric AGPs. (b) Chimeric AGPs are visualized as UpSet plot. Number of common domains of all (green), of all aquatic heterosporous (orange) and all homosporous (magenta) ferns are highlighted. For detailed knowledge of domains, see Figure S5.

DISCUSSION

Polysaccharides of ferns cell walls

Plant terrestrialsation was accompanied by drought stress and leading to diversification of land plants through innovative strategies to reduce dependence on water availability. Structural innovations of tracheophytes include those that enhance transport of water and solutes, as well as taller and turgor-stabilised upright stems for improved spore dispersal and more efficient light capture (Bateman *et al.*, 1998; Eeckhout *et al.*, 2014). Cell wall modifications are important at all levels of plant growth and development and it is likely that the evolutionary pressures brought about the differences in cell wall composition that occurred during the colonisation of land and the emergence of the tracheophytes. With increasing focus on the molecular processes of plant evolution, different groups have contributed to the knowledge of specific cell wall characteristics in ferns using a variety of methods. Often, immunocytochemical workflows (Eeckhout *et al.*, 2014; Leroux *et al.*, 2011; Leroux *et al.*, 2013b; Leroux *et al.*, 2015; Popper 2006; Chernova *et al.*, 2020; Harholt *et al.*, 2012; Carafa *et al.*, (2005)) were applied using various monoclonal antibodies against glycan epitopes (Meikle *et al.*, 1994, McCartney *et al.*, 2005; Marcus *et al.*, 2008; Pedersen *et al.*, 2012; Puhlmann *et al.*, 1994; Marcus *et al.*, 2010). Furthermore, enzyme-assisted digestion with (partial) characterization of the released oligosaccharides was used and shed light on fern xyloglucans (Peña *et al.*, 2008; Hsieh and Harris 2012), mannans (Frankova and Fry, 2011; Popper 2006; Silva *et al.*, 2011) as well as mixed-linkage glucans (Popper and Fry, 2003; Soerensen *et al.*, 2008; Fry *et al.*, 2008; Xue and Fry (2012). All these studies fostered the conclusion that fern cell walls share basic features with those of seed plants, such as the occurrence of cellulose, hemicelluloses and pectic polysaccharides (Leroux *et al.*, 2013a; Matsunaga *et al.*, 2004; Popper and Fry, 2004; Popper, 2008). Yet they differ from them, for example, in their composition of lignin (Weng *et al.*, 2008, see introduction), suggesting that lineage-specific cell wall properties have evolved after the split of the fern and seed plant lineages. These lineage-specific differences seem to occur mainly in the fine-structure of the cell wall, e.g. through variation of side-chain structures. Our focus on AGPs in ferns using methods ranging from carbo-analytical, immunocytochemical to bioinformatic approaches provide detailed insights into the evolutionary history of AGPs in tracheophytes.

AGPs abound in fern cell walls

Already in the 1970s, the occurrence of AGPs in several leptosporangiate ferns was shown by gel-diffusion assay with Yariv's reagent (Clarke *et al.*, 1978). Monoclonal antibodies directed against arabinogalactan epitopes (e.g. JIM4, JIM8, JIM13, KM1, LM2, LM6 or MAC207 (for epitopes and references see Classen *et al.*, 2019) were used to verify the presence of AGPs in combination with glycan microarrays, ELISA and microscopy to detect AGPs in different monilophytes (Popper, 2006; Moore *et al.*, 2013; Leroux *et al.*, 2015; Bartels and Classen, 2017; Eeckhout *et al.*, 2014; Lopez and Renzaglia, 2014; Lopez and Renzaglia, 2016). However, reliability of these discoveries are sometimes questionable because the exact structures of epitopes of the antibodies are not always known and cross-reactions with other polysaccharides might occur. For example, LM6 is directed against 1,5-linked Araf and binds to arabinans, yet it can also detect AGPs.

Information on the structure of AGPs from seed plants is extensive, while limited data is available for monilophytes and other seedless plants. Such studies are, to the best of our knowledge, currently limited to seven mosses (Geddes and Wilkie, 1971; Kremer *et al.*, 2004; Lee *et al.*, 2005; Fu *et al.*, 2007; Happ and Classen, 2019) and four monilophyte species (Bartels and Classen, 2017). To gain further information on fern AGPs and insight into AGP evolution, we isolated AGPs from *Salvinia*, *Azolla* and *Ceratopteris* by specific precipitation with β GlcY. The amount of *Azolla* AGP was comparable to AGP content of the mosses *Sphagnum* and *Physcomitrium* (Bartels *et al.*, 2017) and slightly higher compared to other monilophytes (in mean 0.12 % – 0.15 %, Bartels and Classen, 2017) whereas AGP amounts of *Salvinia* and *Ceratopteris* were slightly lower and comparable to AGP recovery in the moss *Polytrichastrum* (Bartels *et al.*, 2017). However, variation in AGP amounts is observed at different times of harvest (Bartels and Classen, 2017); thus, it cannot be excluded that some of the observed variation may stem from different times of harvest.

With regard to the AGP protein moieties (high protein and low hydroxyproline content) AGPs from the three fern species investigated here are more similar to some moss AGPs (Bartels *et al.*, 2017; Happ and Classen, 2019) than to those from other ferns (Bartels and Classen, 2017). This may reflect similarities in habitat of the mosses and the water ferns we investigated, including characteristics such as high moisture.

The carbohydrate backbones of AGPs mainly consist of linear chains of β 1,3-linked Galp attached to Hyp, and branched with β 1,6-linked Galp side chains (Ma *et al.*, 2018). Our results reveal that AGPs of the three ferns contain this typical galactan core with Galp in 1-, 1,3- 1,6- and 1,3,6-linkage known from seed plants and also from other fern genera (Bartels and Classen, 2017). A proposal for the structure of the carbohydrate moiety of AGP from *Azolla* is shown in

Figure S3. The lower amounts of 1,6-linked Galp, indicating a highly branched structure, may be a special feature of fern AGPs. For example in AGP from the angiosperm *Echinacea*, 1,6-linked Galp was present in high amounts (Classen *et al.*, 2000). KM1, an antibody directed against 1,6-linked Galp (Ruprecht *et al.*, 2017), has been generated against *Echinacea* AGP (Classen *et al.*, 2004). This antibody showed no reactivity with the fern AGPs tested here (Figure 2d), thus supporting low amounts of 1,6-linked Galp in the three species.

We observed several differences to seed plants with regard to the monosaccharides present at the periphery of the fern AGPs. The unusual monosaccharide 3-*O*-Me-Rha is present as terminal monosaccharide in *Salvinia*, *Azolla* and *Ceratopteris* AGPs. 3-*O*-Me-Rha has been detected in cell walls of streptophyte algae, bryophytes, lycophytes, ferns and gymnosperms before (Popper and Fry, 2003; Pfeifer *et al.*, 2022; Popper, Sadler and Fry, 2004; Matsunaga *et al.*, 2004; Anderson and Munro, 1969), but has never been found in angiosperm cell walls. In *Lycopodium* and different ferns, 3-*O*-Me-Rha occurs in rhamnogalacturonan II (Matsunaga *et al.*, 2004). Several studies now show that 3-*O*-Me-Rha is also part of many moss, fern and gymnosperm AGPs (Fu *et al.*, 2007; Bartels *et al.*, 2017; Bartels and Classen, 2017; Happ and Classen, 2019; Baumann *et al.*, 2021), but it was not found in *Lycopodium* AGP (Bartels and Classen, 2017).

Furanosidic Ara is present in all typical AGPs in substantial amounts, but linkage types differ. The terminal linkage is the preferred one while Araf in 1,2-, 1,3- and/or 1,5-linkage occurs less often. AGPs from *Salvinia*, *Azolla* and *Ceratopteris* had high and comparable amounts of 1,2 linked Araf to other leptosporangiate fern AGPs (except the early diverging species *Osmunda regalis*, Bartels and Classen, 2017). This linkage type is, however, have not been described for angiosperm AGPs so far. It is noteworthy that linkage types can also differ within one species. In AGPs from the medicinal plant *Echinacea purpurea*, Araf was present in 1,5-linkage, but secreted AGPs from cell cultures of the same species predominantly formed a 1,3-Araf linkage (Classen, 2007). The latter is not limited only to cell culture AGPs but is also the predominant type in AGPs from *Arabidopsis* leaves (Tryfona *et al.*, 2012) and *Zostera* (Pfeifer *et al.*, 2020).

Structure of fern AGPs in light of evolution

The comparison of AGP fine structures over the streptophyte lineage by PCA revealed first hints on lineage-specific structural features of AGPs. Generally spoken, angiosperms are most likely more stable regarding the type of side-chain linkages while the other major (land) plant lineages show more flexibility in this direction. The set of angiosperms included in our PCA is composed of members of the monocot order of Poales as well as the two dicot orders Asterales and Fabales. While this dataset does not cover all of angiosperm diversity, the inclusion of

monocots and dicots covers the entire evolutionary distance of angiosperms; thus ruling out that the clustering of the PCA can stem from a sampling bias. Clustering of the aquatic ferns *Ceratopteris*, *Salvinia* and *Azolla* seems to correlate with their aquatic habitat. Overall, the data suggest that both, a close phylogenetic relationship and a very divergent lifestyle can drive the evolution of AGP linkage types.

AGP GTs, AGP as well as other HRGP proteins have diversified in ferns

Transfer of the first Gal onto Hyp as well as biosynthesis of the AGP galactan consisting of a β -1,3-linked Gal with β -1,6-linked Gal side chains is performed by members of the glycosyltransferase family 31. We find homologs of *Arabidopsis* Hyp-*O*-galactosyltransferases, β -1,3-galactosyltransferases, and a β -1,6-galactosyltransferase in the genomes of the three investigated ferns and the transcriptoms of other lepto- and eusporangiate ferns. These data agree with our analytical investigations on fern AGP structure and support that the seed plant-typical AGP galactosylation is present in ferns, and was likely present in the LCA of the two lineages.

The occurrence of terminal Rha, partially present as 3-*O*-MeRha is the most striking difference of fern to seed plant AGPs. Up to now, the only rhamnosyltransferase characterized with regard to cell wall biosynthesis is involved in pectic rhamnogalacturonan I synthesis (Takenaka *et al.*, 2018). Future characterizations of rhamnosyltransferases acting on AGPs will be illuminating. Protein backbones of classical AGPs consist of an N-terminal signal peptide, a protein sequence rich in Pro, Ala, Ser and Thr (PAST) residues and may have an additional C-terminal GPI anchor sequence (Schultz *et al.*, 2000). *In silico* analyses revealed several homologs to classical AGPs, extensins and hybrid HRGPs in ferns such as *Adiantum*, *Alsophila* and *Ceratopteris* in similar amounts as found in seed plants and slightly lower numbers for the ferns *Azolla* and *Salvinia* (Ma *et al.*, 2017; Johnson *et al.*, 2017a,b). The latter two have small genomes compared to other ferns (Li *et al.*, 2018), which could explain our results. In all ferns, the chimeric AGPs comprise mainly protein kinase-like, phytocyanin-like, fasciclin-like and xylogen-like AGPs, which are well described chimeric AGPs in seed plants (Johnson, 2003; Basu *et al.*, 2016; Costa *et al.*, 2019; He *et al.*, 2019; Ma *et al.*, 2022; Shafee *et al.*, 2020). Conservation of AG-attachment sites close to these protein domains underlines the necessity of glycosylation for the correct function of the respective domains (Dragićević *et al.*, 2020). The group of xylogen-like AGPs is of interest with regard to the evolution of vascular tissues (Motosé *et al.*, 2004; Kobayashi *et al.*, 2011). The characteristic pfam domain is among the top ten protein domains conserved in all investigated fern genomes. However, the domain was less abundant in the genomes of the heterosporous ferns *Azolla* and *Salvinia*. Such universal occurrence across fern

species hints towards a fundamental contribution of AGPs to the process of vascular tissue differentiation (see below); lower numbers in some of the water ferns might be connected to their aqueous habitat. While AGP protein sequence numbers of ferns and their galactosylation are similar to that of seed plants, their oligosaccharide structures at the periphery of the AGP molecules differ between ferns and seed plants. This might result in deviating functions and explain lineage-specific differences in cell wall structures of ferns and seed plants.

On possible functions of AGPs in ferns

Functional roles of AGPs in seed plants amongst others include cell division, growth, programmed cell death, pattern formation, and plant-microbe interactions (for reviews see Seifert and Roberts, 2007; Ellis *et al.*, 2010; Ma *et al.*, 2018; Hromadová *et al.*, 2021). Interaction of GPI-anchored AGPs with plasma membrane-bound transmembrane proteins of the same cell or soluble AGPs with receptors in adjacent cells have been proposed (Ellis *et al.*, 2010). Signalling caused by AGPs might also occur by oligosaccharides enzymatically cleaved from the AG glycan moieties or via Ca^{2+} -ions (Lamport *et al.*, 2014). Knowledge on the function of fern AGPs is limited, but their roles in gamete and embryo development (Lopez and Renzaglia, 2014, 2016) and desiccation tolerance (Moore *et al.*, 2013) have been described previously. In *Ceratopteris richardii* eggs and multiflagellated sperm cells (Lopez and Renzaglia, 2014, 2016) are covered by an extraprotoplasmic AGP matrix. Given that seed plant AGPs bind and release Ca^{2+} at the plasmalemma (Lamport and Varnai, 2013), Lopez and Renzaglia (2016) proposed that AGPs from *C. richardii* could facilitate gamete fusion through Ca^{2+} oscillations. These data together with the well-documented role of seed plant AGPs in these processes (for review see Ma *et al.*, 2018; Leszczuk *et al.*, 2019) suggest that AGPs have likely facilitated reproduction and embryogenesis already in the LCA of vascular plants. Comparison of hydrated and desiccated leaf material of the resurrection fern *Mohria caffrorum* revealed that arabinose-rich polysaccharides (arabinan-rich pectins and AGPs) protect cell walls against desiccation (Moore *et al.*, 2013). The Ara-containing polysaccharides act as plasticizers ensuring the maintenance of hydration during drought stress. When the first land plants evolved from an aquatic ancestor, adaptation to water deficiency was a big challenge; the evolution of different kinds of water-transporting mechanisms was likely key for land plants to establish themselves on land and diversify (Woudenberg *et al.*, 2022). Involvement of AGPs in water transport has been suggested for many lineages across the land plant tree of life: antibodies directed against AGP epitopes labelled water-conducting cells of different liverworts and mosses (Ligrone *et al.*, 2002). Additionally, xylogen-type genes are present in the moss *Physcomitrium* as well as the lycophyte *Selaginella* (Kobayashi *et al.*, 2011). The AGP

“xylogen” induces xylem differentiation in suspension cultures of the angiosperm *Zinnia* (Motosé *et al.*, 2004). In *Arabidopsis* AGP epitopes mark the initial cell that gives rise to proto- and metaxylem (Dolan *et al.*, 1995). In roots, stems and leaf stalks of the angiosperm *Echinacea purpurea*, labelling of AGPs is most dominant in the area of the xylem (Bossy *et al.*, 2009; Goellner *et al.*, 2013). The recurrent use of AGPs in water transporting tissues in bryophytes, lycophytes and angiosperms suggest that this function is also conserved in other lineages, including ferns; more data is however needed to support their involvement in development of water-transporting tissues in ferns.

Due to similarities in overall AGP structure, some functions of AGPs might be conserved in bryophytes and tracheophytes. However, differences in fine structure, especially the arabinogalactan moiety, can also cause functional differences. Here we show that *Salvinia*, *Azolla* and *Ceratopteris* reveal high content of Rha and methylated Rha at the periphery of their AGPs. This feature is similar to the structure of AGPs of the bryophytes *Physcomitrium*, *Sphagnum* and *Polytrichastrum* (Fu *et al.*, 2007, Bartels *et al.*, 2017). The cell walls of the streptophyte algae *Spirogyra* contain rhamnogalactan-proteins that are structurally similar to AGPs with nearly complete replacement of Ara by Rha (Pfeifer *et al.*, 2022). Rha and methylated Rha are less polar compared to Ara. This suggests a change from a less hydrophilic AGP surface with Rha and methylated Rha as terminal groups to a more hydrophilic surface dominated by terminal Ara in vascular plants. Given the less hydrophilic features of AGPs in algae, bryophytes and the water ferns it is logical to assume that these AGPs have alternative functions with regard to hydrophobic interactions (Fu *et al.*, 2007). Arabinosylation of existing cell wall polymers has been proposed to be an evolutionary strategy to prevent polymer aggregation during water loss (Moore *et al.*, 2013). If true, one may assume that the challenges of a life on land have selected for more hydrophilic AGPs with higher amounts of Ara, allowing for dessication tolerance in tracheophytes. The modifications observed here for the aquatic ferns may be an adaptation to their reversion to aquatic life.

CONCLUSION

During plant terrestrialization, plants acquired molecular adaptations to cope with the terrestrial environment. Tracheophyte innovations like xylem and stabilised upright stems needed modifications in cell wall composition, either through elaboration of ancestral polymers or through synthesis of new components. Our investigations show that AGPs, which are important cell wall components with signalling functions, are present in the three fern species investigated and their basic molecular features are similar to those known from seed plants.

Phylogenetic analysis of relevant GT31 enzymes confirmed that AGP protein backbones and homologs of the basic enzymes responsible for biosynthesis of the galactan core of AGPs are present in ferns likely underpinning the conservation of AGP structures in tracheophytes. An unusual attribute of the three fern AGPs was the presence of 1,2-linked Araf in high amounts which has also been detected in other leptosporangiate fern AGPs, but not in AGPs from other taxa. Interestingly, fern AGPs share a special feature with moss and also gymnosperm AGPs, the occurrence of terminal 3-*O*-MeRha not present in angiosperms. Identification of enzymes that synthesize AG glycans in non-flowering plants, especially rhamnosyltransferases, is a challenge for the future.

More phylodiverse fern genomes are needed to identify AGP protein backbones and glycosyltransferases involved in polysaccharide biosynthesis and AGP glycosylation in this lineage of tracheophytes. Future studies should also include detailed structural analyses of AGPs from higher numbers of bryophytes and monilophytes. Generation of AGP mutants, e.g. by CRISPR/Cas9 technique, will help to gather new information on AGP functions in the streptophyte lineage. As AGPs are possibly involved in water balance of plants, they might be interesting targets to modulate desiccation tolerance of plants in times of climate change.

EXPERIMENTAL PROCEDURES

Plant material, growth conditions and sampling

The ferns *Salvinia* × *molesta* D. S. MITCHELL (*Salvinia*, *S. molesta*), *Salvinia auriculata* AUBL., *Salvinia cucullata* ROXB., *Salvinia natans* (L.) ALL., *Azolla filiculoides* LAM. (*Azolla*, *A. filiculoides*) and *Ceratopteris richardii* BRONGN. (*Ceratopteris*, *C. richardii*) were cultivated in the greenhouse in the Garden of the Pharmaceutical Institute of the Christian-Albrechts-University of Kiel between August and October 2018 (*Salvinia*), September and January 2019/2020 (*Azolla*) and July and August 2021 (*Ceratopteris*); see Figure 1. Spores of *Ceratopteris* RN3 strain were kind gifts of Péter Szövényi (University of Zurich). For spore germination, gametophyte development and sporophyte culture on C-fern medium, the protocol of Plackett *et al.* (2015) was used. Plant material was cleaned with water and freeze-dried.

Isolation of arabinogalactan-proteins (AGPs)

The freeze-dried and ground plant material was extracted two times (2 h and 21 h) with 70 % acetone solution (V/V) in a ratio of 1:20 (w/V) for *A. filiculoides* and *C. richardii* and in a ratio of 1:30 (w/V) for *S. molesta* under constant stirring at 4 °C to remove phenolic compounds. Afterwards, the air-dried plant residue was extracted with double-distilled water (ddH₂O) in a ratio of 1:20 (w/V) for *A. filiculoides* and *C. richardii* and in a ratio of 1:30 (w/V) for *S. molesta*.

After constant stirring for 21 h at 4 °C, the aqueous extract was separated through a tincture press from the remaining plant material.

The aqueous extract was heated in a water bath at 90 – 95 °C for ten minutes to denature proteins. These proteins were removed by centrifugation (4,122 g, 20 min, 4 °C), and the extract was concentrated with a rotary evaporator at 40 °C and 0,010 mbar to approximately one tenth of its volume. In order to precipitate polysaccharides and AGPs, the aqueous extract was poured into ethanol at 4 °C in a ratio of 1:4 (V/V) and stored overnight at 4 °C. The precipitated material was isolated by centrifugation (19,000 g, 4 °C, 20 min) and freeze-dried (AE).

Following the procedure of Classen *et al.* (2005), AGP was isolated from the AE with the β -Glc-Yariv reagent (β GlcY). After dissolving AE in ddH₂O and β GlcY (1 mg mL⁻¹) in an equal volume of sodium chloride solution (0.3 mol L⁻¹), the AGP was precipitated overnight at 4 °C after addition of the β GlcY solution. The AGP- β GlcY-complex was separated by centrifugation (19,000 g, 4 °C, 20 min) and re-dissolved in ddH₂O. After heating to 50 °C, sodium hydrosulfite was added until the red color disappeared. To purify the aqueous AGP solution, it was dialyzed against demineralized water for four days at 4 °C (MWCO 12 – 14 kDa) and freeze-dried afterwards.

Analysis of monosaccharides

For determination of the neutral monosaccharide composition, a modified method of Blakeney *et al.* (1983) was used. To 1 – 10 mg of sample 1.0 mL trifluoroacetic acid (TFA, 2 mol L⁻¹) and 50 μ L internal standard *myo*-inositol (10 g L⁻¹) were added, incubated for 1 h at 121 °C, washed three times with 5 mL ddH₂O and evaporated. The samples were reduced with 200 μ L ammonium hydroxide (1 mol L⁻¹) and 1.0 mL sodium borohydride in dimethyl sulfoxide (DMSO, 1 g 50 mL⁻¹). After incubation for 1.5 h at 40 °C the reaction was stopped with 100 μ L glacial acetic acid. For the acetylation, 200 μ L of 1-methylimidazole and 2.0 mL of acetic anhydride were added, incubated for 20 min at room temperature and stopped by addition of 10 mL ddH₂O. The samples were acidified with 1.0 mL aqueous sulfuric acid (0.1 mol L⁻¹) and liquid-liquid extraction was performed with an equivalent volume of dichloromethane. The identification and quantification of the neutral monosaccharides was performed by gas chromatography (GC) with flame ionization detection (FID) and mass spectrometry detection (MSD): GC + FID: 7890B; Agilent Technologies, USA; MS: 5977B MSD; Agilent Technologies, USA; column: Optima-225; Macherey-Nagel, Germany; 25 m, 250 μ m, 0.25 μ m; helium flow rate: 1 ml min⁻¹; split ratio 30:1. A temperature gradient was used to achieve peak separation (initial temperature 200 °C, subsequent holding time of 3 min; final temperature

243 °C with a gradient of 2 °C min⁻¹). 3-O-MeRha was identified by retention time and mass spectrum (see Happ and Classen, 2019).

According to a modified method of Blumenkrantz and Asboe-Hansen (1973), the uronic acid (UA) amount was determined photometrically using a linear calibration generated with a mixture of glucuronic and galacturonic acid (1:1, w/w). 200 µL of a 500 µg L⁻¹ sample dissolved in sulphuric acid (4 %, V/V) was mixed with 1.2 mL of sodium tetraborate in sulphuric acid (75 mmol L⁻¹) and incubated at 100 °C in a water bath for 20 min. After cooling for another 10 min on ice, 20 µL of a solution of *meta*-hydroxy-diphenyl (0.15 %, w/V) in NaOH (0.5 %, w/V) was added to the sample. After incubation for 15 min at room temperature, the absorbance was determined at 525 nm. For each sample, a threefold determination was performed and an additional blank sample, containing NaOH (0.5 %, w/V) instead of the color reagent, was subtracted.

Reduction of uronic acids and partial degradation of AGPs

The AGP fraction was first subjected to uronic acid reduction followed by oxalic acid partial hydrolysis. A modified method of Taylor and Conrad (1972) was used to perform a carboxy-reduction of the uronic acids. After dissolving 20 – 30 mg AGP in 20 mL ddH₂O, 216 mg of *N*-cyclohexyl-*N'*-[2-(*N*-methylmorpholino)-ethyl]-carbodiimide-4-toluolsulfonate was added slowly under constant stirring until it was completely dissolved. An autotitrator adjusted the pH to 4.75 with 0.01 M HCl and maintained it for another 2 h. The uronic acids were then reduced by the dropwise addition of sodium borodeuteride solutions in increasing concentrations (2.0 mL of 1 mol L⁻¹; 2.5 mL of 2 mol L⁻¹; 2.5 mL of 4 mol L⁻¹). To avoid strong foaming during the reaction, one to two drops of 1-octanol were added beforehand. In addition, the pH value was set to 7.00 with 2 M HCl by an autotitrator and also maintained for another 2 h after the reduction agent was fully added. Finally, the pH was adjusted to 6.5 with glacial acetic acid, the solution was dialysed for three days at 4 °C against demineralized water (MWCO 12 – 14 kDa) and freeze-dried.

For the oxalic acid hydrolysis, a modified method of Gleeson and Clarke (1979) was used. 10 – 15 mg of the uronic acid reduced sample was dissolved in 2.0 mL of oxalic acid (12.5 mmol L⁻¹) and incubated for 5 h at 100 °C. After cooling to room temperature, the hydrolysate was precipitated in ethanol at a final concentration of 80 % (V/V). The precipitate was separated by centrifugation (19,000 g, 10 min, 4 °C), washed twice with 80 % ethanol (V/V), dissolved in 2 mL ddH₂O and freeze-dried.

Structural characterization of arabinogalactan moiety of the AGP

Structure elucidation of AGPs was performed by a modified method according to Harris *et al.* (1984) with potassium methylsulfinyl carbanion (KCA) and iodomethane (IM) in DMSO. The sample (1-5 mg freeze-dried AGP) was treated stepwise with the KCA and IM (1. 100 μ L KCA for 10 min; 2. 80 μ L IM for 5 min; 3. 200 μ L KCA for 30 min; 4. 150 μ L IM for 30 min; 5. 500 μ L KCA for 30 min; 6. 400 μ L IM for 60 min). The permethylated sample was dissolved in 3.0 mL dichloromethane/methanol in a ratio of 2:1 (V/V), washed three times with 2.0 mL water and centrifuged (5 min, 2,500 g). 2.0 mL 2,2-dimethoxy propane and 20 μ L glacial acid were added to the sample, heated to 90 °C and dried under a stream of nitrogen. The samples were hydrolyzed with trifluoroacetic acid (2.0 mol L⁻¹) at 121 °C for 1 h, mixed with 2.0 mL water and freeze-dried. Afterwards, the partially methylated monosaccharides were reduced by addition of sodium-borohydride (0.5 mol L⁻¹), dissolved in ammonium hydroxide (2.0 mol L⁻¹), incubated at 60 °C for 1 h, and the reaction stopped by 0.5 mL acetone. Acetylation was performed by addition of 200 μ L glacial acid, 1.0 mL ethyl acetate, 3.0 mL acetic anhydride and 100 μ L perchloric acid and stopped by demineralized water and 100 μ L 1-methylimidazole. The permethylated alditol acetates were extracted with dichloromethane and separated and detected by GLC-mass spectroscopy as described above (instrumentation see above: "Analysis of monosaccharides"; column: Optima-1701, 25 m, 250 μ m, 0.25 μ m; helium flow rate: 1 mL min⁻¹; initial temperature: 170 °C; hold time 2 min; rate 1 °C min⁻¹ until 210 °C was reached; rate: 30 °C min⁻¹ until 250 °C was reached; final hold time 10 min).

Principal Component Analysis (PCA)

Based on the resulting biochemical data of the methylation analyses, a PCA was performed with the mean values after standardization by using SigmaPlot (build 14.5.0.101) with default settings. The proportion of the terminal rhamnose (unmethylated) to the terminal 3-*O*-Me-Rha was calculated from the compositional data of the acetylation analyses. See Figure 1 for full plant names and phylogenetic position as well as Figure 3 for references.

Determination of the protein moiety and the hydroxyproline content

According to the method of Kjeldahl (1883), the protein content was calculated from the nitrogen content (factor 6.25). The nitrogen content was measured by elemental analysis in the Chemistry Department of CAU Kiel University, Kiel, Germany (HEKAtech CHNS Analyzer). For the quantification of hydroxyproline (Hyp), the methodology of Stegemann and Stalder, 1967 was used with slight modifications. AGPs (10 mg mL⁻¹) were hydrolyzed in a 6 M HCl solution at 110 °C for 22 h. After cooling to room temperature, the hydrolysate was centrifuged

at 25,000 g for 10 min. 160 μ L of the supernatant were diluted with 3840 μ L ddH₂O and 0.6 mL of this dilution was measured in triplicate, as well as a blank value. The blank value was mixed with 0.3 mL of oxidation buffer (pH 6.8; 2.6 g citric acid monohydrate; 7.8 g sodium acetate anhydrous; 1.4 g sodium hydroxide; 25 mL 1-propanol filled to 100 mL ddH₂O) and the samples with 0.3 mL of an oxidating solution (210 mg chloramine T in 15 mL oxidation buffer pH 6.8) and incubated for 20 min at room temperature in the dark. After addition of 0.3 mL colour reagent (1.5 g 4-dimethylaminobenzaldehyde; 5.25 mL perchloric acid, 60 % (V/V); 9.25 mL 2-propanol) to all samples, they were incubated for 15 min in a water bath at 60 °C. After cooling under running tap water for 3 minutes, incubation followed for 30 min at room temperature, before the absorbance was measured at 558 nm with an UV/Vis-spectrophotometer. To determine the hydroxyproline content, a linear regression analysis was performed, using 4-hydroxy-L-proline as a standard.

Indirect Enzyme-linked immunosorbent assay (ELISA)

96-well plates were coated with 100 μ l per well of the sample in the concentrations 12.5 μ g mL⁻¹, 25 μ g mL⁻¹ and 50 μ g mL⁻¹ in ddH₂O and incubated at 37.5 °C for 3 days with open cover. After washing the plates three times with 100 μ l phosphate buffered saline (PBS)-T (pH 7.4, 0.05 % Tween® 20) per well, they were blocked with 200 μ l of BSA (bovine serum albumin, 1 % (w/V)) in PBS per well and incubated again at 37.5 °C for 1 h. The plates were again washed three times with 100 μ l of PBS-T per well. After addition of 100 μ l primary antibody solution (JIM13, KM1, LM2, LM6, LM10, LM15, LM19, LM20, LM25) per well in 1:20 (V/V) PBS 7.4 dilution, the plates were incubated for 1 h at 37.5 °C and washed again three times with 100 μ l PBS-T per well. This was repeated with the secondary antibody (anti-mouse-IgG (KM1) or anti-rat-IgG (others) conjugated with alkaline phosphatase, produced in goat, Sigma-Aldrich Chemie GmbH, Taufkirchen, Germany) in a dilution of 1:500 (V/V) in PBS 7.4. Finally, 100 μ l of the substrate *p*-nitro-phenylphosphate was added per well and the plates were incubated in the dark at room temperature. The absorbance was measured at 405 nm with a plate reader after ten minutes. The samples were analyzed in triplicate. For visualization, the absorbance of the control was set 0 and the highest signal in the dataset was set 1.0. Epitopes of the antibodies and key references are listed in Table S6.

Gel diffusion assay

In an agarose gel (Tris-HCl, 10 mmol L⁻¹; CaCl₂, 1 mmol L⁻¹; NaCl, 0.9 % w/V; agarose, 1 % w/V), several cavities were stamped. The cavities in the first row were filled with dilutions (100 mg mL⁻¹) of each sample and one of them with the positive control, AGP from *Echinacea*

purpurea (10 mg mL⁻¹). In the second line, the cavities were filled with the β GlcY solution (1 mg mL⁻¹). After incubation in the dark at room temperature for 22 h, a red precipitation line appears if the sample contains AGPs.

Phylogenetic analysis of glycosyltransferase family 31 (GT31)

Putative GT31 homologs of ferns were identified by using the BLASTp interface (E-value of 0.01) at the 1KP database (Carpenter *et al.*, 2019; Leebens-Mack *et al.*, 2019) webserver as well as blasting the translated genomes of *A. filiculoides* (v1.1), *C. richardii* (v2.1) and *S. cucullata* (v1.2) (Table S7). AGP-relevant GT31 protein sequences from group A and B of *A. thaliana* were used as query sequences against all accessible leptosporangiate and eusporangiate ferns (accessed at June, 23rd, 2022). The resulting candidate sequences as well as the query sequences were aligned with L-INS-I using MAFFT (version 7.490; Katoh and Standley, 2013). All sequences with a minimum of 200aa were included in the dataset. the phylogenetic tree was constructed by using IQ-Tree using model JTT+I+G4 identified by model finder in-built in IQ-TREE (multicore version 1.5.5 ; Letunic and Bork, 2021). 100 bootstrap replicates were performed.

AGP backbone sequence identification and classification

The annotated protein sequences from the ferns *A. filiculoides* (v1.1), *Adiantum capillus-veneris*, *Alsophila spinulosa* (version 5), *C. richardii* (v2.1), *S. cucullata* (v1.2) were downloaded from the respective web resources (Table S7) and imported into the R environment. By using the R-package “ragp” (Dragićević *et al.*, 2020), the N-terminal signal sequences were identified and the maab-

pipeline (Johnson *et al.*, 2017b) as implemented in the R-package was used to classify the proteins based on their motifs and amino acid biases. All small (< 90 amino acids), highly similar (≥ 0.95 similarity) and chimeric sequences (containing any Pfam domain, E-value < 1e-5) were excluded from the classification. To differentiate the classes 1 and 4 the bigPI algorithm (Eisenhaber *et al.*, 2003) was used to predict GPI-anchor signals.

Chimeric AGP sequences were identified by detecting (STAGV)P by using the implementation in the “ragp”-package with the strict mode (at least four dipeptided in a maximal distance of four amino acids) used by Paunović *et al.* (2021). All dipeptides in an annotated pfam domain (by querying the Pfam database *via* the CDD webtool, Lu *et al.*, 2020) or in the signal sequence were not count. The candidate sequences were length-filtered (≥ 90 amino acids) and highly-similar sequences (> 0.95 similarity) were discarded.

For each translated genome, the chimeric AGPs were grouped by their largest domain and the number of sequences was plotted as bars in Figure S5. An analysis for common domains in the different ferns was performed and visualized by an UpSet plot (Lex *et al.*, 2014) with the R-package “UpSetR” (Conway *et al.*, 2017).

ACKNOWLEDGEMENTS

Funding: LP and BC (project-number 440046237; CL448/3-1), JdV (project-number 440231723; VR132/4-1), and PSZ (project-number 440370236; PSLJ1111/1) are grateful for funding within the framework of MAdLand (<http://madland.science>), priority programme 2237 of the German Research Foundation (DFG). JdV further thanks the European Research Council for funding under the European Union’s Horizon 2020 research and innovation programme (Grant Agreement No. 852725; ERC-StG “TerreStriAL”). Additional funding was received from the Swiss National Science Foundation (grant nos. 160004, 184826, and 212509 to PS); project funding through the University Research Priority Program “Evolution in Action” of the University of Zurich to PS; a Georges and Antoine Claraz Foundation grant to PS.

AUTHORS CONTRIBUTIONS and CONFLICT OF INTEREST

BC and LP planned and designed the research. KM, LP and LS cultivated the plant material, in case of *Ceratopteris* from spores delivered by PS. KM, LP and LS performed the extractions as well as carbohydrate and ELISA experiments. LP, SdV, JdV and KJ performed bioinformatic searches. LP created all main text figures. All authors analysed the data (BC, KM, LS and LP: carbohydrate analysis; LP, SdV and JdV: bioinformatics search for glycosyltransferases; LP and KJ: bioinformatics search for AGP protein backbones). BC wrote the draft manuscript with help of KM and LP; all authors revised the manuscript, read and approved the final manuscript. The authors declare that they have no competing interests.

DATA AVAILABILITY STATEMENT

All relevant experimental data can be found within the manuscript and its supporting materials. Datasets for bioinformatic analyses can be found here:
<https://figshare.com/s/50d87902e1fba3ad98c2>

SUPPORTING INFORMATION

Table S1. Yields of water-soluble polysaccharides (AE) from *S. molesta*, *A. filiculoides*, and *C. richardii* in % of dry plant material (w w⁻¹).

Yields	<i>S. molesta</i>	<i>A. filiculoides</i>	<i>C. richardii</i>
AE	4.5	5.6	3.4

Table S2. Neutral monosaccharide composition of water-soluble polysaccharides (AE) from *A. filiculoides*, *S. molesta* and *C. richardii* in % (mol mol⁻¹).

Neutral monosaccharide	<i>S. molesta</i> AE (n=9)	<i>A. filiculoides</i> AE (n=3)	<i>C. richardii</i> AE (n=3)
3- <i>O</i> -Me-Rha	2.6 ± 0.2	tr	3.0 ± 0.3
Rha	4.2 ± 0.3	5.1 ± 0.1	1.9 ± 0.1
Fuc	2.2 ± 0.2	6.5 ± 0.1	2.9 ± 0.1
Rib	2.6 ± 1.0	tr	1.2 ± 0.2
Ara	30.5 ± 2.8	10.8 ± 0.6	19.8 ± 0.6
Xyl	5.4 ± 1.1	23.5 ± 1.5	22.6 ± 0.8
Man	6.8 ± 0.5	12.3 ± 1.0	9.0 ± 1.5
Gal	25.8 ± 1.8	21.7 ± 0.3	23.7 ± 1.5
Glc	19.9 ± 1.8	20.1 ± 1.1	15.9 ± 1.9

tr: trace value < 1 %

Table S3. Colorimetric determination of the content of uronic acids in the water-soluble polysaccharides (AE) from *S. molesta*, *A. filiculoides* and *C. richardii* in % (w w⁻¹).

Uronic acids	<i>S. molesta</i>	<i>A. filiculoides</i>	<i>C. richardii</i>
AE	1.8 ± 0.2	8.4 ± 0.3	4.4 ± 0.1

Table S4. Neutral monosaccharide composition of AGPs and partially hydrolysed AGPs_{UrOx} from *S. molesta*, *A. filiculoides* and *C. richardii* in % (mol mol⁻¹).

Neutral monosaccharide	<i>S. molesta</i>		<i>A. filiculoides</i>		<i>C. richardii</i>	
	AGP (n=5)	AGP _{UrOx} (n=1)	AGP (n=3)	AGP _{UrOx} (n=1)	AGP (n=3)	AGP _{UrOx} (n=1)
3- <i>O</i> -Me-Rha	4.5 ± 0.3	2.9	tr	tr	8.3 ± 0.7	5.7
Rha	4.3 ± 0.1	2.1	9.2 ± 0.2	6.1	tr	tr
Fuc	1.7 ± 0.2	tr	1.9 ± 0.0	tr	2.8 ± 0.2	tr
Ara	35.2 ± 2.1	10.0	29.1 ± 0.5	14.7	32.3 ± 1.0	8.0
Xyl	1.2 ± 0.2	tr	1.7 ± 0.1	1.1	tr	-
Man	2.4 ± 0.4	1.7	3.8 ± 0.1	2.6	tr	tr
Gal	45.7 ± 2.6	75.6	51.7 ± 0.5	70.4	51.6 ± 1.7	75.9
Glc	5.0 ± 0.5	7.7	2.6 ± 0.6	5.1	5.0 ± 0.3	10.4
Ara : Gal	1 : 1.3 ± 0.2	1 : 7.6	1 : 1.8 ± 0.0	1 : 4.8	1 : 1.6 ± 0.1	1 : 9.5

tr: trace value < 1 %

Table S5. Galactosyltransferase sequences of family GT31 present in genomes (*Azolla*, *Salvinia*, *Ceratopteris*) compared to transcriptomes of other ferns

		Number of species included	Clade I + II* CAGE GALT8 GALT31 A UPEX1	Clade III* HPG T 1-3	Clade IV* GALT9	Clade V* GALT1 GALT3	Clade VI* GALT2 GALT4-6
Genomes							
	<i>Arabidopsis thaliana</i>	1	8	3	3	2	4
	<i>Azolla filiculoides</i>	1	8	3	2	1	3
	<i>Salvinia cucullata</i>	1	6	1	2	1	2
	<i>Ceratopteris richardii</i>	1	10	2	1	1	3
Transcriptomes							
Leptosporangiates							
Polypodiales	Aspleniaceae	2	8	1	2	1	2
	Athyriaceae	4	23	4	4	3	2
	Blechnaceae	1	4	1	1	1	2
	Cystopteridaceae	5	27	7	6	7	12
	Davalliaceae	1	4	0	1	0	4
	Dennstaedtiaceae	1	4	1	1	1	2
	Diplazipsidaceae	1	2	1	1	2	1
	Dryopteridaceae	1	6	1	1	1	2
	Elaphoglossaceae	1	3	1	1	0	0
	Hypodematiaceae	2	8	1	1	1	2
	Lindsaeaceae	3	19	3	3	3	4
	Lomariopsidaceae	1	5	0	2	1	3
	Lonchitidaceae	1	2	1	1	2	2
	Onocleaceae	1	2	1	0	1	1
	Polypodiaceae	6	36	8	7	8	14
	Pteridaceae	14	89	15	15	12	29
	Thelypteridaceae	1	4	1	1	1	0
	Woodsiaceae	2	12	2	0	2	2
Cyatheales	Culcitaceae	1	3	0	0	2	1
	Cyatheaceae	1	0	1	0	0	1
	Thyrsopteridaceae	1	4	1	0	2	1
Plagiogyriales	Plagiogyriaceae	1	3	1	0	1	0
Salviniales	Marsileaceae	1	5	2	1	2	1
	Salvinaceae	1	6	2	1	0	2
Schizeales	Anemiaceae	1	3	0	1	1	2
	Lygodiaceae	1	2	1	1	0	2
Gleicheniales	Dipteridaceae	1	3	1	1	1	1
Hymenophyllales	Hymenophyllaceae	3	1	0	1	0	1
Osmundales	Osmundaceae	4	6	5	3	2	6
Eusporangiates							
Marattiales	Marattiaceae	4	7	5	2	3	8
Equisetales	Equisetaceae	2	4	4	2	2	4
Psilotales	Psilotaceae	2	4	3	1	0	0
Ophioglossales	Ophioglossaceae	4	7	1	0	1	4

* according to Qu *et al.* (2008)

Table S6. Antibodies tested for binding to fern cell wall AGPs

Antibody	Epitope	Key References
JIM13	AGP glycan, e.g. β -D-GlcAp-(1 \rightarrow 3)- α -D-GalAp-(1 \rightarrow 2)- α -L-Rha	Pfeifer <i>et al.</i> (2022); Yates <i>et al.</i> (1996)
KM1	(1 \rightarrow 6)- β -D-Galp units in AGs type II	Classen <i>et al.</i> (2004); Ruprecht <i>et al.</i> (2017)
LM2	(1 \rightarrow 6)- β -D-Galp units with terminal β -D-GlcAp in AGP	Ruprecht <i>et al.</i> (2017); Smallwood <i>et al.</i> (1996)
LM6	(1 \rightarrow 5)- α -l-Araf oligomers in arabinan or AGP	Verhertbruggen <i>et al.</i> (2009a)

Table S7. Accessed resources for the analysis of translated fern genomes.

Plant species	Genome version	Resource
<i>Adiantum capillus-veneris</i>	version 1 (accessed October 6 th , 2022)	https://figshare.com/s/47be9fe90124b22d3c0e
<i>Alsophila spinulosa</i>	version 5	https://figshare.com/articles/dataset/A_spinulosa_genome_rar/19075346/5
<i>Azolla filiculoides</i>	version 1.1	https://feribase.org/
<i>Ceratopteris richardii</i>	version 2.1	https://phytozome-next.jgi.doe.gov/
<i>Salvinia cucullata</i>	version 1.2	https://feribase.org/

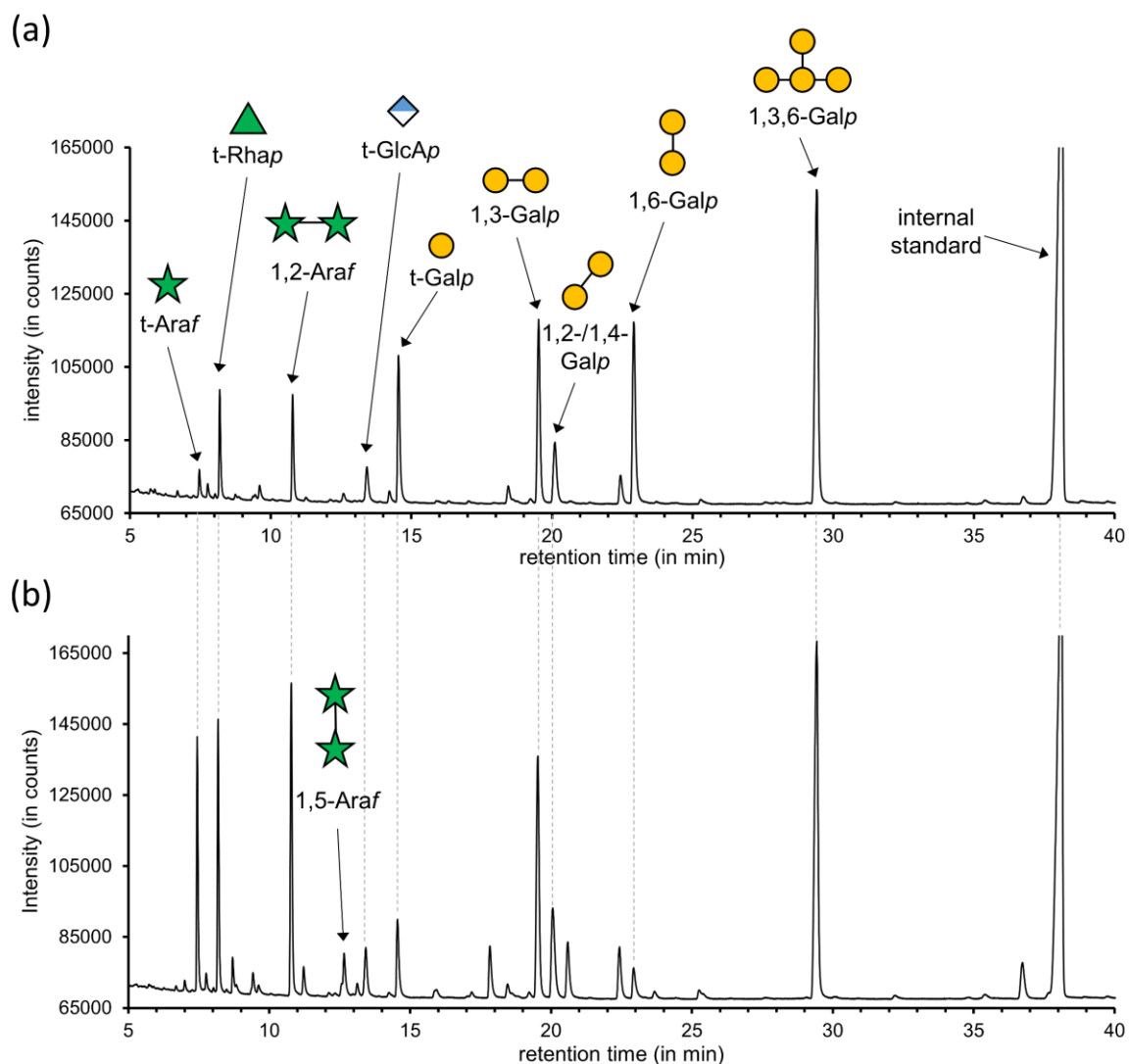


Figure S1. FID chromatograms of *Salvinia* AGPs after GLC analysis. (a) Partially methylated alditol acetates (PMAAs) of the oxalic acid degraded *Salvinia* AGP_{Uro} (see also Figure 2) in direct comparison to the native sample (b) AGP_{Ur}. The relevant linkage-types are highlighted by schematic representations.

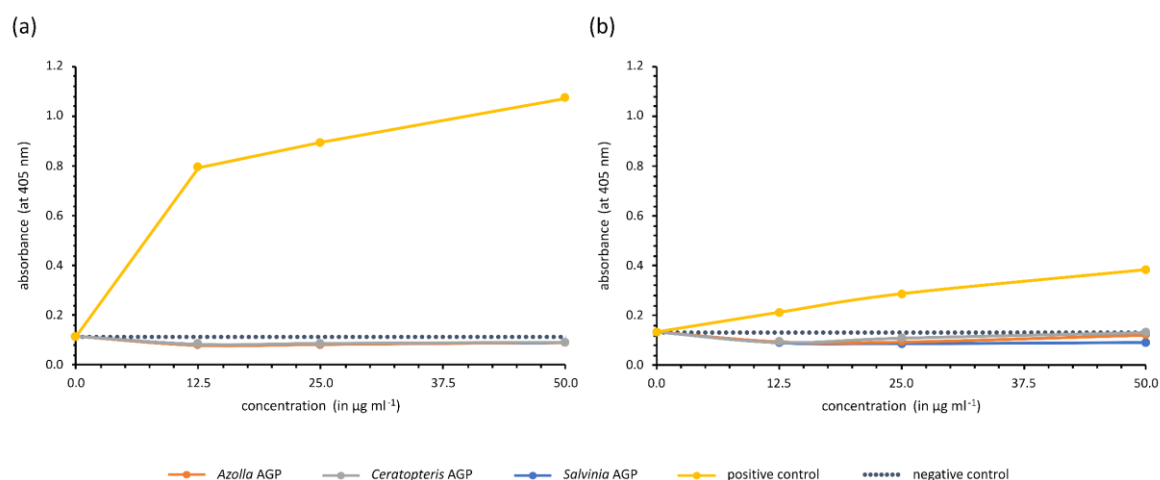


Figure S2. Results of ELISA experiments with fern AGPs in comparison to the positive control *Echinacea purpurea* AGP. (a) Binding of monoclonal antibody KM1 (b) Binding of monoclonal antibody LM6.

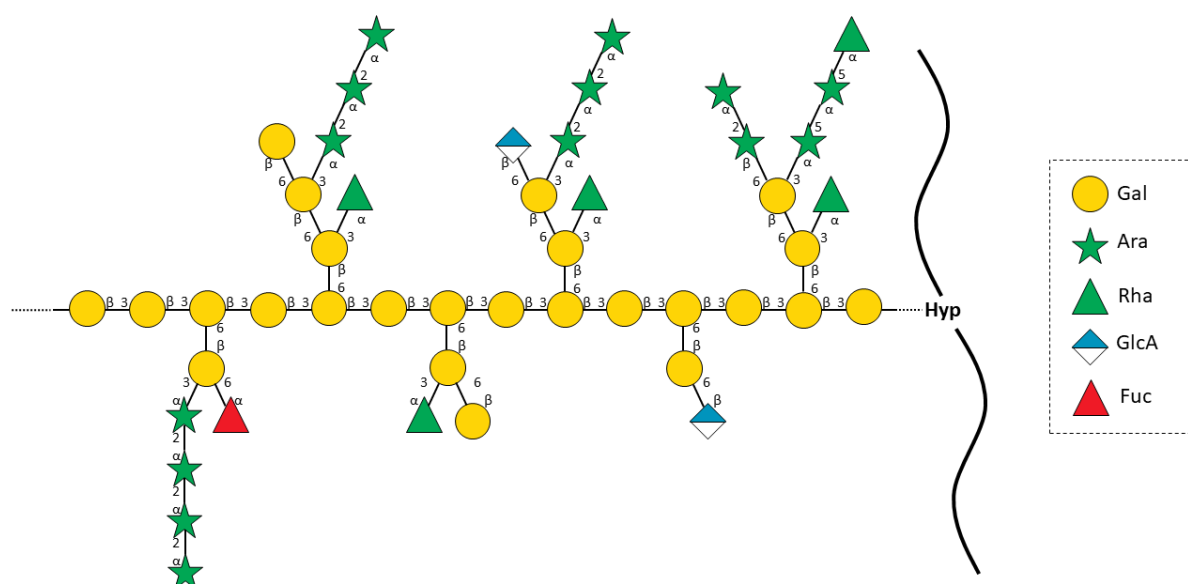


Figure S3. Proposed structure for the carbohydrate moiety of AGPs from *Azolla filiculoides*. The proposal was derived from the compositional, immunocytochemical, and linkage-type analyses of AGP and hydrolysed AGPs.

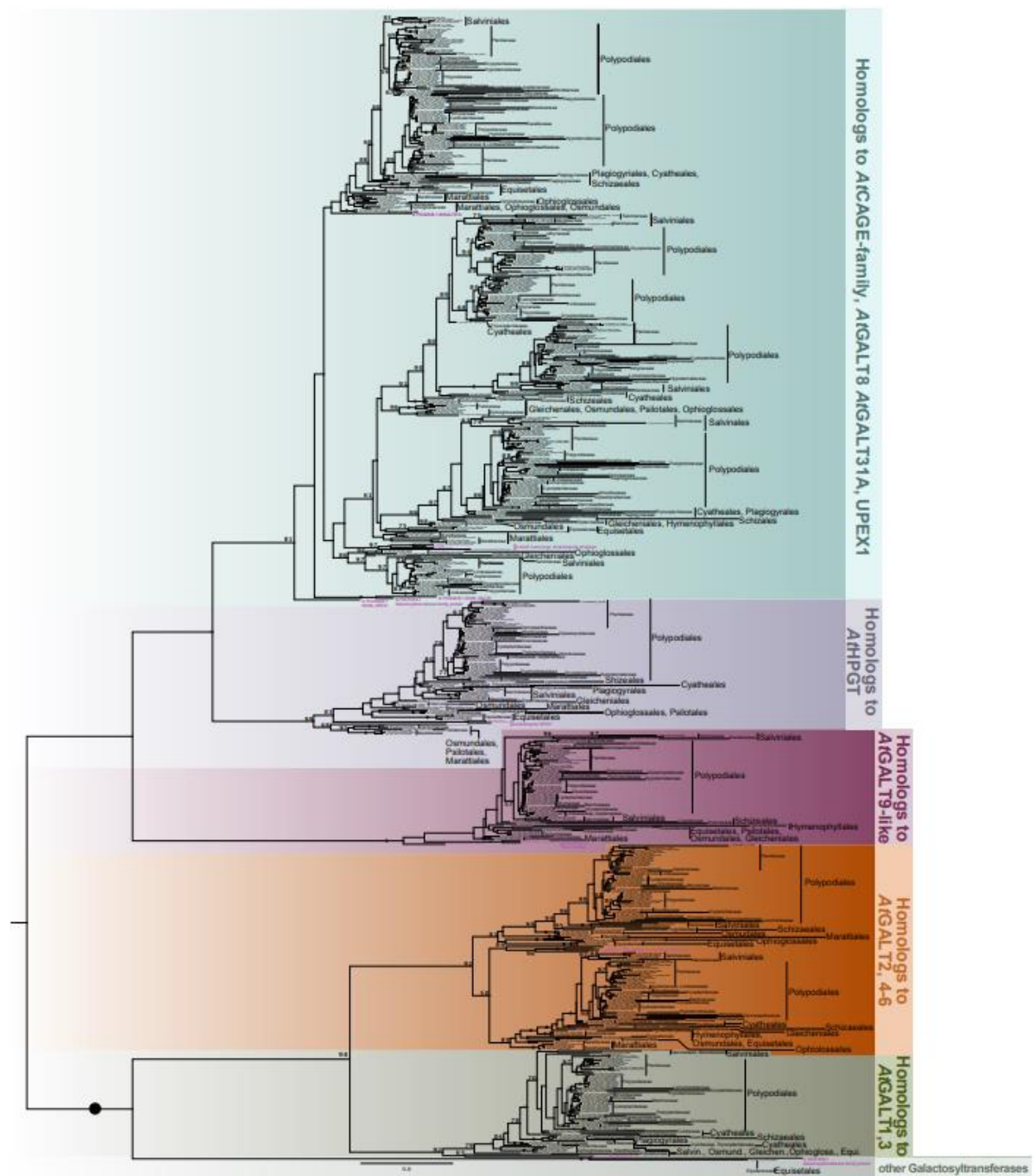
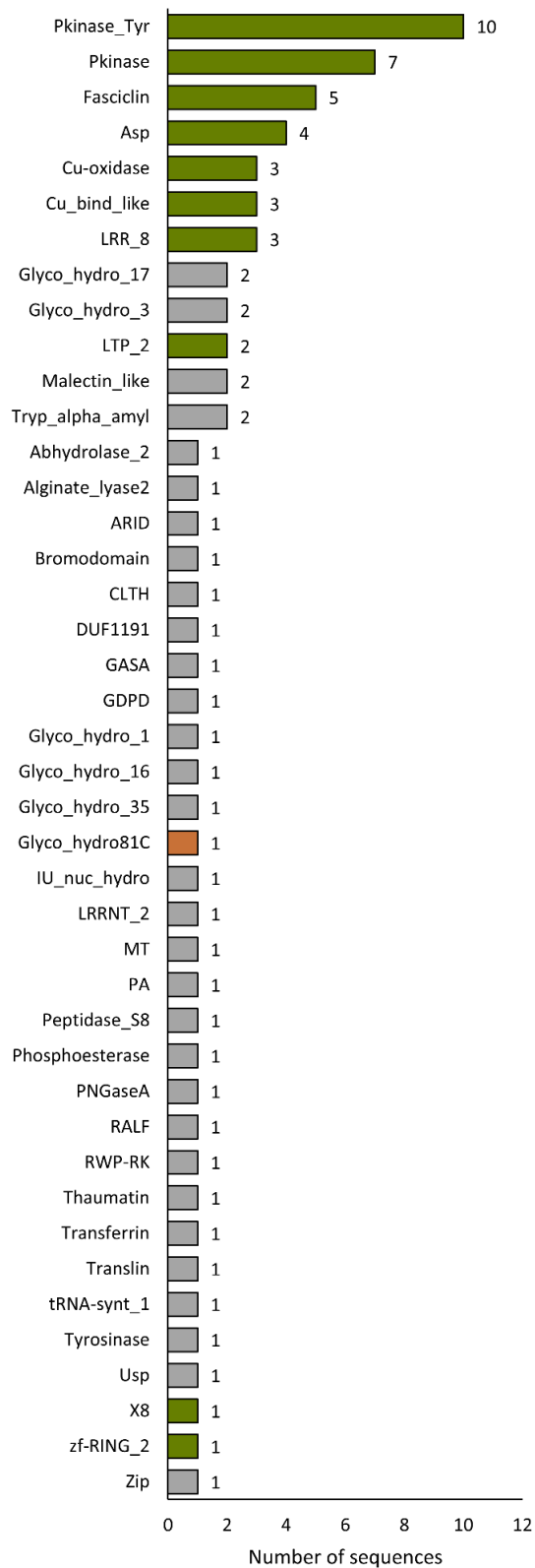
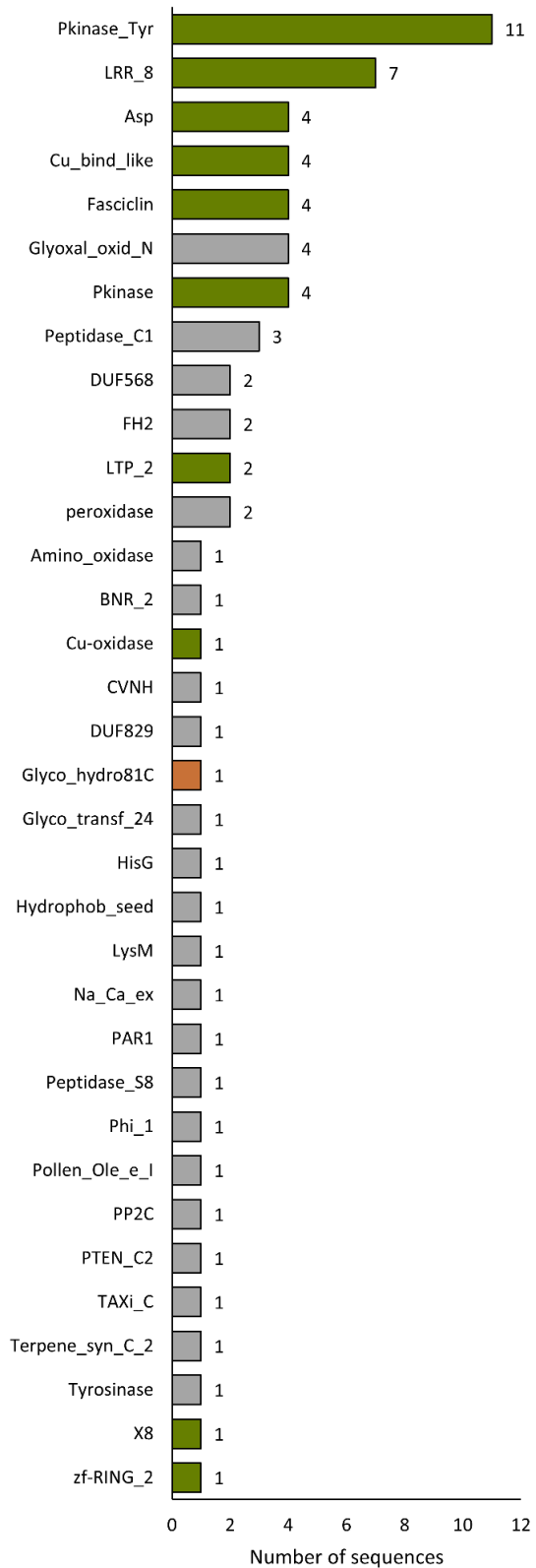


Figure S4. Phylogeny of GT31 enzymes throughout the different groups of ferns. The phylogeny was built using the model JTT+I+G4 and 100 bootstrap replicates. Bootstrap values ≤ 50 are not shown. Bootstrap values of 100 are indicated by black circles. Fern families and orders are indicated next to the phylogeny; here multiple accessions belonged to the same family or genus are group by lines. Solid lines indicate phylogenetically supported clades and dashed lines indicate that the accessions belonging to the same taxonomic association do either not group in a clade or that this clade has no phylogenetic support. *Arabidopsis thaliana* sequences are indicated in bold and purple. The phylogeny is midpoint rooted.

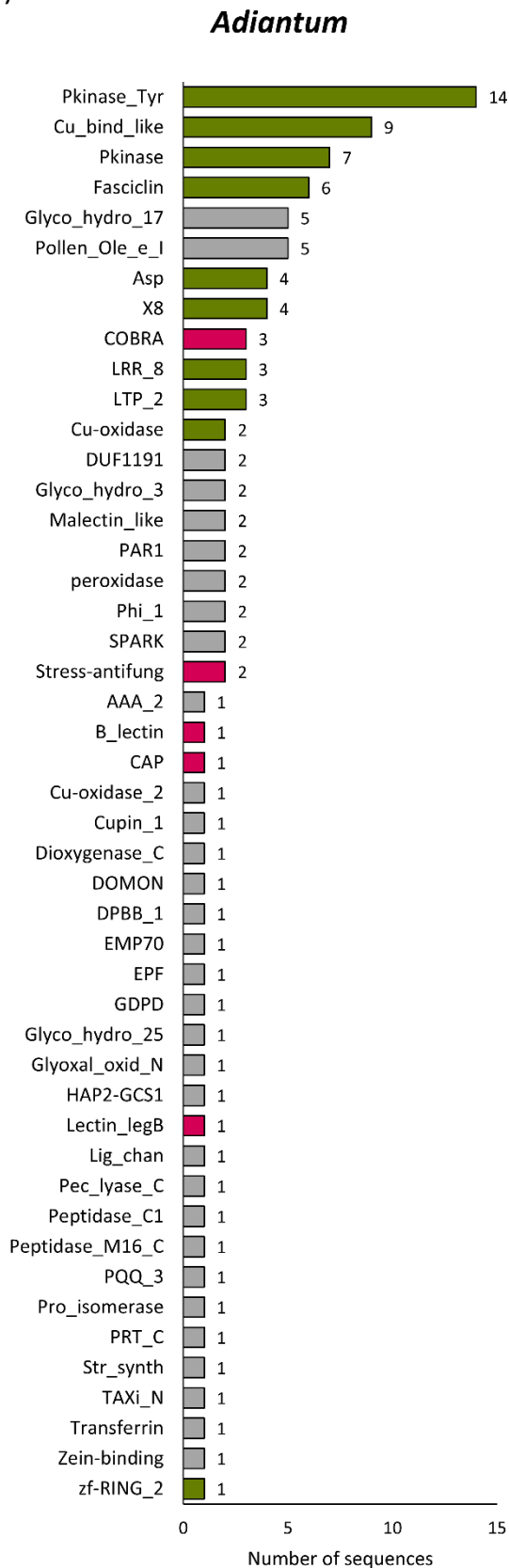
(a)

Azolla

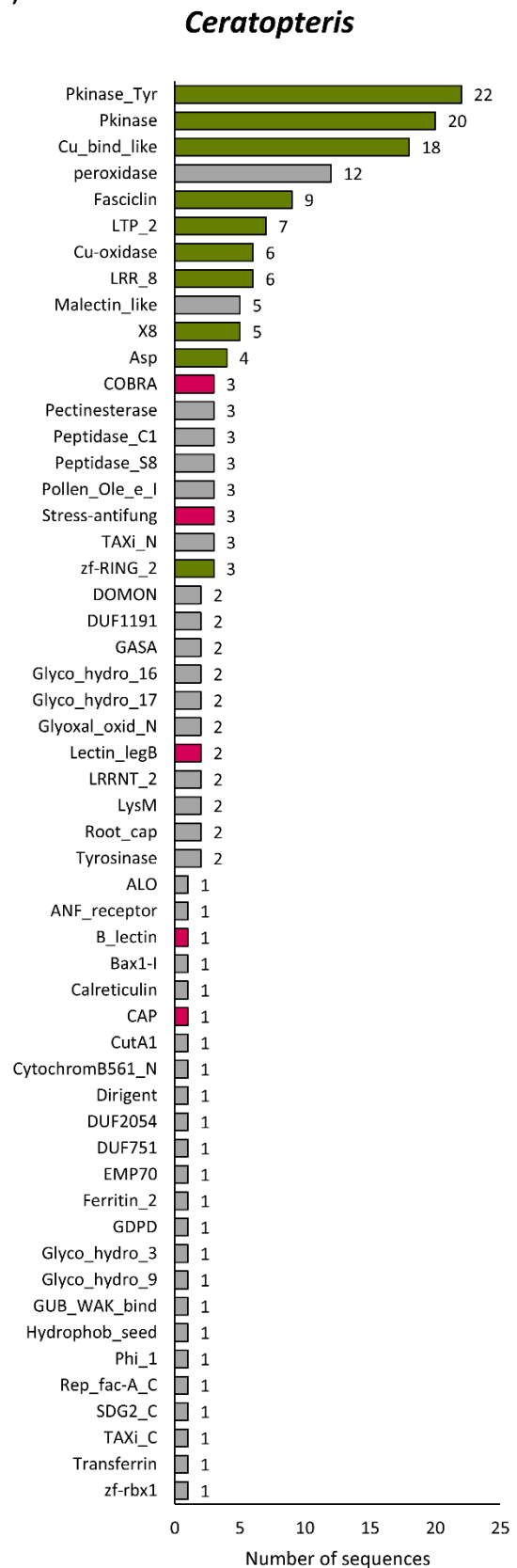
(b)

Salvinia

(c)



(d)



(e)

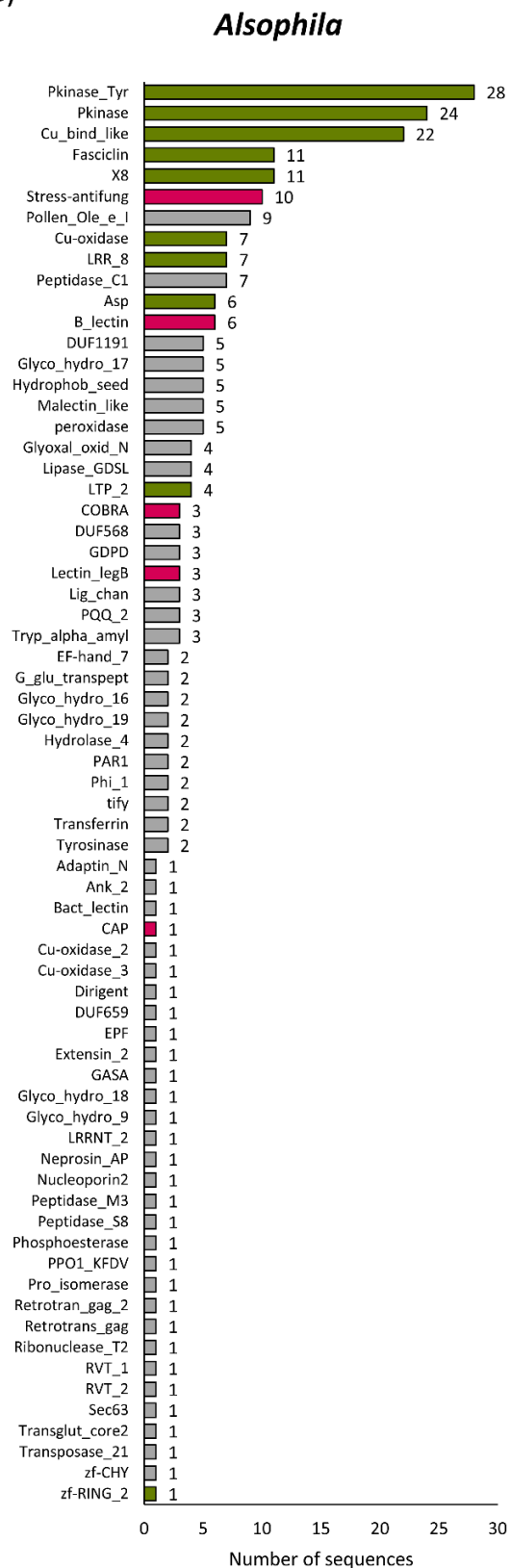


Figure S5: Chimeric AGPs of all investigated fern genomes ranked by decreasing numbers. If multiple domains occur in one protein sequence, the longest was counted. The color code of Figure 5 was used for common domains. (a) *Azolla*, (b) *Salvinia*, (c) *Adiantum*, (d) *Ceratopteris*, (e) *Alsophila*.

Discussion, Conclusion and Outlook

The cell wall of plants is a highly dynamic and complex construct with essential functions for survival. Over millions of years, during evolution, the cell wall had to adapt to different environmental conditions and was therefore subject to constant change. These adaptations were most extreme when the latest common ancestor of all land plants colonised the land from a freshwater habitat.

The main components of the cell wall, the polysaccharides cellulose, pectins and hemicelluloses, as well as cell wall glycoproteins, could be found in the cell walls of individuals all over the *green lineage*. However, there were differences in the quantity and in the fine structure of these molecules. The components within the members of the streptophytes are summarized in Table 1.

Cell wall composition in the streptophyte lineage

Cellulose, the most abundant polysaccharide in the plant cell wall, and callose, the polysaccharide involved in wound healing, have been shown to be conserved.

Hemicelluloses primarily provide stabilisation of the cell wall. Different types of these were identified in the clades of the streptophytes. Mannans are present in cell walls of lycophytes and eusporangiate ferns as well as in those of liverworts and mosses (Popper & Fry, 2004). Hornwort cell walls probably contain lower contents of mannans, which has to be verified by analysing further hornwort species. Glucans, like mixed-linkage glucans (MLG) with a (1→3),(1→4)-β-D-Glcp structure, had only been found in the order Poales as well as in species of the genus *Equisetum* and in the green algae *Micrasterias* (Popper & Fry, 2004; Eder *et al.*, 2008; Sørensen *et al.*, 2008). A glucan with a similar structure, but with (1→3)-Araf residues instead of (1→3)-Glcp, was detected in the moss *Physcomitrium* (Roberts *et al.*, 2018). Genes that could synthesise this unusual arabinoglucan were also identified in hornworts and liverworts by bioinformatic search (Roberts *et al.*, 2018), so further investigations are needed in the future to clarify the presence of this glucan in the other bryophyte clades. The occurrence of xylans was also confirmed in cell walls of the whole *green lineage*, except for those of liverworts. In addition, it should be taken into account that the detection of xylans in the cell walls from streptophyte algae and hornworts was only performed by immunocytochemistry, which should be verified by isolation studies in the future. In contrast, glucuronoxylans were found in the moss *Physcomitrium* and in the lycophyte *Selaginella*, which lack some side chain types of these xylans from gymnosperms and angiosperms (Kulkarni *et al.*, 2012). The xyloglucans of the most streptophytes feature a XXXG pattern, which first occurred in land plants in cell walls of hornworts. While liverworts possessed a XXGG pattern, also common in

Lamiids, and mosses a XXGGG type known from grasses, lycophytes contain both XXXG and XXGG motifs (for detailed review, see Peña *et al.*, 2008). Furthermore, xyloglucans of several KCM and ZCC members were investigated, which also contained the XXXG pattern, which raises the question of whether this structure is conserved or reappeared during the evolution of xyloglucans (Mikkelsen *et al.*, 2021).

Pectins, which can be subdivided into homogalacturonan (HG), rhamnogalacturonan-I (RG-I), and rhamnogalacturonan-II (RG-II), were differently represented in the *green lineage*. While HG and RG-I could be detected mostly by immunocytochemistry, the presence of RG-II in streptophyte algae and especially in bryophytes is still uncertain. The determination of RG-II from cell walls of bryophytes was based only by analysis of the boron content, which is involved in the ester cross-linking of RG-II. This showed a boron content of 1 % of the boron content isolated from cell walls of angiosperms (Matsunaga *et al.*, 2004). Bioinformatic search for RG-I backbone synthesising genes revealed four genes in *Arabidopsis thaliana* encoding RG-I rhamnosyltransferases (AtRRTs), which belong to the glycosyltransferases (GT) family 106 (Takenaka *et al.*, 2018). However, only one homologous gene was found in the streptophyte alga *Klebsormidium flaccidum* and in the bryophytes *Marchantia polymorpha* and *Physcomitrium patens* as well as two in *Selaginella moellendorffii* (Takenaka *et al.*, 2018; Wachananawat *et al.*, 2020). Another enzyme, which is involved in biosynthesis of the RG-I backbones, is the galacturonosyltransferase RGGAT1, belonging to the GT116 family. This family is phylogenetically part of the galacturonosyltransferase (GAUT) family, which is responsible for HG synthesis (Amos *et al.*, 2022). In this study, presence of homologous genes to RGGAT1 could be shown in two bryophyte members as well as one lycophyte and one fern, but is still unknown in streptophyte algae.

To summarise, there are generally only hints for the presence of RG-I in cell walls of streptophyte algae as well as RG-I and RG-II in those of bryophytes. Up to now, no RG-I and RG-II have been isolated from cell walls of streptophyte algae and bryophytes, so this will be a task for future research. In addition, a new monoclonal antibody raised against angiosperm RG-II was developed (Zhou *et al.*, 2018), which should be tested on cell walls of streptophyte algae and bryophytes. At least, further bioinformatic search for genes involved in the synthesis of RG-I and RG-II in genomes of streptophyte algae as well as spore-producing land plants will provide further insights into the presence or absence of these polysaccharides in cell walls of these plants. The ARAD genes, members of the GT47 family, which are involved in the biosynthesis of the α -1,5-L-arabinan side chains of RG-I in *Arabidopsis*, show also potential for this purpose (Harholt *et al.*, 2006).

Lignins are abundant in secondary cell walls and sclerenchyma tissues of tracheophytes and consist of different monolignols in varying quantities. The streptophyte algae and bryophytes are not vascularised and therefore do not contain lignins. However, some monolignols have been detected in bryophytes and also some phenylpropanoid biosynthesis genes in streptophyte algae and the bryophytes *Marchantia* and *Physcomitrium* (see the review of Pfeifer *et al.*, 2022).

Table 1. Summary of cell wall components throughout the streptophyte lineage.

Cell wall component	Streptophyte algae	Hornworts	Liverworts	Mosses	Lycophytes	Eusporangiate ferns	Leptosporangiate ferns	Gymnosperms	Angiosperms	comments
Cellulose	✓	✓	✓	✓	✓	✓	✓	✓	✓	
Mannan	✓	✓	✓	✓	✓	✓	✓	✓	✓	
MLG	(✓) ¹	×	×	(✓) ²	×	(✓) ³	×	×	✓ ⁴	Only detected in the green alga <i>Micrasterias denticulata</i> ¹ , <i>Equisetum</i> species ³ and within the order Poales ⁴ ; in <i>P. patens</i> a MLG like arabinoglucan was identified ²
Xylan	✓	✓	×	✓ ⁵	✓ ⁵	✓	✓	✓	✓	Based only on antibody detection in streptophyte algae and hornworts; modified glucuronoxylans were found ⁵
Xyloglucan type XXXG	✓	✓	XXGG	XXGGG	✓ +XXGG	✓	✓	✓	✓ +XXGG (Lamiids) +XXGGG (grasses)	
HG	✓	✓	✓	✓	✓	✓	✓	✓	✓	
RG-I	(✓) ⁶	(✓) ⁶	(✓) ⁶	(✓) ⁶	(✓) ⁶	(✓) ⁶	(✓) ⁶	✓	✓	Based on detection of RG-I with antibodies against side chains ⁶
RG-II	×	(✓) ⁷	(✓) ⁷	(✓) ⁷	✓	✓	✓	✓	✓	Based only on detection of small amounts of boron ⁷
Callose	✓	✓	✓	✓	✓	✓	✓	✓	✓	
“true” lignin	× ⁸	×	× ⁸	× ⁸	✓	✓	✓	✓	✓	Some monolignols are found (bryophytes); some phenylpropanoid biosynthesis genes are detected ⁸
HRGPs (AGPs, EXTs, PRPs)	(✓), ✓ ⁹ , ✓ ⁹	✓, ✓ ⁹ , × ⁹	✓, ✓ ⁹ , × ⁹	✓, ✓ ⁹ , ✓ ⁹	✓, ✓ ⁹ , × ⁹	✓, ✓ ⁹ , × ⁹	✓, ✓ ⁹ , ✓ ⁹	✓, ✓, ✓ ⁹	✓, ✓, ✓	For streptophyte algae only based on antibody detection, only isolation of RGP in <i>S. pratensis</i> . EXTs and PRPs are based on bioinformatic search ⁹

Preparation based on this work, Scherp *et al.*, 2001; O'Neill *et al.*, 2004; Popper *et al.*, 2010; Leroux *et al.*, 2015; Johnson *et al.*, 2017a; de Vries *et al.*, 2021; Pfeifer *et al.*, 2022, 2023.

HRGPs in the streptophyte lineage with focus on AGPs

Beside polysaccharides, the cell wall consists of cell wall glycoproteins, mainly hydroxyproline-rich glycoproteins (HRGPs). These HRGPs can be categorized according to their glycosylation degree, which is marginal in proline-rich proteins (PRPs), about 50 % in extensins (EXT) and up to 90 % in arabinogalactan-proteins (AGPs; Johnson *et al.*, 2018). While bioinformatic search in transcriptomes revealed sequences for AGPs and EXTs in all streptophytes, low sequence levels were identified for PRPs in streptophyte algae and mosses, but none could be found in hornworts, liverworts, lycophytes and eusporangiate ferns (Johnson *et al.*, 2017a). By isolating AGPs of the cell wall from the hornwort *Anthoceros* in this work, AGPs have now been isolated and characterized from all land plant lineages.

Current knowledge about the occurrence of AGPs in streptophyte algae is controversial. The presence of AGPs was only determined by antibody detection in various studies (Eder *et al.*, 2008; Domozych *et al.*, 2009; Sørensen *et al.*, 2011; Ruiz-May *et al.*, 2018; Palacio-López *et al.*, 2019; Permann *et al.*, 2021a,b). However, these antibodies only recognized the polysaccharide part of these glycoproteins. The study by Pfeifer *et al.* (2022) demonstrated that an isolated aqueous extract of *Nitellopsis obtusa*, a member of the Charophyceae, contained a high protein part and also polysaccharides, which epitopes reacted with AGP antibodies, and consisted of Ara and Gal, but hydroxyproline (Hyp), the linkage element of both parts from AGPs, could not be detected. Consequently, no pure AGP could be isolated. This led to the assumption, that, at least in this species, the biosynthetic machinery for AGPs might not be present or functional.

This hypothesis was confirmed by the work published by Pfeifer *et al.* 2023, which is part of this work. In this study, four other Charales representatives were analysed for the occurrence of AGPs, and only the galactan backbone was identified, but again no Hyp. A bioinformatic search for prolyl 4-hydroxylases (P4Hs) revealed that only one of seven P4H-homologs in the genome of *Chara braunii* would be able to fulfil its function but showed structural variations to P4Hs of *Arabidopsis*.

Protein part of AGPs

Table 2 offers an overview of the amounts of protein and hydroxyproline in AGPs all over the streptophyte lineage analysed in our working group. High protein amounts were present in the AGPs of the most bryophytes, the lycophyte *Lycopodium* and the two aquatic ferns *Salvinia* and *Azolla* (Tab. 2).

Table 2. Protein (% w w⁻¹ of AGP) and hydroxyproline content (% w w⁻¹ of AGP and of protein) in AGPs from different organs of several species of the *green lineage*.

	Species	Organ	Protein (%)	Hyp (%)	Hyp of protein (%)
Algae	Charales ^{1,2}	Whole plant	No AGP		
	<i>Spirogyra pratensis</i> ²	Whole plant	11,3	0,57	5,1
Bryophytes	<i>Anthoceros agrestis</i> ³	Whole plant	16,3	0,31	1,9
	<i>Marchantia polymorpha</i> ⁴	Whole plant	24,9	0,31	1,2
	<i>Sphagnum</i> sp. ⁵	Whole plant	4,6	0,27	5,8
	<i>Polytrichastrum formosum</i> ⁵	Whole plant	17,8	0,16	0,9
	<i>Physcomitrium patens</i> ³	Whole plant	16,9	0,25	1,5
Lycophytes	<i>Lycopodium annotinum</i> ⁶	Aerial part	17,3	1,00	5,8
	<i>Huperzia squarrosa</i> ⁷	Aerial part	11,9	0,79	6,6
	<i>Equisetum arvense</i> ⁸	Aerial part	6,4	1,02	15,9
	<i>Psilotum nudum</i> ³	Aerial part	5,4	0,33	6,1
Ferns	<i>Osmunda regalis</i> ⁸	Aerial part	9,9	0,52	5,3
	<i>Salvinia molesta</i> ⁸	Whole plant	14,6	0,36	2,5
	<i>Azolla filiculoides</i> ⁸	Whole plant	19,4	0,29	1,5
	<i>Ceratopteris richardii</i> ⁸	Aerial part	11,1	0,55	5
	<i>Pteridium aquilinum</i> ⁸	Aerial part	8,3	0,51	6,1
	<i>Dryopteris filix-mas</i> ⁸	Aerial part	12,3	0,47	3,8
	<i>Cycas revoluta</i> ⁹	Leaves	5,1	1,10	21,6
Gymnosperms	<i>Ginkgo biloba</i> ⁹	Leaves	7,2	0,50	6,9
	<i>Ephedra distachya</i> ⁹	Aerial part	7,4	0,70	9,5
	<i>Triticum aestivum</i> ¹⁰	Fruits	6	0,59	9,9
Angiosperms	<i>Secale cereale</i> ¹¹	Fruits	7	1,10	15,1
	<i>Avena sativa</i> ¹²	Fruits	5,4	1,00	16,6
	<i>Baptisia tinctoria</i> ¹³	Roots	5,5	0,35	6,3
	<i>Echinacea pallida</i> ¹⁴	Roots	3,9	0,65	17,3
	<i>Echinacea purpurea</i> ¹⁵	Roots	5	0,64	12,7

Heatmap validation: lowest value set 0 % and highest value 100 %; ¹Pfeifer *et al.*, 2023; ²Pfeifer *et al.*, 2022; ³This work; ⁴Happ & Classen, 2019; ⁵Bartels *et al.*, 2017; ⁶Bartels & Classen, 2017; ⁷Schuldt, 2021; ⁸Mueller *et al.*, 2023; ⁹Baumann *et al.*, 2021; ¹⁰Goellner *et al.*, 2010; ¹¹Goellner *et al.*, 2013; ¹²Goellner *et al.*, 2011; ¹³Wack *et al.*, 2005; ¹⁴Thude & Classen, 2005; ¹⁵Bossy *et al.*, 2009.

High amounts of Hyp were detected in the lycophyte AGPs as well as in those of the eusporangiate fern *Equisetum* and also in those of some seed plants. The Hyp content of the total protein is highest in almost all seed plants, especially in the gymnosperm *Cycas*, as well as in the fern *Equisetum*. In contrast, the Hyp content in the AGP protein parts of most mosses and water ferns are significantly lower.

In AGPs with a low protein content, Hyp residues are located closer to each other, which might lead to polysaccharide chains that can only be slightly branched to avoid steric hindrance. Conversely, this implies that AGPs with a higher protein content and less Hyp could have polysaccharide chains, which are probably more highly branched. This is illustrated in Figure 1.

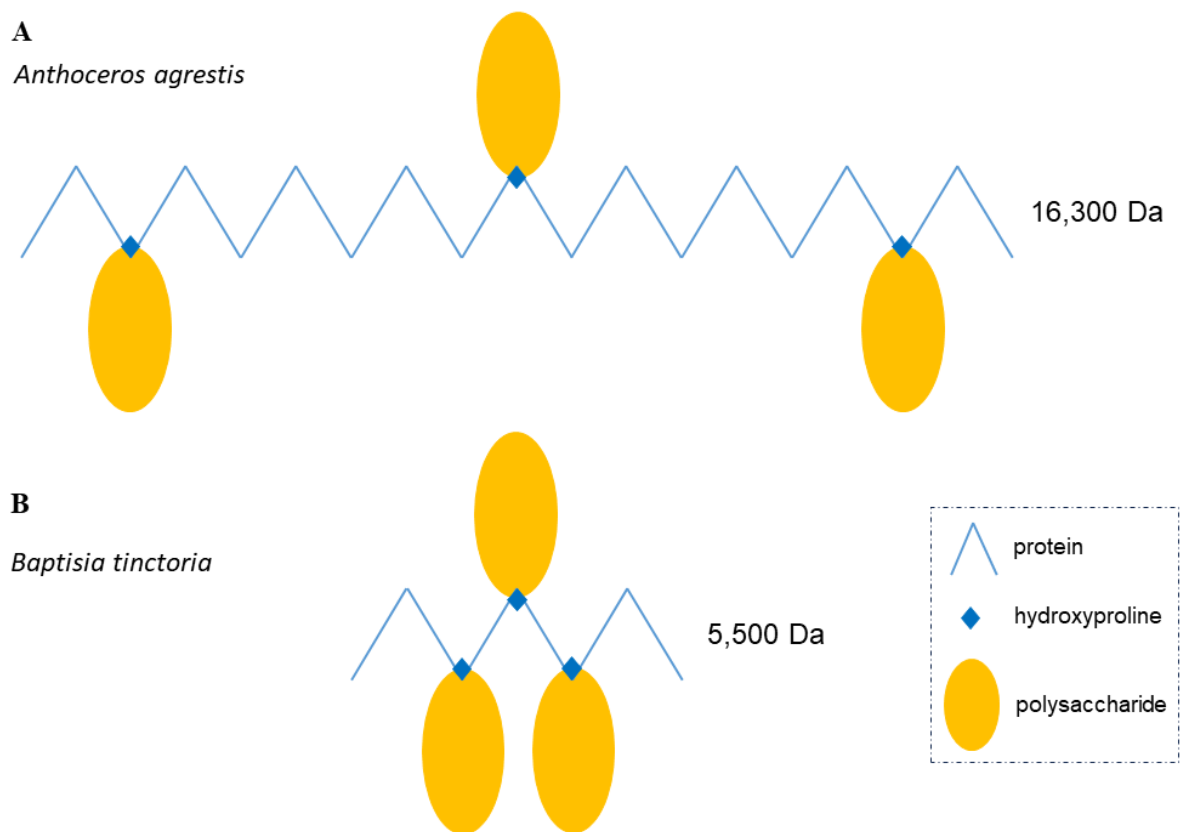


Figure 1. Structural proposal of AGPs with different protein glycosylation according to Fincher *et al.* (1983), calculated with the protein and hydroxyproline content of table 2 and a theoretical molecular weight of both AGPs of 100,000 Da and an average molecular weight of amino acids of 110 Da. **A:** AGP of the hornwort *Anthoceros agrestis*. **B:** AGP of the angiosperm *Baptisia tinctoria*.

Polysaccharide part of AGPs

Figure 2 offers an overview on the composition of the polysaccharide moieties of AGPs all over the streptophyte lineage.

Whereas all land plant AGPs are dominated by Gal and Ara, the two investigated streptophyte algae are different. Algae from the Charales order possessed no AGPs at all (see also above), but galactans with structural motifs of the AGP galactan cores. In addition to Gal, the galactan core structure contained the unusual 3-*O*-MeGal in high amounts. In general, methylated monosaccharides are common in algae and were detected in several chlorophyte and streptophyte algae (Allard & Casadevall, 1990; Ogawa *et al.*, 1994, 1997, 2001; Jander, 2023). The study by Pfeifer *et al.* (2022) determined these methylated monosaccharides, including the 3-*O*-MeGal, in cell wall fractions of *Spirogyra pratensis*, a member of the Zygnematophyceae. This study is the only investigation that isolated a glycoprotein similar to that of AGPs. However, this glycoprotein consisted mainly of the monosaccharides Rha and Gal and was therefore named RGP, a rhamnogalactan protein. The RGP of this alga contained methylated Rha in addition to the 3-*O*-MeGal. High amounts of Rha and 3-*O*-MeRha were also present in land plant AGPs of bryophytes, ferns and gymnosperms, whereas the Rha content in

angiosperm AGPs is generally lower and always completely free of 3-*O*-MeRha (Fig. 2A). The AGPs of both representatives of the lycophytes lack both types of Rha, but the AGP of *Huperzia* contained 3-*O*-MeGal, which was found in cell wall fractions of other lycophytes as well (Popper *et al.*, 2001). This raises the question of whether the methylation of monosaccharides is a typical feature in the streptophyte lineage from algae to gymnosperms, which has been lost in angiosperms.

The uronic acid content of all AGPs investigated are variable but are always below 12 % (Fig. 2B). However, no uronic acids were detectable in the AGPs of the investigated monocotyledonous plants. This could be due to the fact that the AGPs were only isolated from fruits and not from the whole plant. Further studies on other parts of the plant are necessary to determine whether this is a typical feature of monocotyledonous AGPs or restricted to cereals.

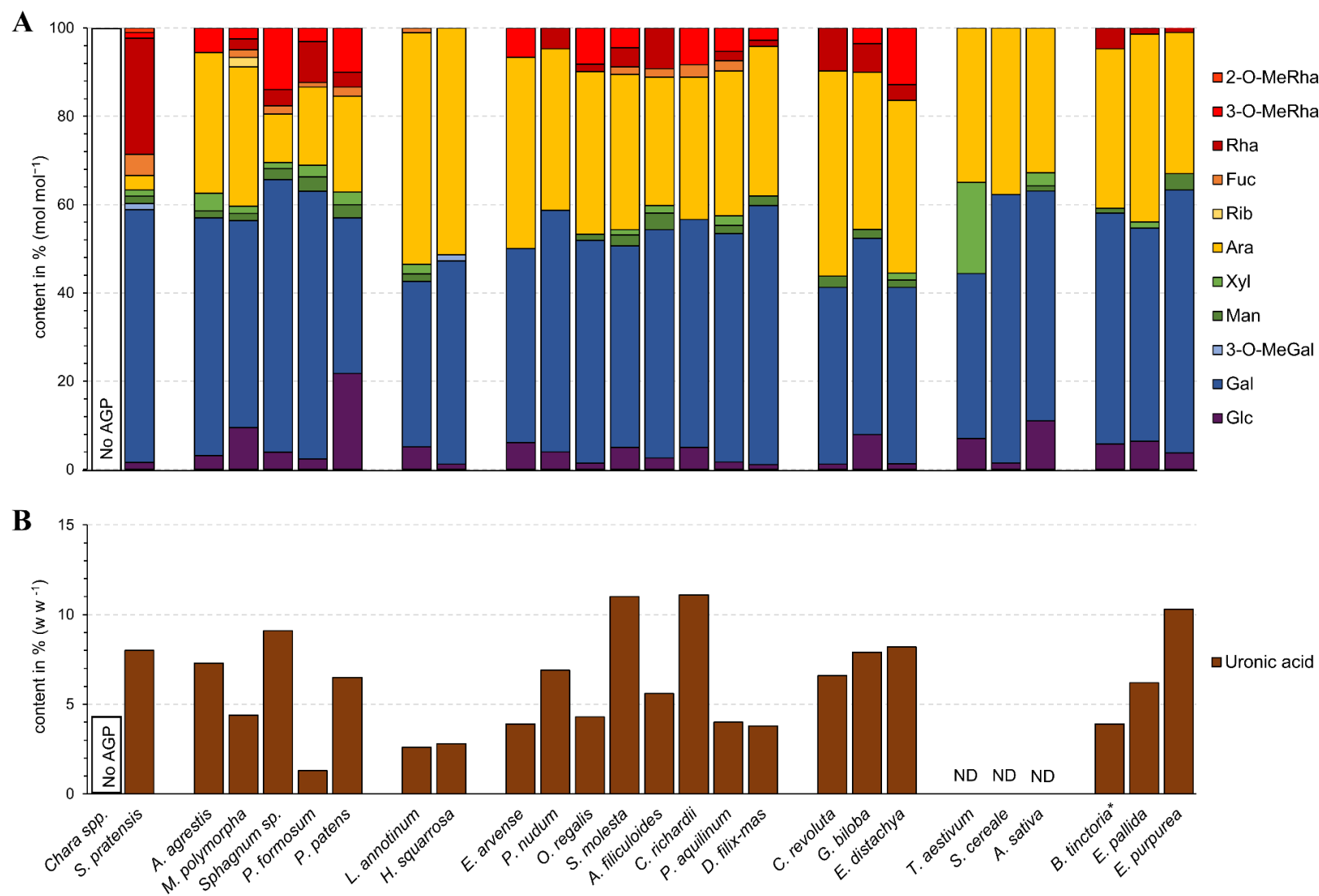


Figure 2. Monosaccharide composition of the RGP and AGPs from several species of the *green lineage*. **A:** Relative neutral monosaccharide composition determined by gas chromatography (GC; % mol mol⁻¹). **B:** Absolute content of uronic acids determined by colorimetric assay (% w w⁻¹ of dry fraction weight). ND: not detected; *: uronic acid content based on carboxy-reduction. For references, see Table 2.

Table 3. Linkage type analysis of AGPs throughout the streptophyte lineage in % (mol mol⁻¹). For references, see Table 2.

		1,3,6-Galp	1,3,4-Galp	1,2,3-Galp	1,3-Galp	1,6-Galp	t-Galp	1,2-Araf	1,3-Araf	1,5-Araf	t-Araf	t-Arap	t-Rhap	t-3-O-MeRhap	1,3-Rhap	1,4-/1,2-Hexp	others
Streptophyte alga	<i>S. pratensis</i>	30.7	0.0	0.0	9.8	5.8	0.0	0.0	0.0	0.0	1.1	0.0	24.7	2.0	20.0	0.0	5.9
	<i>A. agrestis</i>	27.7	6.5	0.0	20.1	0.0	1.4	0.0	2.4	0.0	23.7	1.7	0.0	8.4	0.0	0.0	8.1
	<i>M. polymorpha</i>	27.1	0.0	0.0	19.2	0.0	0.0	0.0	4.3	2.7	36.3	0.0	1.1	1.1	0.0	4.3	3.9
Bryophytes	<i>Sphagnum</i> sp.	27.5	0.0	4.8	17.8	7.3	7.0	0.0	0.5	5.3	3.9	0.0	1.9	7.2	0.0	11.1	5.7
	<i>P. formosum</i>	28.2	0.0	6.6	14.5	2.6	14.2	0.6	3.4	1.8	9.2	0.0	7.4	2.5	0.0	6.8	2.2
	<i>P. patens</i>	22.3	0.0	0.0	11.0	1.4	1.6	0.0	0.0	11.0	9.4	0.0	4.2	12.5	0.0	23.4	3.2
Lycophytes	<i>L. annotinum</i>	29.2	0.0	0.0	19.5	1.1	1.3	0.2	15.2	1.0	11.8	13.4	0.0	0.0	0.0	3.1	4.2
	<i>H. squarrosa</i>	23.4	0.0	0.0	25.1	0.0	0.0	0.0	19.3	0.0	5.1	21.5	0.0	0.0	0.0	0.0	5.6
	<i>E. arvense</i>	26.4	1.7	0.0	16.3	1.8	2.4	0.5	0.2	14.3	23.1	0.0	0.0	3.4	0.0	5.2	4.7
	<i>P. nudum</i>	34.4	0.0	0.0	21.9	3.4	3.5	0.0	10.3	1.4	7.1	9.9	3.6	0.0	0.0	3.4	1.1
	<i>O. regalis</i>	35.5	0.8	0.0	19.7	1.3	3.4	2.9	0.8	2.4	15.9	0.0	1.1	5.1	0.0	6.3	4.8
Ferns	<i>S. molesta</i>	30.7	0.0	0.0	15.2	2.1	2.1	17.2	0.0	3.9	9.6	0.0	5.4	5.6	0.0	5.3	2.9
	<i>A. filiculoides</i>	27.0	0.0	0.0	15.5	2.6	3.4	16.9	0.0	4.4	8.5	0.0	9.5	0.0	0.0	7.9	4.3
	<i>C. richardii</i>	35.9	0.0	0.0	16.4	2.2	6.0	11.5	0.0	7.3	6.4	0.0	0.0	7.8	0.0	3.0	3.5
	<i>P. aquilinum</i>	29.7	2.9	0.0	20.6	2.2	10.6	9.6	1.7	2.5	4.6	0.0	0.5	1.3	0.0	7.6	6.2
	<i>D. filix-mas</i>	23.7	4.0	0.0	18.5	2.9	9.0	5.0	1.7	2.9	15.2	0.0	0.7	1.3	0.0	4.8	10.3

Gymnosperms	<i>C. revoluta</i>	32.4	0.0	0.0	13.2	3.8	2.1	1.5	7.1	6.9	21.7	3.7	4.4	0.0	0.0	1.1	2.1
	<i>G. biloba</i>	12.6	0.0	0.0	2.8	1.3	2.3	1.0	2.3	13.0	8.4	1.0	2.1	1.2	0.0	47.3	4.7
	<i>E. distachya</i>	39.2	0.0	0.0	7.3	4.0	0.9	0.7	0.0	3.7	27.4	0.5	2.4	8.7	0.0	5.2	0.0
Angiosperms	<i>T. aestivum</i>	37.7	0.0	0.0	19.0	3.0	1.2	0.0	0.0	9.0	30.1	0.0	0.0	0.0	0.0	0.0	0.0
	<i>S. cereale</i>	36.3	0.0	0.0	14.2	6.4	3.3	0.0	0.0	7.7	32.1	0.0	0.0	0.0	0.0	0.0	0.0
	<i>A. sativa</i>	36.8	0.0	0.0	19.6	6.1	3.6	0.0	0.0	7.3	26.6	0.0	0.0	0.0	0.0	0.0	0.0
	<i>B. tinctoria</i>	24.2	0.0	0.0	16.7	5.8	3.6	0.0	1.7	9.4	33.2	1.9	1.7	0.0	0.0	1.8	0.0
	<i>E. pallida</i>	26.9	0.0	0.0	16.5	6.3	2.5	0.0	0.0	14.2	29.4	0.0	0.0	0.0	0.0	0.0	4.2
	<i>E. purpurea</i>	31.8	0.0	0.0	12.7	15.4	0.0	0.0	0.0	11.7	24.8	0.0	0.0	0.0	0.0	0.0	3.6
		1,3,6-Galp	1,3,4-Galp	1,2,3-Galp	1,3-Galp	1,6-Galp	t-Galp	1,2-Araf	1,3-Araf	1,5-Araf	t-Araf	t-Arap	t-Rhap	t-3-O-MeRhap	1,3-Rhap	1,4-/1,2-Hexp	others

Table 3 offers an overview on monosaccharide linkage types present in the carbohydrate part of different AGPs. The galactan core structure of angiosperm AGPs consists mainly of pyranosidic 1,3-, 1,6-, and 1,3,6-galactose (Galp) linkages. These were also detected in the AGPs of spore-producing land plants, with the exception of only low amounts of 1,6-Galp. Higher amounts of 1,6-Galp induce longer galactan side chains of angiosperm AGPs.

Bryophyte and fern AGPs also showed unusual branching patterns. The AGPs of the mosses *Sphagnum* and *Polytrichastrum* exhibited a unique 1,2,3-Galp linkage, while the hornwort AGP and some AGPs of ferns revealed 1,3,4-Galp branching.

In angiosperm AGPs, the side chains are mainly decorated with furanosidic Ara (Araf) residues, terminal or 1,5-linked. This pattern was also found in the moss *Physcomitrium*. Other mosses as well as the liverwort *Marchantia* contained 1,3-Araf linkages in addition to both Araf linkages. This 1,3-Araf linkage was also present in the AGP of the hornwort *Anthoceros* and in those of both lycophytes. Besides t-Araf, the hornwort AGP included low amounts of the unusual t-Arap, which were detected in high contents in the lycophyte AGPs. Ara linkage types of the AGP of the eusporangiate fern *Equisetum* were similar to those of angiosperms, while those of *Psilotum* shared the same Ara linkage distribution with the AGP of *Lycopodium*. All other leptosporangiate ferns had 1,2-linked Araf and t-Araf in common. In contrast, the gymnosperm AGPs revealed all Araf linkage types and both terminal residues in different amounts.

Based on the methylation data, a principal components analysis (PCA) was performed in the study of Mueller *et al.* (2023), included in this work. This analysis demonstrated that the angiosperm AGPs were highly conserved, while those of bryophyte, fern and gymnosperm AGPs were more variable. The PCA also showed significant modifications in the AGP of *Lycopodium* due to the 1,3-Araf and t-Arap linkages as well as in the RGP of the streptophyte alga *Spirogyra*. In addition to high amounts of pyranosidic terminal rhamnose (Rhap), this RGP also contained unique 1,3-linked Rhap linkages.

Various GTs belonging to different families are responsible for the AGP glycosylation. The most studied GTs are GT29 and GT31 for galactosylation, GT77 for arabinosylation, GT14 for glucuronosylation (Showalter & Basu, 2016). Other GTs, especially those which are responsible for rhamnosylation, are still unknown (Silva *et al.*, 2020). Thus, there is still a lot of work to be done in the future. In addition, recently published genomes of streptophyte algae and spore producing land plants provide an opportunity for bioinformatic search to investigate the presence of these GTs (Feng *et al.*, 2023 preprint; Sekimoto *et al.*, 2023).

In an evolutionary context, the fact that an AGP-like glycoprotein (RGP) is present in *Spirogyra*, but none was detectable in the Charales members, supports the hypothesis that land

plants are descended from streptophyte algae closely related to the extant Zygnematophyceae (de Vries & Archibald, 2018). To confirm this assumption, further streptophyte algae representatives need to be tested for the occurrence of AGPs and, if present, these have to be isolated and characterized in future research. In addition, further spore producing land plant AGPs, especially those of bryophytes and lycophytes, need to be analysed to get a much clearer picture of similarities and differences in AGP structures within the *green lineage*. An excellent candidate for future research would be the liverwort *Riccia fluitans*. This bryophyte can live both on land and in water and the phenotypes of the aquatic and terrestrial forms differ significantly (Althoff *et al.*, 2022).

Altogether, this work offers an overview on cell wall composition and AGP structure in the course of evolution.

References

- Akiyama, T., Tanaka, K., Yamamoto, S. (1987) An arabinogalactan-rich protein containing 3-*O*-methylrhmannose (Acofriose) in young plants of *Osmunda japonica*. *Agricultural and Biological Chemistry*, **51**, 2599–2600.
- Allard, B. & Casadevall, E. (1990) Carbohydrate composition and characterization of sugars from the green microalga *Botryococcus braunii*. *Phytochemistry*, **29**, 1875–1878.
- Allsobrook, A. J. R., Nunn, J. R., Parolis, H. (1974) The linkage of 4-*O*-methyl-L-galactose in the sulphated polysaccharide of *Aeodes ulvoidea*. *Carbohydrate Research*, **36**, 139–145.
- Althoff, F., Wegner, L., Ehlers, K., Buschmann, H., Zachgo, S. (2022) Developmental plasticity of the amphibious liverwort *Riccia fluitans*. *Frontiers in Plant Science*, **13**, article909327.
- Amos, R. A., Atmodjo, M. A., Huang, C., Gao, Z., Venkat, A., Tadjale, R. *et al.* (2022) Polymerization of the backbone of the pectic polysaccharide rhamnogalacturonan I. *Nature Plants*, **8**, 1289–1303.
- Anderson, C. T. & Kieber, J. J. (2020) Dynamic construction, perception, and remodelling of plant cell walls. *Annual Review of Plant Biology*, **71**, 39–69.
- Anderson, D. M. & King, N. J. (1961a) Polysaccharides of the Characeae. II. The carbohydrate content of *Nitella translucens*. *Biochimica et Biophysica Acta*, **52**, 441–449.
- Anderson, D. M. & King, N. J. (1961b) Polysaccharides of the Characeae. III. The carbohydrate content of *Chara australis*. *Biochimica et Biophysica Acta*, **52**, 449–454.
- Anderson, D. M. W. & Munro, A. C. (1969) The presence of 3-*O*-Methylrhmannose in *Araucaria* resinous exudates. *Ohytochemistry*, **8**, 633–634.
- Aquino, R. S., Grativol, C., Mourão, P. A., S. (2011) Rising from the Sea: Correlations between sulfated polysaccharides and salinity in plants. *PLoS ONE*, **6**, e18862.
- Araki, S., Satake, M., Ando, S., Hayashi, A., Fujii, N. (1986) Characterization of a diphosphonopentaosylceramide containing 3-*O*-methylgalactose from the skin of *Aplysia kurodai* (sea hare). *Journal of Biological Chemistry*, **261**, 5138–5144.
- Arbeitsgruppe Characeen Deutschlands Hrsg. (2016) Armleuchteralgen. Die Characeen Deutschlands, *Springer Spektrum*, Rostock, Germany, 1–618.
- Atmodjo, M. A., Hao, Z., Mohnen, D. (2013) Evolving views of pectin biosynthesis. *Annual Review of Plant Biology*, **64**, 747–779.
- Avci, U., Peña, M. J., O'Neill, M. A. (2018) Changes in the abundance of cell wall apiogalacturonan and xylogalacturonan and conservation of rhamnogalacturonan II structure during the diversification of the Lemnoideae. *Planta*, **247**, 953–971.
- Banks, J. A. (1999) Gametophyte development in ferns. *Annual Review of Plant Physiology and Plant Molecular Biology*, **50**, 163 – 186.
- Banks, J. A., Nishiyama, T., Hasebe, M., Bowman, J. L., Gribskov, M., de Pamphilis, C. *et al.* (2011) The *Selaginella* genome identifies genetic changes associated with the evolution of vascular plants. *Science*, **332**, 960–963.
- Bar-Peled, M., Urbanowicz, B. R., O'Neill, M. A. (2012) The synthesis and origin of the pectic polysaccharide rhamnogalacturonan II – insights from nucleotide sugar formation and diversity. *Frontiers in Plant Science*, **3**, 92.
- Barnes, W. J., Koj, S., Black, I. M., Archer-Hartmann, S. A., Azadi, P., Urbanowicz, B. R. *et al.* (2021) Protocols for isolating and characterizing polysaccharides from plant cell walls: a case study using rhamnogalacturonan-II. *Biotechnology for Biofuels*, **14**, 142.
- Barolo, L., Abbriano, R. A., Commault, A. S., George, J., Kahlke, T., Fabris, M. *et al.* (2020) Perspectives for glyco-engineering of recombinant biopharmaceuticals from microalgae. *Cells*, **9**, 633.
- Barsett, H. & Paulsen, B. S. (1992) Separation, isolation and characterization of acidic polysaccharides from the inner bark of *Ulmus glabra* Huds. *Carbohydrate Polymers*, **17**, 137–144.
- Bartels, D., Baumann, A., Maeder, M., Geske, T., Heise, E. M., von Schwartzberg, K. *et al.* (2017) Evolution of plant cell wall: Arabinogalactan-proteins from three moss genera show structural differences compared to seed plants. *Carbohydrate Polymers*, **163**, 227–235.
- Bartels, D. & Classen, B. (2017) Structural investigations on arabinogalactan-proteins from a lycophyte and different monilophytes (ferns) in the evolutionary context. *Carbohydrate Polymers*, **172**, 342–351.
- Barthlott, W., Wiersch, S., Čolić, Z., Koch, K. (2009) Classification of trichome types within species of the water fern *Salvinia*, and ontogeny of the egg-beater trichomes. *Botany*, **87**, 830–836.
- Barthlott, W., Schimmel, T., Wiersch, S., Koch, K., Brede, M., Barczewski, M., *et al.* (2010) The *Salvinia* paradox: superhydrophobic surfaces with hydrophilic pins for air retention under water. *Advanced Materials*, **22**, 2325–2328.
- Basile, D. V. & Basile, M. R. (1987) The occurrence of cell wall-associated arabinogalactan proteins in the Hepaticae. *The Bryologist*, **90**, 401–404.

- Basile, D. V., Basile, M. R., Mignone, M. M. (2000) Arabinogalactan-proteins, place-dependent suppression and plant morphogenesis. In: Nothnagel EA, Bacic A, Clarke AE, eds. Cell and developmental biology of arabinogalactan-proteins. Springer, Boston, MA, 169–178.
- Basu, D., Wang, W., Ma, S., DeBrosse, T., Poirier, E., Emch, K. *et al.* (2015a) Two hydroxyproline galactosyltransferases, GALT5 and GALT2, function in arabinogalactan-protein glycosylation, growth and development in *Arabidopsis*. *PLoS ONE*, **10**, e0125624. doi: 10.1371/journal.pone.0125624.
- Basu, D., Tian, L., Wang, W., Bobbs, S., Herock, H., Travers, A. *et al.* (2015b) A small multigene hydroxyproline-O-galactosyltransferase family functions in arabinogalactan-protein glycosylation, growth and development in *Arabidopsis*. *BMC Plant Biology*, **15**, 295.
- Basu, D., Tian, L., Debrosse, T., Poirier, E., Emch, K., Herock, H. *et al.* (2016) Glycosylation of a fasciclin-like arabinogalactan-protein (SOS5) mediates root growth and seed mucilage adherence via a cell wall receptor-like kinase (FEI1/FEI2) pathway in *Arabidopsis*. *PLoS ONE*, **11**, e0145092, doi: 10.1371/journal.pone.0145092.
- Bateman, R. M., Crane, P. R., DiMichele W. A., Kenrick, P. R., Rowe N. P., Speck, T. *et al.* (1998) Early evolution of land plants: phylogeny, physiology, and ecology of the primary terrestrial radiation. *Annual Review of Ecology and Systematics*, **29**, 263–292.
- Baumann, A., Pfeifer, L., Classen, B. (2021) Arabinogalactan-proteins from non-coniferous gymnosperms have unusual structural features. *Carbohydrate Polymers*, **261**, 11783.
- Bechteler, J., Peñaloza-Bojacá, G., Bell, D., Burleigh, J.G., McDaniel, S. F., Davis, E. C. *et al.* (2023) Comprehensive phylogenomic time tree of bryophytes reveals deep relationships and uncovers gene incongruences in the last 500 million years of diversification. *American Journal of Botany*, **110**, e16249.
- Becker, B. & Marin, B. (2009) Streptophyte algae and the origin of embryophytes. *Annals of botany*, **103**, 999–1004.
- Becker, B., Feng, X., Yin, Y., Holzinger, A. (2020) Desiccation tolerance in streptophyte algae and the algae to land plant transition: evolution of LEA and MIP protein families within the Viridiplantae. *Journal of Experimental Botany*, **71**, 3270–3278.
- Beňová-Kákošová, A., Dignonnet, C., Goubet, F., Ranocha, P., Jauneau, A., Pesquet, E. *et al.* (2006) Galactoglucomannans increase cell population density and alter the protoxylem/metaxylem tracheary element ratio in xylogenetic cultures of *Zinnia*. *Plant Physiology*, **142**, 696–709.
- Berry, E. A., Tran, M. L., Dimos, C. S., Budziszek, Jr. M. J., Scavuzzo-Duggan, T. R., Roberts, A. W. (2016) Immuno and affinity cytochemical analysis of cell wall composition in the moss *Physcomitrella patens*. *Frontiers in Plant Science*, **7**, 248.
- Blakeney, A. B., Harris, P. J., Henry, R. J., Stone, B. A. (1983) A simple and rapid preparation of alditol acetates for monosaccharide analysis. *Carbohydrate Research*, **113**, 291–299.
- Blindow, I. & Schütte, M. (2007) Elongation and mat formation of *Chara aspera* under different light and salinity conditions. *Hydrobiologia*, **584**, 69 – 76.
- Blumenkrantz, N. & Asboe-Hansen, G. (1973) New method for quantitative determination of uronic acids. *Analytical Biochemistry*, **34**, 484–489.
- Boerjan, W., Ralph, J., Baucher, M. (2003) Lignin Biosynthesis. *Annual Review of Plant Biology*, **54**, 519–546.
- Bolig, K., Lamshöft, M., Schweimer, K., Marner, F.-J., Budzikiewicz, H., Waffenschmidt, S. (2007) Structural analysis of linear hydroxyproline-bound O-glycans of *Chlamydomonas reinhardtii*—conservation of the inner core in *Chlamydomonas* and land plants. *Carbohydrate Research*, **342**, 2557–2566.
- Bossy, A., Blaschek, W., Classen, B. (2009) Characterization and immunolocalization of arabinogalactan-proteins in roots of *Echinacea purpurea*. *Planta Medica*, **75**, 1526–1533.
- Bowles, A. M. C., Paps, J., Bechtold, U. (2021) Evolutionary origins of drought tolerance in spermatophytes. *Frontiers in Plant Science*, **12**, article655924.
- Bowman, J. L. (2013) Walkabout on the long branches of plant evolution. *Current Opinion in Plant Biology*, **16**, 70–77.
- Bowman, J. L., Kohchi, T., Yamato, K. T., Jenkins, J., Shu, S., Ishizaki, K. *et al.* (2017) Insights into land plant evolution garnered from the *Marchantia polymorpha* genome. *Cell*, **171**, 287–304.e15.
- Bowman, J. L. (2022) The origin of a land flora. *Nature Plants*, **8**, 1352–1369.
- Brinkhuis, H., Schouten, S., Collinson, M. E., Sluijs, A., Sinninghe-Damsté, J. S., Dickens, G. *et al.* (2006) Episodic fresh surface waters in the Eocene Arctic Ocean. *Nature*, **441**, 606–609.
- Brown, R. M. Jr. (1985) Cellulose microfibril assembly and orientation: recent developments. *Journal of Cell Science Supplement*, **2**, 13–32.
- Brown, R. M. Jr., Sexana, I. M., Kudlicka, K. (1996) Cellulose biosynthesis in higher plants. *Trends in Plant Science*, **1**, 149–156.
- Brownsey, P. J. & Lovis, J. D. (1987) Chromosome numbers for the New Zealand species of *Psilotum* and *Tmesipteris*, and the phylogenetic relationships of the Psilotales. *New Zealand Journal of Botany*, **25**, 439–454.
- Buckeridge MS, Dos Santos HP, Tiné MAS. (2000) Mobilisation of storage cell wall polysaccharides in seeds. *Plant Physiology and Biochemistry*, **38**, 141–156.

- Buckeridge, M. S.** (2010) Seed cell wall storage polysaccharides: models to understand cell wall biosynthesis and degradation. *Plant Physiology*, **154**, 1017–1023.
- Burton, R. A. & Fincher, G. B.** (2009) (1,3;1,4)- β -D-glucans in cell walls of the poaceae, lower plants, and fungi: a tale of two linkages. *Molecular Plant*, **2**, 873–882.
- Burton, R. A. & Fincher, G. B.** (2014) Evolution and development of cell walls in cereal grains. *Frontiers in Plant Science*, **5**, 456.
- Burton, R. A., Wilson, S. M., Hrmova, M., Harvey, A. J., Shirley, N. J., Stone, B. A. et al.** (2006) Cellulose synthase-like CslF genes mediate the synthesis of cell wall (1,3;1,4)- β -D-glucans. *Science*, **311**, 1940–1942.
- Caffall, K. H. & Mohnen, D.** (2009) The structure, function, and biosynthesis of plant cell wall pectic polysaccharides. *Carbohydrate Research*, **344**, 1879–1900.
- Capek, P.** (2008) An arabinogalactan containing 3-O-methyl-D-galactose residues isolated from the aerial parts of *Salvia officinalis* L. *Carbohydrate Research*, **343**, 1390–1393.
- Carafa, A., Duckett, J. G., Knox, J. P., Ligrone, R.** (2005) Distribution of cell-wall xylans in bryophytes and tracheophytes: new insights into basal interrelationships of land plants. *New Phytologist*, **168**, 231–240.
- Carpenter, E. J., Matasci, N., Ayyampalayam, S., Wu, S., Sun, J., Yu, J. et al.** (2019) Access to RNA-sequencing data from 1,173 plant species: the 1000 plant transcriptomes initiative (1KP). *GigaScience*, **8**, 1–7.
- Carpita, N. C. & Gibeaut, D. M.** (1993) Structural models of primary cell walls in flowering plants: consistency of molecular structure with the physical properties of the walls during growth. *The Plant Journal*, **3**, 1–30.
- Carpita, N. C. & McCann, M. C.** (2002) The functions of cell wall polysaccharides in composition and architecture revealed through mutations. *Plant and Soil*, **247**, 71–80.
- Cavalier, D. M., Lerouxel, O., Neumetzler, L., Yamauchi, K., Reinecke, A., Freshour, G. et al.** (2008) Disrupting two *Arabidopsis thaliana* xylosyltransferase genes results in plants deficient in xyloglucan, a major primary cell wall component. *The Plant Cell*, **20**, 1519–1537.
- Cary, P. R. & Weerts, P. G. J.** (1983) Growth of *Salvinia molesta* as affected by water temperature and nutrition I. effects of nitrogen level and nitrogen compounds. *Aquatic Botany*, **16**, 163–172.
- Chen, X.-Y. & Kim J.-Y.** (2009) Callose synthesis in higher plants. *Plant Signaling & Behavior*, **4**, 489–492.
- Chen, J. & Varner, J. E.** (1985) Isolation and characterization of cDNA clones for carrot extensin and a proline-rich 33-kDa protein. *Proceedings of the National Academy of Sciences*, **82**, 4399–4403.
- Chernova, T., Ageeva, M., Mikshina, P., Trofimova, O., Koslova, L., Lev-Yadun, S. et al.** (2020) The living fossil *Psilotum nudum* has cortical fibers with mannan-based cell wall matrix. *Frontiers in Plant Science*, **11**, 488.
- Clarke, A. E., Knox, R. B., Jermyn, M. A.** (1975) Localization of lectins in legume cotyledons. *Journal of Cell Science*, **19**, 157–167.
- Clarke, A. E., Gleeson, P. A., Jermyn, M. A., Knox, R. B.** (1978) Characterization and localization of β -lectins in lower and higher plants. *Australian Journal of Plant Physiology*, **5**, 707–722.
- Clarke, A. E., Anderson, R.L., Stone, B.A.** (1979) Form and function of arabinogalactans and arabinogalactan-proteins. *Phytochemistry*, **18**, 521–540.
- Classen, B., Witthohn, K., Blascheck, W.** (2000) Characterization of an arabinogalactan-protein isolated from pressed juice of *Echinacea purpurea* by precipitation with the β -glucosyl Yariv reagent. *Carbohydrate Research*, **327**, 497–504.
- Classen, B., Csávas, M., Borbás, A., Dingermann, T., Zündorf, I.** (2004) Monoclonal antibodies against an arabinogalactan-protein from pressed juice of *Echinacea purpurea*. *Planta Medica*, **70**, 861–865.
- Classen, B., Mau, S.-L. & Bacic, A.** (2005) The arabinogalactan-proteins from pressed juice of *Echinacea purpurea* belong to the hybrid class of hydroxyproline-rich glycoproteins. *Planta Medica*, **71**, 59–66.
- Classen, B.** (2007) Characterization of an arabinogalactan-protein from suspension culture of *Echinacea purpurea*. *Plant Cell Tissue organ Cult*, **88**, 267–275.
- Classen, B., Baumann, A., Utermohlen, J.** (2019) Arabinogalactan-proteins in spore-producing land plants. *Carbohydrate Polymers*, **210**, 215–224.
- Cocuron, J. C., Lerouxel, O., Drakakaki, G., Alonso, A. P., Liepman, A. H., Keegstra, K. et al.** (2007) A gene from the cellulose synthase-like C family encodes a β -1,4 glucan synthase. *Proceedings of the National Academy of Sciences*, **104**, 8550–8555.
- Conway, J.R., Lex, A. & Gehlenborg, N.** (2017) UpSetR: an R package for the visualization of intersecting sets and their properties. *Bioinformatics*, **33**, 2938–2940.
- Corrêa-Ferreira, M. L., Viudes, E. B., de Magalhães, P. M., de Santana Filho, A. P., Sasaki, G. L., Pacheco, A. C. et al.** (2019) Changes in the composition and structure of cell wall polysaccharides from *Artemisia annua* in response to salt stress. *Carbohydrate Research*, **483**, 107753.
- Cosgrove, D. J.** (2018) Diffuse growth of plant cell walls. *Plant Physiology*, **176**, 16–27.
- Costa, M., Pereira, A. M., Pinto, S. C., Silva, J., Pereira, L. G., Coimbra, S.** (2019) In silico and expression analyses of fasciclin-like arabinogalactan proteins reveal functional conservation during embryo and seed development. *Plant Reproduction*, **32**, 353–370.
- Cove, D.** (2001) The moss, *Physcomitrella patens*. *Journal of Plant Growth Regulation*, **19**, 275–283.

- Cove, D. J., Perroud, P.-F., Charron, A. J., McDaniel, S. F., Khandelwal, A., Quatrano, R. S. (2009) Culturing the moss *Physcomitrella patens*. *Cold Spring Harbor Protocols*, **2009**, pdb prot5136.
- Cox, C. J., Li, B., Foster, P. G., Embley, T. M., Civián, P. (2014) Conflicting phylogenies for early land plants are caused by composition biases among synonymous substitutions. *Systematic Biology*, **63**, 272–279.
- Cui, S., Hu, J., Guo, S., Wang, J., Cheng, Y., Dang, X., Wu, L., He, Y. (2012) Proteome analysis of *Physcomitrella patens* exposed to progressive dehydration and rehydration. *Journal of Experimental Botany*, **63**, 711–726.
- Deane-Coe, K. K. & Stanton, D. (2017) Functional ecology of cryptogams: scaling from bryophyte, lichen, and soil crust traits to ecosystem processes. *New Phytologist*, **213**, 993–995.
- Dehors, J., Mareck, A., Kiefer-Meyer, M.-C., Menu-Bouaouiche, L., Lehner, A., Mollet, J.-C. (2019) Evolution of cell wall polymers in tip-growing land plant gametophytes: composition, distribution, functional aspects and their remodeling. *Frontiers in Plant Science*, **10**, 441.
- Delaux, P.-M., Hetherington, A. J., Coudert, Y., Delwiche, D., Dunand, C., Gould, S. *et al.* (2019) Reconstructing trait evolution in plant evo–devo studies. *Current Biology*, **29**, R1105–R1121.
- Del Bem, L. E. (2018) Xyloglucan evolution and the terrestrialization of green plants. *New Phytologist*, **219**, 1150–1153.
- Del Bem, L. E. V. & Vincentz, M. G. A. (2010) Evolution of xyloglucan-related genes in green plants. *BMC Evolutionary Biology*, **10**, 341.
- Delwiche, C. F. & Cooper, E. D. (2015) The evolutionary origin of a terrestrial flora. *Current Biology*, **25**, R899–R910.
- de O. Buanafina, M. M. (2009) Feruloylation in grasses: current and future perspectives. *Molecular Plant*, **2**, 861–872.
- de Sousa, F., Foster, P. G., Donoghue, P. C. J., Schneider, H., Cox, C. J. (2019) Nuclear protein phylogenies support the monophyly of the three bryophyte groups (bryophyta schimp.). *New Phytologist*, **222**, 565–575.
- de Vree, B. T., Steiner, L. M., Glazowska, S., Ruhnow, F., Herburger, K., Persson, S. *et al.* (2021) Current and future advances in fluorescence-based visualization of plant cell wall components and cell wall biosynthetic machineries. *Biotechnology for Biofuels*, **14**, 78.
- de Vries, J., Stanton, A., Archibald, J. M., Gould, S. B. (2016) Streptophyte terrestrialization in light of plastid evolution. *Trends in Plant Science*, **21**, 467–476.
- de Vries, J. & Archibald, J. M. (2018) Plant evolution: Landmarks on the path to terrestrial life. *New Phytologist*, **217**, 1428–1434.
- de Vries, S., de Vries, J., Teschke, H., von Dahlen, J., Rosem L. E., Gould, S. B. (2018) Jasmonic and salicylic acid response in the fern *Azolla filiculoides* and its cyanobiont. *Plant, Cell & Environment*, **41**, 2530–2548.
- de Vries, S., Fürst-Jansen, J. M. R., Irisarri, I., Ashok, A. D., Ischebeck, T., Feussner, K., *et al.* (2021) The evolution of the phenylpropanoid pathway entailed pronounced radiations and divergences of enzyme families. *The Plant Journal*, **107**, 975–1002.
- de Vries, S. & de Vries, J. (2022) Evolutionary genomic insights into cyanobacterial symbioses in plants. *Quantitative Plant Biology*, **3**, e16.
- DiTomaso, J. M., Kyser, G. B., Oneto, S. R., Wilson, R. G., Orloff, S. B., Anderson, L. W. *et al.* (2013). Weed control in natural areas in the western United States. Davies, CA: *Weed Research and Information Center, University of California*, 544.
- Dhugga, K. S., Barreiro, R., Whitten, B., Stecca, K., Hazebroek, J., Randhawa, G. S. *et al.* 2004. Guar seed beta-mannan synthase is a member of the cellulose synthase super gene family. *Science*, **303**, 363–366.
- Doblin, M. S., Pettolino, F. A., Wilson, S. M., Campbell, R., Burton, R. A., Fincher, G. B. *et al.* (2009) A barley cellulose synthase-like CSLH gene mediates (1,3;1,4)-beta-D-glucan synthesis in transgenic *Arabidopsis*. *Proceedings of the National Academy of Sciences*, **106**, 5996–6001.
- Dolan, L., Linstead, P., Roberts, K. (1995) An AGP epitope distinguishes a central metaxylem initial from other vascular initials in the *Arabidopsis* root. *Protoplasma*, **189**, 149–155.
- Domozych, D. S., Sørensen, I. and Willats, W. G. T. (2009) The distribution of cell wall polymers during antheridium development and spermatogenesis in the Charophycean green alga, *Chara corallina*. *Annals of Botany*, **104**, 1045–1056.
- Domozych, D. S., Sørensen, I., Sacks, C., Brechka, H., Andreas, A., Fangel, J. U. *et al.* (2014) Disruption of the microtubule network alters cellulose deposition and causes major changes in pectin distribution in the cell wall of the green alga, *Penium margaritaceum*. *Journal of Experimental Botany*, **65**, 465–479.
- Domozych, D. S. & Bagdan, K. (2022) The cell biology of charophytes: exploring the past and models for the future. *Plant Physiology*, **190**, 1588–1608.
- Doner, L. W. & Hicks, K. B. (1997) Isolation of hemicellulose from corn fiber by alkaline hydrogen peroxide extraction. *Cereal Chemistry*, **74**, 176–181.
- Donoghue, P. C. J., Harrison, C. J., Paps, J., Schneider, H. (2021) The evolutionary emergence of land plants. *Current Biology*, **31**, R1–R18.
- Dragičević, M. B., Paunović, D. M., Bogdanović, M. D., Todorović, S. I., Simonović, A. D. (2020) ragp: pipeline for mining of plant hydroxyproline-rich glycoproteins with implementation in R. *Glycobiology*, **30**, 19–35.

- Dubois, M., Gilles, K. A., Hamilton, J. K., Rebers, P. A., Smith, F. (1956) Colorimetric method for determination of sugars and related substances. *Analytical Chemistry*, **28**, 350–356.
- Eder, M., Tenhaken, R., Driouich, A., Lütz-Meindl, U. (2008) Occurrence and characterization of arabinogalactan-like proteins and hemicelluloses in *Micrasterias* (Streptophyta). *Journal of Phycology*, **44**, 1221–1234.
- Eder, M. & Lütz-Meindl, U. (2008) Pectin-like carbohydrates in the green alga *Micrasterias* characterized by cytochemical analysis and energy filtering TEM. *Journal of Microscopy*, **231**, 201–214.
- Eder, M. & Lütz-Meindl, U. (2010) Analyses and localization of pectin-like carbohydrates in cell wall and mucilage of the green alga *Netrium digitus*. *Protoplasma*, **243**, 25–38.
- Eeckhout, S., Leroux, O., Willats, W. G. T., Popper, Z. A., Viane, R. L. L. (2014) Comparative glycan profiling of *Ceratopteris richardii* ‘C-Fern’ gametophytes and sporophytes links cell-wall composition to functional specialization. *Annals of Botany*, **114**, 1295–1307.
- Eisenhaber, B., Wildpaner, M., Schultz, C. J., Borner, G. H. H., Dupree, P., Eisenhaber, F. (2003) Glycosylphosphatidylinositol lipid anchoring of plant proteins. Sensitive prediction from sequence- and genome-wide studies for *Arabidopsis* and *Rice*. *Plant Physiology*, **133**, 1691–1701.
- Ellis, M., Egelund, J., Schultz, C. J., Bacic, A. (2010) Arabinogalactan-proteins: key regulators at the cell surface?. *Plant Physiology*, **153**, 403–419.
- Ensikat, H. J., Ditsche-Kuru, P., Barthlott, W. (2010) Scanning electron microscopy of plant surfaces: simple but sophisticated methods for preparation and examination. In: Méndez-Vilas A, Diaz J (eds) *Microscopy: science, technology, applications and education*. FORMATEX Microscopy series No. **4**, Formatex Research Center, Badajoz, 248–225.
- Espiñeira, J. M., Uzal, E. N., Gómez Ros, L. V., Carrión, J. S., Merino, F., Ros Barceló, A. (2011) Distribution of lignin monomers and the evolution of lignification among lower plants. *Plant Biology*, **13**, 59–68.
- Estevez, J.M., Fernández, P.V., Kasulin, L., Dupree, P., Ciancea, M. (2009) Chemical and in situ characterization of macromolecular components of the cell walls from the green seaweed *Codium fragile*. *Glycobiology*, **19**, 212–228.
- Estevez, J.M., Leonardi, P.I., Alberghina, J.S. (2008) Cell wall carbohydrate epitopes in the green alga *Oedogonium bharuchae* f. *minor* (Oedogoniales, Chlorophyta). *Journal of Phycology*, **44**, 1257–1268.
- Fang, Y., Qin, X., Liao, Q., Du, R., Luo, X., Zhou, Q. *et al.* (2022) The genome of homosporous maidenhair fern sheds light on the euphyllophyte evolution and defences. *Nature Plants*, **8**, 1024–1037.
- Feng, X., Zheng, J., Irisarri, I., Yu, H., Zheng, B., Ali, Z. *et al.* (2023) Chromosome-level genomes of multicellular algal sisters to land plants illuminate signaling network evolution. *Preprint at bioRxiv*10.1101/2023.01.31.526407.
- Ferris, P. J., Woessner, J. P., Waffenschmidt, S., Kilz, S., Drees, J., Goodenough, U. W. (2001) Glycosylated polyproline II rods with kinks as a structural motif in plant hydroxyproline-rich glycoproteins. *Biochemistry*, **40**, 2978–2987.
- Fincher, G. B., Stone, B. A., and Clarke, A. E. (1983). Arabinogalactan-proteins: structure, biosynthesis, and function. *Annual Review of Plant Physiology*, **34**, 47–70.
- Forno, I. W. (1983) Native distribution of the *Salvinia auriculata* complex and keys to species identification. *Aquatic Botany*, **17**, 71–83.
- Forno, I. W. & Harley, K. L. S. (1979) The occurrence of *Salvinia molesta* in Brazil. *Aquatic Botany*, **6**, 185–187.
- Frangedakis, E., Shimamura, M., Villarreal, J. C., Li, F.-W., Tomaselli, M., Waller, M. *et al.* (2021) The hornworts: morphology, evolution and development. *New Phytologist*, **229**, 735–754.
- Franková, L. & Fry, S. C. (2011) Phylogenetic variation in glycosidases and glycanases acting on plant cell wall polysaccharides, and the detection of transglycosidase and trans- β -xylanase activities. *The Plant Journal*, **67**, 662–681.
- Franková, L. & Fry, S.C. (2021) Hemicellulose-remodelling transglycanase activities from charophytes: towards the evolution of the land-plant cell wall. *The Plant Journal*, **108**, 7–28
- Fry, S. C., York, W. S., Albersheim, P., Darvill, A., Hayashi, T., Joseleau, J.-P. *et al.* (1993) An unambiguous nomenclature for xyloglucan-derived oligosaccharides. *Physiologia Plantarum*, **89**, 1–3.
- Fry, S. C., Nesselrode, B. H. W. A., Miller, J. G., Mewburn, B. R. (2008) Mixed-linkage (1–3, 1–4)-beta-D-glucan is a major hemicellulose of *Equisetum* (horsetail) cell walls. *New Phytologist*, **179**, 104–115.
- Fu, H., Yadav, M., P., Nothnagel, E. A. (2007) *Physcomitrella patens* arabinogalactan proteins contain abundant terminal 3-O-methyl-L-rhamnosyl residues not found in angiosperms. *Planta*, **226**, 1511–1524.
- Galloway, A. F., Pedersen, M. J., Merry, B., Marcus, S. E., Blacker, J., Benning, L. G. *et al.* (2018) Xyloglucan is released by plants and promotes soil particle aggregation. *New Phytologist*, **217**, 1128–1136.
- Galtier, J. & A. C. Scott. (1985) Diversification of early ferns. *Proceedings of the Royal Society Edinburgh, Section B; Biology*, **86**, 289–301.
- Geddes, D.S. & Wilkie, K. C. B. (1971) Hemicelluloses from the stem tissues of the aquatic moss *Fontinalis antipyretica*. *Carbohydrate Research*, **18**, 333–335.
- Geng, Y., Yan, A., Zhou, Y. (2022) Positional cues and cell division dynamics drive meristem development and archegonium formation in *Ceratopteris* gametophytes. *Communications Biology*, **5**, 650.

- George, T. G. & Jothi, G. J. (2015) Morphology, phytochemical constituents and thin layer chromatography profiles of secondary and tertiary growth stages of *Salvinia molesta* MITCHELL (Salviniaceae). *The Journal of Phytochemistry, Photon*, **116**, 328–343.
- Geshi, N., Johansen, J. N., Dilokpimol, A., Rolland, A., Belcram, K., Stephane Verger, S. *et al.* (2013) A galactosyltransferase acting on arabinogalactan protein glycans is essential for embryo development in *Arabidopsis*. *The Plant Journal*, **76**, 128–137.
- Gleeson, P. A. & Clarke, A. E. (1979) Structural studies on the major component of gladiolus style mucilage, an arabinogalactan-protein. *Biochemical Journal*, **181**, 607–621.
- Goellner, E. M., Blaschek, W., Classen, B. (2010) Structural investigations on arabinogalactan-protein from wheat, isolated with Yariv reagent. *Journal of agricultural and food chemistry*, **58**, 3621–3626.
- Goellner, E. M., Ichinose, H., Kaneko, S., Blaschek, W., Classen, B. (2011) An arabinogalactan-protein from whole grain of *Avena sativa* L. belongs to the wattle-blossom type of arabinogalactan-proteins. *Journal of Cereal Science*, **53**, 244–249.
- Goellner, E. M., Gramann, J. C., Classen, B. (2013) Antibodies against Yariv's reagent for immunolocalization of arabinogalactan-proteins in aerial parts of *Echinacea purpurea*. *Planta Medica*, **79**, 175–180.
- Gomes, A. R., Freitas, Í. N., da Luz, T. M., Guimarães, A. T. B., da Costa Araújo, A. P., Kamaraj, C. *et al.* (2023) Multiple endpoints of polyethylene microplastics toxicity in vascular plants of freshwater ecosystems: a study involving *Salvinia auriculata* (Salviniaceae). *Journal of Hazardous Materials*, **450**, 131069.
- Gotelli, I. B. & Cleland, R. (1968) Differences in the occurrence and distribution of hydroxyproline-proteins among the algae. *American Journal of Botany*, **55**, 907–914.
- Goubet, F., Jackson, P., Deery, M. J., Dupree, P. (2002) Polysaccharide analysis using carbohydrate gel electrophoresis: a method to study plant cell wall polysaccharides and polysaccharide hydrolases. *Analytical Biochemistry*, **300**, 53–68.
- Goubet, F., Barton, C. J., Mortimer, J. C., Yu, X., Zhang, Z., Miles, G. P. *et al.* (2009) Cell wall glucomannan in *Arabidopsis* is synthesised by CSLA glycosyltransferases, and influences the progression of embryogenesis. *The Plant Journal*, **60**, 527–538.
- Hahsler, M. & Nagar, A. (2019). rBLAST: R Interface for the basic local alignment search tool. R package version 0.99.2, <https://github.com/mhahsler/rBLAST>.
- Happ, K. & Classen, B. (2019) Arabinogalactan-proteins from the liverwort *Marchantia polymorpha* L., a member of a basal land plant lineage, are structurally different to those of angiosperm. *Plants*, **8**, 460.
- Harholt, J., Krüger Jensen, J., Sørensen, S. O., Orfila, C., Pauly, M., Scheller, H. V. (2006) ARABINAN DEFICIENT 1 is a putative arabinosyltransferase involved in biosynthesis of pectic arabinan in *Arabidopsis*. *Plant Physiology*, **140**, 49–58.
- Harholt, J., Sørensen, I., Fangel, J., Roberts, A., Willats, W. G. T., Scheller, H. V. *et al.* (2012) The glycosyltransferase repertoire of the spikemoss *Selaginella moellendorffii* and a comparative study of its cell wall. *PLoS ONE*, **7**, e35846.
- Harholt, J., Moestrup, Ø., Ulvskov, P. (2016) Why plants were terrestrial from the beginning. *Trends in Plant Science*, **21**, 96–101.
- Harris, P. J., Henry, R. J., Blakeney, A. B., Stone, B. A. (1984) An improved procedure for the methylation analysis of oligosaccharides and polysaccharides. *Carbohydrate Research*, **127**, 59–73.
- Harris, B. J., Clark, J. W., Schrempf, D., Szöllösi, G. J., Donoghue, P. C. J., Hetherington, A. M., Williams, T. A. (2022) Divergent evolutionary trajectories of bryophytes and tracheophytes from a complex common ancestor of land plants. *Nature Ecology & Evolution*, **6**, 1634–1643.
- Harrison, J. C. (2017) Development and genetics in the evolution of land plant body plans. *Philosophical Transactions of the Royal Society B, Biological Science*, **372**, 20150490, doi:10.1098/rstb.2015.0490.
- Hatfield, R. D., Rancour, D. M., Marita, J. M. (2016) Grass cell walls: a story of cross-linking. *Frontiers in Plant Science*, **7**, 2056.
- Hayashi, T. (1989) Xyloglucans in the primary cell wall. *Annual Review of Plant Physiology and Plant Molecular Biology*, **40**, 139–168.
- He, J., Zhao, H., Cheng, Z., Ke, Y., Liu, J., Ma, H. (2019) Evolution analysis of the fasciclin-like arabinogalactan proteins in plants shows variable fasciclin-AGP domain constitutions. *International Journal of Molecular Sciences*, **20**, 1945.
- Henry, J. S., Lopez, R. A., Renzaglia, K. S. (2020) Differential localization of cell wall polymers across generations in the placenta of *Marchantia polymorpha*. *Journal of Plant Research*, **133**, 911–924.
- Henry, J. S., Ligrone, R., Vaughn, K. C., Lopez, R. A., Renzaglia, K. S. (2021) Cell wall polymers in the *Phaeoceros* placenta reflect developmental and functional differences across generations. *Bryophyte Diversity & Evolution*, **043**, 265–283.
- Henry, J. S. & Renzaglia, K. S. (2021) The placenta of *Physcomitrium patens*: transfer cell wall polymers compared across the three bryophyte groups. *Diversity*, **13**, 378.
- Herburger, K., Xin, A., Holzinger, A. (2019) Homogalacturonan accumulation in cell walls of the green alga *Zygnema* sp. (Charophyta) increases desiccation resistance. *Frontiers in Plant Science*, **10**, 540.

- Hervé, C., Siméon, A., Jam, M., Cassin, A., Johnson, K. L., Salmeán, A. A. *et al.* (2016) Arabinogalactan proteins have deep roots in eukaryotes: Identification of genes and epitopes in brown algae and their role in *Fucus serratus* embryo development. *New Phytologist*, **209**, 1428–1441.
- Herzog, R. (1934) Anatomische und experimentell-morphologische Untersuchungen über die Gattung *Salvinia*. *Planta*, **22**, 490–514.
- Hess, S., Williams, S. K., Busch, A., Irisarri, I., Delwiche, C. F., de Vries, S. *et al.* (2022) A phylogenomically informed five-order system for the closest relatives of land plants. *Current Biology*, **20**, 4473–4482.e7.
- Hieta, R. & Myllyharju, J. (2002) Cloning and characterization of a low molecular weight prolyl 4-hydroxylase from *Arabidopsis thaliana*. *The Journal of Biological Chemistry*, **277**, 23965–23971.
- Hickok, L. G., Warne, T. R., Slocum, M. K. (1987) *Ceratopteris richardii*: applications for experimental plant biology. *American Journal of Botany*, **74**, 1304–1316.
- Hickok, L. G., Warne, T. R., Fribourg, R. S. (1995) The biology of the fern *Ceratopteris* and its use as a model system. *International Journal of Plant Sciences*, **156**, 332–345.
- Hodgetts, N., Cáliz, M., Englefield, E., Fettes, N., García Criado, M., Patin, L. *et al.* (2019) A miniature world in decline: European Red List of Mosses, Liverworts and Hornworts. Brussels, Belgium: IUCN.
- Hokputsa, S., Harding, S. E., Inngjerdigen, K., Jumel, K., Michaelsen, T. E., Heinze, T. *et al.* (2004) Bioactive polysaccharides from the stems of the thai medicinal plant *Acanthus ebracteatus*: their chemical and physical features. *Carbohydrate Research*, **339**, 753–762.
- Honkanen, S., Jones, V. A. S., Morieri, G., Champion, C., Hetherington, A. J., Kelly, S. *et al.* (2016) The mechanism forming the cell surface of tip-growing rooting cells is conserved among land plants. *Current Biology*, **26**, 3238–3244.
- Hromadová, D., Soukup, A., Tylová, E. (2021) Arabinogalactan proteins in plant roots – an update on possible functions. *Frontiers in Plant Science*, **12**, 674010.
- Hsieh, Y. S. Y. & Harris, P. J. (2012) Structures of xyloglucans in primary cell walls of gymnosperms, monilophytes (ferns sensu lato) and lycophytes. *Phytochemistry*, **79**, 87–101.
- Huang, X., Wang, W., Gong, T., Wickell, D., Kuo, L.-Y., Zhang, X. *et al.* (2022) The flying spider-monkey tree fern genome provides insights into fern evolution and arborescence. *Nature Plants*, **8**, 500–512.
- Ikegaya, H., Hayashi, T., Kaku, T., Iwata, K., Sonobe, S., Shimmen, T. (2008) Presence of xyloglucan-like polysaccharide in *Spirogyra* and possible involvement in cell-cell attachment. *Phycological Research*, **56**, 216–222.
- Ikegaya, H., Nakase, T., Iwata, K., Tsuchida, H., Sonobe, S., Shimmen, T. (2012) Studies on conjugation of *Spirogyra* using monoclonal culture. *Journal of Plant Research*, **125**, 457–464.
- Jander, H. (2023) Analytische Charakterisierung der Zellwand von Jochalgen. *Master thesis*. CAU Kiel University.
- Johnson, K.L., Jones, B.J., Bacic, A., Schultz, C.J. (2003) The fasciclin-like arabinogalactan proteins of *Arabidopsis*. A multigene family of putative cell adhesion molecules. *Plant Physiology*, **133**, 1911–1925.
- Johnson, K. L., Cassin, A. M., Lonsdale, A., Ka-Shu Wong, G., Soltis, D. E., Miles, N. W. *et al.* (2017a) Insights into the evolution of hydroxyproline-rich glycoproteins from 1000 plant transcriptomes. *Plant Physiology*, **174**, 904–921.
- Johnson, K. L., Andrew M. Cassin, A. M., Lonsdale, A., Bacic, A., Doblin, M. S., Schultz, C. J. (2017b) A motif and amino acid bias bioinformatics pipeline to identify hydroxyproline-rich glycoproteins. *Plant Physiology*, **174**, 886–903.
- Johnson, K. L., Jones, B. J., Schultz, C. J., Bacic, A. (2018) Non-enzymic cell wall (glyco)proteins. In: Roberts, J. A., ed. *Annual Plant Reviews online*. Hoboken, NJ: John Wiley & Sons, Ltd. Available from: <https://doi.org/10.1002/9781119312994.apr0070>
- Joseleau, J.-P. & Ruel, K. (1997) Study of lignification by noninvasive techniques in growing maize internodes. *Plant Physiology*, **114**, 1123–1133.
- Karol, K. G., McCourt, R. M., Cimino, M. T., Delwiche, C. F. (2001) The closest living relatives of land plants. *Science*, **294**, 2351–2353.
- Katoh, K. & Standley, D.M. (2013) MAFFT multiple sequence alignment software version 7: improvements in performance and usability. *Molecular Biology and Evolution*, **30**, 772–780.
- Kenrick, P. & Crane, P. R. (1997) The origin and early evolution of plants on land. *Nature*, **389**, 33–39.
- Keskiaho, K., Hieta, M., Sormunen, R., Myllyharju, J. (2007) *Chlamydomonas reinhardtii* has multiple prolyl 4-hydroxylases, one of which is essential for proper cell wall assembly. *The Plant Cell*, **19**, 256–269.
- Kinosian, S. P. & Wolf, P. G. (2022) The biology of *C. richardii* as a tool to understand plant evolution. *eLife*, **11**, e75019.
- Kitazawa, K., Tryfona, T., Yoshimi, Y., Hayashi, Y., Kawauchi, S., Antonov, L. *et al.* (2013) β -galactosyl Yariv reagent binds to the β -1,3-galactan of arabinogalactan proteins. *Plant Physiology*, **161**, 1117–1126.
- Kiyohara, H., Cyong, J.-C., Yamada, H. (1989) Relationship between structure and activity of an anticomplementary arabinogalactan from the roots of *Angelica acutiloba* kitagawa. *Carbohydrate Research*, **193**, 193–200.
- Kjeldahl, J. (1883) Neue Methode zur Bestimmung des Stickstoffs in organischen Körpern. *Zeitschrift für analytische Chemie*, **22**, 366–382.

- Knox, J. P., Linstead, P. J., Perat, J., Cooper, C., Roberts, K. (1991) Developmentally regulated epitopes of cell surface arabinogalactan proteins and their relation to root tissue pattern formation. *The Plant Journal*, **1**, 317–326.
- Kobayashi, Y., Motose, H., Iwamoto, K., Fukuda, H. (2011) Expression and genome-wide analysis of the xylogen-type gene family. *Plant & Cell Physiology*, **52**, 1095–1106.
- Konno, H., Yamaskaki, Y., Katoh, K. (1987) Fractionation and partial characterization of pectic polysaccharides in cell walls from liverwort (*Marchantia polymorpha*) cell cultures. *Journal of Experimental Botany*, **38**, 711–722.
- Koski, M. K., Hieta, M., Böllner, C., Kivirikko, K. I., Myllyharju, J., Wierenga, R.K. (2007) The active site of an algal prolyl 4-hydroxylase has a large structural plasticity. *The Journal of Biological Chemistry*, **282**, 37112–37123.
- Koski, M. K., Hieta, M., Rönkä, A., Myllyharju, J., Wierenga, R.K. (2009) The crystal structure of an algal prolyl 4-hydroxylase complexed with a proline-rich peptide reveals a novel buried tripeptide binding motif. *The Journal of Biological Chemistry*, **284**, 25290–25301.
- Kremer, C., Pettolino, F., Bacic, A., Drinnan, A. (2004) Distribution of cell wall components in *Sphagnum* hyaline cells and in liverwort and hornwort elaters. *Planta*, **219**, 1023–1035.
- Kulkarni, A. R., Peña, M. J., Avci, U. (2012) The ability of land plants to synthesize glucuronoxylans predates the evolution of tracheophytes. *Glycobiology*, **22**, 439–451.
- Lamport, D. T. A. & Varnai, P. (2013) Periplasmic arabinogalactan glycoproteins act as a calcium capacitor that regulates plant growth and development. *New Phytologist*, **197**, 58–64.
- Lamport, D. T. A., Varnai, P., Seal, C. E. (2014) Back to the future with the AGP–Ca²⁺ flux capacitor. *Annals of Botany*, **114**, 1069–1085.
- Lamport, D. T. A. (2023) The growth oscillator and plant stomata: an open and shut case. *Plants*, **12**, 2531.
- Lampugnani, E. R., Khan, G. A., Somssich, M., Persson, S. (2018) Building a plant cell wall at a glance. *Journal of Cell Science*, **131**, jcs207373.
- Lang, D., Ullrich, K. K., Murat, F., Fuchs, J., Jenkins, J., Haas, F. B. *et al.* (2018) The *Physcomitrella patens* chromosome-scale assembly reveals moss genome structure and evolution. *The Plant Journal*, **93**, 515–533.
- Leebens-Mack, J. H., Barker, M. S., Carpenter, E. J., Deyholos, M. K., Gitzendanner, M. A., Graham, S. W. *et al.* (2019) One thousand plant transcriptomes and the phylogenomics of green plants. *Nature*, **574**, 679–685.
- Lee, K. J. D., Sakata, Y., Mau, S.-L., Pettolino, F., Bacic, A., Quatrano, R. S. *et al.* (2005) Arabinogalactan proteins are required for apical cell extension in the moss *Physcomitrella patens*. *The Plant Cell*, **17**, 3051–3065.
- Leroux, O., Knox, J. P., Masschaele, B., Bagniewska-Zadworna, A., Marcus, S. E., Claeys, M. *et al.* (2011) An extensin-rich matrix lines the carinal canals in *Equisetum ramosissimum*, which may function as water-conducting channels. *Annals of Botany*, **108**, 307–319.
- Leroux, O., Eeckhout, S., Viane, R. L. L., Popper, Z. A. (2013a) *Ceratopteris richardii* (C-fern): A model for investigating adaptive modification of vascular plant cell walls. *Frontiers in Plant Science*, **4**, 367.
- Leroux, O., Leroux, F., Mastroberti, A. A., Santos-Silva, F., Van Loo, D., Bagniewska-Zadworna, A. *et al.* (2013b) Heterogeneity of silica and glycan-epitope distribution in epidermal idioblast cell walls in *Adiantum raddianum* laminae. *Planta*, **237**, 1453–1464.
- Leroux, O., Sorensen, I., Marcus, S. E., Viane, R. L., Willats, W. G., Knox, J. P. (2015) Antibody-based screening of cell wall matrix glycans in ferns reveals taxon, tissue and cell-type specific distribution patterns. *BMC Plant Biology*, **15**, 56.
- Leszczuk, A., Szczuka, E., Zdunek, A. (2019) Arabinogalactan proteins: distribution during the development of male and female gametophytes. *Plant Physiology and Biochemistry*, **135**, 9–18.
- Leszczuk, A., Kalaitzis, P., Kulik, J., Zdunek, A. (2023) Review: structure and modifications of arabinogalactan proteins (AGPs). *BMC Plant Biology*, **23**, 45.
- Leterme, P., Londoño, A. M., Muñoz, J. E., Suárez, J., Bedoya, C. A., Souffrant, W. b. Buldgen, A. (2009) Nutritional value of aquatic ferns (*Azolla filiculoides* LAM. and *Salvinia molesta* MITCHELL) in pigs. *Animal Feed Science and Technology*, **149**, 135–148.
- Letunic, I. & Bork, P. (2021) Interactive tree of life (iTOL) v5: an online tool for phylogenetic tree display and annotation. *Nucleic Acids Research*, **49**, W293–W296.
- Lewis, N. G. & Yamamoto, E. (1990) Lignin: Occurrence, biogenesis and biodegradation. *Annual Review of Plant Physiology and Plant Molecular Biology*, **41**, 455–496.
- Lex, A., Gehlenborg, N., Strobel, H., Vuilleumot, R. & Pfister, H. (2014) UpSet: Visualization of intersecting sets. *IEEE Transactions on Visualization and Computer Graphics*, **20**, 1983–1992.
- Li, J., Burton, R. A., Harvey, A. J., Hrmova, M., Wardak, A. Z., Stone, B. A. *et al.* (2003) Biochemical evidence linking a putative callose synthase gene with (1→3)-β-D-glucan biosynthesis in barley. *Plant Molecular Biology*, **53**, 213–225.
- Li, F.-W., Brouwer, P., Carretero-Paulet, L., Cheng, S., de Vries, J., Delaux, P.-M. *et al.* (2018) Fern genomes elucidate land plant evolution and cyanobacterial symbioses. *Nature Plants*, **4**, 460–472.

- Li, J., Nishiyama, T., Waller M., Frangedakis, E., Keller, J., Li, Z. *et al.* (2020) *Anthoceros* genomes illuminate the origin of land plants and the unique biology of hornworts. *Nature Plants*, **6**, 259–272.
- Liepman, A. H., Wilkerson, C. G., Keegstra, K. (2005) Expression of cellulose synthase-like (Csl) genes in insect cells reveals that CslA family members encode mannan synthases. *Proceedings of the National Academy of Sciences*, **102**, 2221–2226.
- Liepman, A. H., Nairn, C. J., Willats, W. G. T., Sørensen, I., Roberts, A. W., Keegstra, K. (2007) Functional genomic analysis supports conservation of function among cellulose synthase-like a gene family members and suggests diverse roles of mannans in plants. *Plant Physiology*, **143**, 1881–1893.
- Ligrone, R., Vaughn, K. C., Renzaglia, K. S., Knox, J. P., Duckett, J. G. (2002) Diversity in the distribution of polysaccharide and glycoprotein epitopes in the cell walls of bryophytes: new evidence for the multiple evolution of water-conducting cells. *New Phytologist*, **156**, 491–508.
- Ligrone, R., Carafa, A., Duckett, J. G., Renzaglia, K. S., Ruel, K. (2008) Immunocytochemical detection of lignin-related epitopes in cell walls in bryophytes and the charalean alga *Nitella*. *Plant Systematics and Evolution*, **270**, 257–272.
- Ligrone, R., Duckett, J. G., Renzaglia, K. S. (2012) Major transitions in the evolution of early land plants: a bryological perspective. *Annals of Botany*, **109**, 851–871.
- Liu, X., Wang, S., Cao, S., He, Q., He, M. *et al.* (2018) Structural characteristics and anticoagulant property in vitro and in vivo of a seaweed sulfated rhamnan. *Marine drugs*, **16**, 243.
- Liu, J., Shao, Y., Feng, X., Oti, V., Matsuura, A., Irshad, M., Zheng, Y., An, P. (2022) Cell wall components and extensibility regulate root growth in *Sueda salsa* and *Spinacia oleracea* under salinity. *Plants*, **11**, 900.
- Lloys, R. M. (1974) Systematics of the genus *Ceratopteris* BRONGN. (Parkeriaceae) II. Taxonomy. *Brittonia*, **26**, 139–160.
- Lopez, R. A. & Renzaglia, K. S. (2014) Multiflagellated sperm cells of *Ceratopteris richardii* are bathed in arabinogalactan proteins throughout development. *American Journal of Botany*, **101**, 2052–2061.
- Lopez, R. A. & Renzaglia, K. S. (2016) Arabinogalactan proteins and arabinan pectins abound in the specialized matrices surrounding female gametes of the fern *Ceratopteris richardii*. *Planta*, **243**, 947–957.
- Loyal, D. S. & Grewal, R. K. (1966) Cytological study on sterility in *Salvinia auriculata* AUBLET with a bearing on its reproductive mechanism. *Cytologia*, **31**, 330–338.
- Lu, S., Wang, J., Chitsaz, F., Derbyshire, M. K., Geer, R. C., Gonzales, N. R. *et al.* (2020) CDD/SPARCLE: the conserved domain database in 2020. *Nucleic Acids Research*, **48**, D265–D268.
- Matsunaga, T., Ishii, T., Matsumoto, S., Higuchi, M., Darvill, A., Albersheim, P., *et al.* (2004) Occurrence of the primary cell wall polysaccharide rhamnogalacturonan II in pteridophytes, lycophytes, and bryophytes. Implications for the evolution of vascular plants. *Plant Physiology*, **134**, 339–351.
- Ma, Y., Yan, C., Li, H., Wu, W., Liu, Y., Wang, Y. *et al.* (2017) Bioinformatics prediction and evolution analysis of arabinogalactan proteins in the plant kingdom. *Frontiers in Plant Science*, **8**, 66.
- Ma, Y., Zeng, W., Bacic, A., Johnson, K. (2018) AGPs through time and space. In: Roberts, J. A., ed. *Annual Plant Reviews online*. Hoboken, NJ: John Wiley & Sons, Ltd. Available from: <https://doi.org/10.1002/9781119312994.apr0608>
- Ma, Y., MacMillan, C.P., de Vries, L., Mansfield, S., Hao, P., Ratcliffe, J., *et al.* (2022) FLA11 and FLA12 glycoproteins fine-tune stem secondary wall properties in response to mechanical stresses. *New Phytologist*, **233**, 1750–1767.
- Maeda, H. & Ishida, N. (1967) Specificity of binding of hexopyranosyl polysaccharides with fluorescent brightener. *The Journal of Biochemistry*, **62**, 276–278.
- Malgas, S., Van Dyk, J. S., Pletschke, B. I. (2015) A review of the enzymatic hydrolysis of mannans and synergistic interactions between β -mannanase, β -mannosidase and α -galactosidase. *World Journal of Microbiology and Biotechnology*, **31**, 1167–1175.
- Marchant, D. B., Chen, G., Cai, S., Chen, F., Schafran, P., Jenkins, J. *et al.* (2022) Dynamic genome evolution in a model fern. *Nature Plants*, **8**, 1038–1051.
- Marcus, S. E., Verhertbruggen, Y., Hervé, C., Ordaz-Ortiz, J. J., Farkas, V., Pedersen, H. L., *et al.* (2008) Pectic homogalacturonan masks abundant sets of xyloglucan epitopes in plant cell walls. *BMC Plant Biology*, **8**, 60.
- Marcus, S. E., Blake, A. W., Benians, T. A. S., Lee, K. J. D., Poyser, C., Donaldson, L. *et al.* (2010) Restricted access of proteins to mannan polysaccharides in intact plant cell walls. *The Plant Journal*, **64**, 191–203.
- Mareri, L., Romi, M., Cai, G. (2018) Arabinogalactan proteins: actors or spectators during abiotic and biotic stress in plants? *Plant Biosystems*, **153**, 173–185.
- Marks, S. A., Hotaling, S., Frandsen, P. B., VanBuren, R. (2021) Representation and participation across 20 years of plant genome sequencing. *Nature Plants*, [Doi.org/10.1038/s41477-021-01031-8](https://doi.org/10.1038/s41477-021-01031-8).
- Martone, P. T., Estevez, J. M., Lu, F., Ruel, K., Denny, M. W., Somerville, C. *et al.* (2009) Discovery of lignin in seaweed reveals convergent evolution of cell-wall architecture. *Current Biology*, **19**, 169–175.
- Matsunaga, T., Ishii, T., Matsumoto, S., Higuchi, M., Darvill, A., Albersheim, P., *et al.* (2004) Occurrence of the primary cell wall polysaccharide rhamnogalacturonan II in pteridophytes, lycophytes, and bryophytes. Implications for the evolution of vascular plants. *Plant Physiology*, **134**, 339–351.

- McCartney, L., Marcus, S. E., Knox, J. P. (2005) Monoclonal antibodies to plant cell wall xylans and arabinoxylans. *Journal of Histochemistry & Cytochemistry*, **53**, 543–546.
- McCourt, R. M., Delwiche, C. F., Karol, K. G. (2004) Charophyte algae and land plant origins. *Trends in Ecology and Evolution*, **19**, 661–666.
- McCourt, R. M., Lewis, L. A., Strother, P. K., Delwiche, C. F., Wickett, N. J., de Vries, J. *et al.* (2023) Green land: multiple perspectives on green algal evolution and the earliest land plants. *American Journal of Botany*, **110**, e16175.
- McFarland, D. G., Nelson, L. S., Grodowitz, M. J., Smart, R. M. Owens, C. S. (2004) *Salvinia molesta* D. S. MITCHELL (Giant *Salvinia*) in the United States: a review of species ecology and approaches to management. *Environmental Laboratory*, U.S. Army Engineer Research and Development Center, Vicksburg, MS, ERDC/EL SR-04-2.
- Meikle, P. J., Bonig, I., Hoogenraad, N. J., Clarke, A. E., Stone, B. A. (1991) The location of (1→3)-β-glucan-specific monoclonal antibody. *Planta*, **185**, 1–8.
- Meikle, P. J., Hoogenraad, N. J., Bonig, I., Clarke, A. E., Stone, B. A. (1994) A (1→3,1→4)-β-glucan-specific monoclonal antibody and its use in the quantitation and immunocytochemical location of (1→3,1→4)-β-glucans. *The Plant Journal*, **4**, 1–9.
- Merced, A. & Renzaglia, K. S. (2019) Contrasting pectin polymers in guard cell walls of *Arabidopsis* and the hornwort *Phaeoceros* reflect physiological differences. *Annals of Botany*, **123**, 579–585.
- Mikkelsen, M. D., Harholt, J., Ulvskov, P., Johansen, I. E., Fangel, J. U., Doblin, M. S. *et al.* (2014) Evidence for land plant cell wall biosynthetic mechanisms in charophyte green algae. *Annals of Botany*, **114**, 1217–1236.
- Mikkelsen, M. D., Harholt, J., Westereng, B., Domozych, D., Fry, S. C., Johansen, I. E. *et al.* (2021) Ancient origin of fucosylated xyloglucan in charophycean green algae. *Communications Biology*, **4**, 754.
- Miller, D. H., Lampert, D. T. A., Miller, M. (1972) Hydroxyproline heterooligosaccharides in *Chlamydomonas*. *Science*, **176**, 918–920.
- Miranda, C. V. & Schwartzburd, P. B. (2016) Aquatic ferns from Viçosa (MG, Brazil): Salviniaceae (Filicopsida; Tracheophyta). *Brazilian Journal of Botany*, **39**, 935–942.
- Miranda, C. V. & Schwartzburd, P. B. (2019) *Salvinia* (Salviniaceae) in southern and southeastern Brazil—including new taxa, new distribution records, and new morphological characters. *Brazilian Journal of Botany*, **42**, 171–188.
- Mitchell, D. S. & Thomas, P. A. (1972) Ecology of water weeds in the neotropics. *UNESCO Technical Papers in Hydrology, United Nations Educational, Scientific and Cultural Organization, Paris, France*, **12**, 1–50.
- Mitchell, D. S. & Tur, N. M. (1975) The rate of growth of *Salvinia molesta* (S. auriculata AUCT.) in laboratory and natural conditions. *Journal of Applied Ecology*, **12**, 213–225.
- Mócsai, R., Göritzer, K., Stenitzer, D., Maresch, D., Strasser, R., Altmann, F. (2021) Prolyl hydroxylase paralogs in *Nicotiana benthamiana* show high similarity with regard to substrate specificity. *Frontiers in Plant Science*, **12**, 63659.
- Mohnen, D. (2008) Pectin structure and biosynthesis. *Current Opinion in Plant Biology*, **11**, 266–277.
- Moller, I., Sørensen, I., Bernal, A. I., Blaukopf, C., Lee, K., Øbro, J. *et al.* (2007) High-throughput mapping of cell-wall polymers within and between plants using novel microarrays. *The Plant Journal*, **50**, 1118–1128.
- Moore, J. P., Nguema-Ona, E. E., Vicré-Gibouin, M., Sørensen, I. Willats, W. G. T., Driouich, A., *et al.* (2013) Arabinose-rich polymers as an evolutionary strategy to plasticize resurrection plant cell walls against desiccation. *Planta*, **237**, 739–754.
- Morris, J. L., Puttick, M. N., Clark, J. W., Edwards, D., Kenrick, P., Pressel, S. *et al.* (2018) The timescale of early land plant evolution. *Proceedings of the National Academy of Sciences*, **115**, E2274–E2283. doi: 10.1073/pnas.1719588115.
- Morrison, J. C., Greve, L. C., Richmond, P. A. (1993) Cell wall synthesis during growth and maturation of *Nitella* internodal cells. *Planta*, **189**, 321–328.
- Motitsoe, S. N., Coetzee, J. A., Hill, J. M., Hill, M. P. (2020) Biological control of *Salvinia molesta* (D.S. MITCHELL) drives aquatic ecosystem recovery. *Diversity*, **12**, 204.
- Motose, H., Sugiyama, M., Fukuda, H. (2004) A proteoglycan mediates inductive interaction during plant vascular development. *Nature*, **429**, 873–878.
- Moussu, S. & Ingram, G. (2023) The EXTENSIN enigma. *The Cell Surface*, **9**, 100094.
- Mueller, K.-K., Pfeifer, L., Schuldt, L., Szövényi, P., de Vries, S., de Vries, J. *et al.* (2023) Fern cell walls and the evolution of arabinogalactan proteins in streptophytes. *The Plant Journal*, **114**, 875–894.
- Nagalingum, N. S., Schneider, H., Pryer, K. M. (2006) Comparative morphology of reproductive structures in heterosporous water ferns and a reevaluation of the sporocarp. *International Journal of Plant Sciences*, **167**, 805–815.
- Narciso, J. O., Zeng, W., Ford, K., Lampugnani, E. R., Humphries, J., Austarheim, I. *et al.* (2021) Biochemical and functional characterization of GALT8, an *Arabidopsis* GT31 β-(1,3)-galactosyltransferase that influences seedling development. *Frontiers in Plant Science*, **12**, 678564.
- Navarro, D. A. & Stortz, C. A. (2008) The system of xylogalactans from the red seaweed *Jania rubens* (Corallinales, Rhodophyta). *Carbohydrate Research*, **343**, 2613–2622.

- Nibbering, P., Castilleux, R., Wingsle, G., Niittylä, T. (2022) CAGEs are golgi-localized GT31 enzymes involved in cellulose biosynthesis in *Arabidopsis*. *The Plant Journal*, **110**, 1271–1285.
- Niklas, K. J. (2004) The cell walls that bind the tree of life. *BioScience*, **54**, 831–841.
- Nishiyama, T., Wolf, P. G., Kugita, M., Sinclair, R. B., Sugita, M., Sugiura, C. *et al.* (2004) Chloroplast phylogeny indicates that bryophytes are monophyletic. *Molecular Biology and Evolution*, **21**, 1813–1819.
- Nishiyama, T., Sakayama, H., de Vries, J., Buschmann, H., Saint-Marcoux, D., Ullrich, K. K. *et al.* (2018) The *Chara* genome: secondary complexity and implications for plant terrestrialization. *Cell*, **174**, 448–464.e24.
- Nitta, J. H., Schuettelpelz, E., Ramírez-Barahona, S., Iwasaki, W. (2022) An open and continuously updated fern tree of life. *Frontiers in Plant Science*, **13**, 909768.
- Ogawa, K., Yamaura, M., Maruyama, I. (1994) Isolation and identification of 3-*O*-methyl-D-galactose as a constituent of neutral polysaccharide of *Chlorella vulgaris*. *Bioscience, Biotechnology, and Biochemistry*, **58**, 942–944.
- Ogawa, K., Yamaura, M. and Maruyama, I. (1997) Isolation and identification of 2-*O*-methyl-L-rhamnose and 3-*O*-methyl-L-rhamnose as constituents of an acidic polysaccharide of *Chlorella vulgaris*. *Bioscience, Biotechnology, and Biochemistry*, **61**, 539–540.
- Ogawa, K., Arai, M., Naganawa, H., Ikeda, Y., Kondo, S. (2001) A new β -D-galactan having 3-*O*-methyl-D-galactose from *Chlorella vulgaris*. *Journal of Applied Glycoscience*, **48**, 325–330.
- Ogawa-Ohnishi, M. & Matsubayashi, Y. (2015) Identification of three potent hydroxyproline O-galactosyltransferases in *Arabidopsis*. *The Plant Journal*, **81**, 736–746.
- Oliver, J. D. (1993) A review of the biology of Giant *Salvinia* (*Salvinia molesta* MITCHELL). *Journal of Aquatic Plant Management*, **31**, 227–231.
- O'Neill, M. A., Ishii, T., Albersheim, P., Darvill, A. G. (2004) Rhamnogalacturonan II: structure and function of a borate cross-linked cell wall pectic polysaccharide. *Annual Review Plant Biology*, **55**, 109–139.
- O'Rourke, C., Gregson, T., Murray, L., Sadler, I.H., Fry, S.C. (2015) Sugar composition of the pectic polysaccharides of charophytes, the closest algal relatives of land-plants: presence of 3-*O*-methyl-D-galactose residues. *Annals of Botany*, **116**, 225–236.
- Palacio-López, K., Tinaz, B., Holzinger, A., Domozych, D. S. (2019) Arabinogalactan proteins and the extracellular matrix of charophytes: a sticky business. *Frontiers in Plant Science*, **10**, 447.
- Pattathil, S., Avci, U., Baldwin, D., Swennes, A. G., McGill, J. A., Popper, Z. *et al.* (2010) A comprehensive toolkit of plant cell wall glycan-directed monoclonal antibodies. *Plant Physiology*, **153**, 514–525.
- Paulsen, B.S., Craik, D. J., Dunstan, D. E., Stone, B. A., Bacic, A. (2014) The Yariv reagent: behaviour in different solvents and interaction with a gum arabic arabinogalactan-protein. *Carbohydrate Polymers*, **106**, 460–468.
- Paunović, D. M., Ćuković, K. B., Bogdanović, M. D., Todorović, S. I., Trifunović-Momčilov, M. M., Subotić, A. R. *et al.* (2021) The arabinogalactan protein family of *Centaurium erythraea* Rafn. *Plants*, **10**, 1870.
- Pedersen, H. L., Fangel, J. U., McCleary, B., Ruzanski, C., Rydahl, M. G., Ralet, M.-C. *et al.* (2012) Versatile high-resolution oligosaccharide microarrays for plant glycobiology and cell wall research. *Journal of Biological Chemistry*, **287**, 39429–39438.
- Pennell, R. I., Janniche, L., Kjellbom, P., Scofield, G., N., Peart, J. M., Roberts, K. (1991) Developmental regulation of a plasma membrane arabinogalactan protein epitope in oilseed rape flowers. *The Plant Cell*, **3**, 1317–1326.
- Penning, B. W., McCann, M. C., Carpita, N. C. (2019) Evolution of the cell wall gene families of grasses. *Frontiers in Plant Science*, **10**, 1205.
- Peña, M. J., Darvill, S. G., Eberhard, S., York, W. S., O'Neill, M. A. (2008) Moss and liverwort xyloglucans contain galacturonic acid and are structurally distinct from the xyloglucans synthesized by hornworts and vascular plants. *Glycobiology*, **18**, 891–904.
- Peña, M. J., Kong, Y., York, W. S., O'Neill, M. A. (2012) A galacturonic acid-containing xyloglucan is involved in *Arabidopsis* root hair tip growth. *Plant Cell*, **24**, 4511–4524.
- Peña, M. J., Kulkarni, A. R., Backe, J., Boyd, M., O'Neill, M. A., York, W. S. (2016) Structural diversity of xylans in the cell walls of monocots. *Planta*, **244**, 589–606.
- Permann, C., Herburger, K., Felhofer, M., Gierlinger, N., Lewis, L.A., Holzinger, A. (2021a) Induction of conjugation and zygosporangium cell wall characteristics in the alpine *Spirogyra mirabilis* (Zygnematophyceae, Charophyta): Advantage under climate change scenarios? *Plants*, **10**, 1740.
- Permann, C., Herburger, K., Niedermeier, M., Felhofer, M., Gierlinger, N. and Holzinger, A. (2021b) Cell wall characteristics during sexual reproduction of *Mougeotia* sp. (Zygnematophyceae) revealed by electron microscopy, glycan microarrays and RAMAN spectroscopy. *Protoplasma*, **258**, 1261–1275.
- Pettolino, F.A., Hoogenraad, N. J., Ferguson, C., Bacic, A., Johnson, E., Stone, B. A. (2001) A (1→4)-beta-mannan-specific monoclonal antibody and its use in the immunocytochemical location of galactomannans. *Planta*, **214**, 235–242.
- Pfeifer, L. & Classen, B. (2020) Validation of a rapid GC-MS procedure for quantitative distinction between 3-*O*-methyl- and 4-*O*-methyl-hexoses and its application to a complex carbohydrate sample. *Separations*, **7**, 42.

- Pfeifer, L., Shafee, T., Johnson, K. L., Bacic, A., Classen, B. (2020) Arabinogalactan-proteins of *Zostera marina* L. contain unique glycan structures and provide insight into adaption processes to saline environments. *Scientific Reports*, **10**, 8232.
- Pfeifer, L., Mueller, K.-K., Classen, B. (2022) The cell wall of hornworts and liverworts: innovations in early land plant evolution?. *Journal of Experimental Botany*, **73**, 4454–4472.
- Pfeifer, L., Utermöhlen, J., Happ, K., Permann, C., Holzinger, A., von Schwartzberg, K. et al. (2022) Search for evolutionary roots of land plant arabinogalactan-proteins in charophytes: presence of a rhamnogalactan-protein in *Spirogyra pratensis* (Zygnematophyceae). *The Plant Journal*, **109**, 568–584.
- Pfeifer, L., Mueller, K.-K., Utermöhlen, J., Erdt, F., Zehge, J. B. J., Schubert, H. et al. (2023) The cell walls of different *Chara* species are characterized by branched galactans rich in 3-*O*-methylgalactose and absence of AGPs. *Physiologia Plantarum*, 175:e13989.
- Pires, N. D. & Dolan, L. (2012) Morphological evolution in land plants: new designs with old genes. *Philosophical Transactions of the royal society*, **367**, 508–518.
- Piršelová, B. & Matušíková, I. (2013) Callose: the plant cell wall polysaccharide with multiple biological functions. *Acta Physiologiae Plantarum*, **35**, 635–644.
- Plackett, A. R. G., Rabbínawitsch, E. H., Langdale, J. A. (2015) Protocol: genetic transformation of the fern *Ceratopteris richardii* through microparticle bombardment. *Plant Methods*, **11**, 37.
- Popper, Z.A., Sadler, I. H., Fry, S.C. (2001) 3-*O*-methyl-D-galactose residues in lycophyte primary cell walls. *Phytochemistry*, **57**, 711–719.
- Popper, Z. A. & Fry, S. C. (2003) Primary cell wall composition of bryophytes and charophytes. *Annals of Botany*, **91**, 1–12.
- Popper, Z. A. & Fry, S. C. (2004) Primary cell wall composition of pteridophytes and spermatophytes. *New Phytologist*, **164**, 165–174.
- Popper, Z. A., Sadler, I. H., Fry, S. C. (2003) α -D-Glucuronosyl-(1→3)-l-galactose, an unusual disaccharide from polysaccharides of the hornwort *Anthoceros caucasicus*. *Phytochemistry*, **64**, 325–335.
- Popper, Z. A., Sadler, I. H., Fry, S. C. (2004) 3-*O*-Methylrhamnose in lower land plant primary cell walls. *Biochemical Systematics and Ecology*, **32**, 279–289.
- Popper, Z. A. (2006) The cell walls of pteridophytes and other green plans – a review. *Fern Gazette*, **17**, 247–257.
- Popper, Z. A. (2008) Evolution and diversity of green plant cell walls. *Current Opinion in Plant Biology*, **11**, 286–292.
- Popper, Z. A. & Tuohy, M. G. (2010). Beyond the green: understanding the evolutionary puzzle of plant and algal cell walls. *Plant Physiology*, **153**, 373–383.
- Popper, Z. A., Michel, G., Hervé, C., Domozych, D. S., Willats, W. G. T., Tuohy, M. G. et al. (2011) Evolution and diversity of plant cell walls: from algae to flowering plants. *Annual Review of Plant Biology*, **62**, 567–590.
- Přerovská, T., Henke, S., Bleha, R., Spiwok, V., Gillarová, S., Yvin, J.-C. et al. (2021) Arabinogalactan-like glycoproteins from *Ulva lactuca* (Chlorophyta) show unique features compared to land plants AGPs. *Journal of Phycology*, **57**, 619–635.
- Proseus, T. E. & Boyer, J. S. (2006) Calcium pectate chemistry controls growth rate of *Chara corallina*. *Journal of Experimental Botany*, **57**, 3989–4002.
- Pryer, K. M., Schuettpehl, E., Wolf, P. G., Schneider, H., Smith, A. R., Cranfill, R. (2004) Phylogeny and evolution of ferns (monilophytes) with a focus on the early leptosporangiate divergences. *American Journal of Botany*, **91**, 1582–1598.
- Pteridophyte Phylogeny Group I (PPG). (2016) A community-derived classification for extant lycophytes and ferns. *Journal of Systematics and Evolution*, **54**, 563–603. doi: 10.1111/jse.12229
- Puhlmann, J., Bucheli, E., Swain, M. J., Dunning, N., Albersheim, P., Darvill, A. G. et al. (1994) Generation of monoclonal antibodies against plant cell wall polysaccharides. I. Characterization of a monoclonal antibody to a terminal α -(1→2)-linked fucosyl-containing epitope. *Plant Physiology*, **104**, 699–710.
- Puttick, M. N., Morris, J. L., Williams, T. A., Cox, C. J., Edwards, D., Kenrick, P. et al. (2018) The interrelationship of land plants and the nature of the ancestral embryophyte. *Current Biology*, **28**, 733–745.
- Pryer, K. M., Schuettpehl, E., Wolf, P. G., Schneider, H., Smith, A. R., Cranfill, R. (2004) Phylogeny and evolution of ferns (monilophytes) with a focus on the early leptosporangiate divergences. *American Journal of Botany*, **91**, 1582–1598.
- Qu, Y., Egelund, J., Gilson, P. R., Houghton, F., Gleeson, P. A., Schultz, C. J. et al. (2008) Identification of a novel group of putative *Arabidopsis thaliana* β -(1,3)-galactosyltransferases. *Plant Molecular Biology*, **68**, 43–59.
- Raimundo, S.C., Avci, U., Hopper, C., Pattathil, S., Hahn, M.G., Popper, Z.A. (2016) Immunolocalization of cell wall carbohydrate epitopes in seaweeds: Presence of land plant epitopes in *Fucus vesiculosus* L. (Phaeophyceae). *Planta*, **243**, 337–354.
- Ralet, M.-C., Tranquet, O., Poulain, D., Moïse, A., Guillon, F. (2010). Monoclonal antibodies to rhamnogalacturonan I backbone. *Planta*, **231**, 1373–1383.

- Ralph, J., Lundquist, K., Brunow, G., Lu, F., Kim, H., Schatz, P. F. *et al.* (2004) Lignins: natural polymers from oxidative coupling of 4-hydroxyphenylpropanoids. *Phytochemistry Reviews*, **3**, 29–60.
- Rebaque, D., Del Hierro, I., López, G., Bacete, L., Vilaplana, F., Dallabernardina, P. *et al.* (2021) Cell wall-derived mixed-linked β -1,3/1,4-glucans trigger immune responses and disease resistance in plants. *Plant Journal*, **106**, 601–615.
- Renault, H., Alber, A., Horst, N. A., Basilio Lopes, A., Fich, E. A., Kriegshauser, L. *et al.* (2017) A phenol-enriched cuticle is ancestral to lignin evolution in land plants. *Nature Communications*, **8**, 14713.
- Renault, H., Werck-Reichhart, D., Weng, J.-K. (2019) Harnessing lignin evolution for biotechnological applications. *Current Opinion in Biotechnology*, **56**, 105–111.
- Rencoret, J., Gutiérrez, A., Marques, G., del Rio, J. C., Tobimatsu, Y., Lam, P. Y. *et al.* (2021) New insights on structures forming the lignin-like fractions of ancestral plants. *Frontiers in Plant Science*, **12**, 740923.
- Rensing, S. A., Lang, D., Zimmer, A. D., Terry, A., Salamov, A., Shapiro, H. *et al.* (2008) The *Physcomitrella* genome reveals evolutionary insights into the conquest of land by plants. *Science*, **319**, 64–69.
- Rensing, S.A. (2017) Why we need more non-seed plant models. *New Phytologist*, **216**, 355–360.
- Rensing, S. A., Goffinet, B., Meyberg, R., Wu, S.-Z., Bezanilla, M. (2020) The moss *Physcomitrium* (*Physcomitrella*) *patens*: a model organism for non-seed plants. *The Plant Cell*, **32**, 1361–1376.
- Renzaglia, K. S. & Warne, T.R. (1995). *Ceratopteris*: an ideal model system for teaching plant biology. *International Journal of Plant Sciences*, **156**, 385–392.
- Renzaglia, K. S., Duff, R. J., Nickrent, D. L., Garbary, D. J. (2000) Vegetative and reproductive innovations of early land plants: implications for a unified phylogeny. *Philosophical Transactions of the Royal Society London B*, **355**, 769–793.
- Renzaglia, K. S., Lopez, R. A., Johnson, E. E. (2015) Callose is integral to the development of permanent tetrads in the liverwort *Sphaerocarpos*. *Planta*, **241**, 615–627.
- Renzaglia, K. S., Villarreal, A. J. C., Piatkowski, B. T., Lucas, J. R., Merced, A. (2017) Hornwort stomata: architecture and fate shared with 400-million-year-old fossil plants without leaves. *Plant Physiology*, **174**, 788–797.
- Renzaglia, K. S., Villarreal, A. J. C., Garbary, D. J. (2018) Morphology supports the setaphyte hypothesis: mosses plus liverworts form a natural group. *Bryophyte Diversity and Evolution*, **40**, 11–17.
- Renzaglia, K. S., Lopez, R. A., Welsh, R. D., Owen, H. A., Merced, A. (2020) Callose in sporogenesis: novel composition of the inner spore wall in hornworts. *Plant Systematics and Evolution*, **306**, 16.
- Roberts, A. W., Lahnstein, J., Hsieh, Y. S. Y., Xing, X., Yap, K., Chaves, A. M. *et al.* (2018) Functional characterization of a glycosyltransferase from the moss *Physcomitrella patens* involved in the biosynthesis of a novel cell wall arabinoglucan. *The Plant Cell*, **30**, 1293–1308.
- Rodríguez-Concepción, M., Pérez-García, A., Beltrán, J. P. (2001) Up-regulation of genes encoding novel extracellular proteins during fruit set in pea. *Plant Molecular Biology*, **46**, 373–382.
- Rodríguez-Gacio, M. D. C., Iglesias-Fernández, R., Carbonero, P., Matilla, A. J. (2012) Softening-up the mannan-rich cell walls. *Journal of Experimental Botany*, **63**, 3976–3988.
- Roig-Oliver, M., Douthe, C., Bota, J., Flexas, J. (2021) Cell wall thickness and composition are related to photosynthesis in Antarctic mosses. *Physiologia Plantarum*, **173**, 1914–1925.
- Room, P. M. (1983). 'Falling apart' as a lifestyle: the rhizome architecture and population growth of *Salvinia molesta*. *Journal of Ecology*, **71**, 349–365.
- Room, P. M., Sands, D. P. A., Forno, I. W. Taylor, M. F. J., Julien, M. H. (1985) A summary of research into biological control of *Salvinia* in Australia. *Proceedings of the VI International Symposium on Biological Control of Weeds*, Vancouver, Canada, 19–25. August 1984 (Ed by E. S. Delfosse), Agriculture Canada, Ottawa, 543–549.
- Ruel, K., Faix, O., Joseleau, J. P. (1994) New immunogold probes for studying the distribution of the different lignin types during plant cell wall biogenesis. *Journal of Trace and Microprobe Techniques*, **12**, 247–265.
- Ruhfel, B. R., Gitzendanner, M. A., Soltis, P. S., Soltis, D. E., Burleigh, J. G. (2014) From algae to angiosperms-inferring the phylogeny of green plants (*Viridiplantae*) from 360 plastid genomes. *BMC Evolutionary Biology*, **14**, 23.
- Ruiz-May, E., Sørensen, I., Fei, Z., Zhang, S., Domozych, D. S., Rose, J. K. C. (2018) The secretome and N-glycosylation profiles of the Charophycean green alga, *Penium margaritaceum*, resemble those of embryophytes. *Proteomes*, **6**, 14.
- Ruprecht, C., Bartetzko, M. P., Senf, D., Dallabernadina, P., Boos, I., Andersen, M. C. F. *et al.* (2017) A synthetic glycan microarray enables epitope mapping of plant cell wall glycan-directed antibodies. *Plant Physiology*, **175**, 1094–1104.
- Ruprecht, C., Bartetzko, M. P., Senf, D., Lakhina, A., Smith, P. J., Soto, M. J. *et al.* (2020) A glycan array-based assay for the identification and characterization of plant glycosyltransferases. *Angewandte Chemie International Edition*, **59**, 12493–12498.
- Šamec, D., Plerz, V., Srividya, N., Wüst, M., Lange, B. M. (2019) Assessing chemical diversity in *Psilotum nudum* (L.) BEAUV., a pantropical whisk fern that has lost many of its fern-like characters. *Frontiers in Plant Science*, **10**, 868.

- Sarkar, P., Bosneaga, E., Auer, M. (2009) Plant cell walls throughout evolution: towards a molecular understanding of their design principles. *Journal of Experimental Botany*, **60**, 3615–3635.
- Scheller, H. V., Jensen, J. K., Sørensen, S. O., Harholt, J., Geshi, N. (2007) Biosynthesis of pectin. *Physiologia Plantarum*, **129**, 283–295.
- Scheller, H. V. & Ulvskov, P. (2010) Hemicelluloses. *Annual Review of Plant Biology*, **61**, 263–289.
- Scherp, P., Grotha, R., Kutschera, U. (2001) Occurrence and phylogenetic significance of cytokinesis-related callose in green algae, bryophytes, ferns and seed plants. *Plant Cell Report*, **20**, 143–149.
- Schneider, S. C., Nowak, P., Von Ammon, U., Ballot, A. (2016) Species differentiation in the genus *Chara* (Charophyceae): considerable phenotypic plasticity occurs within homogenous genetic groups. *European Journal of Phycology*, **51**, 282–293.
- Schneider, R., Hanak, T., Persson, S., Voigt, C. A. (2016) Cellulose and callose synthesis and organization in focus, what's new? *Current Opinion in Plant Biology*, **34**, 9–16.
- Schuette, S., Wood, A. J., Geisler, M., Geisler-Lee, J., Ligrone, R., Renzaglia, K. S. (2009) Novel localization of callose in the spores of *Physcomitrella patens* and phylogenomics of the callose synthase gene family. *Annals of Botany*, **103**, 749–756.
- Schuldt, L. (2021) Arabinogalactan-Proteine aus *Azolla* und *Huperzia*: Vergleichende Analytik eines aquatischen Farns und eines terrestrischen Bärlapps. *Master thesis*. CAU Kiel University.
- Schultz, C. J., Johnson, K. L., Currie, G., Bacic, A. (2000) The classical arabinogalactan protein gene family of *Arabidopsis*. *The Plant Cell*, **12**, 1751–1767.
- Seddiqi, H., Oliaei, E., Honarkar, H., Jin, J., Geonzon, L. C., Bacabac, R.G. et al. (2021) Cellulose and its derivatives: towards biomedical applications. *Cellulose*, **28**, 1893–1931.
- Seifert, G. J. & Roberts, K. (2007) The biology of arabinogalactan proteins. *Annual Review of Plant Biology*, **58**, 137–161.
- Seifert, G.J. (2018) Fascinating fasciclins: a surprisingly widespread family of proteins that mediate interactions between the cell exterior and the cell surface. *International Journal of Molecular Sciences*, **19**, 1628.
- Seifert, G. J., Strasser, R., Van Damme, E. J. M. (2021) Editorial: plant glycobiology - a sweet world of glycans, glycoproteins, glycolipids, and carbohydrate-binding proteins. *Frontiers in Plant Science*, **12**, 751923.
- Sekimoto, H., Komiya, A., Truyuki, N., Kawai, J., Kanda, N., Ootsuki, R. et al. (2022) A divergent RWP-RK transcription factor determines mating type in heterothallic *Closterium*. *New Phytologist*, **237**, 1636–1651.
- Shafee, T., Bacic, A., Johnson, K. (2020) Evolution of sequence-diverse disordered regions in a protein family: Order within the chaos. *Molecular Biology and Evolution*, **37**, 2155–2172.
- Shibaya, T., Kaneko, Y., Sugawara, Y. (2005) Involvement of arabinogalactan proteins in protonemata development from cultured cells of *Marchantia polymorpha*. *Physiologia Plantarum*, **124**, 504–514.
- Shibaya, T. & Sugawara, Y. (2007) Involvement of arabinogalactan proteins in the regeneration process of cultured protoplasts of *Marchantia polymorpha*. *Physiologia Plantarum*, **130**, 271–279.
- Shibaya, T. & Sugawara, Y. (2009) Induction of multinucleation by beta-glucosyl Yariv reagent in regenerated cells from *Marchantia polymorpha* protoplasts and involvement of arabinogalactan proteins in cell plate formation. *Planta*, **230**, 581–588.
- Shimamura, M. (2016) *Marchantia polymorpha*: taxonomy, phylogeny and morphology of a model system. *Plant and Cell Physiology*, **57**, 230–256.
- Showalter, A. M., Keppler, B., Lichtenberg, J., Gu, D., Welch, L. R. (2010). A bioinformatics approach to the identification, classification, and analysis of hydroxyproline-rich glycoproteins. *Plant Physiology*, **153**, 485–513.
- Showalter, A. M. & Basu, D. (2016) Glycosylation of arabinogalactan-proteins essential for development in *Arabidopsis*. *Communicative and Integrative Biology*, **5**, e1177687.
- Silva, G. B., Ionashiro, M., Carrara, T. B., Crivellari, A. C., Tine, M. A. S., Prado, J. et al. (2011) Cell wall polysaccharides from fern leaves: evidence for a mannan-rich type III cell wall in *Adiantum raddianum*. *Phytochemistry*, **72**, 2352–2360.
- Silva, J., Ferraz, R., Dupree, P., Showalter, A. M., Coimbra, S. (2020) Three decades of advances in arabinogalactan-protein biosynthesis. *Frontiers in Plant Science*, **11**, 610377.
- Smallwood, M., Yates, E.A., Willats, W.G.T., Martin, H., Knox, J.P. (1996) Immunochemical comparison of membrane-associated and secreted arabinogalactan-proteins in rice and carrot. *Planta*, **198**, 452–459.
- Smith, M. M. & McCully, M. E. (1978) A critical evaluation of the specificity of aniline blue induced fluorescence. *Protoplasma*, **95**, 229–254.
- Smith, J., Yang, Y., Levy, S., Adelusi, O. O., Hahn, M. G., O'Neill, M. A. et al. (2016) Functional characterization of UDP-apiose synthases from bryophytes and green algae provides insight into the appearance of apiose-containing glycans during plant evolution. *The Journal of Biological Chemistry*, **291**, 21434–21447.
- Smith, P. J., Wang, H.-T., York, W. S., Peña, M. J., Urbanowicz, B. R. (2017) Designer biomass for next-generation biorefineries: leveraging recent insights into xylan structure and biosynthesis. *Biotechnology for Biofuels*, **10**, 286.
- Somerville, C., Bauer, S., Brininstool, G., Facette, M., Hamann, T., Milne, J. et al. (2004) Toward a systems approach to understanding plant cell walls. *Science*, **306**, 2206.

- Sørensen, I., Pettolino, F. A., Wilson, S. M., Doblin, M. S., Johansen, B., Bacic, A. *et al.* (2008) Mixed-linkage (1→3), (1→4)-β-D-glucan is not unique to the Poales and is an abundant component of *Equisetum arvense* cell walls. *The Plant Journal*, **54**, 510–521.
- Sørensen, I., Domozych, D. S., Willats, W. G. T. (2010) How have plant cell walls evolved?. *Plant Physiology*, **153**, 366–372.
- Sørensen, I., Pettolino, F. A., Bacic, A., Ralph, J., Lu, F., O'Neill, M. A. *et al.* (2011) The charophycean green algae provide insights into the early origins of plant cell walls. *The Plant Journal*, **68**, 201–211.
- Speelman, E. N., Van Kempen, M. M. L., Barke, J., Brinkhuis, H., Reichart, G. J., Smolders, A. J. P. *et al.* (2009) The eocene erctic *Azolla* bloom: environmental conditions, productivity and carbon drawdown. *Geobiology*, **7**, 155–170.
- Staudacher, E. (2012) Methylation – an uncommon modification of glycans. *Biological Chemistry*, **393**, 675–685.
- Steffan, W., Kováč, P., Albersheim, P., Darvill, A. G., Hahn, M. G. (1995) Characterization of a monoclonal antibody that recognizes an arabinosylated (1→6)-β-D-galactan epitope in plant complex carbohydrates. *Carbohydrate Research*, **275**, 295–307.
- Stegemann, H. & Stalder, K. (1967) Determination of hydroxyproline. *Clinica Chimica Acta*, **18**, 267–273.
- Steiner, P., Obwegeser, S., Wanner, G., Buchner, O., Lütz-Meindl, U., Holzinger, A. (2020) Cell wall reinforcements accompany chilling and freezing stress in the streptophyte green alga *Klebsormidium crenulatum*. *Frontiers in Plant Science*, **11**, 873.
- Strasser, R., Seifert, G., Doblin, M. S., Johnson, K. L., Ruprecht, C., Pfrengle, F., *et al.* (2021) Cracking the “sugar code”: a snapshot of N- and O-glycosylation pathways and functions in plants. *Frontiers in Plant Science*, **12**, 640919.
- Su, D., Yang, L., Shi, X., Ma, X., Zhou, X., Hedges, S. B. *et al.* (2021) Large-scale phylogenomic analyses reveal the monophyly of bryophytes and neoproterozoic origin of land plants. *Molecular Biology and Evolution*, **38**, 3332–3344.
- Suzuki, T., Narciso, J. O., Zeng, W., Van de Meene, A., Yasutomi, M., Takemura, S. *et al.* (2017) KNS4/UPEX1: a type II arabinogalactan β-(1,3)-galactosyltransferase required for pollen exine development. *Plant Physiology*, **173**, 183–205.
- Suzuki, K. & Terasawa, M. (2020) Biological activities of rhamnan sulfate extracts from the green algae *Monostroma nitidum*. *Marine Drugs* **18**, 228.
- Szövényi, P., Frangedakis, E., Ricca, M., Quandt, D., Wicke, S., Langdale, J. A. (2015) Establishment of *Anthoceros agrestis* as a model species for studying the biology of hornworts. *BMC Plant Biology*, **15**, 98.
- Takenaka, Y., Kato, K., Ogawa-Ohnishi, M., Tsuruhama, K., Kajiura, H., Yagyu, K. *et al.* (2018) Pectin RG-I rhamnosyltransferases represent a novel plant-specific glycosyltransferase family. *Nature Plants*, **4**, 669–676.
- Taylor, R. L. & Conrad, H. E. (1972) Stoichiometric depolymerization of polyuronides and glycosaminoglycuronans to monosaccharides following reduction of their carbodiimide-activated carboxyl groups. *Biochemistry*, **11**, 1383–1388.
- Thomas, R. J. (1977) Wall analyses of *Lophocolea seta* cells (bryophyta) before and after elongation. *Plant Physiology*, **59**, 337–340.
- Thompson, E. W. & Preston, R. D. (1967) Proteins in the cell walls of some green algae. *Nature*, **213**, 684–685.
- Thude, S. & Classen, B. (2005) High molecular weight constituents from roots of *Echinacea pallida*: An arabinogalactan-protein and an arabinan. *Phytochemistry*, **66**, 1026–1032.
- Timme, R. E., Bachvaroff, T. R., Delwiche, C. F. (2012) Broad phylogenomic sampling and the sister lineage of land plants. *Public Library of Science One*, **7**, e29696. doi: 10.1371/journal.pone.0029696.
- Timmings, A., Saint-André, M., de Visser, S. P. (2017) Understanding how prolyl-4-hydroxylase structure steers a ferryl oxidant toward scission of a strong C–H bond. *Journal of the American Chemical Society*, **139**, 9855–9866.
- Tryfona, T., Sorieul, M., Feijao, C., Stott, K., Rubtsov, D. V., Anders, N. *et al.* (2019) Development of an oligosaccharide library to characterise the structural variation in glucuronarabinoxylan in the cell walls of vegetative tissues in grasses. *Biotechnology for Biofuel*, **12**, 109.
- Tryfona, T., Liang, H.-C., Kotake, T., Tsumuraya, Y., Stephens, E., Dupree, P. (2012) Structural characterization of *Arabidopsis* leaf arabinogalactan polysaccharides. *Plant Physiology*, **160**, 653–666.
- Urbaniak, J. & M. Gąbka (2014) Polish Charophytes: an illustrated guide to identification. *Uniwersytet Przyrodniczy we Wrocławiu*, Wrocław, Poland, 1–122.
- Valavan, R. E., Mayilsamy, M., and Rajendran, A. (2016). *Psilotum nudum*: a new medicinal pteridophyte record for the cryptogamic flora of sirumalai hills, Dindigul district, Tamilnadu, India. *Shanlax International Journal of Arts, Science and Humanities*, **3**, 48–52.
- Velasquez, S. M., Ricardi, M. M., Poulsen, C. P., Oikawa, A., Dilokpimol, A., Halim, A. *et al.* (2015) Complex regulation of prolyl-4-hydroxylases impacts root hair expansion. *Molecular Plant*, **8**, 734–746.
- Verhertbruggen, Y., Marcus, S.E., Haeger, A., Verhoef, R., Schols, H.A., McCleary, B.V. *et al.* (2009a) Developmental complexity of arabinan polysaccharides and their processing in plant cell walls. *The Plant Journal*, **59**, 413–425.

- Verhertbruggen, Y., Marcus, S. E., Haeger, A., Ordaz-Ortiz, J. J., Knox, J. P. (2009b) An extended set of monoclonal antibodies to pectic homogalacturonan. *Carbohydrate Research*, **344**, 1858–1862.
- Verhertbruggen, Y., Yin, L., Oikawa, A., Scheller, H. V. (2011) Mannan synthase activity in the CSLD family. *Plant Signaling & Behavior*, **6**, 1620–1623.
- Verma, D.P.S. & Hong, Z. (2001) Plant callose synthase complexes. *Plant Molecular Biology*, **47**, 693–701.
- Vlad, F., Tiainen, P., Owen, C., Spano, T., Daher, F. B., Oualid, F. *et al.* (2010) Characterization of two carnation petal prolyl 4 hydroxylases. *Physiologia Plantarum*, **140**, 199–207.
- Voigt, J., Stolarczyk, A., Zych, M., Malec, P., Burczyk, J. (2014) The cell-wall glycoproteins of the green alga *Scenedesmus obliquus*. The predominant cell wall polypeptide of *Scenedesmus obliquus* is related to the cell-wall glycoprotein gp3 of *Chlamydomonas reinhardtii*. *Plant Science*, **215–216**, 39–47.
- Voiniciuc, C. (2022) Modern mannan: a hemicellulose's journey. *New Phytologist*, **234**, 1175–1184.
- Wachananawat, B., Kuroha, T., Takenaka, Y., Kajiura, H., Naramoto, S., Yokoyama, R. *et al.* (2020) Diversity of pectin rhamnogalacturonan I rhamnosyltransferases in glycosyltransferase family 106. *Frontiers in Plant Science*, **11**, 997.
- Wack, M., Classen, B., Blaschek, W. (2005) An acidic arabinogalactan-protein from the roots of *Baptisia tinctoria* (L.) R. Brown. *Planta Medica*, **71**, 814–818.
- Wagner, A., Tobimatsu, Y., Phillips, L., Flint, H., Geddes, B., Lu, F. *et al.* (2015) Syringyl lignin production in conifers: proof of concept in a pine tracheary element system. *Proceedings of the National Academy of Sciences* **112**, 6218–6223.
- Wang, Q.-H., Zhang, J., Liu, Y., Jia, Y., Jiao, Y.-N., Xu, B. *et al.* (2022) Diversity, phylogeny, and adaptation of bryophytes: insights from genomic and transcriptomic data. *Journal of Experimental Botany*, **73**, 4306–4322.
- Waterhouse, A., Bertoni, M., Bienert, S., Studer, G., Tauriello, G., Gumienny, R. *et al.* (2018) SWISS-MODEL: homology modelling of protein structures and complexes. *Nucleic Acids Research*, **46**, W296–W303.
- Wee, M., Sims, I. M., Goh, K. K. T. (2014) Structure of a shear-thickening polysaccharide extracted from the New Zealand black tree fern, *Cyathea medullaris*. *International Journal of Biological Macromolecules*, **70**, 86–91.
- Weng, J.-K., Li, X., Bonawitz, N. D., Chapple, C. (2008) Emerging strategies of lignin engineering and degradation for cellulosic biofuel production. *Current Opinion in Biotechnology*, **19**, 166–172.
- Wickett, N. J., Mirarab, S., Nguyen, N., Warnow, T., Carpenter, E., Matasci, N. *et al.* (2014) Phylotranscriptomic analysis of the origin and early diversification of land plants. *Proceedings of the National Academy of Sciences of the USA*, **111**, E4859–68.
- Wodniok, S., Brinkmann, H., Glöckner, G., Heide, A. J., Philippe, H., Melkonian, M. *et al.* (2011) Origin of land plants: Do conjugating green algae hold the key?. *BMC Evolutionary Biology*, **11**, 104.
- Woessner, J. P. & Goodenough, U. W. (1994) Volvocine cell walls and their constituent glycoproteins: an evolutionary perspective. *Protoplasma*, **181**, 245–258.
- Woudenberg, S., Renema, J., Tomescu, A. M. F., De Rybel, B., Weijers, D. (2022) Deep origin and gradual evolution of transporting tissues: perspectives from across the land plants. *Plant Physiology*, **kiac304**, doi: 10.1093/plphys/kiac304.
- Xu, Z., Zhang, D., Hu, J., Zhou, X., Ye, X., Reichel, K. L. *et al.* (2009) Comparative genome analysis of lignin biosynthesis gene families across the plant kingdom. *BMC Bioinformatics*, **10**, S3.
- Xue, X., & Fry, S. C. (2012) Evolution of mixed-linkage (1→3, 1→4)-β-D-glucan (MLG) and xyloglucan in *Equisetum* (horsetails) and other monilophytes. *Annals of Botany*, **109**, 873–886.
- Yadav, S., Basu, S., Srivastava, A., Biswas, S., Mondal, R., Jha, V. K. *et al.* (2023) Bryophytes as modern model plants: an overview of their development, contributions, and future prospects. *Journal of Plant Growth Regulation*, **42**, 6933–6950.
- Yariv, J., Rapport, M. M., Graf, L. (1962) The interaction of glycosides and saccharides with antibody to the corresponding phenylazo glycosides. *Biochemical Journal*, **85**, 383–388.
- Yates, E. A., Valdor, J. F., Haslam, S. M., Morris, H. R., Dell, A., Mackie, W. *et al.* (1996) Characterization of carbohydrate structural features recognized by anti-arabinogalactan-protein monoclonal antibodies. *Glycobiology*, **6**, 131–139.
- Ye, Z.-H. & Zhong, R. (2022) Cell wall biology of the moss *Physcomitrium patens*. *Journal of Experimental Botany*, **73**, 4440–4453.
- Yin, Y., Johns M. A., Cao, H., Rupani, M. (2014) A survey of plant and algal genomes and transcriptomes reveals new insights into the evolution and function of the cellulose synthase. *BMC Genomics*, **15**, 260.
- York, W. S. & O'Neill, M. A. (2008) Biochemical control of xylan biosynthesis – which end is up? *Current Opinion in Plant Biology*, **11**, 258–265.
- Youl, J. J., Bacic, A., Oxley, D. (1998) Arabinogalactan-proteins from *Nicotiana glauca* and *Pyrus communis* contain glycosylphosphatidylinositol membrane anchors. *Proceedings of the National Academy of Sciences*, **95**, 7921–26.
- Yuasa, K., Toyooka, K., Fukuda, H., Matsuoka, K. (2005) Membrane-anchored prolyl hydroxylase with an export signal from the endoplasmic reticulum. *The Plant Journal*, **41**, 81–94.

- Zabotina, O. A., Zhang, N., Weerts, R.** (2021) Polysaccharide biosynthesis: glycosyltransferases and their complexes. *Frontiers in Plant Science*, **12**, 625307.
- Zhang, J., Fu, X.-X., Li, R.-Q., Zhao, X., Liu, Y., Li, M.-H. et al.** (2020) The hornwort genome and early land plant evolution. *Nature Plants*, **6**, 107–118.
- Zhou, Y., Kobayashi, M., Awano, T., Matoh, T., Takabe, K.** (2018) A new monoclonal antibody against rhamnogalacturonan II and its application to immunocytochemical detection of rhamnogalacturonan II in *Arabidopsis* roots. *Bioscience, Biotechnology, and Biochemistry*, **82**, 1780–1789.

Acknowledgements

Mein größter und besonderer Dank geht an meine Doktormutter, Birgit Classen, die mich in ihrer Arbeitsgruppe aufnahm und mir so meinen Doktor ermöglichte! Danke, dass du mich mit deiner freundlichen und liebevollen Art empfangen, zu jeder Zeit unterstützt und gefördert hast! Danke, dass du immer ein offenes Ohr für mich hattest und mir zur Seite standest, auch „wenn die Evolution der AGPs mal aus der Reihe tanzte“. Danke, dass du auch heute noch meine Neugier und mein Interesse an der Wissenschaft wachsen lässt und dafür sogar mit mir um die halbe Welt gereist bist (zumindest bis nach Málaga). Ich freue mich unheimlich, weiterhin Teil deines wunderbaren Teams sein zu dürfen! Vielen Dank!

Weiterhin möchte ich mich bei Lukas Pfeifer bedanken. Du standest mir seit Tag 1 mit Rat und Tat zur Seite. Du hast mir so viel beigebracht und keinen Tipp für dich behalten. Ich danke dir, dass ich so viel lernen durfte und vor allem für dein Vertrauen. Nicht zuletzt möchte ich dir auch für die vielen wunderbaren Gespräche und vor allem für die lustigen selbstausedachten Lieder danken, die so manch einen mühsamen Tag verzückt haben. Ohne dich hätte die Zeit nur halb so viel Spaß gemacht! Vielen Dank!

Johanna, Marie-Theres und Calisto, vielen Dank euch für die großartigen Gespräche und für die gemeinsame Zeit. Der Austausch untereinander, die Unterstützung und der Zusammenhalt haben mir viel Kraft gegeben und mich immer wieder zum Lachen gebracht! Vielen Dank!

Zudem möchte ich noch unseren „Haus-Elfen“ Claudia, Conny, Mayra und Kalle, sowie unseren GärtnerInnen Olaf, Steffi und Anna danken, die mir bei jedem noch so plötzlich auftretenden Problem jederzeit zur Seite standen und meine Verzweiflung in Luft aufgelöst haben! Vielen Dank für eure Unterstützung!

Zum Schluss geht mein Dank an meine Familie und meine Freunde, die immer an mich geglaubt und mich darin bestärkt haben, was im Leben wirklich wichtig ist und was wirklich zählt. Danke, dass ihr immer für mich da seid. Ohne euch wäre ich nicht dort, wo ich jetzt stehe! Ich danke euch unendlich für alles, was ihr für mich getan habt, und ich hoffe, ich kann euch irgendwann das zurückgeben, was ihr mir mein Leben lang gebt. Vielen Dank!

Declaration

Hiermit erkläre ich, Kim-Kristine Müller, dass die vorliegende Arbeit zum Zwecke der Promotion im Fachbereich Pharmazeutische Biologie im Pharmazeutischen Institut der Christian-Albrechts-Universität zu Kiel eigenverantwortlich unter der Leitung meiner Doktormutter Frau Professorin Dr. Birgit Classen verfasst wurde.

Es wurden keine weiteren außer in dieser Arbeit angegebenen Hilfsmitteln und Quellen verwendet und nach Einhaltung der Regeln guter wissenschaftlicher Praxis der Deutschen Forschungsgemeinschaft gearbeitet.

Ich möchte darauf hinweisen, dass die Ergebnisse der Grünalge *Chara aspera* auch Teil der Masterarbeit von Felicitas Erdt und die des Schwimmfarns *Azolla filiculoides* sowie des Bärlapps *Huperzia squarrosa* Teil der Masterarbeit von Lina Schuldt waren.

Zudem versichere ich, dass ich diese Arbeit vorher keiner anderen wissenschaftlichen Einrichtung im Rahmen einer Promotion eingereicht habe. Bestimmte Abschnitte dieser Arbeit sind in wissenschaftlichen Fachzeitschriften publiziert worden. Die jeweiligen Co-Autoren und mein entsprechender Anteil an dem Review, den Originalveröffentlichungen und den zur Veröffentlichung vorbereiteten Manuskripten sind unter „Results and Contributions“ beschrieben und den jeweiligen Kapiteln zu entnehmen.

Ich versichere außerdem, dass mir kein akademischer Grad aberkannt wurde.

Kiel, 2024

Kim-Kristine Müller